ISSN 0790 - 0279

Suirbhéireacht Gheolaíochta Éireann

# ASSESSMENT OF THE GEOLOGICAL FACTORS INFLUENCING THE OCCURRENCE OF RADON HAZARD AREAS IN A KARSTIC REGION

P.J. O'Connor, V. Gallagher, J.S. Madden
G. van den Boom, J.P. McLaughlin, I.R. McAulay,
K.J. Barton, J.T. Duffy, R. Müller,
S. Grimley, D. Marsh, G. Mackin, C. MacNiocaill

Geological Survey of Ireland
Report Series RS93/2

## AUTHORS

**P.J. O'Connor, V. Gallagher**

Geological Survey of Ireland, Beggars Bush, Haddington Road, Dublin 4.

**J.S. Madden, J.T. Duffy, G. Mackin**

Radiological Protection Institute of Ireland, 3 Clonskeagh Square, Clonskeagh Road, Dublin 14.

**G. van den Boom, R. Müller**

Bundesanstalt für Geowissenschaften und Rohstoffe, Hanover, Germany.

**J.P. McLaughlin, S. Grimley**

Department of Physics, University College, Belfield, Dublin 4.

**I.R. McAulay, D. Marsh**

Department of Physics, Trinity College, Dublin 2.

**K.J. Barton, C. MacNiocaill**

Applied Geophysics Unit, University College, Galway.

## SUMMARY

Radon is a naturally-occurring radioactive gas derived from the decay of uranium in rocks and minerals. Radon and its decay products in the indoor environment arguably constitute the most significant natural radiological risk to human health in Ireland. No fundamental studies aimed at investigating the underlying geological controls of radon production and migration in Irish rocks were undertaken previously. For this reason, GSI co-ordinated an EC-supported project (contract Bi7-CT90-0059) with this objective in mind during the period 1990-1992.

The project involved close collaboration between a number of Irish institutes (GSI, RPII, UCD, TCD, UCG) and the German Federal Geological Survey (BGR).

The area chosen for the investigation is one of contrasted geology near Moycullen, Co. Galway, where the Galway Granite abuts against karstic limestone. The granite is considerably more enriched in uranium than the limestone but, contrary to expectations, a significant number of houses built on limestone were found to have elevated indoor radon concentrations. Radon entry at specific house sites was found to be due to the existence of *very localized* physical pathways in the underlying bedrock substrates (e.g. fractures, channels, faults, shear zones, etc.) which gave rise to a very considerable increase in permeability. In particular, it was found that karstification of the limestone due to dissolution by circulating groundwater greatly enhanced permeability and such bedrock could act as a very efficient radon conduit. Much of central and western Ireland is underlain by similar limestone formations which have been karstified to a greater or lesser extent. The results of the present study suggest that indoor radon monitoring should be targeted by RPII in these areas as a matter of priority to assess the true extent of the radiological risk to the indigenous population.

The present study also shows that, by combining geological mapping techniques with radon soil-gas surveys, it is possible to define *radon availability* over broad geographic areas. The consequences of such a predictive mapping methodology are that areas designated for urban development may be categorized at the outset in terms of potential radon risk, thereby helping to reduce or avoid the cost of later remedial actions by Local Authorities or other State agencies responsible for radon mitigation and remediation. Further follow-up studies are underway to test the effectiveness of such a predictive radon mapping methodology.

P.J. O'Connor

September 1993

TABLE OF CONTENTS

## 5 OBJECTIVES AND RESULTS OF TCD STUDY

5.1 Correlation of soil $^{226}Ra$ and $^{234}Th$ with indoor radon
5.2 Rock $^{226}Ra$ and $^{234}Th$ results
5.3 Terrestrial gamma measurements
5.4 $^{40}K$ results
5.5 Conclusions

## 6 OBJECTIVES AND RESULTS OF UCG STUDY

6.1 Appraisal of regional gravity data
6.2 Results of field geophysical surveys
6.3 Conclusions

## 7 OBJECTIVES AND RESULTS OF BGR STUDY

7.1 Results of combined Rn-He soil-gas surveys
7.2 Regional Helium-Radon distribution
7.3 Conclusions

## TECHNICAL ANNEXES

Annex 1: Contribution of the Geological Survey of Ireland

Annex 2: Contribution of the Radiological Protection Institute of Ireland

Annex 3: Contribution of University College, Dublin

Annex 4: Contribution of Trinity College, Dublin

Annex 5: Contribution of Bundesanstalt für Geowissenschaften und Rohstoffe

Annex 6: Contribution of University College, Galway

## MAP FOLIO

Containing maps to accompany the technical annexes.
(Colour originals of these maps may be consulted at the Geological Survey of Ireland)

# 1 SUMMARY OF PROJECT GLOBAL OBJECTIVES AND ACHIEVEMENTS

## 1.1 Rationale

Radon and its decay products in the indoor environment arguably constitute the most significant natural radiological impact on human health. For this reason, it is important that we should attempt to understand the nature of radon generation in bedrock and its derivative soil cover and the migratory routes to surface dwellings. Such an understanding will undoubtedly be of assistance in the formulation of effective radon mitigation strategies aimed at limiting the radiological risk to the population at large.

## 1.2 Global Objectives

The primary aim of the project was to carry out an integrated and multidisciplinary investigation of the geological factors controlling the occurrence of certain high radon exhalation sites in Western Ireland. Specifically, the project set out to:-

(i) Determine the geological controls of radon production and migration in karstic limestone terrain.

(ii) Develop a more efficient and effective field sampling methodology for radon detection and test the use of soil-gas helium mapping as an aid in delineating radon migratory routes.

## 1.3 Global Achievements

A field study area was selected by the project team in Western Ireland, centred on the village of Moycullen (Co. Galway), where elevated indoor $^{222}Rn$ levels had been reported during monitoring carried out by U.C.D. in 1987. The study area straddles the NW-SE trending boundary or contact zone between the, in part, uraniferous late Caledonian Galway Granite and its unconformable cover of younger Carboniferous karstic limestones. These bedrock lithologies are overlain by varied, and often thick, glacial deposits which include a substantial component of fluvioglacial sands and gravels. The geological and topographic relationships of the study area are shown schematically in a cross-section (Fig. 1a). Surface dwellings in which indoor $^{222}Rn$ concentrations were measured, are distributed throughout the area and overlie either granite or limestone bedrock.

The technical annexes of this report include details of the methodologies employed, tabulations and statistical summaries of the data obtained, and computer-integrated maps of all spatial geodata that supplement the summary presented here. Colour originals of all the maps enclosed in the Map Folio may be consulted at the Geological Survey of Ireland, Beggars Bush, Haddington Road, Dublin 4. All maps are available in digital form.

### 1.3.1 Results of Geological, Geophysical and Geochemical Investigations

Investigations carried out by GSI comprised systematic field mapping of the bedrock geology (1:10560 scale) and glacial deposit geology (1:25000 scale) of the study area, supported by a reconnaissance total-gamma survey and a diamond drilling campaign (11 boreholes) of selected surface and subsurface targets. These geodata, together with other spatial data depicting the geographic distribution of indoor $^{222}Rn$ concentrations (RPII), soil

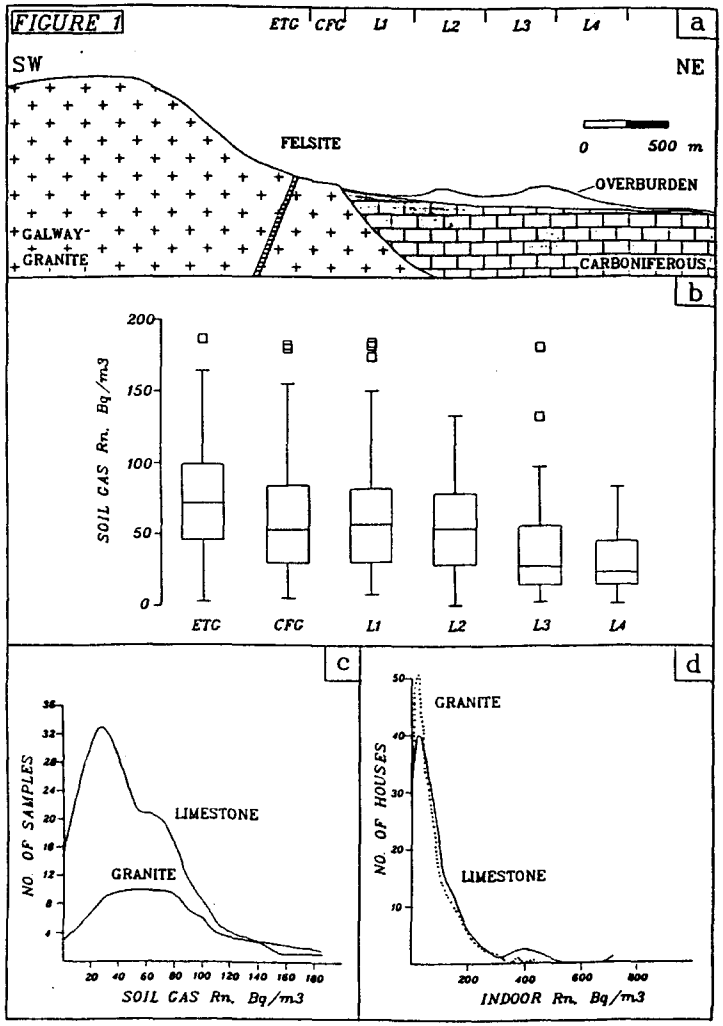


Figure 1 Schematic cross-section of geology in Moycullen area and summary of soil-gas radon data

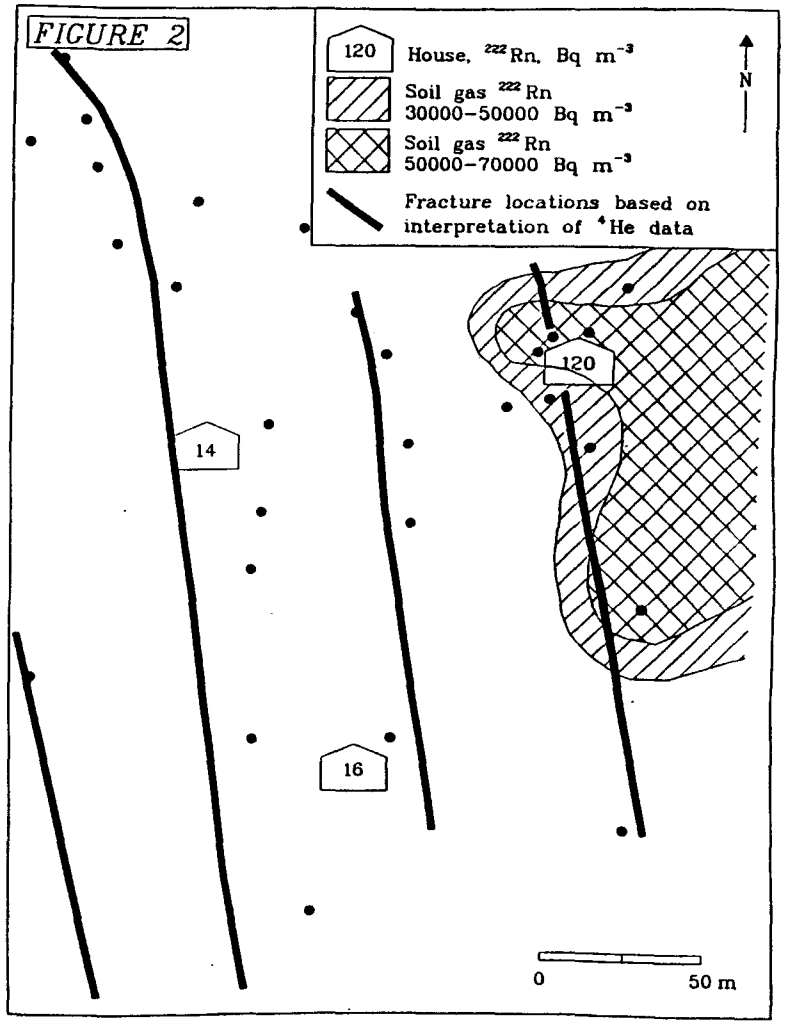


Figure 2 Interpretative map of soil-gas radon and helium concentrations in Ballydotia area, Moycullen.

gas $^{222}Rn$ and $^{4}He$ concentrations (BGR), and soil $^{226}Ra$ activities (TCD) were digitized and computer-integrated to aid interpretation using customized mapping software (AutoCAD) available at GSI.

Geochemical analysis of 82 samples of rocks and soils recovered from surface or in drillcore was completed by TCD, using high resolution gamma spectrometry. The measured $^{226}Ra$, $^{234}Th$, $^{228}Ac$ and $^{40}K$ activities of samples were used to identify potential $^{222}Rn$ sources.

Geophysical investigations carried out by UCG (under subcontract to GSI) involved detailed resistivity surveys (EM-VLF-R, VES and dipole-dipole array) in the vicinity of houses with high indoor $^{222}Rn$ levels in three selected sub-areas. The resistivity data were used to aid definition of subsurface bedrock structures which might act as $^{222}Rn$ migratory routes.

Assessment of the results of geological, geophysical and geochemical investigations identified the likely potential radon sources and migratory routes in the study area, which are summarized in Table 1. Radon availability at a particular house site is controlled by a combination of the proximal existence of a radon source *and* the presence of localized subsurface structures (fractures, faults, shear zones, cavities) in bedrock which act as zones of enhanced permeability.

### 1.3.2 Results of Indoor 222-Rn Surveys

Time-integrated indoor $^{222}Rn$ measurements (≥90 days exposure) using closed passive CR-39 detectors were completed by RPII in 235 houses almost equally divided between granite and limestone terrains. Concentrations ranged from 8 Bq $m^{-3}$ up to 725 Bq $m^{-3}$ with an arithmetic mean concentration of 82 Bq $m^{-3}$ and a median concentration of 53 Bq $m^{-3}$. Overall, 10% of houses had $^{222}Rn$ concentrations in excess of 200 Bq $m^{-3}$ (National Reference Level). When considered in lithological terms, 13% of houses underlain by limestone and 6% of houses underlain by granite had indoor concentrations in excess of 200 Bq $m^{-3}$ (see Fig. 1d). There is no obvious systematic spatial pattern to the indoor $^{222}Rn$ data, and high and low concentrations occur, often contiguously, over both granite and limestone terrains.

### 1.3.3 Site-Specific Investigations

A co-ordinated series of site-specific investigations at 18 houses, completed by RPII, UCD and TCD, involved (i) time-intergrated (passive) and instantaneous (active) soil gas $^{222}Rn$ measurements, (ii) determination of $^{226}Ra$, $^{234}Th$, $^{228}Ac$ and $^{40}K$ in soils, and (iii) terrestrial gamma radiation measurements. UCD successfully developed and tested a new multi-chambered type of CR-39 detector which allowed a much greater range of soil gas $^{222}Rn$ concentrations to be measured. A soil permeability probe was also developed but adverse ground conditions precluded its use in the study area.

The ranges of soil gas $^{222}Rn$ concentrations measured at sites using both passive and active detectors are shown in Table 2.

**Table 1: Radon Sources and Pathways**

| | Source | Radioelement Content | Geographic Distribution | Migratory Pathways |
|---|---|---|---|---|
| 1. | Main Galway Granite | **Moderate** (resistate accessory minerals) | Widespread | Intergranular; along fractures (all scales), altered shear zones; in solution in groundwater |
| 2. | Felsite Dykes | **High** (U, Ra in labile accessory minerals) | Localized linear zones | Along linear fracture zones occupied by dykes |
| 3. | Murvey Granite | **High** (U, Ra in labile accessory minerals) | Not exposed (if present located in contact zone) | Along contact zone (sheared) |
| 4. | Lower Carboniferous Limestone | **Low** (dispersed in matrix) | Widespread | Along joints/fractures and through karst cavities/channels; in solution in circulating groundwater |
| 5. | Basal Carboniferous Black Shale | **High** | Possibly widespread | Along fractures and shear zone at contact; in solution in circulating groundwater |
| 6. | Upper Carboniferous Shales and Phosphorites | **High-Very High** | Not known in study area (eroded) | Along fractures and in downward circulating groundwater leading to deposition within or beneath the cover limestones |
| 7. | Glacial Deposits | **Low** | Widespread | Through open pore spaces (especially in sand/gravel deposits) |

**Table 2** **Ranges of measured soil gas $^{222}Rn$ concentrations using passive and active detectors**

| | Passive (CR-39) | Active (Lucas Cell) |
|---|---|---|
| **Granite** | 340-58760 Bq $m^{-3}$ | 330-108370 Bq $m^{-3}$ |
| **Limestone** | 2600-53010 Bq $m^{-3}$ | 4560-165165 Bq $m^{-3}$ |

Large within-site and between-site variability was encountered. No apparent correlation was observed between measured soil gas and indoor $^{222}Rn$ concentrations, although the within-site variability posed a serious problem to proper interpretation.

Measured $^{226}Ra$ activities in soils at specific house sites ranged from 7 to 89 Bq $kg^{-1}$ (average 48 Bq $kg^{-1}$) and, again no correlation with indoor $^{222}Rn$ levels was apparent.

Terrestrial gamma measurements at specific sites indicated average absorbed doses of 58 nGy $h^{-1}$ over granite and 48 nGy $h^{-1}$ over limestone, consistent with the relative radioelement contents of each lithology.

### 1.3.4 Results of Combined Soil Gas $^{222}Rn$-$^{4}He$ Investigations

A total of 367 soil gas $^{222}Rn$ samples and 447 soil gas $^{4}He$ samples were collected by BGR using a modified grab sampling technique. Radon concentrations were determined on a Pylon AB-5 monitor and helium concentrations by mass spectrometry. A successful intercomparison test of RPII and BGR grab sampling techniques under field and laboratory conditions was also carried out.

A statistical summary of the soil gas $^{222}Rn$ and $^{4}He$ data is shown in Fig. 1c and Table 3.

**Table 3** **Statistical summary of soil-gas data (active sampling)**

| | $^{222}Rn$ (Bq $m^{-3}$) | $^{4}He$ (ppb) |
|---|---|---|
| **Granite** | 2600-186300 (median 65650) | 5013-5685 (median 5283) |
| **Limestone** | 400-184000 (median 37300) | 5092-5759 (median 5267) |

Although the median soil gas $^{222}Rn$ value recorded over limestone is only half that over granite, nearly twice as many houses built on limestone had indoor $^{222}Rn$ levels in excess of 200 Bq $m^{-3}$. For the study area, the maxima of the radon distributions are, perhaps, a better guide as to whether or not an indoor problem is likely to exist.

Soil gas $^{222}Rn$ levels over limestone show a systematic decrease with distance from the granite (Fig. 1b). While such a decrease could reflect a decrease in the permeability of the limestone and/or its glacial overburden, it is thought more likely to reflect the decay of

$^{222}$Rn during transport (by groundwaters?) from the granite source.

Contouring the soil gas $^{222}$Rn data defines a number of high $^{222}$Rn anomalous zones, some up to 500m in maximum dimension. At such scales there is an apparent spatial correlation between some of these anomalous zones and the occurrence of high indoor $^{222}$Rn levels in houses, although when this correlation is examined in detail (site-specific studies) it is not often found to be upheld.

Spatial analysis of the soil gas $^{4}$He data defines a number of linear arrays of high $^{4}$He values, thought to represent zones of enhanced permeability. Such He "lineaments" often correlate with known fracture zones and are often centred on soil gas $^{222}$Rn anomalies. Where a house is sited on a zone of enhanced permeability defined by anomalous $^{4}$He values and within an area underlain by a soil gas $^{222}$Rn anomaly, high indoor $^{222}$Rn levels may occur (see Fig. 2). The existence of both a radon source and a physical pathway for radon migration appear to be equally critical factors in controlling indoor $^{222}$Rn levels. If either is absent, then high indoor levels may not develop.

### 1.3.5 Conclusions and Recommendations

(i) The present study shows that geological mapping, when supported by combined Rn-He soil gas surveys, can succeed in defining radon availability over broad geographic areas of varied geology and pedology. Further development of such predictive mapping methodologies could assist in focussing the indoor monitoring campaigns of EC radiological institutes in a more effective way. Effective soil-gas mapping methodologies may also be used to categorize areas in terms of Rn potential which are designated for urban development and thereby help to reduce or avoid the cost of later remedial actions.

(ii) The mapping methodologies employed suggest that for specific house sites the migratory routes for Rn transport are likely to be very localized physical pathways. Site specific measurements of soil $^{226}$Ra activities and soil gas $^{222}$Rn concentrations may fail to show a meaningful correlation with indoor $^{222}$Rn levels for a variety of reasons.

(iii) Geophysical resistivity-based survey techniques may only achieve partial success in imaging subsurface radon migratory pathways and it is suggested that other geophysical methods (e.g. ground-probing radar) might prove more effective in locating shallow physical pathways for radon ingress beneath houses and in their immediate vicinity (particularly in urban environments).

(iv) Carbonate rocks such as limestone contain very low concentrations of U and Ra and dwellings built on carbonate bedrock might be expected to have low indoor $^{222}$Rn concentrations. However, such rocks are also highly prone to dissolution (karstification) by circulating groundwater which thereby greatly enhances their permeability. The present study shows that they can act as very efficient radon conduits where karstification is well advanced or complete and where U or Ra are mobile.

Recent studies in Denmark and the USA have also reported enhanced $^{222}$Rn levels in dwellings built on limestone sequences and support the view that rock permeability strongly influences $^{222}$Rn availability even in otherwise poorly uraniferous lithologies. Indoor monitoring of $^{222}$Rn should be extended to populated areas of the EC underlain by karstified limestone sequences in order to assess the true extent of the radiological risk to the population of these areas.

### 1.3.6 Publications arising from the study

**Boom, G. van den & Müller, R. (1991).** Bericht uber die Durchfuhrung von Helium-Radon Messungen in funt Testgebieten in der CSFR. Unweltradioaktivitat, Interdisziplinare Umweltforschung, Marianska (CSFR), Vortrag und Bericht BGR, Archiv Nr. 108 990.

**Duffy, J.T. 1992.** Dealing with Radon in Ireland. *Construction 1992*, Vol. 4, p. 7. Published by Environmental Research Unit ISSN 0791-2099.

**Enmotec (1992)** Mogliche Auswirkungen der Grubenflutungen auf die Radonemanation in oberflachennahe Sedimente und potentielle Gefahrdung fur angrenzende Siedlungsbereiche. Workshop der Wismut G.m.b.H. in Chemnitz, Vortrag und Bericht.

**Madden, J.S. (1991)** Radon in Buildings. What is it? Where does it come from? Why are we concerned? Proceedings of the Institution of Engineers of Ireland Seminar on the Investigation and Cure of Sick Buildings, May 1991.

**Madden, J.S. (1992).** The Radon Problem in the West/South of Ireland. Proceedings of the Institution of Engineers of Ireland Seminar on Radon in Buildings, May 1992.

**O'Connor, P.J. (1992)** Recognition of radon hazard in Western Ireland: the role of geological factors. In: Radon et gaz rares dans les Sciences de la Terre et de l'Environment. P. Doremus, L. Dejonghe and J.-M. Charlet (Eds.). *Mém. Expl. Cartes Geologiques et Minières de la Belgique*, No. 32, 83-92.

**O'Connor, P.J. (1992)** Mapping radon migration in karstic limestone terrain in Western Ireland. (Presented at 2nd Irish Environmental Researcher's Colloquium p. 27, Abstracts, Trinity College, Dublin, January 1992).

**O'Connor, P.J., Gallagher, V., van den Boom, G., Hagendorf, J., Müller, R., Madden, J.S., Duffy, J.T., McLaughlin, J.P., Grimley, S., McAulay, I.R. and Marsh, D. (1992)** Mapping of $^{222}$Rn and $^{4}$He in soil gas over a karstic limestone-granite boundary: correlation of high indoor $^{222}$Rn with zones of enhanced permeability. *Journal of Radiation Protection Dosimetry*, Vol. 45, 215 - 218.

# 2 OBJECTIVES AND RESULTS OF GSI STUDY

The objectives of the geological investigations carried out by GSI in the study area were:

(i) To determine the location and geographic extent of radioelement-enriched rock types which might act as potential radon sources.

(ii) To determine the nature and spatial distribution of geological structures which might act as potential radon migratory routes to dwellings at surface.

## 2.1 Methodology

(a) Systematic mapping of bedrock geology (1:10560 scale) and glacial deposit geology (1:25000 scale) of the study area was completed.

(b) A reconnaissance total-gamma radiometric survey, based on 200 stations, was undertaken in support of the mapping programme.

(c) Eleven boreholes were drilled in the depth range 20-80m to investigate the nature of surface and subsurface targets delineated in field surveys by the project team in terms of their radon potential.

(d) Petrographic/mineralogical investigation of recovered geological samples was carried out and samples were analysed by neutron activation in Canada to determine their radioelement contents.

(e) A preliminary investigation of $^{222}$Rn activities in surface and groundwaters in the study area was completed with the assistance of the British Geological Survey.

(f) The compiled geological maps were digitized and integrated with other spatial geodata provided by the other partners using computer-based mapping software (AutoCAD).

## 2.2 Results

### 2.2.1 Identification of Radon Sources

The results of the total-count gamma radiometric survey of the study area show that the granite-limestone contact zone is reflected by a transition from higher total-gamma values recorded over granite terrain to lower values over limestone terrain. Within the area underlain by granite, the detected radiometric anomalies correlate spatially with known fracture zones and, in particular, with occurrences of radioactive felsite dykes which frequently occupy these zones.

Radioelement analysis of samples recovered from outcrop has confirmed high abundances of U (~15ppm), Th (~50ppm) and $^{222}$Ra activity (~160 Bq kg$^{-1}$) in the felsite dyke rocks which are in contrast to lower and more typical radioelement levels in the surrounding main Galway granite. The high radioelement contents of the felsite dykes are similar to those recorded by GSI for the Murvey granite variety of the Galway Granite batholith and to radioelement levels recorded in the granites of Devon and Cornwall in the

U.K., areas which have been designated as "affected" by NRPB. The felsites, therefore, represent localized linear zones of high radon potential within the granitic terrain of the study area and dwellings sited on or close to such zones could develop an indoor radon problem.

The nature of the granite-limestone contact at one locality, Ballycuirke townland, was investigated by GSI in a series of 3 boreholes which were drilled in close proximity to each other to a maximum depth of 80m. The contact was shown to dip at 25°-30° northeastwards beneath the younger limestone cover rocks (Fig. 1a). Intense alteration and deformation of the marginal granite at the contact is evident in drillcore and it is concluded that the contact zone is sheared or faulted along much of its length and that extensive water-rock interaction has occurred in this zone. Petrographic and geochemical analysis of the altered and deformed granitic rocks of the contact zone suggests that $^{222}$Ra, and to a lesser extent $^{234}$Th, have been leached and remobilized by circulating groundwaters. This is consistent with the results of other studies, e.g. those recently reported by U.S.G.S., that shearing of granitic rocks is conducive to the release of their contained radioelements (e.g. U, Ra), mainly as a consequence of the mineralogical changes which occur during the shearing process. There are likely to be a significant number of such unexposed linear shear zones in the granitic terrain of the study area which could represent zones of enhanced radon emanation.

The drillcores recovered from the contact zone boreholes also indicate the presence of a previously unknown and severely deformed black shale unit (>5m thick) at the base of the Carboniferous limestone sequence. Analysis of shale samples (by TCD) shows high $^{226}$Ra activities (~142 Bq kg$^{-1}$). If the shale unit extends laterally beneath the karstic limestone cover rocks throughout the study area, as is likely, then it would represent a significant and geographically-widespread radon source. The limestones themselves are radioelement-poor.

There is a further potential radon source which, from geological considerations, merits attention. To the south of the study area in Co. Clare, the karstic Carboniferous limestones are overlain by uraniferous shales and phosphorites, of Namurian age. It is likely that these uraniferous lithologies once existed in the study area also, but have since been eroded. They would have contributed substantial amounts of U and Ra to downward-circulating groundwaters during post-Carboniferous times. The radioelements in solution may have been deposited at lower stratigraphic levels in the underlying limestone sequence. Later karstification of the limestones, which greatly enhanced their permeability, would allow them to act as a very efficient transport medium for available $^{222}$Rn to migrate upwards to the surface.

A preliminary survey of $^{222}$Rn activities in groundwater samples recovered from both wells and springs in both the granite and limestone terrains was carried out with assistance from personnel of the British Geological Survey who kindly carried out the analyses. The results indicate that the $^{222}$Rn activities of wells on granite bedrock generally exceed 100 Bq l$^{-1}$ and, as might be expected, are approximately twice the activity levels recorded for wells on limestone.

### 2.2.2 Identification of Radon Migratory Routes

Following its generation in U-Ra bearing minerals in rocks, radon migrates by diffusive and convective processes along crystal defects and grain boundaries, through pore spaces and through macroscopic cracks and fractures of different scale on its upward route to the surface. Below the water-table, radon is in solution and hydrogeological factors are also important in its migration. Potential radon migratory routes to surface dwellings are, therefore, dependent on the existence of appropriate physical pathways at any given site. The field geological studies have identified a number of physical pathways which, individually or in combination, are likely to have a significant influence on the radon flux measured at surface. These pathways include:-

(1) Fracture Zones: A substantial number of linearly-disposed fracture zones of varying magnitude and intensity were delineated in both the granite and limestone terrains. Movement (faulting, shearing) has taken place on some of these fractures, particularly in the granite-limestone contact zone. Fracture directions in the granite terrain generally trend N-S or NE-SW and many of the fractures are occupied by later radioelement-rich felsite dykes. The felsite dykes thus represent a potential source of high radon emanation situated in linear zones of high permeability. There is a high fracture density in the limestone terrain, with N-S and E-W trends predominant.

(2) Karstified Limestone: Deeply-jointed karstic pavements are exposed at surface in the limestone terrain with measured solution channels up to 2m deep and 0.5m wide. The probable existence of widespread subsurface cavities or channels in the limestone terrain was indicated in a series of 8 GSI boreholes, drilled to depths of 20-50m, in Ballydotia townland. The boreholes were sited in close proximity to two separate houses where elevated indoor $^{222}$Rn levels had previously been recorded by RPII and where geophysical and soil-gas $^{4}$He surveys by UCG and BGR, respectively, had indicated the possible presence of subsurface discontinuities. The karstified limestone therefore represents a laterally extensive medium of greatly enhanced permeability through which radon could migrate freely. Spatial variation in the radon flux measured at surface may reflect the degree of karstification attained by the limestone from place to place. If the limestone is underlain by a radioelement-rich black shale, as is thought likely, then a widespread potential Rn source is situated below a highly permeable cover.

(3) Permeable Overburden: The fluvioglacial sand and gravel deposits, which have been delineated and overlie the cover limestones, have low radioelement contents and do not represent potential radon sources, but their high permeability suggests that radon would migrate freely through these deposits to the surface. Most of the other glacial materials (drift, boulder-clay) and the soils derived from them are less permeable and are not enriched in radioelements.

## 2.3 Conclusions

The spatial variation observed in the indoor $^{222}$Rn data - where high and low values are often recorded in contiguous houses - suggests that localized subsurface structures (e.g. joints, fractures, faults, shear zones), representing zones of greatly enhanced permeability, control radon migration and ingress at specific house sites.

# 3 OBJECTIVES AND RESULTS OF RPII STUDY

The specific objectives of the Radiological Protection Institute of Ireland (RPII) in this project were:

(i) To approach and obtain on behalf of the Research Group the participation of householders, and to determine the geographical distribution of indoor radon concentrations in selected townlands within the Moycullen postal district.

(ii) To approach and obtain on behalf of the Research Group the further participation of specific householders whose houses were selected for detailed follow-up site investigations, and

(iii) To conduct site investigations incorporating soil gas radon measurements using passive, integrating CR-39 alpha track radon detectors, instantaneous soil gas radon measurements using a grab sampling technique and terrestrial gamma radiation measurements. In addition the RPII supplied passive radon detectors to UCG, a sub-contractor to the GSI, for deployment in several boreholes drilled by GSI in the Moycullen area.

## 3.1 Introduction

The choice of the Moycullen area for this project originates in the discovery by University College Dublin (UCD) in 1985-1989 of elevated indoor radon concentrations in houses on the limestone sequences. Regional follow-up studies by the RPII and UCD in 1989-1991 confirmed these earlier findings and predicted that 14% ± 5% of houses in Co. Galway would exceed the adopted national Reference Level of 200 Bq $m^{-3}$ (Radon gas). In addition the regional survey identified an anomalous area in Co. Galway, which incorporates Moycullen, in which 24% ± 9% of the houses were predicted to exceed the Reference Level. Radon concentrations monitored in houses in the Moycullen area during the regional survey ranged from 42 Bq $m^{-3}$ up to 1751 Bq $m^{-3}$.

## 3.1 Geographical Distribution of Indoor Radon Concentrations

### 3.2.1 Sample Selection

A total of 494 householders in selected townlands within the Moycullen postal district were contacted by the RPII regarding participation in this project, and indoor radon measurements were completed in 235 houses. All houses were plotted on 1:10560 O.S. maps, and their locations subsequently digitised by GSI.

### 3.2.2 Indoor Radon Gas Measurement Technique

Time integrated radon gas concentrations were measured using the standard RPII domestic radon dosemeter. This dosemeter is a passive, closed, alpha track radon detector which is left undisturbed in a ground floor living area or bedroom for a minimum exposure period of 90 days. It consists of a cylindrical plastic bottle with a screw-on lid. The alpha

particle detecting medium i.e. polyallyl-diglycol carbonate or CR-39 is held in position inside the lid by a small plastic insert placed inside the bottle.

On return the detectors were chemically etched and counted by manual microscopy. The etching conditions used were 10N Sodium Hydroxide (NaOH) at $70^0$C for 8 hours. The dosemeters were calibrated by participation in the recent series of intercomparisons carried out by the CEC.

## 3.3 Site Specific Investigations

### 3.3.1 Site Selection

After consultation with other project partners, 20 houses were selected for detailed site investigations. The selected sites contained houses with both high and low indoor radon concentrations and were located on both sides of the granite/country rock geological contact. Investigations were completed at 18 sites and all site locations were plotted on 1:2500 O.S. maps.

### 3.3.2 Measurement Techniques

3.3.2.1 Passive Integrated Soil Gas Radon Measurements

Time integrated soil gas radon concentrations were measured using the standard RPII domestic radon dosemeter. A portable Cobra drill with a 4.5 cm diameter soil sampling head was used under suitable site conditions to penetrate the overburden to a depth of 1m. The hole was then cased with tight fitting plastic tubing to preserve, it and sealed at the surface with an air-tight rubber cap. All detectors were suspended in the pipe so as to remain above the water table.

Difficult and unfavourable ground conditions at most sites dictated that practically all passive radon detectors were deployed and retrieved by manual excavation of the soil. Holes were dug by pick and shovel to practical attainable depths, and the radon detectors positioned on top of a stable base, usually a stone, and then covered with a plastic cup of protection. The holes were then backfilled and marked. After an exposure period of 190 hours the detectors were retrieved for processing. Where possible the measurements were taken in original soil as opposed to imported top soil.

3.3.2.2 Instantaneous Soil Gas Radon Measurements

Soil gas was extracted from the ground by sucking through a 4 mm internal diameter hydraulic pipe into Lucas cells. To ensure a representative sample of soil gas was obtained a flow-through method was adopted whereby at least 1 litre of soil gas was flushed through the Lucas cells.

After a minimum delay period of at least 3 hours the Lucas cells were counted on a Pylon AB-5 Radiation Monitoring System. Radon concentrations were determined using appropriate calibration factors and sample decay corrections. All measurements were taken in original soil where possible.

### 3.3.3 Terrestrial Gamma Radiation Measurements

Terrestrial gamma radiation measurements were taken at 2 locations at each site, at least 10 m away from the nearest building or outcrop. A Mini Instruments Environmental Meter (Type 6-80) was used for this purpose. The energy compensated GM tube was placed

in a vertical position with its centre approximately 1m above ground level. The counting period was 1000 seconds and the results displayed in $\mu$Gy $h^{-1}$. An average cosmic ray contribution of 0.04 $\mu$Gy $h^{-1}$ was subtracted from each reading to give the terrestrial component.

## 3.4 Intercomparison of Instantaneous Soil Gas Radon Measurement Techniques

An intercomparison of the radon grab sampling techniques employed in the field by RPII and BGR was undertaken at the RPII Calibration Facility in Dublin. The intercomparison was performed under laboratory conditions in the walk-in Radon Chamber, and also under typical field conditions in the grounds of UCD.

## 3.5 Results

### 3.5.1 Geographical Distribution of Indoor Radon Concentrations

In the survey area indoor radon concentrations ranged from 8 Bq $m^{-3}$ up to 725 Bq $m^{-3}$ with an arithmetic mean concentration of 82 Bq $m^{-3}$ and a median concentration of 53 Bq $m^{-3}$. There is no obvious systematic spatial pattern in the data, and high and low concentrations occur, often contiguously, over both granite and limestone. Overall, 10% of the houses had concentrations in excess of 200 Bq $m^{-3}$.

From a purely lithological basis the indoor radon concentrations in general tended to be higher in houses underlain by limestone. Thirteen percent of such houses had radon concentrations in excess of 200 Bq $m^{-3}$ as against 6% of houses on the granite.

### 3.5.2 Site Investigations

Instantaneous soil gas radon concentrations ranged from 330 Bq $m^{-3}$ up to 108,000 Bq $m^{-3}$ on the granite side of the geological contact and from 4500 Bq $m^{-3}$ up to 165,000 Bq $m^{-3}$ on the limestone side. On both sides of the geological contact some of the highest recorded instantaneous soil gas radon concentrations on site are often associated with the lowest indoor radon concentrations.

Terrestrial gamma radiation measurements indicated absorbed doses ranging from 38 nGy $h^{-1}$ up to 60 nGy $h^{-1}$ with an average value of 48 nGy $h^{-1}$ over the limestone. Over the granite absorbed doses ranged from 44 nGy $h^{-1}$ up to 70 nGy $h^{-1}$ with an average value of 58 nGy $h^{-1}$. The higher values over the granite are to be expected because of the uraniferous nature of the Galway Granite Batholith.

### 3.5.3 Intercomparison Exercise

The results of the intercomparison of RPII and BGR grab sampling techniques are presented in Table 4. Good agreement between both techniques under laboratory and field conditions is evident.

**TABLE 4**

| | Volume | Counts/10 min | Radon Concentration Bq $m^{-3}$ |
|---|---|---|---|
| Field Test | RPII<br>BGR | 161 ml<br>10 ml | 23320<br>24630 |
| Lab. Test | RPII<br>BGR | 161 ml<br>10 ml | 54260<br>55500 |

### 3.5.4 Passive Radon Detectors Deployed in Deep Boreholes

Soil gas radon concentrations ranged from 657 Bq $m^{-3}$ up to 12974 Bq $m^{-3}$ in measured boreholes. The degree of atmospheric mixing in the boreholes is unknown as is the degree of air mixing from the various open cavities encountered in the boreholes.

## 3.6 Conclusions

No apparent correlation between indoor radon concentrations and site specific soil gas radon concentrations is evident. The occurrence of high and low indoor radon concentrations, often contiguously, over both granite and limestone suggests that other parameters such as house characteristics and site specific geotechnical, geophysical and hydrogeological features must be important influences on radon ingress into domestic dwellings in this area.

# 4 OBJECTIVES AND RESULTS OF UCD STUDY

(i) To determine soil-gas radon concentrations in the granitic/karstic limestone contact region of Moycullen, Co. Galway, using standard techniques and a new type of passive detector being developed for this purpose.

(ii) To integrate, compare and interpret these measurements with those of other collaborating partners.

## 4.1 Development and calibration of a passive alpha track detector for use in soil-gas radon measurement

The objective was to produce miniature multichamber passive radon detectors which could be implanted in the ground in a region where little or no previous knowledge of soil gas radon levels was available. The novel aspect of this approach was to make the chambers of such small dimensions that their response to the alpha particles from radon and its progeny was sufficiently low to considerably reduce track saturation. In this way, the detectors would be used in very high radon concentrations for prolonged periods.

A theoretical model was developed to predict the sensitivity of small cylindrical detector chambers as a function of chamber radius and length (see Figure 3). On the basis of this model a three-chamber detector made from solid perspex was designed which was capable of covering the radon range from 10000 to 150000 Bq $m^{-3}$ for exposure periods from about 1 to 3 weeks without track saturation effects becoming unmanageable (see Figure 4). This is ideal for soil gas radon measurements. A Kitamura CNC high-precision computerized Machine Tool Centre was used to manufacture 150 of these multichamber detectors for the project field work. CR-39 was the detecting medium used. The detectors were intercalibrated against regular radon detectors calibrated at the NRPB (UK) as part of the ongoing CEC radon detection intercalibration programme.

## 4.2 Field measurements

Field work in the Moycullen area of Co. Galway took place mainly in July 1991. Due to the close proximity of the bedrock to the surface and the stony ground, it was very difficult to make radon measurement at depth. In places the soil cover was as shallow as 2 or 3 cm. Therefore the depths of the integrated measurements ranged from about 0.3 to 1.25 m and the depths of the soil-gas grab measurements from 0.3 to 0.7 m. Where possible, the measurements were taken close to each house and in original soil as opposed to imported top soil which the owner had brought into the garden to overcome general soil deficiency.

Instantaneous measurements of radon levels in soil gas were made using a grab sampling technique. Soil gas was pumped from the ground through a hydraulic pipe with 4 mm internal diameter into 100 ml Lucas scintillation cells. Integrated measurements of soil gas radon of duration 10 days were made using both standard and the new multichamber alpha track passive radon detectors.

A soil-gas permeability probe was designed and constructed based on a design by Anders Damkjaer at the Technical University of Denmark (CEC contract B16-347f-114), to make relative measurements of the soil permeability. Unfortunately, the soil and ground

Figure 3: Track production v. radon concentration

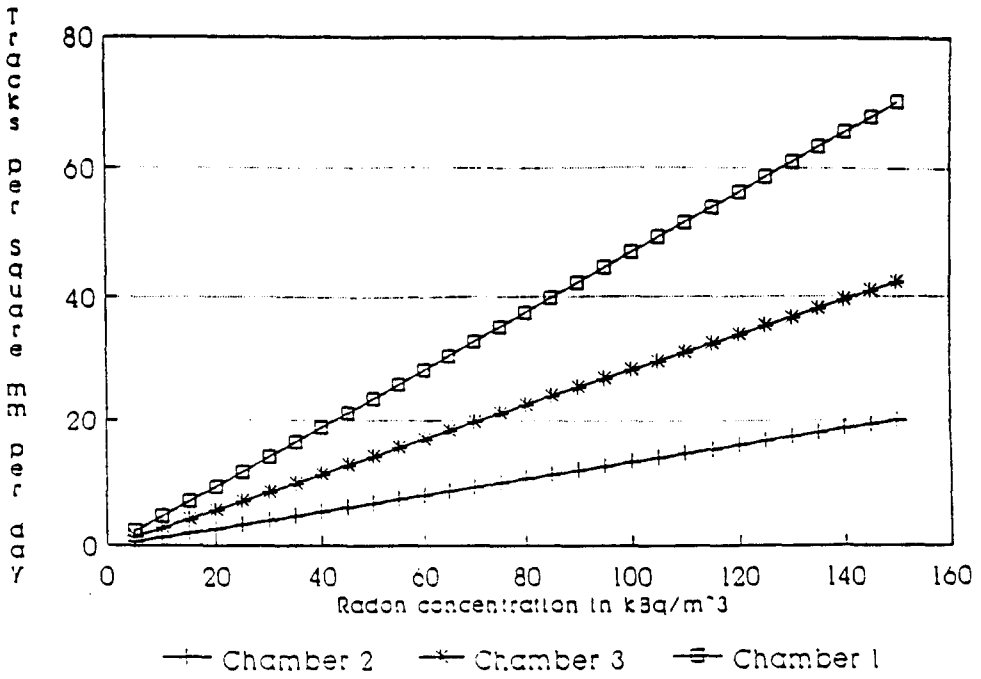


Figure 4: New Multichamber passive detector

Chamber 1: $R_c$ = 0.0060m; D = 0.011m
Chamber 2: $R_c$ = 0.0015m; D = 0.004m
Chamber 3: $R_c$ = 0.0045m; D = 0.005m

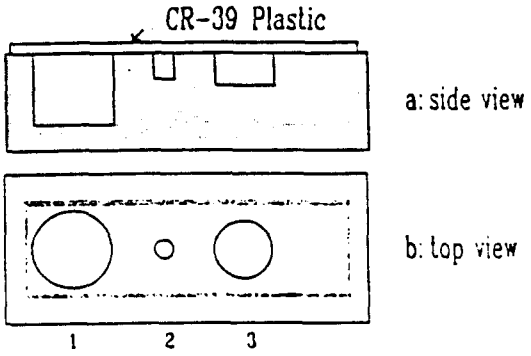


conditions encountered at almost all the sites proved unsuitable for the reliable operation of the permeability probe.

Wide variations were obtained in radon soil gas levels in the field area. The time-integrated soil-gas measurements gave concentrations ranging from a few hundred Bq $m^{-3}$ up to 58000 Bq $m^{-3}$. Most of the higher concentrations occurred on the granitic side of the Moycullen area. The grab samples gave radon concentrations ranging from 330 Bq $m^{-3}$ up to 165000 Bq $m^{-3}$.

It should be noted that at individual house sites considerable variations of soil gas radon levels were found to exist. Radon soil gas level ratios of ten to one between the soil at the front and back of a house were not unusual. Ratios as high as sixty eight to one were detected. These wide variations of soil gas radon levels over a distance of a small number of metres indicates the complexity of the radon migration and availability in the area. This considerably reduces the possibility that area mapping can give rise to a radon prediction

capability of sufficient accuracy and power to predict the existence of a high-radon risk down to the scale of an individual house site.

### 4.3 Conclusions

The general elevation of indoor radon levels in the Moycullen area appears to be due to the underlying uraniferous granite (see reports of other partners for a fuller discussion). No direct correlation was found between the indoor radon concentrations and those in the ground; houses built side-by-side may have indoor radon concentrations differing by several hundred Becquerels. This would suggest that there are other important parameters governing indoor radon concentrations apart from the existence of the granite and the karstic limestone such as:-

(i) House structure, in particular the foundations

(ii) House heating and ventilation

(iii) Soil permeability

(iv) Localized faults and fractures in the underlying bedrock

From a measurement perspective, it was found that the newly designed multichamber radon detector which was designed specifically for this work proved to be very suitable for field work in the unfavourable conditions found in the Moycullen area.

# 5 OBJECTIVES AND RESULTS OF TCD STUDY

(i) To determine by gamma ray spectrometry the radioactivity content of samples of soil and rock collected in the region selected for study.

(ii) To investigate the importance of radium content in the soil and rock samples in assessing the potential for high radon levels in dwellings in the region.

(iii) To study the uranium series disequilibrium in the samples and attempt to determine the significance of this factor in predicting domestic radon concentrations.

## 5.1 Correlation of Soil $^{226}Ra$ and $^{234}Th$ with Indoor Radon

From the results of the initial indoor radon survey, 17 houses were selected for further study, including houses with low and elevated radon levels on each of granite and limestone bedrock. The objective of the soil measurements was to investigate the concentrations of $^{226}Ra$ (the precursor of $^{222}Rn$) in the soil surrounding these selected houses. At the location of each house, a soil sample was collected from a depth of 30-40cm. Care was taken to ensure that the collected sample was of natural soil, and not imported topsoil. When samples were returned to the laboratory they were dried and powdered to be suitable for gamma activity measurement. This powder was then placed in standard Marinelli beakers which have a sample volume of 450ml. Typical sample masses were in the range 300-600 grams. Samples were measured for gamma activity using a high resolution HpGe solid state detector. The naturally occurring radionuclides of interest are $^{234}Th$ (93 KeV) and $^{226}Ra$ (186 KeV) from the uranium-238 series, $^{228}Ac$ (911 KeV) from the thorium-232 series and $^{40}K$ (1461 KeV). The figures in parathesis indicate the energies in the spectrum at which the nuclide activity is measured. Sample measurement time varied but most were counted for approximately 24 hours which yields a lower detection limit of about 11 Bq $kg^{-1}$ for $^{226}Ra$.

No significant degree of correlation was found for indoor radon levels when tested against any of the other quantities measured for soils. However, the $^{226}Ra$ values found in the Moycullen soils were considerably less than those found in other parts of Ireland. Values up to 430 Bq $kg^{-1}$ had previously been found within 60km of Moycullen and over 500 Bq $kg^{-1}$ in the Kerry area further to the south. The highest values for $^{234}Th$ in this survey were 149 Bq $kg^{-1}$ as compared with a maximum value of 543 Bq $kg^{-1}$ found in an earlier national survey consisting of 651 samples taken on the basis of the 10 km grid. The disequilibrium found in the Moycullen soils was also much lower than found elsewhere in the country with the highest measured value for the $^{226}Ra/^{234}Th$ ratio in this series of measurements being 1.91 compared with values up to 10 in some samples from Co. Clare. The average values of radium in soil found in the national survey was 46 Bq $kg^{-1}$ which compares with the Moycullen soils mean of 48 Bq $kg^{-1}$; the corresponding values for $^{234}Th$ were 39 Bq $kg^{-1}$ nationally and 49 Bq $kg^{-1}$ in the Moycullen samples.

## 5.2 Rock $^{226}Ra$ and $^{234}Th$ Results

No significant correlations were found for relationships between the different activity concentrations as measured in rock outcrop and drillcore samples supplied by GSI. The radium concentrations appear in general to be rather lower in the core samples than in the

soils and there is even less evidence for disequilibrium in the $^{226}Ra/^{234}Th$ ratio.

A series of surface or near-surface rock samples had also been referred for analysis by GSI for Galway granites in general and for specific rock types in the Moycullen area investigated in this project. In the case of the Galway granites, some degree of correlation was found (R2=0.615) between $^{234}Th$ and $^{226}Ra$ values and also between $^{226}Ra/^{234}Th$ ratio and $^{226}Ra$ values (R2=0.798). This indicates a slight increase in degree of disequilibrium with increasing activity concentrations of $^{226}Ra$, though it must be stressed that the degree of disequilibrium was never large and in most cases was not detectably different to unity.

In the case of the Moycullen rock samples, the radium values were lower than for the granites, but a reasonable degree of correlation (R2=0.759) was found between $^{226}Ra$ and $^{234}Th$ activity concentrations. For most of these samples the degree of disequilibrium appeared to be less than one, but it should again be noted that for individual samples it would be difficult to interpret this as having any relevance to the geological factors influencing the nature of the rocks. The geological significance of $^{226}Ra$ activities measured on rock samples are further discussed in the report of GSI.

## 5.3 Terrestrial Gamma Measurements

A number of measurements were made of gamma radiation dose rates above the ground in the Moycullen area. The dose rate obtained over exposed limestone slabs was 13 nGy $h^{-1}$, which is extremely low but consistent with values measured elsewhere in the country over similar limestone terrain. Dose rates measured over soil in and around Moycullen and over granitic terrain averaged 70 nGy $h^{-1}$, which is in the range recognised as the highest found in a series of measurements made over the whole country.

## 5.4 $^{40}K$ Results

Potassium-40 was measured in all samples and the activity concentrations were high for all rock samples whether core or surface, with similar values being obtained for the means within each classification. In the case of the soil samples, generally lower values of $^{40}K$ were found, with the mean for this grouping being about 2/3 that of the means for the rock samples.

## 5.5 Conclusions

It may therefore be concluded that the $^{226}Ra$ activities present in the soils do not in this survey provide a reliable indicator to the radon levels found in houses built on such soils. The degree of disequilibrium between $^{226}Ra$ and $^{234}Th$ found in the measurements was not large and it would therefore not be justified to draw any general conclusions between this ratio and the potential for high radon levels in houses. The mean values for $^{226}Ra$ in the soil and in the rock core measurements were close to and below the national average respectively, which again does not provide any justification for drawing general conclusions.

# 6 OBJECTIVES AND RESULTS OF UCG STUDY

(i) To assess and report on the available regional gravity data in the Moycullen area in order to identify any structural geological trends which may influence radon migration.

(ii) To carry out and report on detailed geophysical surveys to aid the geological appraisal of three follow-up locations in the Moycullen area as specified by a sub-contract with the Geological Survey of Ireland. These locations are designated: (a) Ballydotia; (b) Moycullen Village and (c) Uggool.

## 6.1 Appraisal of Regional Gravity Data

Gravity data were gridded and contoured to produce a regional map for the Moycullen area. The available data were of limited geographical extent and the station density was poor in the follow-up locations. The data provided no evidence of hidden, major deep geological structures but confirmed the gentle NE dip of the granite/limestone contact in the Moycullen region.

## 6.2 Results of Field Geophysical Surveys

A detailed ElectroMagnetic-Very Low Frequency-Resistivity (EM-VLF-R) survey was carried out in the Ballydotia area which lies on limestone bedrock. An apparent resistivity high, abutted by a low, was found to coincide with a house having high indoor-radon values. A second house which had high, but variable, indoor-radon values was found to lie close to an apparent resistivity gradient. In the first case, the anomalous apparent resistivity values encountered are thought to be caused by current channeling associated with a zone, or zones, of cavities in the limestone bedrock. In the second case, the resistivity gradient is thought to represent a jointing pattern in otherwise massive limestone.

A colinear, dipole-dipole array resistivity survey was carried out in the vicinity of each house in order to further define features found from the EM-VLF-R survey. The results, plotted on resistivity pseudosections, are interpreted as indicating a zone of low resistivity, weathered limestone, with possible cavities, to the north of the first house and probably a joint in limestone lying to the west of the second house. The resistivity data indicate the zone of weathering to be approximately 25m deep to the north of the first house and the limestone in the area of survey near the second house to be largely unweathered.

Two resistivity, Vertical Electrical Soundings (VES) were carried out in the vicinity of the first house in order to quantify the extent, depth and nature of the overburden and limestone strata to the north and south of the weathered zone. The first sounding, to the north, showed overburden to be less than 2 metres thick and underlain in turn by a 5.5m thick layer of weathered limestone and then competent limestone. The second sounding, in the south, showed a thin overburden of 0.6m lying on competent limestone.

Subsequent drilling by the Geological Survey of Ireland in the vicinity of, and under, the first house found a number of small cavities associated with the weathered zone. Competent limestone was encountered to the south of the house and the weathered zone. Drillholes near the second house proved massive limestone with a very small cavity at depth to the west of the house. This cavity was not imaged by the geophysical surveys.

The EM-VLF-R survey carried out over limestone bedrock near Moycullen Village,

was limited in its extent by powerlines and access difficulties due to the high density of housing in the area. The result showed a simple apparent resistivity gradient increasing in a NE direction. This pattern may be related to either a thinning overburden or more massive limestone occuring in a NE direction. No further geophysical surveys were carried out in this area.

In the Uggool area, the EM-VLF-R survey was carried out over granite bedrock. The survey, around a high indoor-radon house, was hindered by powerlines, roads and steep topography. As a consequence, the results could not easily be interepreted, but lower apparent resistivities are thought to be influenced by the more clayey nature of the overburden. No distinct pattern, which might relate to geological structure, could easily be discerned from the limited data collected. No further geophysical surveys were carried out in this area.

## 6.3 Conclusions

Geophysical surveys proved the most successful in the Ballydotia area where a zone of weathered limestone containing cavities was identified in the vicinity of a house having high indoor-radon. Geophysical surveys in the vicinity of high density housing were hampered by cultural noise. Further work is necessary to investigate the possible radon migration pathways from cavities in the limestone bedrock, through the foundations, and into selected high indoor-radon houses in the Ballydotia area. The foundations of these houses should be assessed using ground probing radar and active indoor-radon measurements to map possible migration pathways.

# 7 OBJECTIVES AND RESULTS OF BGR STUDY

The objectives of the research project carried out in 1991/92 by the BGR in the Galway area (Western Ireland) were:

(i) Tests and applications of new methodologies in defining potential areas with high radon concentrations and migration paths for mobile terrestrial gases (helium and radon).

(ii) Correlation of outdoor radon anomalies with radon-polluted buildings and attempt to predict radon contamination of populated areas based on a combined helium-radon mapping method.

## 7.1 Results of combined Rn-He Soil Gas Surveys

In summer 1991 soil gas investigations were carried out in the study area near Galway (Western Ireland). A newly developed methodology using a combination of the noble gases radon and helium was applied in the field to allow the detection and identification of gas migration paths and the documentation of accompanying radon anomalies especially in populated areas. This new methodology has opened up new possibilities to delimit the boundaries of radon contaminated regions. The co-operation with the Irish group of physicists that carried out indoor measurements was very productive and successful.

The investigation included outdoor measurements of radon concentration in soil air in populated areas and detailed sampling around individual houses. The number of radon samples collected was 367. For determination of migration paths for radon a total of 447 soil air samples were collected from 90cm depth and analysed for their helium concentration. It was assumed that helium as a very mobile and inert noble gas would prove advantageous in detecting migration channels used by other terrestrial gases (in this case radon) and their dispersion pattern in the overlying soil cover. Specially designed stainless steel gas probes were used for sampling both radon and helium. The sampling procedure guarantees that no ambient air contaminates the soil gas sample. A detailed description of the sampling method is given in the technical annex to this report.

The results of the statistical data evaluation in brief are the following:

Radon soil gas values measured show a wide range between 400 and 186000 Bq $m^{-3}$. The ranges measured for both limestone and granite sample groups are similar. The distribution histogram of all collected radon samples shows two clearly separated populations. The lower one includes radon concentration values <50000 Bq $m^{-3}$. The upper population covers samples with values >50000 Bq $m^{-3}$. If one considers the two lithologies separately, it is obvious that the granite population is skewed towards higher radon values as expected, but has no major influence on the distribution shape in the histogram of all collected samples. The very distinct division of the limestone-radon population is approximately the same as the total population. This means that the majority of the granite values are gathered in the upper population. The statistical parameteres of the measured radon values in soil air above both lithological units are as follows:

Granite Area

N total: 110 samples; Minimum value: 2600 Bq $m^{-3}$;
Maximum value: 186300 Bq $m^{-3}$;
Median: 65650 Bq $m^{-3}$;

Limestone Area

N total: 256 samples; Minimum value: 400 Bq $m^{-3}$;
Maximum value: 184000 Bq $m^{-3}$;
Median: 37300 Bq $m^{-3}$;

Surprisingly, the maximum values of the granite and limestone soil gas radon populations are approximately the same, but the median values of the granite population are nearly double that recorded for the limestone population.

However the radon hazard has almost the same impact on the populated areas in the limestone region as in the granite region (as is evident from the results obtained from the indoor radon surveys in houses carried out by RPII).

The statistical parameters of the helium distribution for the two areas of different lithology are:

Granite Area

N total: 151 samples; Minimum value: 5013 ppb(v);
Maximum value: 5685 ppb(v);
Median: 5283 ppb(v);

Limestone Area

N total: 295 samples; Minimum value: 5092 ppb(v);
Maximum value: 5759 ppb(v);
Median: 5267 ppb(v);

Taking into account that the worldwide helium concentration in atmospheric air is 5240 ppb(v), the median of the limestone area is in accordance with the theoretical value. As expected, the corresponding granite value is slightly higher.

### 7.2 Regional Helium-Radon Distribution

Three separate sub-areas were surveyed to determine the spatial distribution of soil gas radon and helium. Two of the sub-areas are situated in the limestone region: Ballydotia and Moycullen. In the granite region, the sub-area of Uggool was studied.

The Ballydotia and Moycullen sub-areas are contiguous and are situated east of the Galway-Oughterard highway. The geological contact between the granite and the limestone has been mapped by the GSI and runs parallel to this road. It is inferred from borehole investigations that this contact is marked by a NW-SE striking major fault or shear zone. Samples were collected exclusively in the limestone area where radon contaminated houses were known to occur. The application of the combined helium-radon mapping method necessitated sampling traverses close to the populated areas. The distribution patterns of both noble gases indicate the location and direction of migration paths with high radon haloes in their vicinity. Houses which have high indoor radon levels are very often located in a zone of high permeability, most probably a fracture zone, which coincides with both high helium

and/or radon concentrations in soil air, whereas an adjacent house less than 50m distant, with low indoor radon levels may not be influenced by the radon emanation from the migration channel. This suggests that houses located a short distance away from the fracture zone may not develop an indoor radon problem. The migration paths deduced from the helium-radon data correlate spatially with different fracture systems e.g. N-S, the main joint direction in the limestone and NW-SE, the direction of major faulting (for example the granite/limestone contact). The highest soil gas radon values were observed near the intersections of the two systems.

The sub-area of Uggool is situated within the granite terrain. Here, also, the helium-radon soil gas data suggest the same similar directions of migration channels. The spatial correlation between radon concentrations in soil gas and indoor radon data is also evident in this sub-area but not to the extent observed in the limestone area.

## 7.3 Conclusions

The radon contamination of buildings and dwellings is often, especially in areas overlain by sedimentary rocks, not controlled by the lithology or pedology but mainly by highly permeable fracture zones which serve as migration paths for the terrestrial radon gas.

The combined helium-radon mapping method applied in the present study has been successful in the detection of such permeable migration zones.

# ANNEX 1

**Contribution of the Geological Survey of Ireland**

**V. Gallagher and P.J. O'Connor**

# Contents

## 1.1 Introduction

Carbonate rocks such as limestone contain very low concentrations of U and Ra and dwellings built on carbonate bedrock might be expected to have low indoor $^{222}Rn$ concentrations. However, such rocks are also highly prone to dissolution (karstification) by circulating groundwater which thereby greatly enhances their permeability. They can act as very efficient radon conduits where karstification is well advanced or complete and where U or Ra are mobile. Recent studies in Denmark (Damkjaer and Korsbech 1988) and the USA (Hand and Banikowski 1988) have reported enhanced $^{222}Rn$ levels in dwellings built on limestone sequences and support the view that rock permeability strongly influences $^{222}Rn$ availability even in otherwise poorly uraniferous lithologies.

In a regional survey carried out in 1989 by workers at University College, Dublin (UCD) and the Radiological Protection Institute of Ireland (RPII) in counties Galway and Mayo in western Ireland in areas largely underlain by Carboniferous limestone, approximately 10% of dwellings had indoor $^{222}Rn$ levels in excess of the 200 $Bq/m^3$ national reference level (McLaughlin 1990). The present study was aimed at assessing the geological factors responsible for the occurrence of such radon hazard areas overlying karstic limestone terrain.

A study area was selected, centred on the village of Moycullen, Co. Galway, 10 km northwest of Galway City. Elevated levels of indoor $^{222}Rn$ were discovered by UCD in this area in 1987. The area lies on the boundary between the uraniferous late Caledonian Galway Granite batholith and its cover of younger Carboniferous karstic limestones. Most of the area is, in turn, overlain by a variety of ice-contact deposits, including fluviatile sands and gravels.

The results of geological and geochemical investigations carried out by the Geological Survey of Ireland during the course of the project are described below together with a summary of the regional geology.

## 1.2 Regional geology

### 1.2.1 Connemara Dalradian: Metagabbro and Gneiss Complex

The Moycullen areas lies at the eastern extremity of Connemara (Fig. 1). The geology of Connemara has been extensively studied since the first maps were produced by the Geological Survey of Ireland in the last century (Wager 1932; Burke 1957; Leake and Leggo 1963; Wright 1964; Bradshaw et al. 1969; Evans and Leake 1970; Coats and Wilson 1971; Leake 1974; Tanner and Shackleton 1979; Leake 1986; Leake 1989; Tanner 1990). The oldest rocks in the region are the metapelites, quartzites, marbles and metavolcanics of the Dalradian Supergroup (Harris and Pitcher 1975; Harris et al. 1978). These were previously considered to be late Precambrian to Ordovician in age but recent U-Pb dating has suggested the correlative Dalradian of Scotland to be entirely pre-590 Ma in age, i.e. Precambrian (Rogers et al. 1989)

Deposition of the Dalradian metasediments and Metavolcanics was followed by high grade regional metamorphism and folding (M1, D1 - Grampian Orogeny) (Leake and Leggo 1963) and by a second, amphibolite facies metamorphism and associated deformation (M2, D2) prior to 590 Ma (Tanner 1990). As the rocks were cooling from the D2 event they were intruded by a belt of mafic-acid igneous rocks (Leake 1989), now preserved as the metagabbros, orthogneisses and migmatites of the Metagabbro and Gneiss Complex (MGC). These were emplaced along a magmatic arc of early Ordovician age which was established

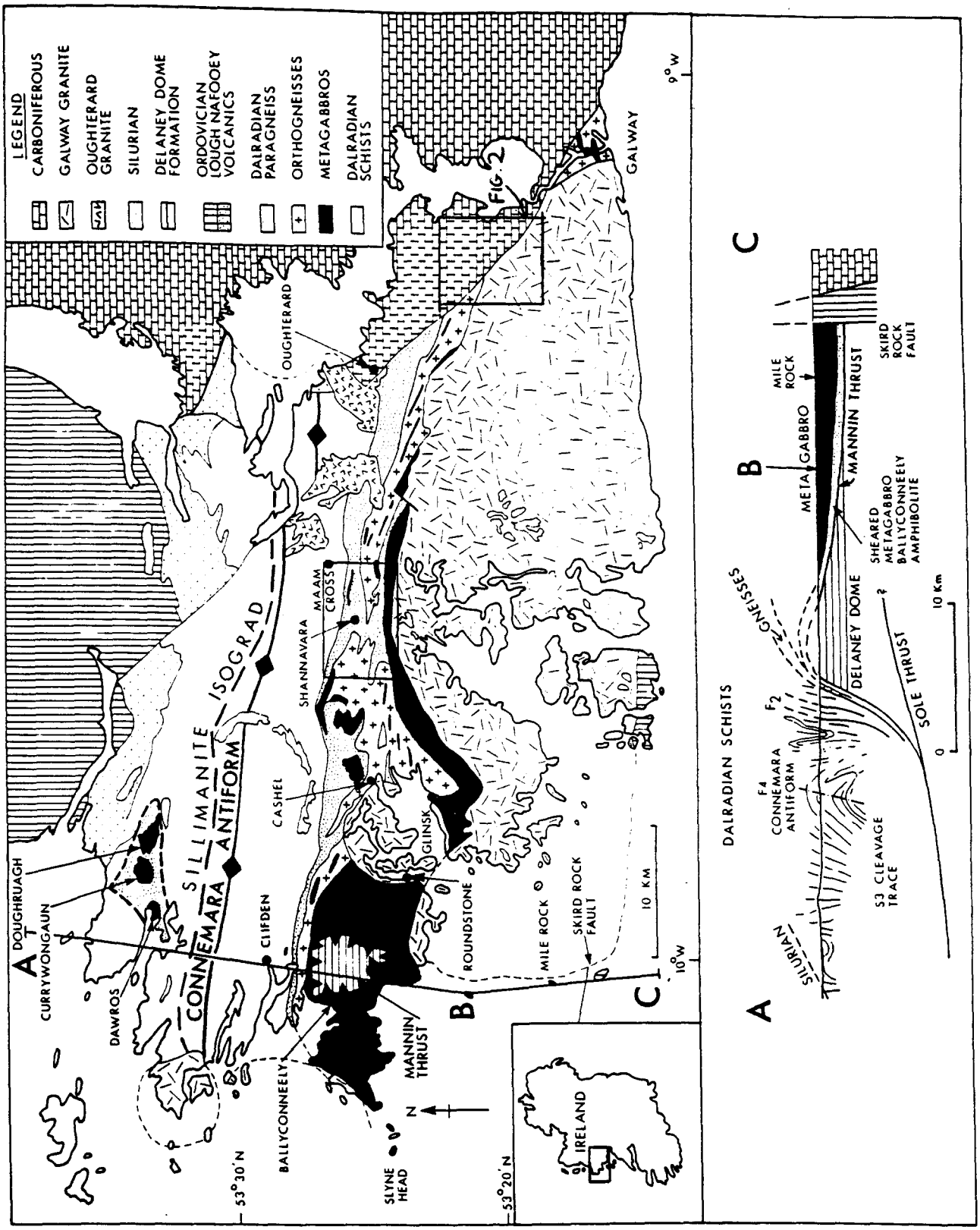


**Figure 1. Regional geology (from Leake 1989). Area of Figure 2 shown.**

along a northwards-dipping subduction zone on the southeastern edge of the Appalachian-Caledonian fold belt (Tanner 1990). The intrusive rocks included gabbros, quartz diorites, tonalities, granodiorites and granites (Leake 1989). The gabbros were intruded at 490 Ma (Jagger et al. 1988.) shortly before the onset of D3 deformation during which they were folded and deformed. Syn-tectonic acid intrusions followed and the latest of these, K-feldspar orthogneisses, were emplaced at the waning stages of D3 (Leake 1989). The MGC provided heat for hornfelsing (M3) of the Dalradian succession to sillimanite grade. Major uplift and retrogressive metamorphism (D4, M4) between c. 460 and 440 Ma followed (Tanner 1990). Much of the MGC was consumed during passive intrusion of the Galway Granite batholith at c. 400 Ma.

### 1.2.2 The Galway Granite

The Galway Granite is an east-west elongated composite post-kinematic batholith (Max et al. 1978). It was intruded passively but is weakly foliated throughout. The batholith comprises two main intrusion centres, the Carna and Galway-Kilkieran Domes, underlying an area c. 60 x 25 km in extent (Max et al. 1978; Leake 1978) (Fig. 1). The satellite Roundstone Dome occurs immediately north of the main Galway Granite exposure. The Oughterard Granite, just west of Oughterard village, 15km northwest of Moycullen, is of uncertain age: Kennan et al. (1987) recently suggested that Rb-Sr isotope data indicated an age of 407± 23 Ma, essentially coeval with the Galway Granite, whereas its age has previously been regarded as Mid Ordovician (Leggo et al. 1966; Leake 1988).

The lithologies of the Galway Granite range from granodiorite to alkali leucogranite. They have been categorized by Max et al. (1978):

(a) The **Carna Granite** is a granodiorite; both K-feldspar-poor and K-feldspar-rich varieties occur. The K-feldspar-poor variety is a medium-grained grey biotite granodiorite with occasional plagioclase megacrysts and rare K-feldspar megacrysts. The K-feldspar-rich variety contains K-feldspar megacrysts (up to 20mm in size) in a pink groundmass of quartz and feldspar with biotite and hornblende. This is locally granite. Average modal composition of the Carna Granite (K-feldspar-poor type) is 24% quartz, 24% K-feldspar, 42% plagioclase, 4% biotite, 3% chlorite, 2% hornblende, with accessory sphene, epidote, magnetite and apatite (Wright 1964).

(b) The **Errisbeg Townland Granite** occurs in the centre and east of the batholith and as a rim to Carna Granite. It is a biotite-hornblende granite with pink-grey megacrysts (20-50mm) of K-feldspar and plagioclase in a medium grained groundmass. Variations in the content of mafics occur, particularly at the eastern end of the batholith (Coats and Wilson 1971) where there is a rise in mafic content inwards from the margin. The **Callowfinish Granite** is an equigranular variant of Errisbeg Townland Granite and has a medium- to coarse-grained anhedral groundmass with fewer megacrysts and more biotite. It is chemically similar to the more mafic Errisbeg Townland Granite. Mean modal composition of the Errisbeg Townland Granite (Wright 1964) is 29% quartz, 31% K-feldspar, 34% plagioclase, 4% biotite, 2% chlorite, $<1$% hornblende with accessory sphene, epidote, magnetite and apatite. The Callowfinish Granite has a mean composition (Wright 1964) of 27% quartz, 31% k-feldspar, 32% plagioclase, 6% biotite, 2% chlorite with accessory hornblende, sphene, epidote, magnetite and apatite.

(c) The **Spiddal Granite**, a granodiorite, is similar to the Carna Granite and also contains both K-feldspar-rich and K-feldspar-poor varieties (Max et al. 1978).

(d) **Murvey Granite** is the youngest granite and occurs in isolated patches around the margins of the batholith and in a large outcrop at Costelloe where it is believed to form a roof zone. It is a fine-grained leucogranite (2-5mm), in places aplitic in character. Wright (1964) gives a mean modal composition of 34% quartz, 34% K-feldspar, 30% plagioclase, <2% biolite and chlorite, and trace amounts of sphene, epidote, magnetite, apatite and garnet.

(e) The **Roundstone Granite** is similar to but coarser grained than the Errisbeg Townland Granite. It is structurally distinct from the latter, however (Max et al. 1978), and is generally not treated as part of the Galway Granite.

The Carna Dome at the western end of the batholith comprises a central granodiorite (Carna Granite) surrounded by a rim of granite (Errisbeg Townland Granite) which passes outward to marginal alkaline leucogranite (Murvey Granite). According to Leake (1974), the Carna Granite crystallized from its margins inwards and marginal Murvey Granite formed from an interstitial melt pressed out of unconsolidated Errisbeg Townland Granite magma by foundering of unconsolidated block of country rock. Within the Galway-Kilkieran Dome, the Spiddal Granite may represent a separate magma (Max et al. 1978) which intruded Errisbeg Townland Granite. Late aplite, pegmatite, felsite and porphyry dykes are abundant within the batholith and typically trend north-south, following the major fracture direction (c.f. Coats and Wilson 1971).

The Galway Granite lithologies have invariably undergone retrogressive alteration. Plagioclase, especially in its cores, and, to a lesser extent, K-feldspar have generally been altered to kaolin, sericite ± calcite, ± epidote ± pyrite ± Fe-oxide. Biotite is generally altered in part or whole to chlorite ± Fe-oxide ± pyrite. In many samples, quartz and feldspar are extremely turbid due to an abundance of contained secondary fluid inclusions on cross-cutting, annealed fractures (Jenkin et al. 1992).

Chemical variations within the Galway Granite (Coats and Wilson 1971; Wright 1964; Leake 1974; Lawrence 1975; Feely and Madden 1988) are typical of calc-alkaline evolutionary trends: progressive increases in Si and alkalies are matched by corresponding decreases in Fe, Mg, Ti, Ca, Al, Mn and P, Sr and Zr decrease and Rb increases with increasing Si content.

Radioelement concentrations in the Galway Granite are notably high in comparison with other late Caledonian granites in Ireland: mean contents of 10 and 12 ppm U and 46 and 56 ppm Th for the Errisbeg Townland Granite and Murvey Granite, respectively, compare with values for U and Th in other Irish granites which are generally less than 6 and 15 ppm, respectively (O'Connor 1986). The Murvey Granite, especially, is radioelement-rich (Feely and Madden 1986), particularly at Costelloe (O'Connor 1981) where accessory uraninite and U-bearing thorite, monazite and zircon have been recognized (Feely et al. 1989). U was also remobilized along late fractures and grain boundaries (Feely 1982). U and Th abundances within the Galway Granite increase with increasing acidity among granite types, from granodiorite to leucogranite (Feely and Madden 1988). U and Th levels within the batholith are comparable to those of the Hercynian granites of southwest England and to those of Irish Tertiary granites (O'Connor et al. 1983). Moreover, as with the high-heat-producing southwest England granites, there is evidence for long-lived post-crystallization circulation of water in and around the Galway batholith, both in the intensity and pervasiveness of retrogressive alteration of the granites and in recent fluid inclusion and isotopic studies (Feely and Hogelsberger 1991; Jenkin et al. 1992; Gallagher et al. in press).

### 1.2.3 The Carboniferous succession

The Galway Granite, the Connemara Dalradian and the MGC are overlain uncomformably by a Carboniferous limestone and basal clastic succession around and east of Oughterard (Kinahan 1869; Kinahan and Nolan 1870; Coats and Wilson 1971) (Fig. 1). At Oughterard, beds of conglomeritic limestone with clasts of quartz become more abundant and thicker close to the contact of the Carboniferous with the Galway Granite and MGC (Kinahan and Nolan 1870). Shale and yellow and red sandstones occur at the boundary. The junction of limestone and sandstones is marked by dolomite. East of Oughterard, conglomerates are found along the contact zone between granite or MGC and limestone; occasionally, sandstones occur (Kinahan 1869). The limestone beds lie almost horizontally or dip slighty to northeast or east, with the highest dips occuring closest to the granite contact.

The limestone is extensively karstified. Dissolution channels and caves formed predominantly along the main joint direction which runs north-south (Kinahan and Nolan 1970). A second joint set runs E-W. The karstification appears to extend over the whole of the area underlain by limestone. Caves and channels are conduits for groundwater flow. The two major lakes in the region, Lough Corrib and Lough Moy, are linked in this way (Kinahan and Nolan 1870).

## 1.3 Local geology

### 1.3.1 Introduction

The project area covers approximately 70km$^2$ centred on the village of Moycullen, 10km northwest of Galway City on the main Galway-Oughterard road (Map 1). Southwest of the road are uplands underlain by the Galway Granite; to the northeast, the low-lying, relatively flat land is underlain by Lower Carboniferous sediments, predominantly limestone which has undergone karstification; to the west, the eastern extremity of the Connemara MGC crops out.

The granite uplands in the south and southwest of the area reach maximum heights of c. 200m and in places slope steeply to the road which runs along or close to the slope break which marks the contact of limestone and granite. The granite is covered by extensive deposits of bog and rocky drift. The thickness of overburden varies from a few centimetres to several metres. Exposure is good in patches, especially above 100m. The granite uplands are drained by numerous streams which run generally northwards (Map 1); these rarely reach more than 3m in width and are commonly less than 1m wide over much of their length. The granite is extensively fractured and is an aquifer: springs are common on the hills and near the contact with the limestone.

In contrast, the ground north of the main road is generally flat; what topographic variation does occur is generally due to the presence of thick glacial deposits, notably fluviatile sands and gravels, rather than to variations in bedrock elevation. Overburden in areas without sand and gravel cover is typically a thin layer of limestone drift; some large areas of bare limestone pavement occur but exposure is otherwise generally poor. The granite-limestone contact is marked by a slope break but is nowhere exposed. Streams which cross the granite-limestone boundary either terminate in lakes or enter swallow holes and continue underground through the extensively karstified limestone (Map 1).

The Moycullen area has received relatively little attention since it was surveyed by the Geological Survey in the 19th Century (Kinahan 1869). Coats and Wilson (1971) mapped

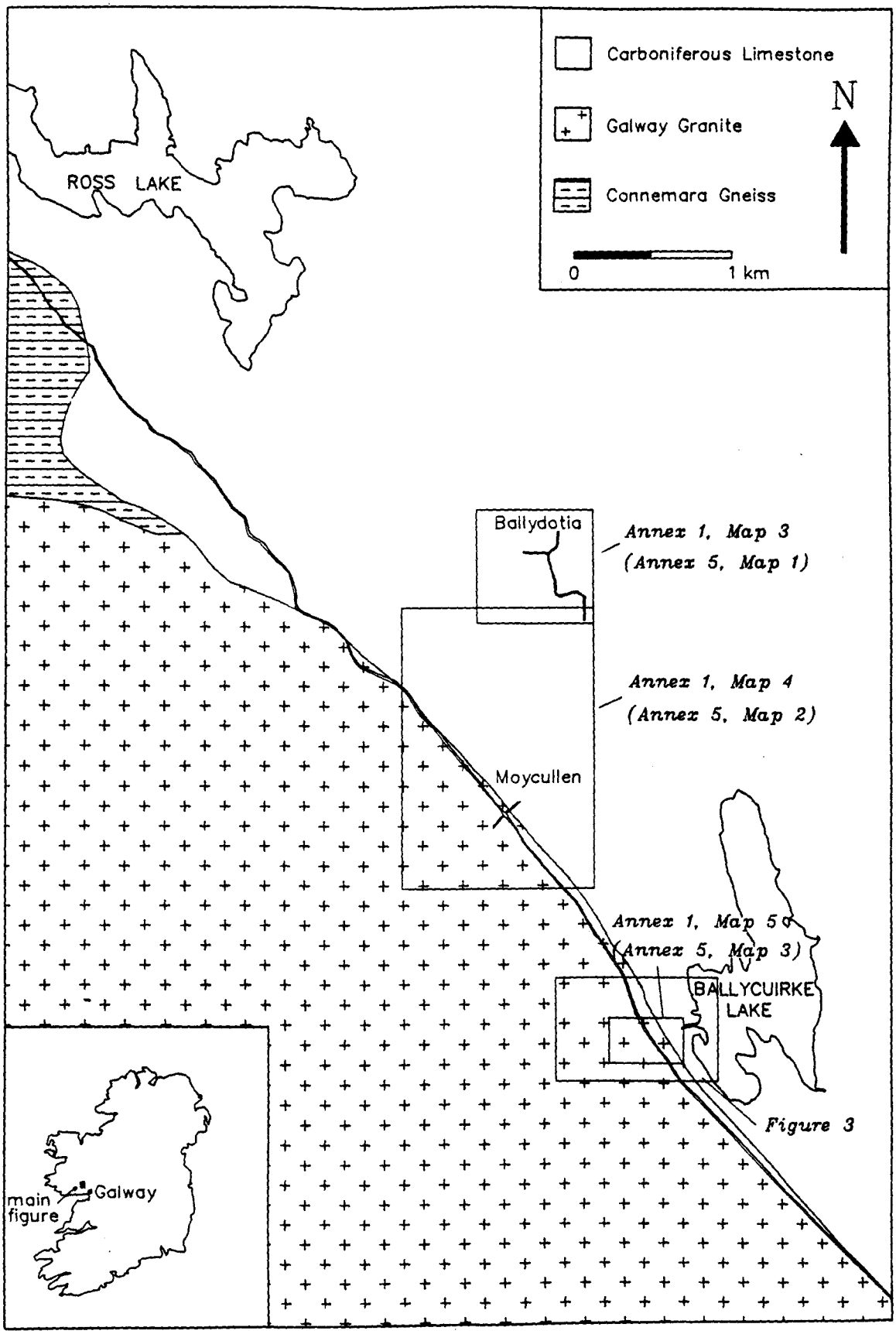


**Figure 2. Moycullen area: general geology; area covered by maps also shown.**

the eastern end of the Galway batholith, including the southeastern part of the project area and the reconnaissance map of Max et al. (1978) includes the areas of the granite-limestone contact. The most recent map was produced by Carey (1990) who mapped the area immediately north of Moycullen which is covered by 1:10560 sheet 68.

Field mapping (1:10560 scale) undertaken by the Geological Survey of Ireland during this project was aimed at providing more information about: 1) the granite-limestone contact, 2) the extent and nature of the marginal granite facies and 3) the possible existence of U-enriched lithologies in the granite or Carboniferous succession. The granite-limestone contact was drilled at Ballycuirke townland (Map 1) where mapping had defined the contact to within 30m. Further short boreholes were drilled in the limestone in Ballydotia (Map 1) to assess the nature and extent of karst formations around houses with high indoor Rn activity. Petrographic analyses were carried out on 42 samples from along the granite margin (Appendix 1). In addition, a 1:25000 scale map of Quaternary deposits in the area was compiled by C. Delaney from field observations, old Geological Survey maps and aerial photographs.

### 1.3.2 Metagabbro and Gneiss Complex

The Connemara Metagabbro and Gneiss Complex extends eastwards into the project area near Newtown (Map 1). According to the map of Max et al. (1978), the complex terminates against a north-south trending fault traversing the granite-limestone contact at Drimcong Bridge. Carey (1990) mapped gneiss at Drimcong Bridge also but recorded this as the first of two gneiss enclaves which occur along the granite margin southeast of the main body of gneiss which he mapped as terminating at Newtown. Mapping during this project has failed to find evidence for a continuous belt of gneiss southeast of Newtown - between the enclaves mapped by Carey (1990) there is no outcrop but the float is entirely granitic. Detailed mapping along the stream south of Drimcong Bridge has revealed that the area underlain by gneiss is considerably wider here than previously suggested (Map 1).

Petrographic descriptions of samples from and around the MGC enclave are given in Appendix 1 (Samples 91.1019-21, 91.1023-24, 91.1042). Lithologies present include grey **quartz-plagioclase-biotiteparagneiss, quartz-plagioclase-biotite-(K-feldspar)orthogneiss,** which resembles, in hand specimen, the marginal granite of the area, and **psammite.** The gneiss is heavily fractured and even brecciated in places. The final outcrop in the stream before the marginal granite is a strongly altered, severly crushed quartz-K-feldspar-plagioclase-biotite rock, resembling mylonitized granite or orthogneiss. It contains 30% quartz which suggests it is granite since orthogneiss at this locality has been found to have 50-60% quartz. Although the contact between the MGC and Galway Granite is typically transgressive (Leake and Leggo 1963), it may be faulted here.

### 1.3.3 The Galway Granite

Two varieties of Galway Granite occur in the area as well as numerous felsite, aplite, porphyry and pegmatite dykes. The Errisbeg Townland Granite occupies all but the margins of the batholith. It is typically a biotite-hornblende granite containing distinctive megacrysts (10-80mm) of pink or cream K-feldspar. Within 100-500m of the limestone contact, the ground is underlain by equigranular biotite-poor, sometimes leucocratic granite. Max et al. (1978) first identified this granite and classified it as Callowfinish Granite (Wright 1964), a finer grained, equigranular variety of Errisbeg Townland Granite.

Errisbeg Townland Granite shows considerable variation in modal composition, especially in the femic minerals, but average modal composition for the eastern end of the

batholith (Coats and Wilson 1971) is 29% quartz, 30% K feldspar, 34% plagioclase and less than 6% biotite and chlorite. This conforms to the mean modal composition in the type area at the western end of the batholith and to the mean modal composition of Callowfinish Granite (Wright 1964). The marginal granite at Moycullen shows considerable variation in modal composition (Appendix 1) but chemical analyses (below, section 1.6) appear to confirm that it can be classified as Callowfinish Granite and that it is quite distinct from the radioelement-rich Murvey variety which has not been encountered in outcrop or in drillcore in the project area.

The typical marginal granite at Moycullen (e.g. samples 91.1002, 91.1005, 91.1092) has 20-30% quartz, 20-30% K feldspar, 30-40% plagioclase and less than 3% biotite. Quartz comprises over 50% of some samples, however, and the ratio of K-feldspar to plagioclase varies from 1:6 to 2:1. The rock is generally equigranular with grain size of 2-5mm: rare megacrysts, particularly of K-feldspar, reach 10mm in size. Virtually all samples examined have suffered deformation ranging from pervasive fracturing to intense cataclasis of grains. Quartz has generally been recrystallized into mosaics of smaller grains with sutured contacts. Plagoclase is granulated along grain boundaries and may also have recrystallized to smaller, intergrown plagioclase grains. Alteration ranges from the retrogressive alteration typical of the Galway Granite (Wright 1964; Coats and Wilson 1971) (plagioclase replaced by sericite and kaolin, especially in centre of grains; biotite partially supplanted by chlorite and/or Fe-oxide) to an extremely intensive alteration near the limestone contact which has rendered the granite soft and friable. This latter alteration, observed in core, is notable for the abundance of carbonate as a replacement of feldspar and the high density of fluid inclusions in quartz. It can be seen in core that alteration and deformation of the granite increase in intensity as the contact with the Carboniferous succession is approached. The contact rock is an extremely friable granite with a bimodal grain size (1-1.5mm and 0.3-0.6mm) and its reduced size and crushed texture suggest it is a mylonite. The contact is interpreted as a thrust fault at Ballycuirke (see below, section 1.5).

Field mapping suggests that the contact between the Errisbeg Townland Granite and the Callowfinish Granite is gradational; indeed, it is not always clear whether the rock is Callowfinish Granite or simply a less megacrystic Errisbeg Townland Granite. Whereas the Callowfinish Grainte is whitish or grey near the contact with limestone, it is in many places pinkish further from the contact. A pink variety was found at the end of one borehole at Ballycuirke (DH1) (section 1.5).

Minor intrusions in the granite along the margin of the Galway batholith include felsite, porphyry and aplite. Pegmatites tend to occur further from the contact. The felsites are flow banded, very fine grained brownish rocks with a matrix ($<0.1$mm grain size) of recrystallized quartz, feldspar and white mica. Quartz and feldspar also occur as phenocrysts (0.2-0.5mm), in some cases in a chain-linked texture. A spherulitic texture in which spherules have a dark brown colour is common. The reason for this colour is not clear; it does not appear to be limonite. Small porphyry dykes were mapped in only a few localities but they account for a very significant portion of the core drilled through the contact at Ballycuirke (DH1-3) (section 1.5). These grey green rocks have a matrix of fine quartz and feldspar ($\ll 0.1$mm) and phenocrysts of euhedral feldspar (0.5-4.0mm) and near-euhedral quartz (0.25-0.5mm). Minor chlorite, apparently primary, accounts for their colour. Feldspar comprises approximately 60% of the rock; the remainder is mainly quartz with 2-3% minor material, including chlorite. The porphyries are altered in much the same way as granite at the contact: feldspar is replaced by calcite and sericite, pyrite is also replacive

and fills fractures. However, these compact rocks have resisted deformation much better than granite and largely retain their original texture.

### 1.3.4 Lower Carboniferous succession

Prior to this work the only Carboniferous lithologies recognized in the Moycullen area were Carboniferous Limestone and limestone conglomerate. Kinahan (1869) reported the latter as occurring "all along the boundary" with the granite and noted an *in situ* occurrence in Newtown. Such rocks have not been noted nearer Moycullen, however. Drilling at Ballycuirke, southeast of Moycullen, has revealed that a basal black shale unit occurs between limestone and granite (Fig. 4, section 1.5). The lower part of the limestone is dolomitized. No limestone breccia was noted in core.

The shale is finely laminated. Complex, apparently syn-sedimentary faulting has disrupted the lamination and later intense brecciation further broke up the original sedimentary structures. The shale is composed of a mixture of silicate and calcareous clasts, the latter including both fossil debris and lithic fragments. Silicates include quartz and plagioclase (andesine) - the quartz, like that in the altered contact granite, is very rich in secondary fluid inclusions but the feldspar is notably less altered than its granitic counterpart. Pyrite is abundant, occurring in distinct layers or irregularly shaped replacive grains. The shale occupies a zone of intensive crushing and is severely fragmented. Immediately above the contact with the granite, it is wholly disaggregated and appears as a black mud. The thickness of the shale unit is difficult to estimate at any point because of core loss in the contact zone but overall it varies between 4 and 8m.

Shale passes upwards into dolomitic limestone through a zone of intensely fractured, shaley material in which bedding is highly disrupted. Dolomite appears as a pale grey granular rock with a matrix of ill-defined white clasts c. 1mm in size. It contains abundant calcite veins. The thickness of the dolomite varies from approximately 2 to 3.5m in core.

The limestone in core at Ballycuirke is typical of the bedrock in the area northeast of the Galway Granite. It is a grey argillaceous bioclastic limestone massive over much of its thickness. Crinoids, typically <2mm in size, are the dominant bioclast but large brachiopod fragments are scattered throughout and are also concentrated in 0.1-0.3m thick clast rich zones. Shaley laminae and partings are common and the limestone is stylolitic in most occurrences. Calcite veins are ubiquitous but are rarely thicker than 1-2mm. Brecciation is associated with thicker veins.

Carey (1990) detailed the faunal assemblage found in limestone. It includes gastropods (*Straparollus sp.*), productids (Linoproductids, *Overtonia fimbriata*, *Giganto productus varians*), terebratulids (*Dielasma sp.*), athyrids (*Actinoconchus planosulcatus*) and rugose corals (*Caninia sp.*). He concluded that it was Brigantian in age and in life position.

Karstification of the limestone is obvious in numerous areas of limestone pavement throughout the area and further surface indicators include swallow holes and turloughs which are common in areas not covered by sand and gravel, e.g. Ballydotia (Map 1, Annex 6). Drilling in the latter area revealed the presence of numerous cavities: most are small (0.1-0.2m) but some reach over a metre in size.

## 1.4 Quaternary geology

### 1.4.1 Introduction

The area was examined in two ways: information was compiled from the aerial photograph coverage of the area and from the old G.S.I. maps and selected areas were mapped in detail. A map was drafted at 1:25000 scale. For comparative purposes, this is reproduced at 1:15000 scale (Map 2).

### 1.4.2 Information from aerial photographs

A number of terrains could be recognized from the photographs (Map 2) and are described below. The term drift is used to indicate undifferentiated glacial deposits.

1. Bedrock at surface

This category is applied to limestone areas only, as areas of karst pavement can be recognized by their high reflectancy. Similar areas of exposed bedrock in granite are not easily identified, and may be confused with boulder strewn areas.

2. Mixed bedrock and bog

This category is applied to the upland areas underlain by granite; the terrain is distinguished by a highly irregular surface, the absence of any agriculture, and a variable reflectance thought to be due to the mix of bare rock and vegetation.

3. Mixed limestone pavement and drift

The terrain is characterized by a mixture of scrub and vegetated land, often associated with ridges and terraces which are in alignment with bedrock lineaments in nearby areas of karst pavement and with areas where the development field patterns indicate a reasonable soil cover. This pattern is thought to indicate a mixture of: 1) drift cover, where soil cover is thick and agriculture can take place, and 2) areas where bedrock is extremely close to the surface, and soils are probably developed from organic accumulation.

4. Drift-covered areas

These are areas where soil cover is well-developed, as indicated by the development of fields, and where no bedrock control can be observed in the alignment of ridges and hummocks. The absence of sand pits from these areas suggests that the underlying sediments are not well-sorted and are likely to be dominated by diamicts.

5. Sand and gravel dominated areas

These features are indicated by the presence of excavations. Where excavations occur and where the GSI field maps indicate that the pits are gravel pits, the entire landform is interpreted as being dominantly of well-sorted material. Two such landforms were identified in the area. The southern form was in part examined in the field and is discussed below. The northern landform is a narrow linear ridge extensively exploited for gravel; its form indicates that it is an esker.

6. Alluvium and Peat

These areas are flat, and have a higher reflectance than the surrounding terrains, due to water saturation.

### 1.4.3 Proofing the aerial photography map

Because of the short amount of time available, field-checking of the data compiled was limited. The old G.S.I. six-inch field maps were therefore used to supplement field studies. The accuracy of the map appears to vary according to the terrain type.

1. Limestone at surface: Both field mapping and examination of the G.S.I. maps indicates that this is more extensive than shown on the map; some of the area categorized as mixed pavement and drift may be largely limestone pavement covered in scrub vegetation.

2. Mixed bedrock and bog: These areas were not examined in detail in the field, other than at Area 1 (see below). However, examination of the GSI maps indicates that a large amount of these areas may in fact be covered in what is termed "rocky drift" on the old maps. The meaning of this term is unclear. It may refer to boulder trains resting on the bedrock surface, or surrounded by peat; or more likely to till with a high boulder content, which would indicate that bedrock is close to the surface. "Stony-drift" - a term though to indicate till - is also used in this area; however, it normally refers to areas which have been mapped as dominantly drift from the air photographs. This terrain is therefore though to show considerably more variation than indicated on the map.

3. Mixed limestone pavement and drift: The drift in these areas is termed stony drift or rocky drift on the old G.S.I. maps and is considered to mean glacial till. Field mapping at Areas 3 and 4 (Map 2; see below) indicates that glacial drift cover is thin and is found mostly in lows in the topography; however, till ridges were also identified in Ballynahallia and Gortachalla townlands. Exposure in the northmost ridge indicates that the ridge is underlain by a clast-rich diamiction with a sandy matrix. The material is though to be an ablation till deposited at the ice margin rather than lodgement till and the landform is interpreted as an end moraine. Because of this, the exposure cannot be considered typical of the drift underlying this terrain.

4. Drift-covered areas: Examination of the G.S.I. maps indicates that small patches of bedrock may occur in these areas; however they are not extensive. The G.S.I. maps also indicate that gravelly drift may also occur in these areas, implying that some of the material is waterlain. However, both field mapping in the area around Moycullen and the old maps indicate that the majority of the landforms are composed of diamicton rather than of well-sorted material. Where gravelly material is found, it is located along the break, of slope marking the change from upland granite to low-lying limestone and is associated with streams draining the upland areas. The material may therefore have been deposited as paraglacial fans; the sorting and therefore the permeability is dependent on whether or not the material was deposited into standing water.

Ridges in the lowland area are usually scattered with large boulders and are though to be composed of boulderly diamicton; however this may form a drape over well-sorted sediments below.

6. Alluvium and Peat: Distribution shown on the map appears to be reasonably accurate when compared to G.S.I. maps and to field mapping.

### 1.4.4 Field Mapping

Six areas (Map 2) were examined in some detail, as they are associated with particularly large soil radon anomalies.

Area 1. Uggool Townland

Exposure in this area was extremely poor, however some deductions could be made about the glacial deposits. The remains of an old sandpit near the main road in the southern part of the area indicate that some waterlain deposition has occurred; comparison with the air photographic evidence suggests that a fan of debris may have been deposited at this point. The exposure is too degraded to see the section; however sediments are in excess of 2m depth. Upvalley, bedcrock appears at the surface within 100m of the excavation; this is the point at which the anomaly is located. At Loc. 1 (Map 2), trial holes dug by the landowner show 50cm of peat overlying 1m or more of weathered granite; the rock has disintegrated into a muddy coarse sand.

To the north of the river the land rises to form a ridge; the high part of the ridge is of bedrock with a sparse covering of soil; the bedrock in places is glacially smooth and striated. The flanks of the ridge have a better soil covering; this may merely represent the movement of colluvium downslope, but is more likely to be due to a covering of glacial till. Bedrock appears to be within 1-2m of the surface everywhere except in a narrow zone parallel to the main road.

Area 2. Leagaun and Ballydotia Townlands.

This area was mapped to examine the extent and nature of the sands and gravels being exploited. A large ice-marginal kame was identified from the air photos and from field evidence. Examination of sections indicate that this is a delta, underlain by well-sorted, predominantly sand-sized sediments. The southwest-facing slope is steep and contains boulders and is interpreted as the ice-contact face; some diamict may underly this slope, but no exposure was seen. The kame appears to be composed of more than one lobe, as a number of higher, flat-topped areas could be identified within the landforms. Foreset dip directions indicate progradation was to the north and northeast.

The sediments at Loc.2 are somewhat coarser than those at Loc.3 and appear to be associated with a separate lobe, as the two areas are separated by a steep slope. Loc. 2 deposits fine northwards and eastwards. The southern sections are composed of alternating pebble and cobble gravels and coarse sands; these are overlain by medium and fine silty sands in the most easterly part of the exposure. The northern sections are composed of foresets of fine planar-or ripple-laminated sands with occasional silt drapes alternating with fine pebble gravels. Foresets prograde in an arc between 345° NW and 360° N. The steep slope northwards from the pit is thought to be the delta front at this point.

Sediments at Loc. 3 also show a northwards fining. Exposures in the south side of the pit are mostly of fine sand and silt in foresets with occasionally silty clay drapes; however in places pebble and cobble gravels are exposed underlying the sands. Large boulders are also present on the floor of the pit indicating a coarsening in sediment size downwards. The northern sections may be divided into two parts; the lower part of the section shows a fining-upwards sequence from medium and fine sands to laminated silts and clays; these are thought to be toesets and proximal lake sediments. This is overlain by a sequence of foresets dipping gently north to northeast composed of sand and pebble gravels.

A similar sequence is seen at Loc. 5 to the southeast. Exposures noted in the field and on the aerial photographs of the area indicates that the sand and gravel continues to the

southeast; however the large numbers of boulders in the area immediately to the north of the slope break indicates that there is a marked change in sediment type in this direction. No exposure was found in this direction; however, the size of the boulders indicates that glacial cover is unlikely to be in excess of 3m.

Bench marks along the road in Leagaun Townland indicate that the sand deposit is at least 7m thick at this point.

The major soil radon anomaly in this area is positioned just north of the break of slope marking the northern boundary of the kame; it may therefore be associated with a change in soil permeability.

Area 3 Gortachalla

The area is predominantly composed of limestone pavement partly masked by scrub vegetation. Soil covering is confined to slight hollows; it is unclear whether drift is found in these hollows, or whether the soil is a colluviual deposit. The anomaly is located on bedrock.

Area 4 Ballynahalia

The area may be divided into two parts; a southern part which is forested and which appears to be composed of a mixture of drift and exposed limestone pavement, and a northern part underlain by raised bog. The bog is associated with a break of slope in the limestone.

The overburden in the forested area was difficult to map; however an exposure at the roadside to the east (Loc. 4) in sandy till in the side of a ridge (described below) indicates that some drift is present. This area is hummocky in topography; the drift is thought to be supraglacial and deposited at the ice margin, and is therefore likely to have a low clay content and be somewhat permeable.

The location of the soil radon anomaly at the boundary between raised bog to the north and mixed bedrock and drift to the south may again be associated with a change in permeability in the subsoil.

Area 5. Killarainy and Ballycuirke West Townlands

A series of ridges trending northwest-southeast and separated by distinct depressions are located north of Moycullen village; these have large boulders of granite on their slopes and are interpreted as end moraines or crevasse fills made of diamict. The southeastern part of the area is one of hummocky moraine; no exposure was found in this area, but it is likely that the hummocks are underlain by sandy till with thin beds of stratified material; permeabilities would be low.

The only pattern seen in the location of the soil radon anomalies in this area is that they appear to lie at the base of steep slopes; this may be associated with a change in permeabilities and drainage.

Area 6. Newtown Townland

Overburden is again variable in this area. The cover of drift is of varying thickness; to the north the hill by Newtown village appears to be of drift, probably till. Glacial deposits also appear to be banked up against the side of Newtown Hill, and north of the village these are gravelly in character; these may represent a fan deposited at the break of the slope. An area of peaty soil is associated with the Sruffaunderracony stream; the area immediately to

the south of this is hummocky in topography and these mounds may be of drift; however bedrock is exposed in a drainage channel, as shown on the map. The area around Lough Beg is underlain by post-glacial peat bog. The area south of the road is drift-covered, with hummocks, no exposure was found.

The soil radon anomaly is located in the area of hummocky moraine where bedrock is close to the surface.

### 1.4.5 Summary

Examination of the six areas does not highlight any strong pattern in the location of the soil radon anomalies, since strikingly different terrains are involved. However, two possible connections between the areas may exist.

Firstly, the soil radon anomalies may be associated with a change from a drift cover to bedrock at the surface. At Areas 1, 3 and 4, the bedrock is overlain by unconsolidated material within 100m of the location of the anomaly; at area 1 by poorly sorted sand, and by peat at area 4. At area 6 bedrock is exposed in a drain immediately south of the anomaly; it may be that bedrock is very close to the surface at sites 2 and 5.

A second possibility is that each anomaly is associated with a change in permeability in each case. This possibility is mentioned in association with each area above; however the changes in permeability are not likely to be similar, and the connection is somewhat tenous.

## 1.5 Drilling programme

### 1.5.1 Introduction

Core drilling was undertaken in the Moycullen area during September and October 1991 in support of geological, geochemical and geophysical work on the EC radon project. A cumulative total of 437 m was drilled in 11 boreholes.

The aims of the drilling were to:

1) establish the nature of the granite/limestone contact;

2) assess the permeability of rocks along the contact zone;

3) recover material for further geochemical analysis, specifically the determination of U, Ra contents and Rn activity;

4) assess the permeability of the karstified limestone in the light of the geophysical surveys;

5) check for U-bearing lithologies intercalated with the limestone.

### 1.5.2 Drilling

Drilling was carried out by the GSI mobile drilling unit under the supervision of K. Crilly. Two target areas were drilled, firstly at Ballycuirke along the granite-limestone contact and secondly at Ballydotia over limestone (Map 1, Fig. 2).

A Ballycuirke (DH 1-3)

This area is beside the Loughkip river, 250 m north of Clydagh Bridge which is 1.6 km SE of Moycullen on the main Galway-Clifden road (Map 1, Fig. 3). Granite is exposed in the river about 150 m north of the bridge and limestone has been recorded on the old GSI six-inch maps (Galway 68) a further 100m to the north. The granite here is marginal white biotite granite. Minor outcrops of grey-green porphyry or felsite were noted and boulders of breccia with clasts of felsite are common in the walls beside the river.

Drilling sites were chosen about 60 m NE of the slope break believed to define the granite-limestone contact. Three holes were drilled on two sites 42 m apart, DH 1 on one site and DH 2 and DH 3 on the other (Fig. 3). A section is given in Fig. 4. A summary of the core logs is given below.

(1) Moycullen DH 1

Angle 45°; orientation 222°; length 56.6 m; core type NQ

Depth:

0.0- 5.5 m: Not recovered

5.5-22.2 m: Grey bioclastic limestone, often argillaceous matrix. Crinoids, typically <2 mm in size, are dominant bioclast. Larger brachiopod fragments are scattered throughout and occur in clast-rich zones 0.1-0.3 m thick (at 10.4, 15.2 and 16.0 m). Shale laminae are common, noted especially where limestone has parted along them. Numerous stylolites. Limestone fractured and core broken in several places, notably at 7.6 and 21.8 m. calcite veins are ubiquitous but usually only mm thick. Brecciation is associated with thicker veins.

22.2-24.5 m: Dolomite lies immediately below fractured limestone with disseminated Fe-sulphide. Dolomite appears as a pale grey granular rock with matrix of ill-defined white clasts c. 1 mm in size. Many calcite veinlets.

24.5-29.0 m: Transition from dolomite to finely laminated shale is marked by broken shaley material. Laminae are curved. Complex, apparently syn-sedimentary faulting present at internal contacts. At 26.5 m, shale is intensely fractured and and bedding highly disrupted. Fine-grained Fe sulphide is present in concentrations up to 20 mm in size. Fracturing is often parallel to bedding.

29.0-30.9 m: Brecciated shale. Core very broken - 70% recovery over next 6 m. Possible fault gouge at base of this interval.

30.9-33.6 m: Below gouge (fault) lithology appears to be highly sheared granite. Brecciation or cataclasis apparent. Quartz fragments 20-30 mm in size.

33.6-34.5 m: Possible fault suggested by gouge. Granite below it is sheared and intensely altered (kaolinized?). Grain size: 2-4 mm.

34.5-39.6 m: Granite is more competent after 34.5 m. Alteration manifests itself as green-yellow phyllosilicate and disseminated Fe sulphide. Granite is white, "Callowfinish" type. Brecciation at 36.7 m.

39.6-50.6 m: Greenish, altered porphyry, sheared at top. 1-2 mm grain size, hard dark grey quartzo-feldspathic matrix. Feldspar occurs as single grains up to 5 mm in size and gives the porphyrytic texture. Veins throughout contain carbonate and greenish material similar to that in altered granite. Brecciation or shearing in places.

50.6-56.6 m: Granite. Contact not preserved. As before, fractured or sheared in places, sulphide-rich. Much green alteration sufficiently intense to cause incipient disaggregation in places. At 52.8 m, gradual development of pink tint in feldspar begins. Below 53 m, feldspar has a strong pink colour. Green alteration phase remains. Texturally and compositionally, the granite resembles "Callowfinish" type rather than pink K-feldspar-bearing ETG.

(2) Moycullen DH 2

Angle 66°; orientation 232°; length 79.8 m; core type NQ

Depth:

0.0- 5.3 m: Not recovered

5.3-23.6 m: Grey bioclastic limestone, typically crinoidal with larger bioclasts scattered throughout and concentrated in 0.1-0.2 m thick zones of shelly debris. Very fractured core at 11.0 and 23-23.6m; brecciation at 21-23 m. Some faults or joints have buff-coloured dried clay coating. Stylolites common. Solution pits, some prismatic in shape, at 17.6-18.2 m.

23.6-25.6 m: Dolomite, as in DH 1. Transition after 24.6 m to shale through shaley dolomite to banded shale. 30% core loss between 23.9 and 26.9 m is within shale.

25.6-30.1 m: Banded, sheared shale above sheared granite - only 50% core recovery between 26.9 and 30.1 m and contact is somewhere between. Contact was observed when core was recovered but was destroyed in transport as core is friable. Contact observed was an unconformity not a fault, i.e. apparent overstep of shale onto granite. Granite below contact is highly sheared at top, altered and friable due to dissolution along grain boundaries. Fe sulphide disseminated throughout. Little core loss in granite below 29.8 m so core loss over this interval is mainly within sheared shale.

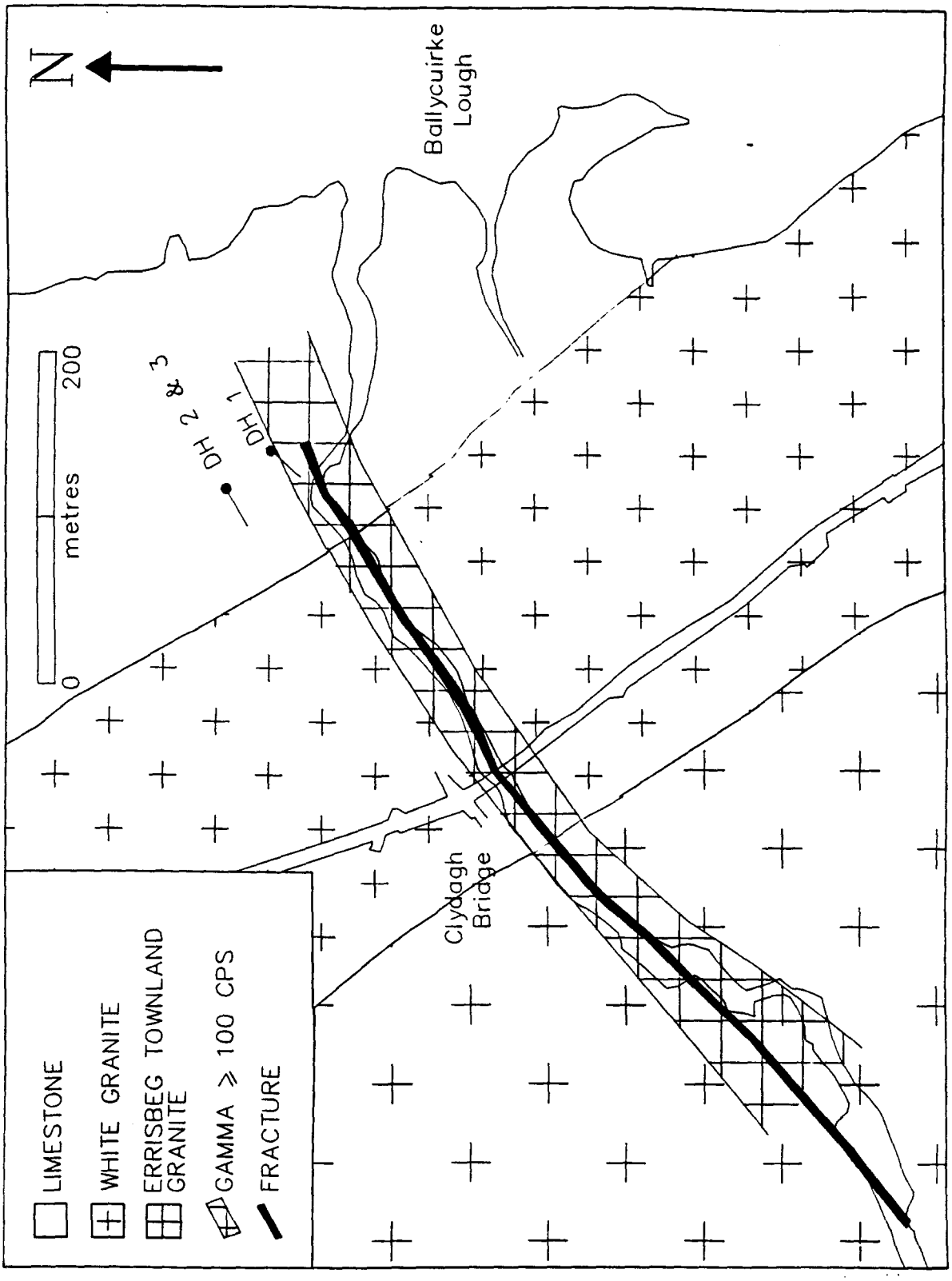


**Figure 3. Ballycuirke area, showing geology and location of boreholes.**

30.1-45.0 m: Altered porphyry. Many veins of green talc-like mineral; carbonate in places. Feldspar phenocrysts up to 5 mm in size. Shearing and associated cataclasis in places.

45.0-60.4 m: Granite. Contact with porphyry preserved - some cataclasis of granite along contact. Granite is sheared throughout all this section. Zones of cataclasis common - large feldspars (>5 mm) reduced to 1-3 mm in size. Fe sulphide common along fractures. Green alteration present, mainly below 54 m. Shearing especially intense between 54.6 and 56.6 m. Granite very sheared for 0.2 m above porphyry contact (60.2-60.4 m).

60.4-61.6 m: Porphyry, relatively little altered; increase in size and abundance of feldspar phenocrysts toward upper and lower contacts.

61.6-69.0 m: Granite. Intensely sheared for 0.2 m below contact. Sheared throughout. Core fractured above contact with underlying porphyry.

69.0-74.8 m: Porphyry. Altered, veined, sheared, fractured. Relatively fine grained; porphyrytic crystals more abundant after 71 m.

74.8-79.8 m: Sheared granite, altered as before.

(3) Moycullen DH 3

Angle 45°; orientation 232°; length 33.4 m; core type NQ

Depth:

0.0- 5.0 m: Not recovered.

5.0-18.8 m: Typical bioclastic limestone of area, mainly crinoidal with scattered brachiopods. Minor faulting at 5.8 m, minor brecciation at 11.4 and 17.8 m. Stylolitic. Occasional 0.1-0.2 m thick zones rich in shelly debris.

18.8-22.2 m: Dolomite. Abundant shaley interlaminations containing Fe sulphide.

22.2-24.2 m: Transition zone, increasing component of shale occurring as fine laminae often only 10's mm in length or as larger intercalations.

24.2-26.8 m: Typical banded shale, sheared. Brecciation and veining between 25.4 and 26.6 m.

26.8-29.8 m: Black mud which may be intensely sheared shale. Wet, can be disaggregated in water. Occasional, more competent zones of brecciated dolomite or limestone.

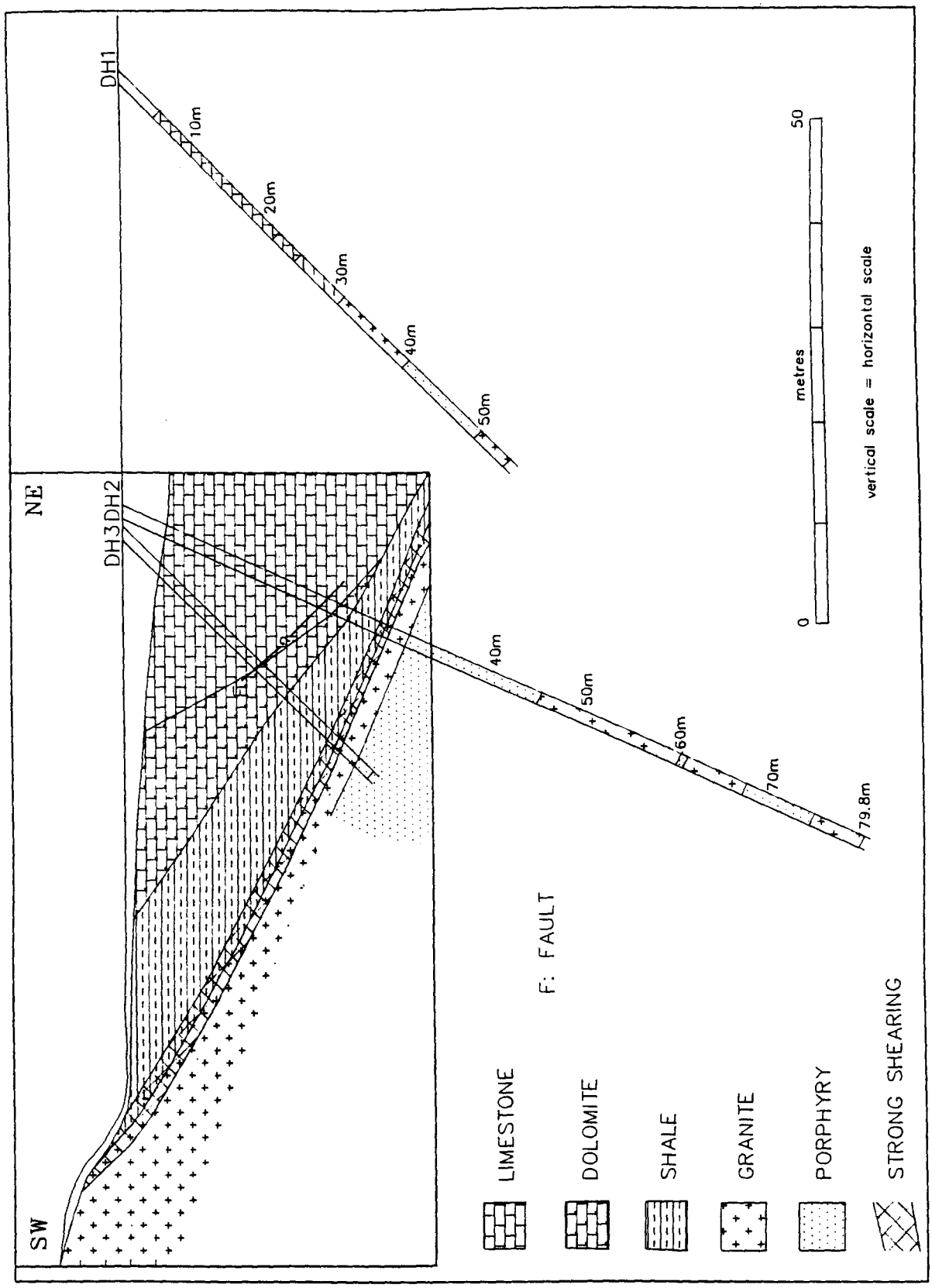


**Figure 4. Cross-section based on DH 2 and 3, Ballycuirke.**

29.8-32.4 m: Granite. Possible gouge at contact suggests fault but because overlying material is so disaggregated it is hard to say if it is a fault gouge or mud. Granite is sheared, Fe sulphide abundant on fractures. Cataclasis of granite in places. Greenish, talc-like alteration phase as before.

32.4-33.4 m: Porphyry. Contact with granite not preserved.

Conclusions

Several conclusions can be drawn from the drilling at Ballycuirke:

1) The dip of the Galway Granite-Lower Carboniferous contact is very shallow, 25-30° (Fig. 4). In one core an apparently unconformable contact was observed so that a simple overlap of sediment onto a gently sloping eroded granite surface is suggested. However, the presence of what appears to be mylonitized or intensely sheared granite immediately below the contact is also suggestive of a shear zone or thrust fault parallel to the contact.

2) The NW-SE trending slope break in the area is confirmed to be a topographic expression of the contact.

3) Faulting and fracturing are important features of the recovered core but their significance, whether local or regional, cannot be estimated. Photolinears suggest that an important N-S trending fracture zone is present at Ballycuirke (Fig. 3) and breccias have been noted in float. It is possible, therefore, to regard most of the deformation observed in core as of local significance.

4) Porphyry is an important component of the intrusive suite here, far more so than is apparent from surface mapping.

5) Alteration of the igneous rocks is very strong. The granite is partially disaggregated. This suggests pervasive circulation of water along the contact zone where alteration is strongest. Shale also appears to show the effects of deformation and fluid circulation where it has been reduced to incompetent mud. It is important to distinguish between the effects of recent water circulation and of that associated with the formation and cooling of the granite some 400 m.y. ago, although it may be impossible to do so.

6) Dolomite at the base of the limestone is of variable thickness and is an alteration product of limestone. The timing of alteration is as yet unclear but since the dolomite lies immediately above the zone of deformation around the contact where alteration is most intense it can stated that dolomitization followed deformation.

B Ballydotia (DH 4-11)

Ballydotia lies 1.6 km N of Moycullen village (Map 1, Fig. 2). The area is underlain by Carboniferous limestone and was the site of detailed geochemical (soil gas Rn and He, house Rn, soil Ra) and geophysical (resistivity and VLF) surveys (Annexes 2, 3, 4, 5 and 6). Significant indoor Rn anomalies recorded here have been correlated with high-resistivity anomalies (Annex 6). Drilling was carried out in the eastern and western parts of the area

(Fig. 5) around two houses (Nos. 6 and 10) with high indoor Rn activity. In the western part, the affected house (No. 10) is close to the centre of a broad resistivity anomaly (Map 1, Annex 6). In the eastern part, the affected house (No. 6) lies on a zone of high soil gas Rn and He (Map 3).

Eight holes were drilled, five in the western part and three in the east. DH 4 was sited behind the affected house (No. 10) about 40 m from the centre of the resistivity anomaly. DH 5 and 6 (Map 1, Annex 6) were drilled at the centre of the anomaly, beside an old well. DH 7 (Map 1, Annex 6) was drilled across a linear geophysical feature which coincides with a small slope break and which is thought to be a major fault or joint. In the eastern part, DH 8 was drilled vertically into a broad zone of high resistivity (Map 1, Annex 6). The EM traverse in this area defined a zone of high values across the line between two swallow holes on either side of the affected house (No. 6). This line coincides with a broad zone of elevated Rn and He soil gas values (Map 3). DH 9 and 10 were drilled across this structure intercepting it at different heights (Map 1, Annex 6). In February 1992, after the completion of geophysical surveys, a further borehole, DH 11, was drilled diagonally below house No. 10 in an attempt to intersect a possible north-south-trending fracture or cavity zone.

No detailed core logs were done as the aim of the drilling was to assess the structure of bedrock rather than its lithological composition. A brief description of each core follows.

(1) Moycullen DH 4
Vertical; length 25.8 m; core type NQ

DH 4 intersected a small cavity, c. 0.2 m thick. Rounded granite pebbles, among others, are evidence for water flow within the limestone.

(2) Moycullen DH 5
Angle 55°; orientation 100°; length 21.7 m; core type NQ

DH 5 was drilled across and below the old well and intersected a 0.6 m wide cavity 13 m below the surface, a few metres beyond the vertical projection of the well (Fig. 5).

(3) Moycullen DH 6
Vertical; length 40.4 m; core type NQ

DH 6 was drilled at the same site as DH 5 to test whether a larger cavity existed but which may have been missed by the angled hole. No cavity was intersected.

(4) Moycullen DH 7
Angle 45°; orientation 260°; length 31.6 m; core type NQ

DH 7 was drilled into the small slope break which coincides with a sharp break between zones of higher and lower EM values. A cavity, almost 2 m wide, was intersected almost directly below the slope break, confirming the geophysical interpretation of a major joint or fault (Fig. 5).

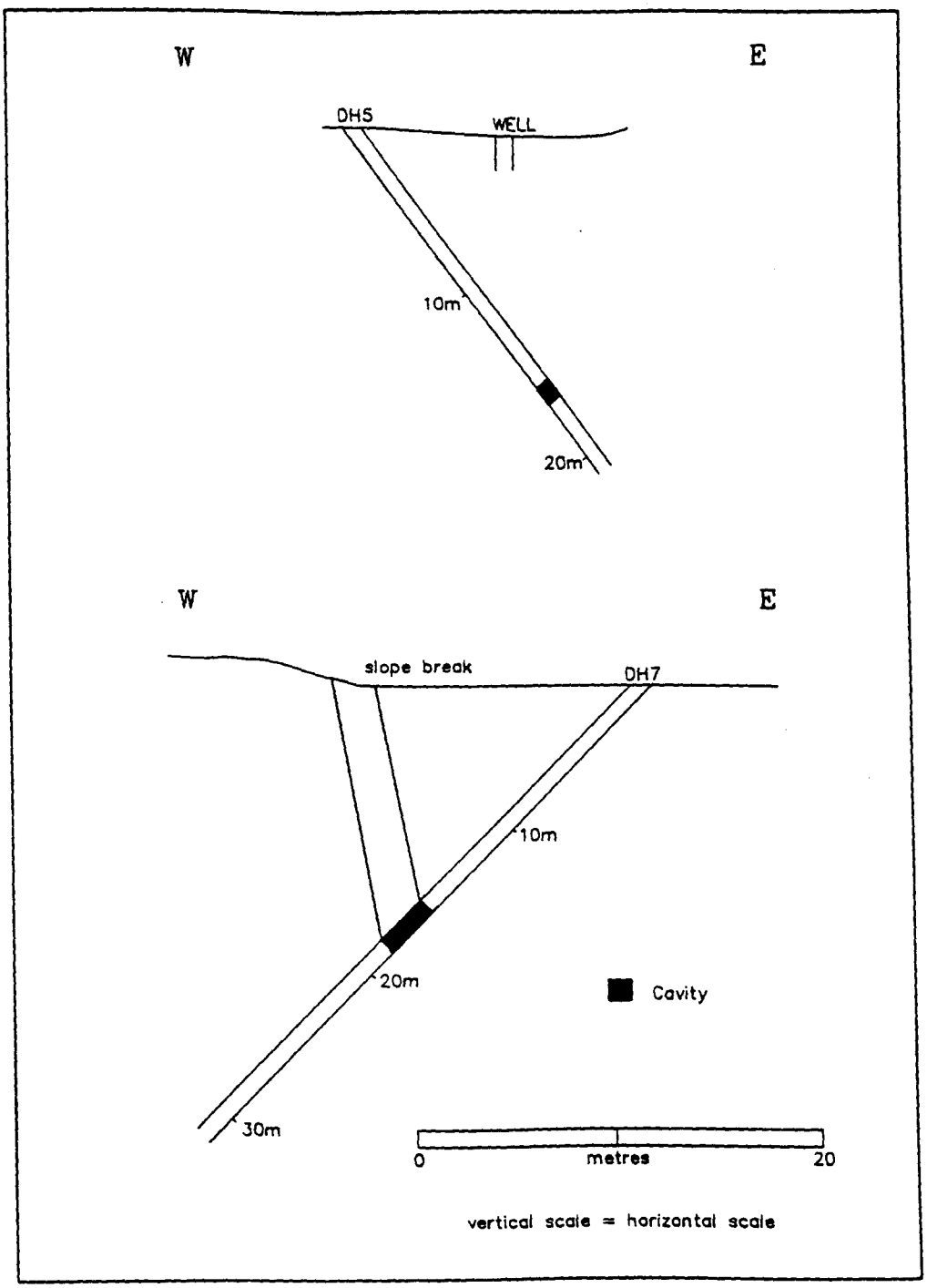


**Figure 5. Cross-sections, DH 5 and 7.**

(5) Moycullen DH 8
Vertical; length 34.8 m; core type NQ

DH 8 was drilled into a broad zone of high EM 95 m west of the major N-S linear anomaly in the eastern part of Ballydotia. A small channel was intersected at 25 m.

(6) Moycullen DH 9
Angle 47°; orientation 262°; length 39.5 m; core type NQ

DH 9 was drilled westwards across the trend of the line joining the two swallow holes, intersecting it at a depth of 14-16 m. A small channel intersected at 34 m cannot be related to the position of the swallow holes or the geophysical anomalies coincident with them.

(7) Moycullen DH 10
Angle 45°; orientation 262°; length 21.5 m; core type NQ

DH 10 was drilled in the same direction as but above DH 9. It intersected the line between the swallow holes at 4-6 m. No channels were intersected.

(8) Moycullen DH 11
Angle 45°; orientation 240°; length 51.8 m; core type NQ

DH 11 was drilled in a southwesterly direction below house No. 10. It intercepted two narrow cavities, the first c. 0.45 m wide and the second c. 0.8 m wide. In the first cavity, a 0.15 m thick band of buff-coloured clay containing fine comminuted limestone was found at the base (sample 91.1093) (Table 4, Annex 4). In the second, a 0.1 m thick red-brown clay contained granite fragments (sample 91.1094). The cavities were found at 21.3 and 22.0m, respectively, in core, at a vertical depth of c. 15 m close to the centre of the house.

Conclusions

1) In the western part of Ballydotia drilling gave some support to the geophysical interpretation, notably in DH 7 which intersected a 2 m thick cavity directly below the slope break. Although cavities were intersected in DH 5, near the well, and in DH 11 below house no. 10, it is clear that the major resistivity anomaly here does not imply a single large cavity below the surface, rather, perhaps, a series of small channels.

2) It is possible that the two holes drilled across the line of swallow holes and across the linear geophysical anomaly passed below or above existing cavities but this suggests that if cavities exist they must be relatively small. Small channels through which water is flowing, carrying silt and granitic and other exotic pebbles, do exist.

3) Resistivity and EM anomalies may reflect the existence of a network of small (100's mm maximum dimension), ramifying channels throughout the limestone.

## 1.6 Results of geochemical investigations

### 1.6.1 Introduction

Geochemical studies undertaken by GSI and TCD were chiefly directed towards assessing the radioelement content of rocks and soils in the Moycullen area. Whole-rock samples were collected by GSI from outcrop and core in Moycullen; additionally, a suite of granite samples, representative of Galway Granite lithologies in general, were taken from the GSI Geochemistry Section collection for comparative studies. Soil samples from around selected houses in the project area were collected by TCD. A preliminary study of the $^{222}Rn$ activity in ground- and surface waters was carried out by GSI in collaboration with BGS. The TCD report, covering the soil radioelement results, is appended as Annex 4. The background to GSI's sampling and a discussion of the results of lithological and water sampling follows.

### 1.6.2 Whole-rock sampling

Objectives

A programme of geochemical analyses was begun by GSI in order to follow up earlier field mapping in the Moycullen area. The aims were:

1) to classify the marginal granite variety at Moycullen and establish its radioelement content;
2) to provide essential information on the levels of $^{226}Ra$, $^{234}Th$ and $^{40}K$ (determined by TCD) in the Galway granite as a whole and in specific lithologies in the Moycullen area;
3) to make a preliminary assessment of potential U-Ra sources in the Moycullen area.

Samples

Thirteen samples of Galway granite were selected from those collected by GSI Geochemistry Section in 1988. They include Errisbeg Townland granite (2), Spiddal granite (1), Inveran granite (1), Callowfinish granite (3), Murvey granite (4), Oughterard granite (1) and a crushed granite, probably Murvey granite (1). A full list is given in Table 1. The Moycullen field samples include marginal white granite (4),felsite (2) and 4 samples taken vertically from topsoil down to a depth of 3m from a sand quarry overlying Carboniferous Limestone (Table 1).

A suite of samples was taken from drill core recovered at Ballycuirke (DH 1 and 2) and analysed at TCD. These samples provided a high degree of geological control not otherwise attainable. In particular, they allowed an assessment of how alteration and/or deformation affect the contents of radioelements in granite. The samples are listed in Table 2 and the analytical results are given in Annex 4. Two samples of clay, which were found in small cavities in limestone at Ballydotia (DH 11), were also analysed at TCD.

### 1.6.3 Geochemistry of field samples

Whole-rock geochemical analyses of the GSI 1988 Galway granite samples were completed previously. Three marginal white granite samples and two felsite samples from Moycullen were analysed at the Geology Department, University of Leeds, for major elements and 13 trace elements, though only 8 trace elements are considered here. The results are given in Table 3 and are illustrated in Figs. 6-8.

Figs. 6 and 7, in which data are plotted with Wright's (1964) data for the Galway

Table 1

Samples analysed from the Galway Granite and Moycullen area

**Galway granite:**

| Sample | Townland | Grid Ref. | Granite type |
|---|---|---|---|
| 882001 | Costelloe | L 9936 2339 | Murvey |
| 882020 | Costelloe | L 9739 2675 | Inveran |
| 882021 | Lissagurraun | M 2390 2866 | Murvey |
| 882040 | E. Loughaunkey | M 0867 2520 | Spiddal |
| 882046 | Dangan | M 2818 2618 | Murvey |
| 882057 | Lettercraffroe | M 0715 3754 | Callowfinish (?) |
| 882058 | Kilcummin | M 0271 2205 | Murvey |
| 882082 | Knockatee | M 1491 3090 | Errisbeg Townland |
| 882083 | Arderoo Lough | M 1335 3195 | Errisbeg Townland |
| 882138C | Kilkieran | L 8358 3225 | Crushed, hematized |
| 882143 | W. Glentrasna | L 9745 4055 | Callowfinish (?) |
| 882146 | N. Lough Avally | L 8960 3980 | Callowfinish (?) |
| 882148 | Lackavrea | L 9723 4920 | Oughterard |

**Moycullen area:**

| Sample | Townland | Grid Ref. | Sample type |
|---|---|---|---|
| 911004 | Clydagh | M 2226 3120 | White granite |
| 911007 | Carrowlustraun | M 2086 3320 | Felsite |
| 911052 | Carrowlustraun | M 2005 3325 | Felsite |
| 911054 | Gortnamona E. | M 2047 3357 | White granite |
| 911055 | Clydagh | M 2240 3135 | White granite |
| 911060 | Carrowlustraun | M 2046 3344 | White granite |
| 911062(1) | Moycullen | M 2210 3380 | Topsoil |
| 911062(2) | Moycullen | M 2210 3380 | Sand & gravel |
| 911062(3) | Moycullen | M 2210 3380 | Sand & gravel |
| 911062(4) | Moycullen | M 2210 3380 | Sand & gravel |

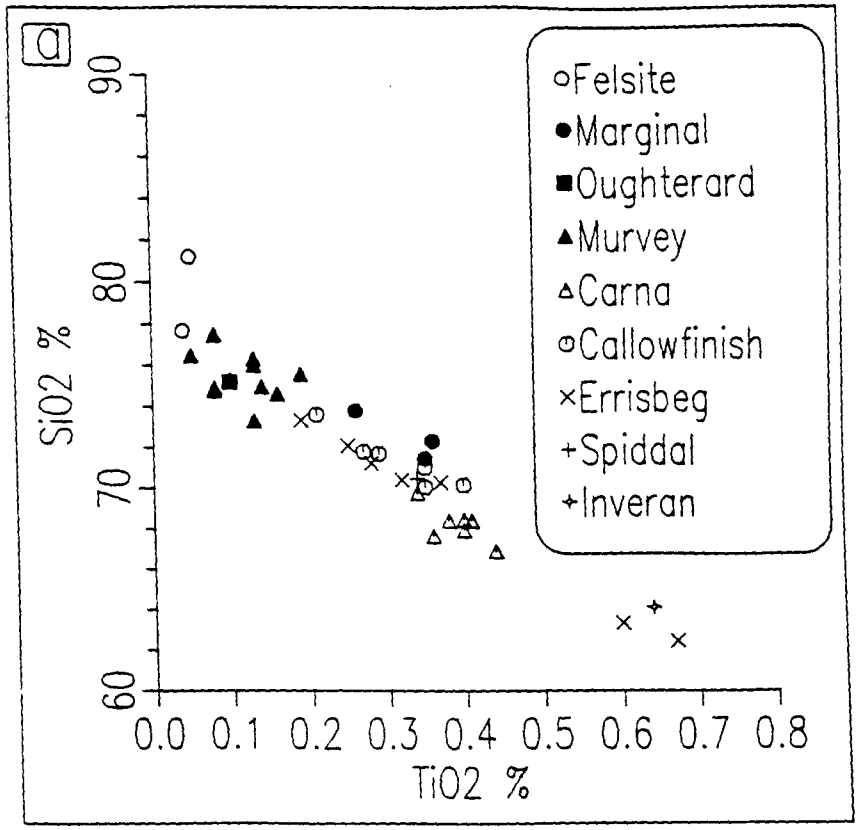


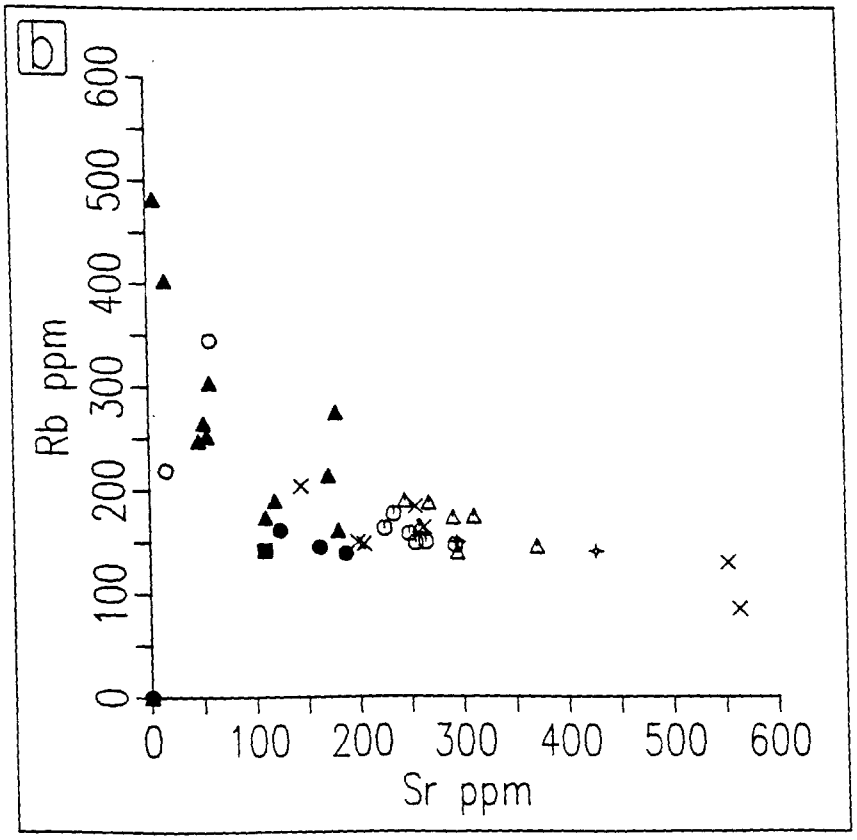


**Figure 6.** **$SiO_2$ v $TiO_2$ (a) and Rb v Sr (b) for Galway Granite and Moycullen field samples**

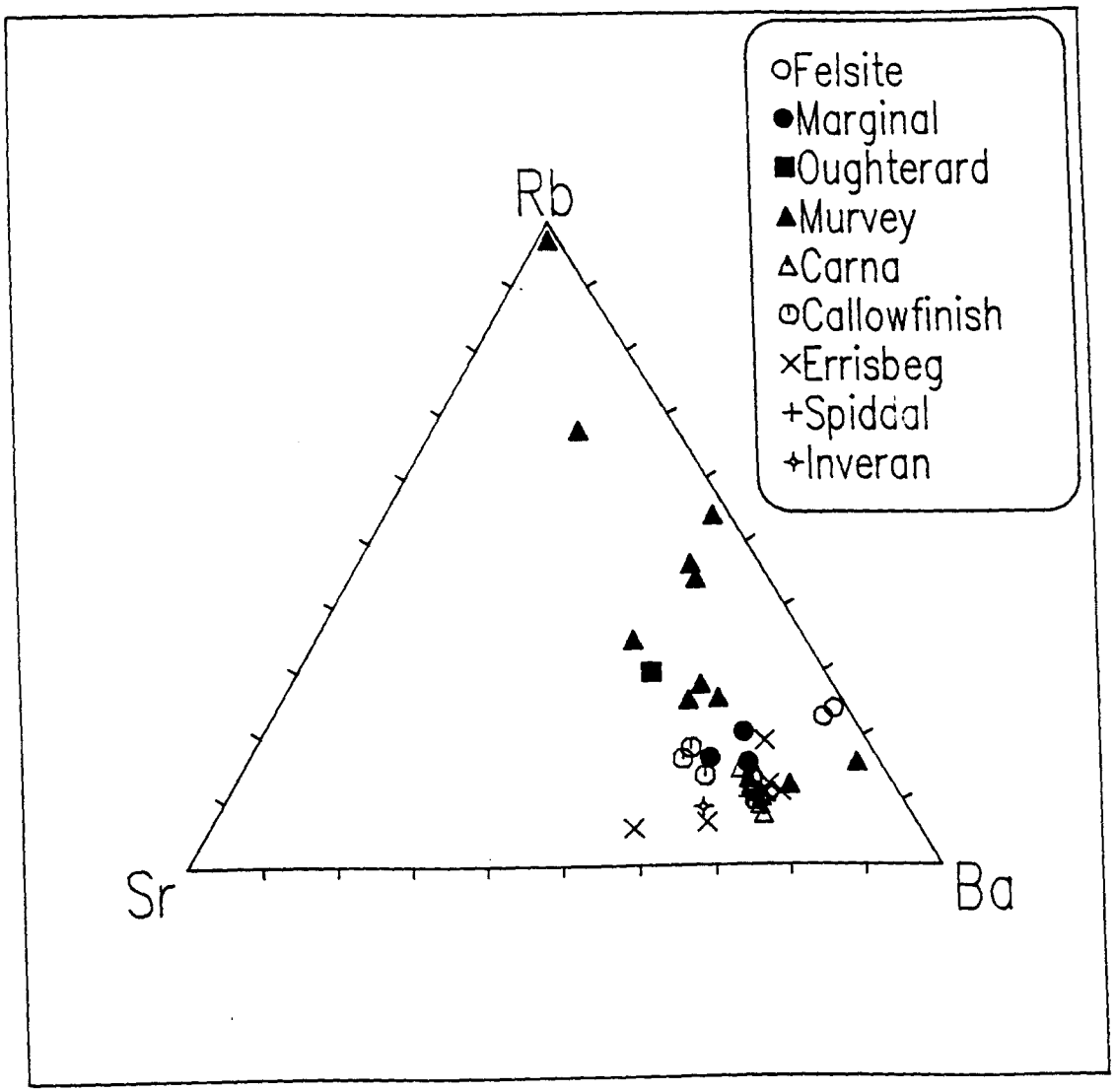


**Figure 7. Rb-Sr-Ba for Galway Granite and Moycullen field samples.**

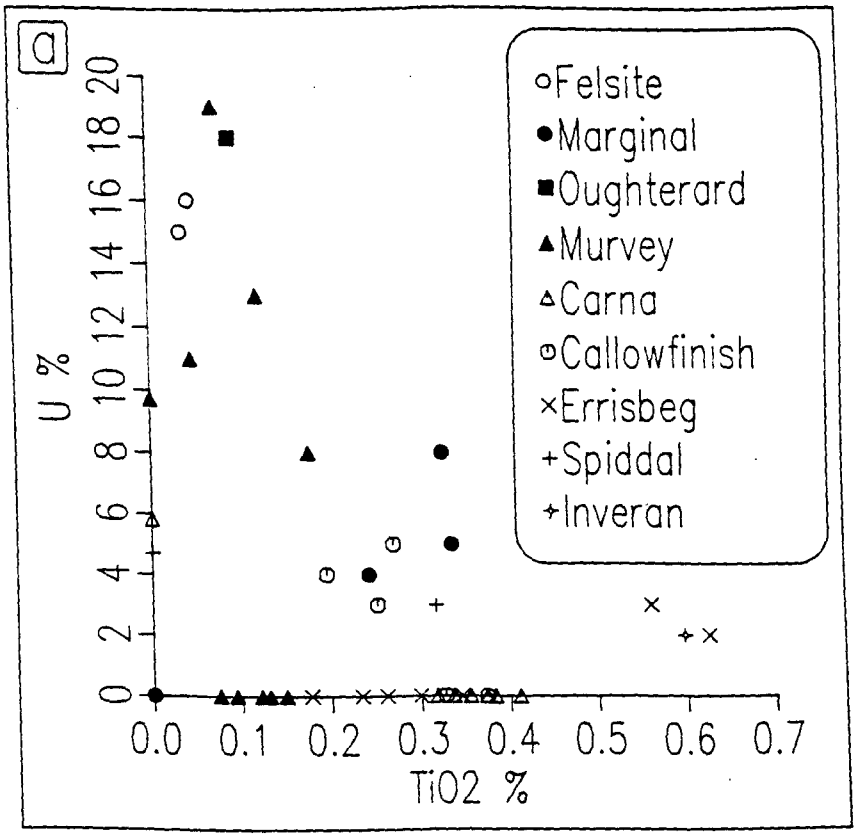


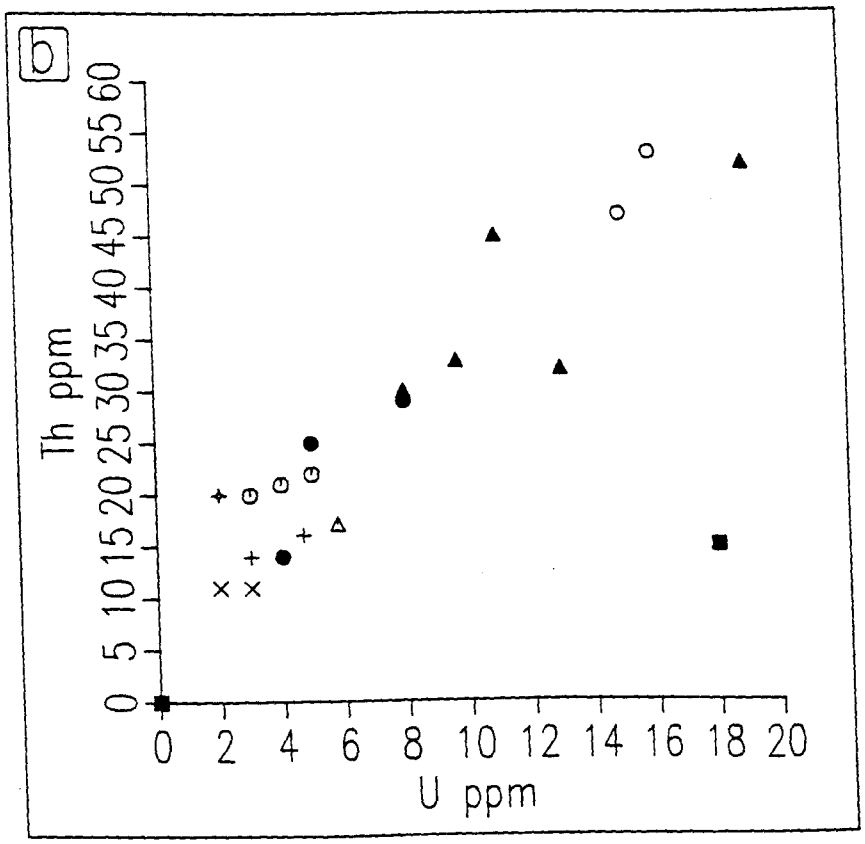


**Figure 8. U v $TiO_2$ (a) and Th v U (b) for Galway Granite and Moycullen field samples**

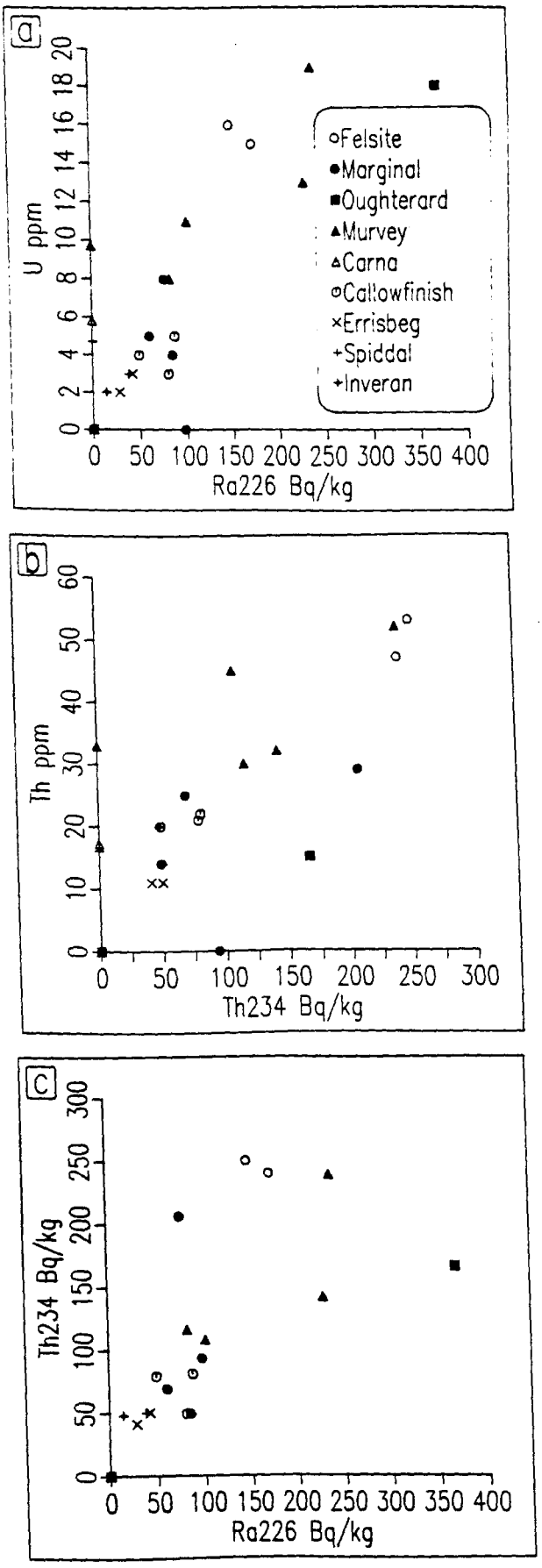


**Figure 9.** **U v $^{226}$Ra (a), Th v $^{234}$Th (b) and $^{234}$Th v $^{226}$Ra for Galway Granite and Moycullen field samples**

granite, clearly demonstrate the fractionation trend for the granite. The marginal white granite at Moycullen has a similar chemistry to the Callowfinish granite and to Wright's Errisbeg Townland granite. The Errisbeg Townland granite samples from the GSI 1988 collection are notably more basic in composition and may be a mafic variety. Of interest is the very acid nature of the single sample of Oughterard granite (Fig. 6). On the Rb v. Sr diagram (Fig. 7), both the white granite at Moycullen and the Oughterard granite appear to be depleted in Rb relative to other granite types. Felsites from Moycullen appear similar to the Murvey granite except on the Rb-Sr-Ba diagram where their relatively low Rb and high Ba contents distinguish them.

Plots of U v. $TiO_2$ (Fig. 8a) for the GSI 1988 and Moycullen data (Wright (1964) did not analyse for U or Th) show 3 distinct groupings:

- low U, high $TiO_2$ : mafic (?) Errisbeg Townland granite, Inveran granite
- med. U, med. $TiO_2$ : Callowfinish, Spiddal, Marginal Granite (Moycullen)
- high U, low $TiO_2$ : Murvey, Oughterard granite, felsite dykes

The Oughterard granite sample has the second highest U content of all analysed samples (18ppm).

In Fig. 8b there is a broad linear relationship between Th and U though the Oughterard granite sample has notably low Th. The felsites from Moycullen are among the most radioelement-rich lithologies analysed; white marginal granite again plots with Callowfinish granite and is relatively radioelement-poor.

$^{226}Ra$, $^{234}Th$ and $^{40}K$ analyses were carried out at TCD (see Annex 4, Table 2). $^{234}Th$ is plotted against $^{226}Ra$ in Fig. 9c. There is a broad linear trend from low $^{234}Th$, $^{226}Ra$ values to higher values. Oughterard granite, consistent with its high U content, has a very high $^{226}Ra$ content.

Figs. 9a and 9b display the relationship between Th and $^{234}Th$ and between U and $^{226}Ra$. The data points are somewhat scattered but there is a broad, skewed trend from low to high values.

In addition to the whole-rock results, two results have been obtained to date for the sand quarry samples (Table 3): $^{226}Ra$ and $^{234}Th$ are both present in relatively low quantities suggesting a very low potential as a radon source.

Summary

1. The Marginal Granite at Moycullen, although it does not strongly resemble the type Callowfinish granite in the field or petrographically, is geochemically similar and is radioelement-poor.

2. Felsites appear to be the only intrusive rocks in the Moycullen area with relatively high radioelement contents. The Oughterard granite has a very high U and $^{226}Ra$ content despite the low gamma count recorded over its eastern part.

### 1.6.4 Geochemistry of core samples

The results of gamma-ray spectroscopy of core samples from DH 1 and DH 2 at Ballycuirke are given in Table 3, Annex 4. The results are illustrated in Fig. 10. It is clear from this figure that, whereas the results appear uninformative in the context of the overall levels of $^{226}Ra$, $^{234}Th$ and $^{40}K$ recorded (Annex 4), there is a strong downhole variation in radioelement activities which can be related to geology.

The rocks around the granite-Carboniferous contact are strongly deformed (section

1.3). The contact granite is crushed and intensely altered so that it has become friable. Shale within the contact zone has been disaggregated and reduced to a mud. Below the contact zone, the granite in many cases is intensely altered and strongly deformed and is cut by networks of fractures. Many of these fractures are filled by calcite and pyrite. Quartz is extremely rich in secondary fluid inclusions distributed along planar arrays. Some of the alteration observed undoubtedly occurred in the immediate aftermath of emplacement of the batholith some 400 m.y. ago since retrograde alteration of feldspars, in particular, is prevalent throughout the batholith. Disaggregation of both shale and granite is presumably a consequence of recent groundwater flow since it might be expected that cementation would have occurred if alteration had been more ancient. The abundance of calcite in the core samples and its relative absence in altered granite further from the contact suggests that calcite was derived from dissolution of overlying limestone by fluids circulating through granite and limestone. Thus, the geological evidence suggests pervasive fluid flow through the granite and basal Carboniferous sediments over an extended period of time, perhaps even continuously or intermittently from 400 Ma to present day.

In Fig. 10 it can be seen that most core samples analysed from DH 1 have rather low $^{226}$Ra activities. A notable exception is shale immediately above the contact with the granite which has a $^{226}$Ra activity of 142 Bq kg$^{-1}$. A second shale sample, 5m above it in core, has a much lower activity of 15 Bq kg$^{-1}$. The high-$^{226}$Ra sample corresponds with the peak identified in the down-hole natural gamma log (Annex 6). Both limestone and dolomitized limestone have low $^{226}$Ra activity, close to the limit of detection of 11 Bq kg$^{-1}$. The granite samples generally have $^{226}$Ra activities below the limit of detection or just above it. This contrasts with four samples of marginal white granite collected in the field further from the granite contact (Table 3) which have a median activity value of 80 Bq kg$^{-1}$. The degree of alteration in these samples is much less than in core. Four porphyry samples have variable $^{226}$Ra activity, two conspicuously altered samples having lower values (16 and 22 Bq kg$^{-1}$) than two samples that appear, in hand specimen, to be relatively unaltered (42 and 44 Bq kg$^{-1}$). The implication is that $^{226}$Ra activity decreases as the degree of alteration increases. This is also supported by trends observed in samples from DH 2 (Fig. 10): $^{226}$Ra activity increases in granite with increasing distance from the contact and decreasing intensity of alteration and deformation, reaching 116 Bq kg$^{-1}$ in sample 91.1091.

Similar trends are observed in both DH 1 and DH 2 for $^{234}$Th. The high-$^{226}$Ra activity shale sample (91.1079) also has high $^{234}$Th activity (94 Bq kg$^{-1}$). Like $^{226}$Ra activity, the activity of $^{234}$Th also increases with increasing depth in DH 2. A similar increase is observed for the deepest granite samples in DH 1. This, together with the fact that $^{234}$Th activity is in many cases only slightly below the median value for field samples, suggests that $^{226}$Ra is more readily remobilized than $^{234}$Th.

The $^{40}$K activity is also shown on Fig. 10. In most samples, $^{40}$K activity seems to vary inversely with the activities of $^{226}$Ra and $^{234}$Th so that the $^{40}$K activity is higher in core than the median value for field samples. This might be expected on the basis of the mineralogical and chemical changes associated with alteration in the granites: the growth of kaolin and sericite in place of plagioclase implies a net gain in K. Thus, $^{40}$K may, in a general way, be regarded as an indicator of alteration in the granite samples. Porphyries and sediments have low $^{40}$K activities, consistent with their low content of K-bearing minerals.

In summary, the activities of $^{226}$Ra, $^{234}$Th and $^{40}$K in core samples on the granite-

**Table 2**

**Analysed drillcore samples**

| Sample | Drillhole, depth | Lithology |
|---|---|---|
| 91.1063 | DH 1, 30.7-33.7 m | Crushed granite immediately below contact |
| 91.1064 | DH 1, 35.2 m | Highly altered granite, friable |
| 91.1065 | DH 1, 35.3 m | Altered granite, more competent |
| 91.1066 | DH 1, 36.2 m | Competent, altered granite |
| 91.1067 | DH 1, 37.2 m | Competent, altered granite |
| 91.1068 | DH 1, 39.1 m | Competent, altered granite |
| 91.1069 | DH 1, 40.6 m | Altered porphyry |
| 91.1070 | DH 1, 41.3 m | Altered porphyry |
| 91.1071 | DH 1, 44.3 m | Highly altered porphyry |
| 91.1072 | DH 1, 47.6 m | Altered porphyry |
| 91.1073 | DH 1, 51.2 m | Competent, altered granite |
| 91.1074 | DH 1, 52.3 m | Competent, altered granite |
| 91.1075 | DH 1, 55.2 m | Pink K-feldspar granite |
| 91.1076 | DH 1, 25.4 m | Highly deformed shale |
| 91.1077 | DH 1, 30.8 m | Highly deformed shale |
| 91.1078 | DH 1, 23.7 m | Dolomitized limestone |
| 91.1079 | DH 1, 21.1 m | Massive limestone |
| 91.1080 | DH 2, 29.6 m | Crushed granite near contact |
| 91.1081 | DH 2, 31.1 m | Altered porphyry |
| 91.1082 | DH 2, 38.5 m | Altered porphyry |
| 91.1083 | DH 2, 35.5 m | Altered porphyry |
| 91.1084 | DH 2, 47.6 m | Competent, altered granite |
| 91.1085 | DH 2, 51.4 m | Competent, altered granite |
| 91.1086 | DH 2, 55.7 m | Competent, altered granite |
| 91.1087 | DH 2, 54.9 m | Sheared, altered granite |
| 91.1088 | DH 2, 59.4 m | Competent, altered granite |
| 91.1089 | DH 2, 63.5 m | Competent, altered granite |
| 91.1090 | DH 2, 67.0 m | Competent, altered granite |
| 91.1091 | DH 2, 75.6 m | Competent, altered granite |
| 91.1092 | DH 2, 78.7 m | Competent, altered granite |

## Table 3

## Geochemistry of samples from the Galway Granite and from the Moycullen area

| | 911004 | 911055 | 911060 | 911007 | 911052 | 882001 | 882020 | 882021 | 882040 | 882046 |
|---|---|---|---|---|---|---|---|---|---|---|
| SiO2 | 72.34 | 71.50 | 73.84 | 81.18 | 77.68 | 77.47 | 64.13 | 75.99 | 70.50 | 75.80 |
| TiO2 | 0.36 | 0.35 | 0.26 | 0.05 | 0.04 | 0.08 | 0.84 | 0.13 | 0.34 | 0.19 |
| Al2O3 | 14.62 | 14.28 | 14.53 | 10.82 | 11.38 | 12.06 | 16.35 | 12.74 | 15.04 | 12.81 |
| Fe2O3 | 1.70 | 2.03 | 1.05 | 1.15 | 1.10 | 0.93 | 4.47 | 0.94 | 2.58 | 1.34 |
| MnO | 0.05 | 0.04 | 0.01 | 0.05 | 0.04 | 0.08 | 0.11 | 0.07 | 0.07 | 0.07 |
| MgO | 1.00 | 0.84 | 0.13 | 0.58 | 0.57 | 0.03 | 1.90 | 0.22 | 0.87 | 0.35 |
| CaO | 0.47 | 0.83 | 0.27 | 0.11 | 0.31 | 0.53 | 3.66 | 0.68 | 1.31 | 0.69 |
| Na2O | 3.66 | 3.96 | 4.14 | 0.09 | 0.38 | 3.91 | 3.91 | 3.86 | 4.05 | 3.61 |
| K2O | 4.65 | 4.36 | 4.39 | 4.15 | 7.30 | 4.53 | 3.56 | 4.65 | 4.35 | 4.90 |
| P2O5 | 0.17 | 0.16 | 0.05 | 0.03 | 0.02 | 0.01 | 0.27 | 0.03 | 0.11 | 0.06 |
| L.O.I. | 1.17 | 1.35 | 1.10 | 1.98 | 1.48 | 0.56 | 0.54 | 0.26 | 1.21 | 0.53 |
| Total | 100.19 | 99.70 | 99.77 | 100.19 | 100.30 | 100.19 | 99.54 | 99.57 | 100.43 | 100.15 |
| Rb | 145.00 | 139.00 | 161.00 | 219.00 | 345.00 | 482.00 | 141.00 | 304.00 | 156.00 | 214.00 |
| Sr | 162.00 | 187.00 | 124.00 | 16.00 | 59.00 | 7.00 | 427.00 | 58.00 | 295.00 | 171.00 |
| Y | 6.00 | 9.00 | 3.00 | 53.00 | 37.00 | 60.00 | 17.00 | 9.00 | 12.00 | 10.00 |
| Nb | 12.00 | 12.00 | 11.00 | 22.00 | 26.00 | 31.00 | 12.00 | 17.00 | 8.00 | 11.00 |
| Zr | 123.00 | 115.00 | 90.00 | 102.00 | 95.00 | 92.00 | 181.00 | 69.00 | 137.00 | 94.00 |
| Ba | 611.00 | 514.00 | 501.00 | 675.00 | 1112.0 | 7.00 | 1007.0 | 88.00 | 1000.0 | 451.00 |
| Th | 25.00 | 29.00 | 14.00 | 53.00 | 47.00 | 52.00 | 20.00 | 13.00 | 14.00 | 14.00 |
| U | 5.00 | 8.00 | 4.00 | 16.00 | 15.00 | 19.00 | 2.30 | 10.00 | 2.70 | 2.70 |
| Ra226 | 60.00 | 76.00 | 84.00 | 148.00 | 172.00 | 236.00 | 14.00 | 227.00 | 88.00 | 82.00 |
| Th234 | 69.00 | 206.00 | 49.00 | 250.00 | 240.00 | 289.00 | 48.00 | 142.00 | 50.00 | 116.00 |
| K40 | 1274.0 | 1184.0 | 1205.0 | 1128.0 | 1934.0 | 1219.0 | 940.00 | 1241.0 | 1195.0 | 1292.0 |

| | 882057 | 882058 | 882082 | 882083 | 882138 | 882143 | 882146 | 882148 |
|---|---|---|---|---|---|---|---|---|
| SiO2 | 71.35 | 76.48 | 62.46 | 63.36 | 74.51 | 73.65 | 71.73 | 75.19 |
| TiO2 | 0.27 | 0.05 | 0.67 | 0.60 | 0.17 | 0.21 | 0.29 | 0.10 |
| Al2O3 | 13.89 | 12.49 | 17.19 | 16.69 | 13.52 | 13.54 | 14.54 | 13.63 |
| Fe2O3 | 2.02 | 1.00 | 4.58 | 4.29 | 1.44 | 1.63 | 2.22 | 1.13 |
| MnO | 0.08 | 0.05 | 0.11 | 0.10 | 0.05 | 0.06 | 0.07 | 0.04 |
| MgO | 0.83 | 0.02 | 2.05 | 1.98 | 0.27 | 0.64 | 0.83 | 0.16 |
| CaO | 1.41 | 0.49 | 2.80 | 3.83 | 0.38 | 1.32 | 2.11 | 0.43 |
| Na2O | 3.59 | 3.94 | 4.28 | 4.29 | 2.90 | 3.45 | 3.60 | 3.74 |
| K2O | 4.66 | 4.67 | 3.99 | 2.86 | 4.96 | 4.53 | 4.18 | 4.46 |
| P2O5 | 0.11 | 0.01 | 0.33 | 0.32 | 0.03 | 0.06 | 0.10 | 0.04 |
| L.O.I. | 1.41 | 0.58 | 1.78 | 0.94 | 1.23 | 1.02 | 0.51 | 0.91 |
| Total | 100.12 | 99.78 | 100.24 | 99.26 | 99.46 | 100.11 | 100.18 | 99.83 |
| Rb | 150.00 | 403.00 | 130.00 | 85.00 | 277.00 | 158.00 | 177.00 | 143.00 |
| Sr | 265.00 | 17.00 | 553.00 | 563.00 | 90.00 | 249.00 | 234.00 | 109.00 |
| Y | 8.00 | 63.00 | 14.00 | 12.00 | 13.00 | 9.00 | 10.00 | 19.00 |
| Nb | 10.00 | 32.00 | 9.00 | 10.00 | 15.00 | 8.00 | 10.00 | 36.00 |
| Zr | 96.00 | 97.00 | 174.00 | 175.00 | 79.00 | 74.00 | 82.00 | 44.00 |
| Ba | 673.00 | 325.00 | 1300.0 | 839.00 | 291.00 | 555.00 | 566.00 | 223.00 |
| Th | 20.00 | 45.00 | 11.00 | 11.00 | 24.50 | 21.40 | 22.40 | 15.00 |
| U | 3.10 | 11.00 | 2.30 | 2.70 | 17.00 | 4.10 | 5.00 | 18.00 |
| Ra226 | 80.00 | 101.00 | 28.00 | 42.00 | 267.00 | 49.00 | 87.00 | 367.00 |
| Th234 | 49.00 | 188.00 | 41.00 | 50.00 | 188.00 | 79.00 | 81.00 | 166.00 |
| K40 | 1050.0 | 1266.0 | 1058.0 | 806.00 | 1352.0 | 1201.0 | 1097.0 | 1212.0 |

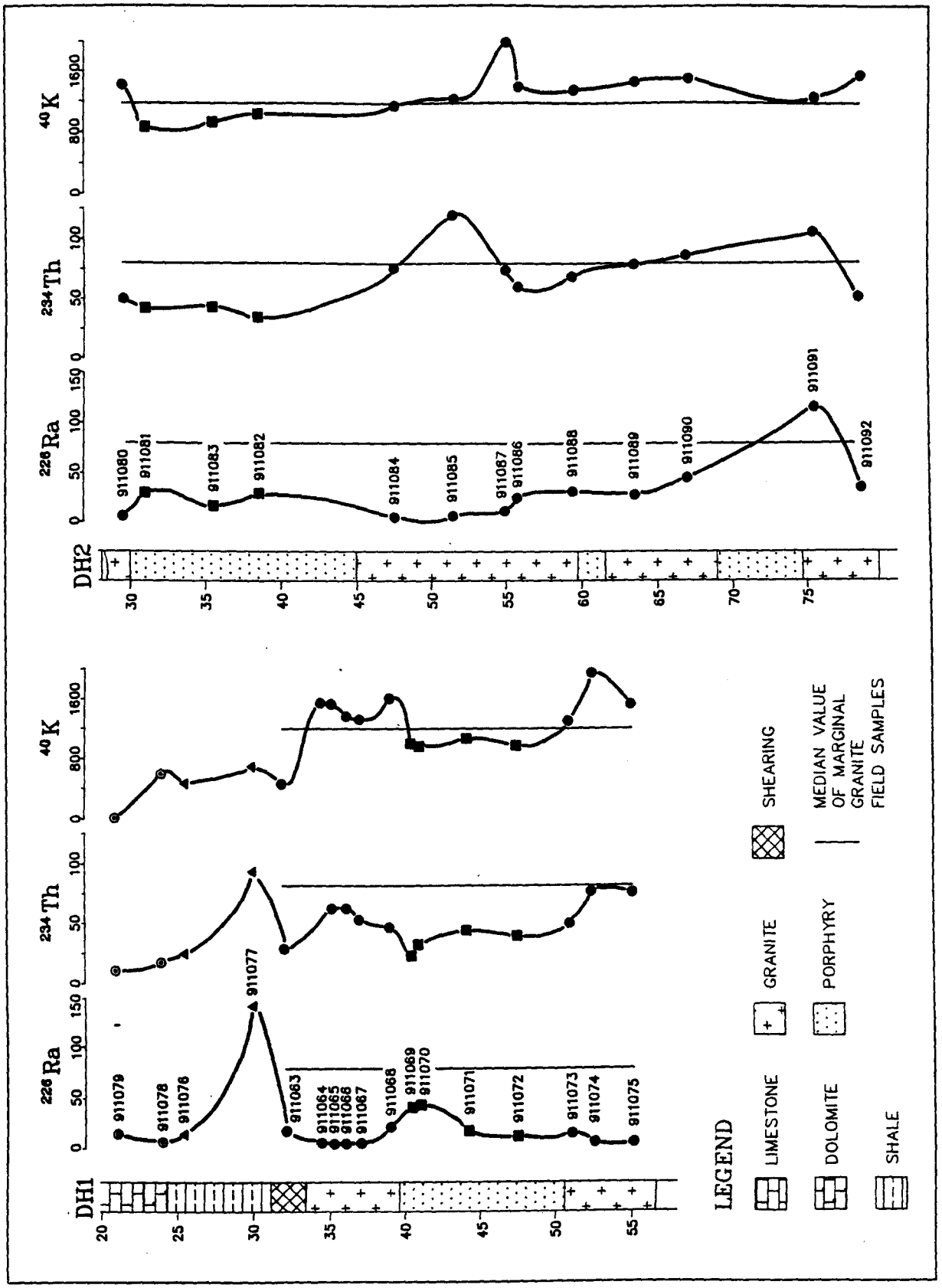


**Figure 10. Variation in $^{226}$Ra, $^{234}$Th and $^{40}$K in cores DH1 and DH2.**

Carboniferous contact at Ballycuirke suggest that Ra and Th have been leached from deformed and altered lithologies. Altered granites have gained K and thus have relatively high $^{40}K$ activities. The *degree* of alteration is also reflected in activities of radionuclides, the most intensely modified granites having the lowest $^{226}Ra$ and $^{234}Th$ activities.

### 1.6.5 Radon in water samples

Introduction

Samples of water were collected from streams, springs and wells in the Moycullen area (Map 1) and analysed for $^{222}Rn$ (Table 4). A total of 22 samples were taken from 20 different sources, which included 4 wells and 2 springs on granite bedrock, 1 well and 1 spring on limestone and 12 streams on granite. Although the Carboniferous limestone is a major aquifer, there are very few springs or wells available for sampling in the area. At least 4 wells marked on 1:2500 maps, which were last surveyed in 1981, have since been lost during land clearance and reclamation. In the future, boreholes preserved as part of the drilling programme may be used to monitor groundwater $^{222}Rn$ activities in limestone. The results of this study, therefore, represent only a preliminary survey.

Analytical techniques

Samples were analysed in the Radiometric Services Laboratory of the British Geological Survey under the supervision of D.K. Talbot and T.K. Ball. The analyses were carried out in accordance with the British Geological Survey's quality assurance procedure "Laboratory detection of Radon in water samples". The results represent the Rn activity at the time of sampling. Correction factors to account for Rn decay between the time of sampling and analysis and for instrument calibration were applied.

Results

1. Granite bedrock

Values of $^{222}Rn$ activity in groundwater taken from wells on granite bedrock range from 63.6 to 125.4 Bq $l^{-1}$. The two lowest values were taken from the same source within 2 minutes of each other. The two spring sources gave values of 27.3 and 38.0 Bq $l^{-1}$, the first from a spring issuing several metres south of the granite margin. Two of the well samples exceed 100 Bq $l^{-1}$ and at least one of these (MYWA 3) is a source of piped drinking water.

In contrast to the values obtained for groundwater in granite, stream water has very low $^{222}Rn$ activity, ranging from 0.0 to 16.2 Bq $l^{-1}$ (median value = 1.4 Bq $l^{-1}$). The two highest values, 16.2 and 12.3 Bq $l^{-1}$, are from small (0.1 to 0.2 m wide) streams near the source. The source is covered by bog: the water seeps from the bog and it is not clear what contact, if any, it has with the granite bedrock which lies close to the surface. Samples MYWA 4 and 5 illustrate the possible relationship: MYWA 4 (16.2 Bq $l^{-1}$) was taken close to the source of the stream, MYWA 5 (1.0 Bq $l^{-1}$) 50 m further downstream.

2. Limestone bedrock

MYWA 12 and 13 were collected from the mouth of a spring. Their $^{222}Rn$ activities of 12.6 and 15.1 Bq $l^{-1}$ are much lower than those in springs on granite. The well sample has a value of 43.8 Bq $l^{-1}$. Thus, both spring and well samples on limestone have $^{222}Rn$

**Table 4**

**Radon in water samples in Moycullen area**

| Sample | Bedrock | Source Type | Radon Activity, Bq $l^{-1}$ |
|---|---|---|---|
| MYWA1 | Limestone | Well | 43.6 |
| MYWA2 | Granite | Well | 89.4 |
| MYWA3 | Granite | Well | 102.2 |
| MYWA4 | Granite | Stream | 16.2 |
| MYWA5 | Granite | 50 m downstream from MYWA4 | 1.1 |
| MYWA6 | Granite | Well | 63.6 |
| MYWA7 | Granite | Same well as MYWA6 | 71.8 |
| MYWA8 | Granite | Well | 125.4 |
| MYWA9 | Granite | Stream, 20 m from source spring | 38.0 |
| MYWA10 | Granite | Loughkip river | 6.1 |
| MYWA11 | Granite | Loughkip river | 0.9 |
| MYWA12 | Limestone | Spring | 12.6 |
| MYWA13 | Limestone | Spring, same as MYWA12 | 15.1 |
| MYWA14 | Granite | Stream, near source | 12.3 |
| MYWA15 | Granite | Spring, at margin of granite | 27.3 |
| MYWA16 | Granite | Stream, near source spring | 6.5 |
| MYWA17 | Granite | Stream | 1.5 |
| MYWA18 | Granite | Stream | 1.5 |
| MYWA19 | Granite | Stream | 0.4 |
| MYWA20 | Granite | Stream, near source | 0.0 |
| MYWA21 | Granite | Stream, near source | 0.0 |
| MYWA22 | Granite | Stream | 1.3 |

activities which are approximately 50% of those on granite bedrock.

## 1.7 Radon in soil gas and dwellings

### 1.7.1 Introduction

Collection and measurement of radon in soil gas and in dwellings in the Moycullen area are described in Annexes 2 and 5 where the results are discussed. In addition to these contributions, the Geological Survey of Ireland carried out studies of the data collected by RPII and BGR in order to:

1) produce integrated maps at 1:2500 scale showing soil gas $^{222}Rn$ and $^{4}He$, $^{222}Rn$ in dwellings and $^{226}Ra$ in soil which can be compared directly with geological and geophysical maps;

2) provide comparative statistical treatment of all $^{222}Rn$ data.

### 1.7.2 Maps

Maps 3, 4 and 5 show $^{222}Rn$ in soil gas and dwellings, $^{4}He$ in soil gas and $^{226}Ra$ in soil in the Ballydotia, Moycullen and Uggool areas, respectively. No attempt has been made to interpret the soil gas $^{4}He$ data which are discussed in detail in Annex 5. The soil gas $^{222}Rn$ data collected by BGR were contoured using GEOEAS, a geostatistical environmental assessment software package developed by the U.S. Environmental Protection Agency. A variogram model of the data was first constructed, then the sample values were kriged and the resulting grid file contoured. The contour maps show broad areas where high and low values of soil gas $^{222}Rn$ might be found. These maps are intended to complement the manually-contoured maps made by BGR. The machine contours do not allow for small, localized anomalies since they are based on weighted averages of many sample points; the manually contoured maps necessarily involve a significant degree of subjectivity.

### 1.7.3 Statistical treatment

The results of analyses of $^{222}Rn$ in soil gas and dwellings are presented and discussed in Annexes 2, 3 and 5. GSI undertook comparative statistical treatment of all data in order to provide detailed geological control of the results. Figs. 11-17 compare the activity of $^{222}Rn$ in soil gas and dwellings to bedrock and soil type.

Fig. 11 is a histogram of soil gas $^{222}Rn$ (Annex 5) subdivided according to bedrock type. The soil gas over granite has a higher median $^{222}Rn$ activity (65500 Bq $m^{-3}$) than that on limestone (37300 Bq $m^{-3}$), although the range for both is similar (2600-186300 and 400-184400 Bq $m^{-3}$, respectively). Fig. 12 shows a more detailed breakdown of the soil gas $^{222}Rn$ activity. Soil gas over Errisbeg Townland Granite has a somewhat higher median $^{222}Rn$ activity (71700 Bq $m^{-3}$) than that over Marginal (Callowfinish) Granite (53300 Bq $m^{-3}$). Soil gas over limestone bedrock within 800 m of the granite-limestone contact has a similar median $^{222}Rn$ activity to that over marginal granite but there is a sharp reduction in overall $^{222}Rn$ activity with increasing distance from the contact. This is well illustrated in Fig. 13 where there is a decrease in the median value of soil gas $^{222}Rn$ activity in soils from within 400m of the contact (median, 57750 Bq $m^{-3}$) to soils over 1200m from the contact (median, 23350 Bq $m^{-3}$). At first sight, this suggests that the Galway Granite is a significant source of $^{222}Rn$ in soil over limestone.

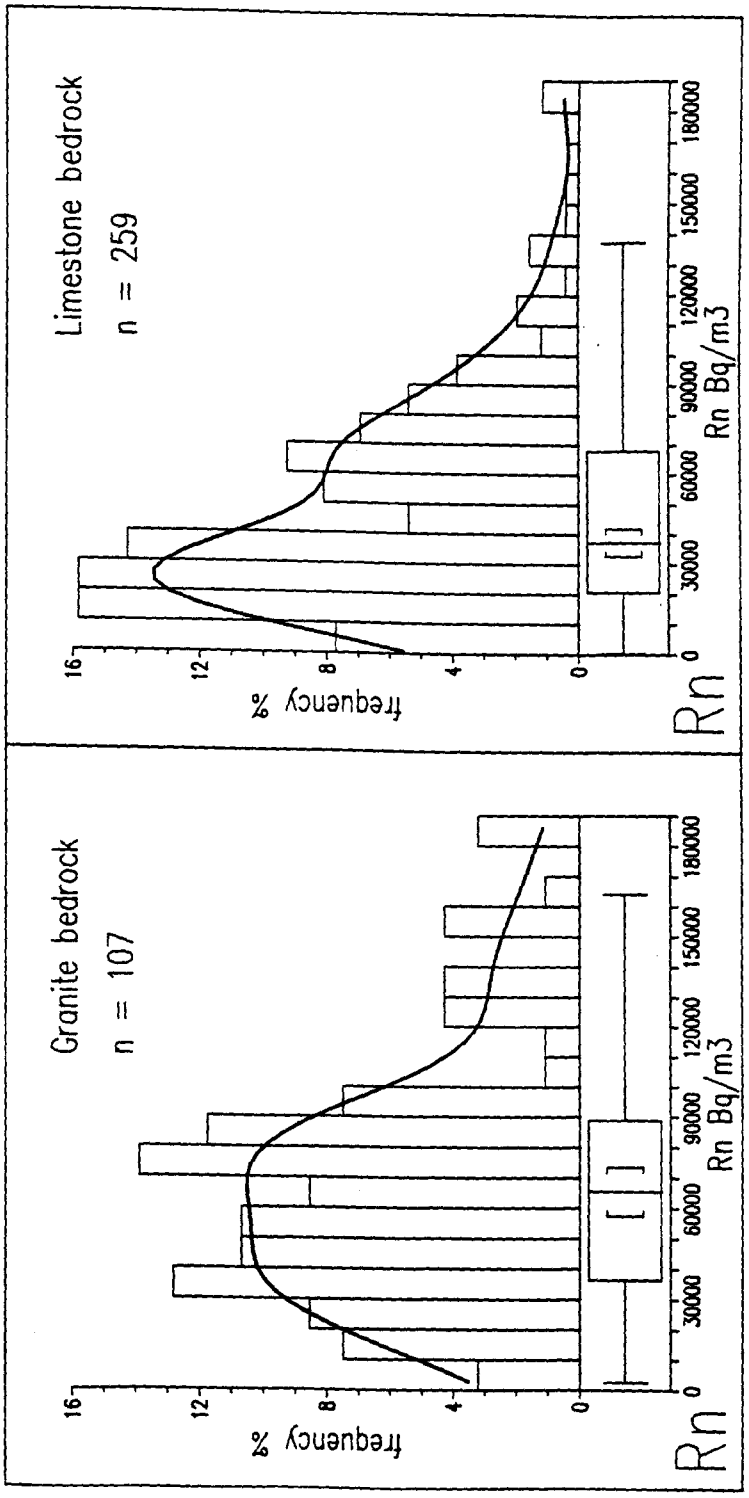


**Figure 11.** **Histograms, density traces and boxplots for soil gas radon activity (BGR) v bedrock type.**

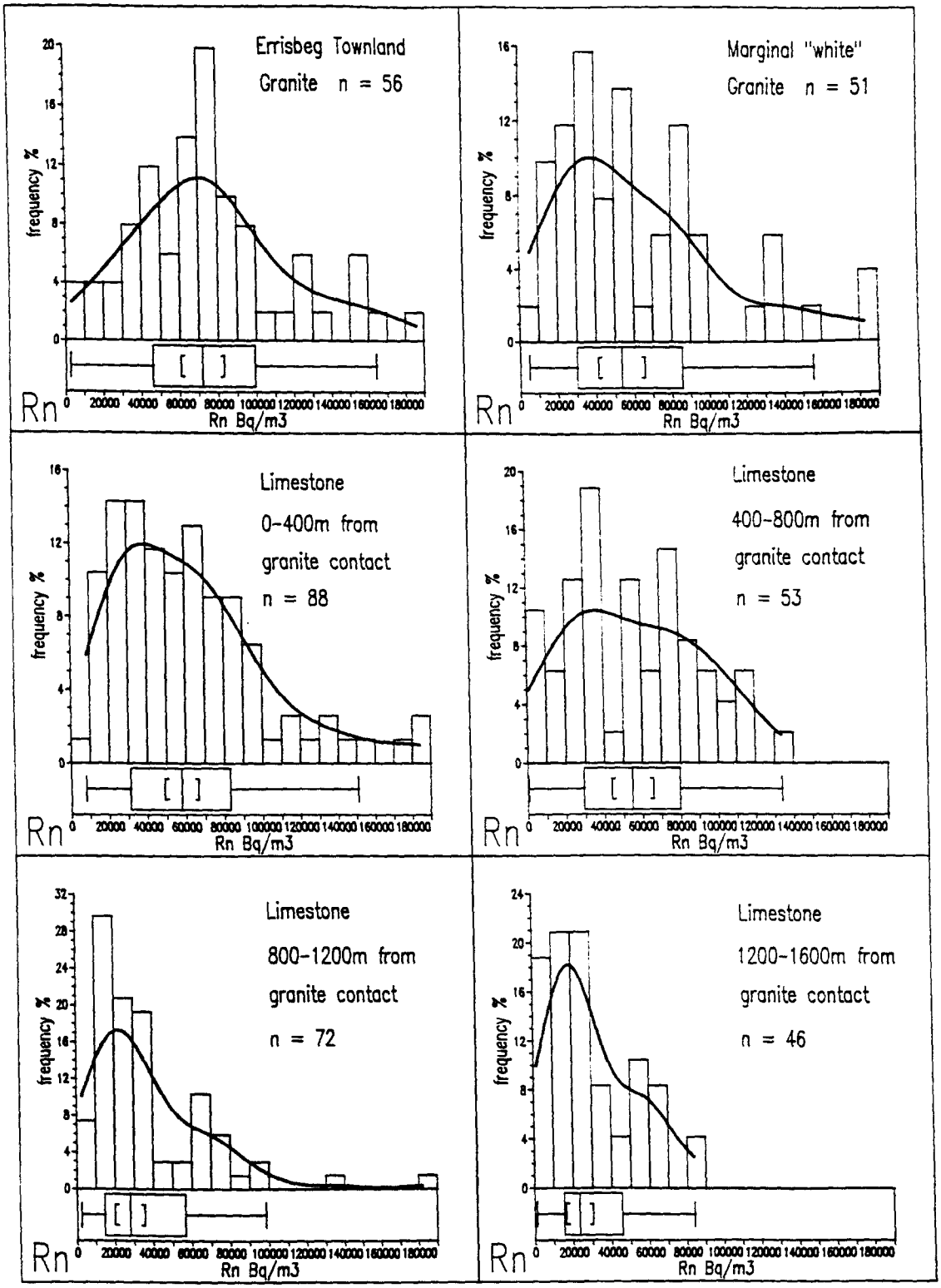


**Figure 12. More detailed breakdown of soil gas radon activity (BGR) v bedrock type.**

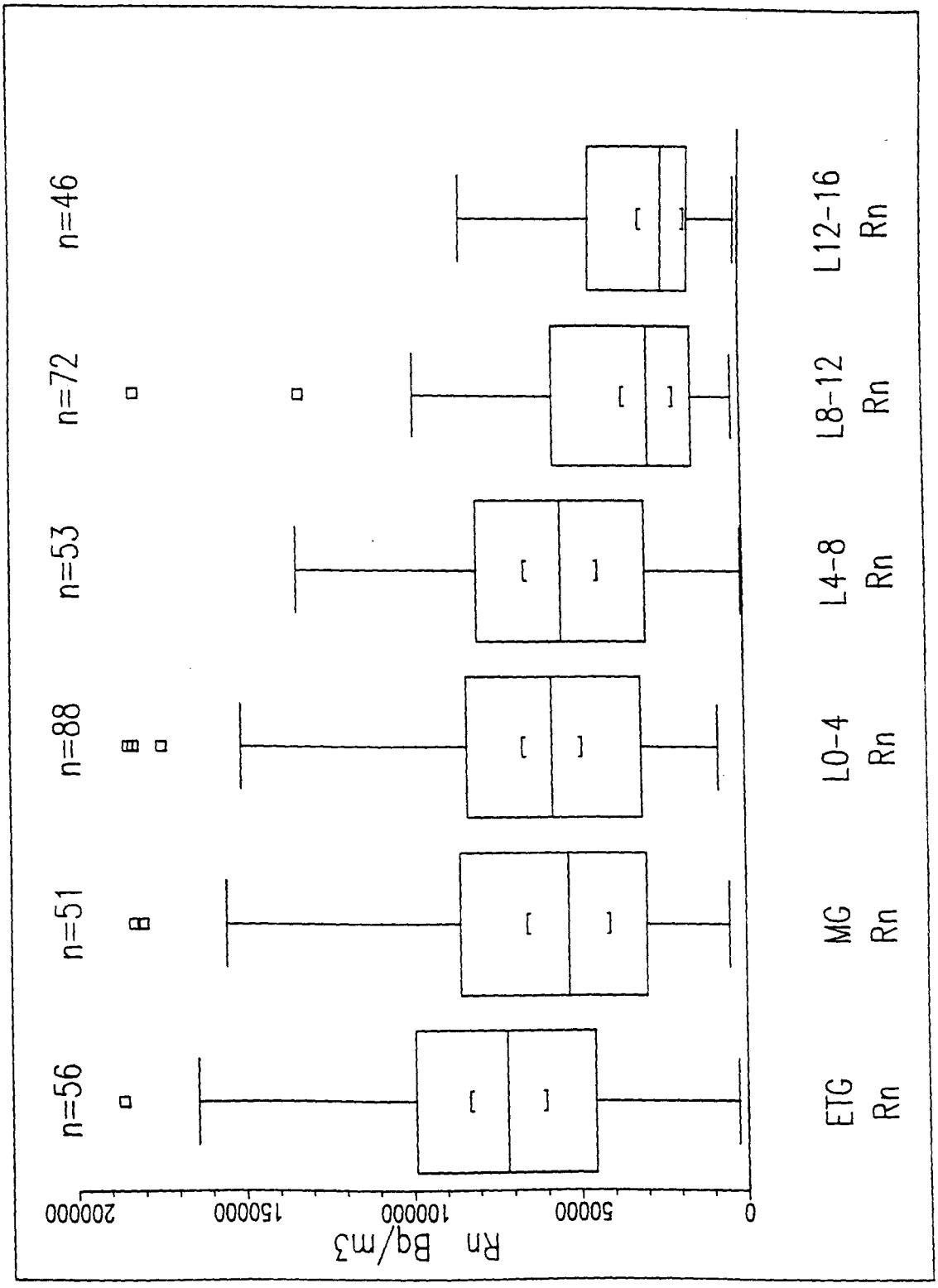


**Figure 13. Boxplots of soil gas radon activity (BGR) grouped according to distance from granite-limestone contact.**

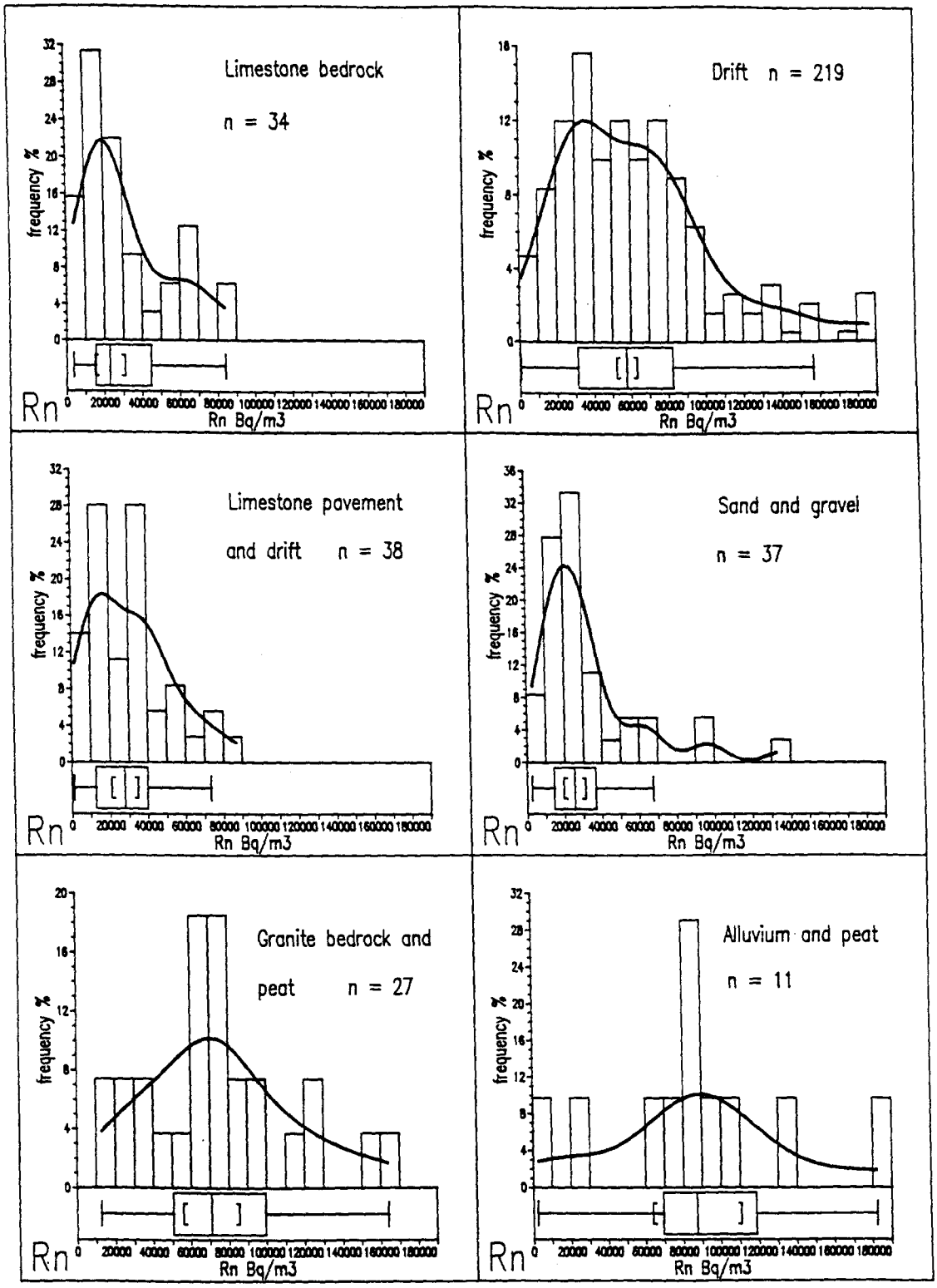


**Figure 14. Soil gas radon activity (BGR) v overburden type.**

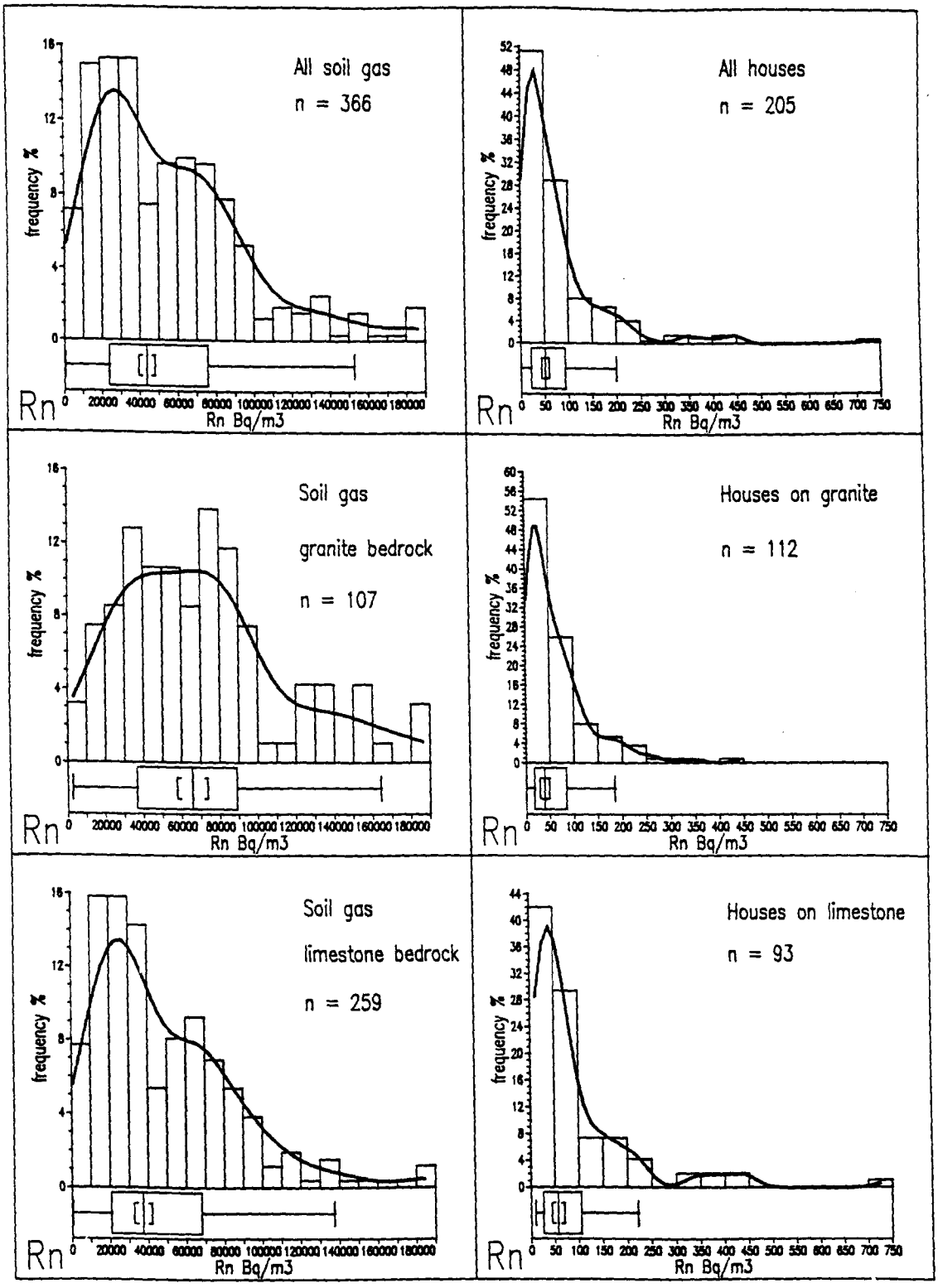


**Figure 15. Indoor radon activity (RPII) v bedrock type**

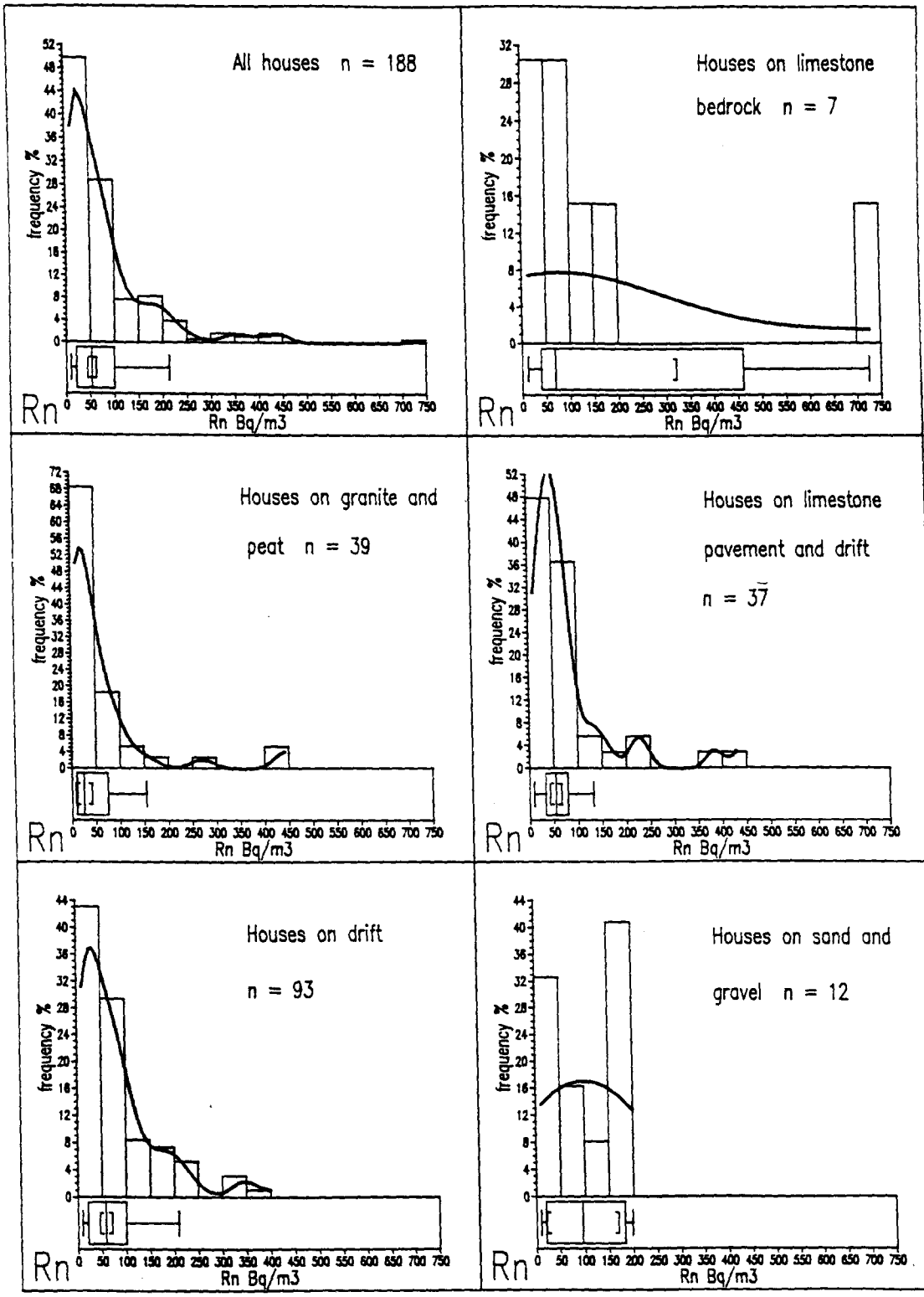


**Figure 16. Indoor radon activity (RPII) v overburden type**

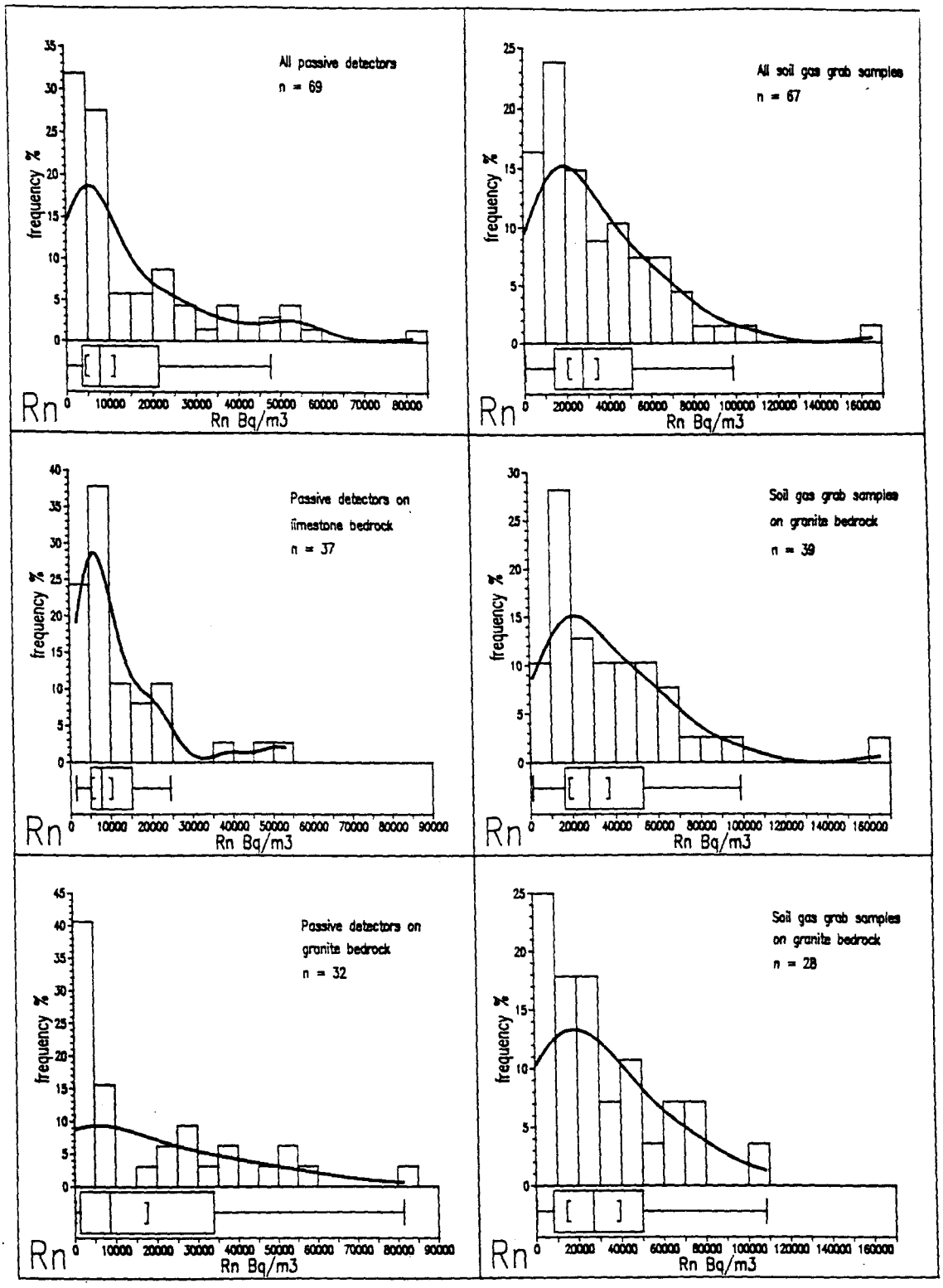


**Figure 17. Soil gas radon activity (RPII, UCD) v bedrock type**

Fig. 14 shows soil gas $^{222}Rn$ compared to overburden (soil) type as defined in section 1.4. The highest median activity values are found in soils overlying granite (drift, peat). An exception is alluvium and peat (median activity 87300 Bq $m^{-3}$) which forms the soil at the margins of lakes, along the contact of the limestone and granite and in upland areas underlain by granite (Map 2). $^{222}Rn$ activities of soil gas in sand and gravel, in drift on limestone and in thin soils covering limestone bedrock are relatively low (median values of 25200, 27750 and 22850 $Bqm^{-3}$, respectively).

Fig. 15 compares the $^{222}Rn$ activity in soil gas and dwellings for granite and limestone bedrock. It is apparent that houses on limestone have a higher range and median value for $^{222}Rn$ activity (range 10-725, median 57 Bq $m^{-3}$) than those on granite (range 0-440, median 39 Bq $m^{-3}$), the opposite of the situation with soil gas. Fig. 16 shows house data on the basis of overburden type. As with soil gas data, it is difficult to detect any strong correlation between $^{222}Rn$ activity and soil type. It can be seen, however, that numerous houses on those areas where the soil is described as limestone pavement and drift and limestone bedrock (Map 2), i.e. very thin soil cover, have values of $^{222}Rn$ activity exceeding 200 Bq $m^{-3}$. In contrast, the soil cover on granite is generally thicker.

Fig. 17 illustrates the soil gas data collected by RPII (Annex 2) and UCD (Annex 3) using active and passive detectors. Median values for soil gas grab samples are similar for both limestone and granite bedrock (27386 and 26765 Bq $m^{-3}$, respectively). Soil gas data collected by using passive detectors have a significantly higher $^{222}Rn$ activity over granite than over limestone (range 60-81463, median 8572 Bq $m^{-3}$ and range 1485-53010, median 7699 Bq $m^{-3}$, respectively).

## 1.8 Acknowledgements

Malachy Carey provided field assistance at various stages of the project and carried out the total-count gamma ratemeter survey (Annex 6). Catherine Delaney compiled the report on the quaternary geology of the project area (section 1.4). Barry Long and Conor MacDermot (Geological Survey of Ireland) provided invaluable insight into the geology of the region.

## 1.9 References

**Bradshaw, R., Plant, A.G., Burke, K.C. and Leake, B.E. (1969)** The Oughterard Granite, Connemara, Co. Galway. *Proceedings of the Royal Irish Academy*, **68B**, 39-65.

**Burke, K.C. (1957)** An outline of the structure of the Galway Granite. *Geological Magazine*, **94**, 452-464.

**Carey, M. (1990)** The geology of Moycullen, Co. Galway. *Unpublished B.Sc. thesis, University College, Dublin.*

**Coats, J.S. and Wilson, J.R. (1971)** The eastern end of the Galway Granite. *Mineralogical Magazine*, **38**, 138-151.

**Damkjaer, A. and Korsbech, U. (1988)** A search for correlation between local geology and indoor radon concentration. *Radiation Protection Dosimetry*, **24 (1)**, 51-58.

**Evans, B.W.E. and Leake, B.E. (1970)** The geology of the Toombeola district, Co. Galway. *Proceedings of the Royal Irish Academy*, **70B**, 105-139.

**Feely, M. (1982)** Geological, geochemical and geophysical studies on the Galway Granite in the Costelloe/Inveran sector, Western Ireland. *Unpublished Ph.D. thesis, National University of Ireland.*

**Feely, M. and Högelsberger, H. (1991)** Preliminary fluid inclusion studies of the Mace Head Mo-Cu deposit in the Galway Granite. *Irish Journal of Earth Sciences*, **11**, 1-10.

**Feely, M. and Madden, J.S. (1986)** A quantitative regional gamma ray survey on the main Galway Granite, Western Ireland. In Andrew, C.J., Crowe, R.W.A., Finlay, S., Pennell, W.M. and Pyne, J.F. (eds.) *The geology and genesis of mineral deposits in Ireland*, Irish Association for Economic Geology, 195-200.

**Feely, M. and Madden, J.S. (1988)** Trace element variation in the leucogranites within the main Galway Granite, Connemara, Ireland. *Mineralogical Magazine*, **52**, 139-146.

**Feely, M., Mccabe, E. and Williams, C.T. (1989)** U, Th and REE-bearing accessory minerals in a high-heat production leucogranite within the Galway Granite, Western Ireland. *Transactions of the Institution for Mining and Metallurgy*, **98**, B27-32.

**Gallagher, V., Feely, M., Högelsberger, H., Jenkin, G.R.T. and Fallick, A.E. (in press)** Geological, fluid inclusion and stable isotope studies of Mo mineralization, Galway Granite, Ireland. *Mineralium Deposita.*

**Hand, B.M. and Banikowski, J.E. (1988)** Radon in Onondaga County, New York: palaeohydrology and redistribution of uranium on Palaeozoic sedimentary rocks. *Geology*, **16**, 775-778.

**Harris, A.L. and Pitcher, W.S. (1975)** The Dalradian Supergroup. In Harris, A.L. and Pitcher, W.S. (eds.) *A correlation of Precambrian rocks in the British Isles*. Special Report of the Geological Society of London, **6**, 52-75.

**Harris, A.L., Baldwin, C.T., Bradbury, H.J., Johnson, H.D. and Smith, R.D. (1978)** Ensialic basin sedimentation: the Dalradian Supergroup. In Bowes, D.R. and Leake, B.E. (eds.) *Crustal evolution in northwestern Britain and adjacent regions*. Geological Journal Special Issue No. 10, 115-138.

**Jagger, M.D., Max, M.D., Aftalion, M. and Leake, B.E. (1988)** U-Pb ages of basic rocks and gneisses intruded into the Dalradian rocks of Cashel, Connemara, W. Irealnd. *Journal of the Geological Society, London*, **145**, 645-648.

**Jenkin, G.R.T., Fallick, A.E. and Leake, B.E. (1992)** A stable isotope study of retrograde alteration in SW Connemara, Ireland. *Contributions to Mineralogy and Petrology*, **110**, 269-288.

**Kennan, P.S., Feely, M. and Mohr, P. (1987)** The age of the Oughterard Granite, Connemara, Ireland. *Geological Journal*, **22**, 273-280.

**Kinahan, G.H. (1869)** Memoirs of the Geological Survey of Ireland (sheet 105).

**Kinahan G.H. and Nolan, J. (1870)** Memoirs of the Geological Survey of Ireland (sheet 95).

**Lawrence, G. (1975)** The use of Rb/Sr ratios as a guide to mineralization in the Galway Granite, Ireland. In Elliot, I.L. and Fletcher, W.K. (eds.) *Geochemical exploration*, Elsevier, 353-370.

**Leake, B.E. (1974)** The crystallization history and mechanism of emplacement of the western part of the Galway Granite, Connemara, Western Ireland. *Mineralogical Magazine*, **39**, 498-513.

**Leake, B.E. (1978)** Granite emplacement: the granites of Ireland and their origin. In Bowes, D.R. and Leake, B.E. (eds.) *Crustal evolution in northwest Britain and adjacent regions*, Geological Journal Special Issue No. 10, 221-248.

**Leake, B.E. (1986)** The geology of SW Connemara, Ireland: a fold and thrust Dalradian and metagabbro-gneiss complex. *Journal of the Geological Society, London*, **143**, 221-236.

**Leake, B.E. (1988)** Comments on the age of the Oughterard Granite, Connemara, Ireland. *Geological Journal*, **23**, 271-272.

**Leake, B.E. and Leggo, P.J. (1963)** On the age relations of the Connemara migmatites and the Galway Granite, west of Ireland. *Geological magazine*, **100**, 193-204.

**Leggo, P.J., Compston, W. and Leake, B.E. (1966)** The geochronology of the Connemara granites and its bearing on the antiquity of the Dalradian series. *Quarterly Journal of the Geological Society of London*, **122**, 91-188.

**Max, M.D., Long, C.B. and Geoghegan, M.A. (1978)** The Galway Granite. *Geological Survey of Ireland Bulletin*, **2**, 223-233.

**McLaughlin, J.P. (1990)** Indoor radon: sources, health effects and control. *Technology Ireland*, **July/August**, 27-30.

**O'Connor, P.J. (1981)** Radioelement geochemistry of Irish granites. *Mineralogical Magazine*, **44**, 485-495.

**O'Connor, P.J. (1986)** Uranium mineralization in the Irish Caledonides. In Andrew, C.J., Crowe, R.W.A., Finlay, S., Pennell, W.M. and Pyne, J.F. (eds.) *The geology and genesis of mineral deposits in Ireland*, Irish Association for Economic Geology, 157-175.

**O'Connor, P.J., Long, C.B. and Hennessy, J. (1983)** Radioelement geochemistry of Irish Newer Caledonian granites. *Geological Survey of Ireland Bulletin*, **3**, 125-140.

**Rogers, G., Dempster, T.J., Bluck, B.J. and Tanner, P.W.G. (1989)** A high-precision U-Pb age for the Ben Vuirich granite: implications for the evolution of the Scottish Dalradian Supergroup. *Journal of the Geological Society, London*, **146**, 789-798.

**Tanner, P.W.G. (1990)** Structural age of the Connemara gabbros, western Ireland. *Journal of the Geological Society, London*, **147**, 599-602.

**Tanner, P.W.G. and Shackleton, R.M. (1979)** Structure and stratigraphy of the Dalradian rocks of the Bennabeola area, Connemara, Eire. In Harris, A.L., Holland, C.H. and Leake, B.E. (eds.) *Caledonides of the British Isles - reviewed*, Geological Society of London Special Publication No. 8, 243-256.

**Wager, L.R. (1932)** The geology of the Roundstone district, Co. Galway. *Proceedings of the Royal Irish Academy*, **41B**, 46-72.

**Wright, P.C. (1964)** The petrology, chemistry and structure of the Galway Granite of the Carna area, Co. Galway. *Proceedings of the Royal Irish Academy*, **63B**, 239-264.

## APPENDIX

**Petrographic descriptions of rock samples from the Moycullen area, Co. Galway.**

### A. Granites and minor dyke rocks: field samples

**91.1002**

Hand specimen: Coarse-grained marginal granite; altered fsp; pyrite in fractures.
Mineralogy: Plag, Kfsp, qz, sericite, biot, chlorite, opaque.
Texture: Granitic; plag euhedral-subhedral.
Grain size: Qz typically 3-5mm; plag 2-4mm; Kfsp up to 10mm; biot 1-2mm.
Deformation: Fracturing, break up of plag and development of sub-grains; strain extinction in qz; biot flexed.
Alteration: Plag to sericite; calcite not identified; biot to chlorite; pyrite to limonite.
Modal comp.: 50% plag; 15-20% Kfsp; 25-30% qz; 2-3% biot.
Comments: Well preserved primary textures; most Kfsp is perthite, some is microcline.

**91.1004**

Hand specimen: Equigranular, white, c. 5mm gr. size, little biot.
Mineralogy: Qz, plag, Kfsp (perthite), biot, chlor, sphene, apatite, zircon, ?rutile, pyrite, Fe-oxide.
Texture: Equigranular; fsp in clusters of euhedral xtals; some biot clusters; "granitic" texture.
Grain size: 3-7mm (qz, fsp); mean 4-5mm.
Deformation: Qz, fsp: strong strain extinction; no obvious fabric; some fractures.
Alteration: Fsp strongly sericitized, identity uncertain; biot->chlor; limonite along fractures, cleavage.
Modal comp: 53% qz; 31% sericitized fsp; 10-12% perth; 4-6% biot (incl. altered biot).
Comment: Heavily altered fsp seems to be either twinned or zoned, i.e. plag, not Kfsp.

**91.1005**

Hand specimen: Grey med-coarse grained granite; abundant pyrite in fractures and in cavities; euhedral drusy qz in cavities.
Mineralogy: Kfsp, plag, qz, biot, chlor, pyrite, sericite.
Texture: Granitic.
Grain size: Qz 1-3mm; plag mostly 2-5mm but some up to 8mm; Kfsp 3-5mm, up to 8mm; biot 0.5-1mm.
Deformation: Strain extinction in qz; fracturing; flexed biot.
Alteration: Fsp to sericite; biot to chlorite and pyrite.
Modal comp.: 20-25% qz; 40-45% plag; 25-30% Kfsp; 3-5% biot and other mafics.
Comments: Well preserved textures; drusy cavities unusual.

contd/

**91.1007**

Hand specimen: Banded brown rk with abund. clustered, chain-linked fsp (< 1mm).
Mineralogy: Matrix: recryst. qz; porph. fsp? - intensely altered, brown in ord. light (cream in H.S.), corroded, brown col. due to limonite; pyrite inclusions, esp at margin.
Texture: Banded; clusterd fsp (?) strung out // banding.
Grain size: Matrix: 0.05-0.15mm; porph. material: 0.25-0.5mm.
Deformation: Apparent fabric defined by elongation of porph. material and its tendency to be strung out // banding; Matrix: no fabric, recryst, strain ext. Some fractures.
Alteration: Of porph. material.
Modal comp: Matrix (almost pure qz) c. 50%.
Comment: This could be a gneiss as suggested by CBLong (pers. comm.) but overall texture suggests a felsite.

**91.1009**

Hand specimen: Fine-grained equigranular grey microgranite.
Mineralogy: Qz, plag, Kfsp, perth, pyrite, kaolin, ? garnet (at one edge).
Texture: Equigr., crushed, remnant euhedral fsp; essentially granitic, but much deformed, recryst.
Grain size: 1-2mm.
Deformation: Crushing, strain extinct., edges of qz granulated, recrystallized.
Alteration: Kaolinization of fsp intense in cores but outer zones may be little altered; grains may be wholly unaffected; ore in cracks & in fsp.
Modal comp: C. 40% qz, 60% fsp.
Comment: Notable absence of biot/mica; fine grain size a factor in low degree of alteration?

**91.1010**

Hand specimen: Fractured, limonite-stained equigranular granite.
Mineralogy: Qz, perth, plag, pyrite, kaolin, sericite, apatite, ?garnet.
Texture: Equigranular, granitic; euhedral fsp.
Grain size: 2-5mm; mean c. 4mm for fsp, qz.
Deformation: Intensely fractured; fsp xtals crenulated; strain extinct. fsp, qz; grain bdy granulation.
Alteration: Intense kaolinization of fsp; py in fractures; py replaces fsp in cores and zones linked by fractures.
Modal comp: 30-40% qz, rest is mostly fsp (Kfsp:plag: 2:1).
Comments: Intense fracturing/alteration make estimate of modal comp difficult. Notably intense conc. of fluid inclusions in qz.

contd/

**91.1012**

Hand specimen: Altered granite; fractured; limonite-stained;crushed (?).
Mineralogy: Plag, Kfsp (perthite, microcline), qz, biot, chlorite, sericite, opaque, apatite.
Texture: Granitic but much granulation, flattening of qz and destruction of interlocking texture.
Grain size: Kfsp up to 10mm and typically 3-6mm; plag 2-4mm; biot < 0.25mm.
Deformation: Fracturing; granulation; foliation of qz; biot, plag and qz bent.
Alteration: Fsp to sericite; biot to chlorite; py along fractures.
Modal comp.: 30% qz; 40-45% plag; 25-30% Kfsp.
Comments: Notably crushed.

**91.1013**

Hand specimen: Pink aplite, coarser material in contact with it.
Mineralogy: Qz, Kfsp (perth, microcline), plag, opaque(py?), chlor, ?apatite.
Texture: Fine aplitic texture.
Grain size: 0.25-0.5mm.
Deformation: Strain extinct., crushing, recryst. and obliteration of clear xtal faces.
Alteration: Kaolinization of fsp; chlor after ?biot; fsp -> opaque.
Modal comp: 30-40% qz; rest is fsp, Kfsp > plag (>2:1).
Comment: At edge of thin section, coarser material in contact with albite consists of qz, Kfsp (incl. microcline). 4mm. Heavily altered. ETG?

**91.1016**

Hand specimen: Yellow-white fsp with grey qz; med gr. grey granite.
Mineralogy: Qz, plag, perth, microcline, chlor, py, Fe ox., biot, apatite, sphene(?).
Texture: Clusters of euhedral fsp; equigranular; granitic.
Grain size: 2-3mm fsp.
Deformation: Fractured; qz, fsp very strained; incipient fabric development // fractures.
Alteration: Biot->chlor; fsp->kaolin;
Modal comp: 30-40% qz; < 5% biot, opaque, chlor etc. Kfsp > plag (1:1 - 2:1).
Comment: Same locality as 91.1010; resembles a more altered variant of 91.1004.

**91.1017**

Hand specimen: Weathered granite; fractured, pyrite-rich, limonite-stained, coarse-grained, white-yellow fsp
Mineralogy: Plag, Kfsp, qz, biot, musc, sericite, pyrite, sphene, chlorite.
Texture: Granitic
Grain size: Plag 2-4mm, Kfsp 3-7mm, qz 1-3mm, mica 0.3-1mm.
Deformation: Severe strain in qz; granulation & recrystallization of qz between larger fsp; biot, musc flexed; fractured.
Alteration: Fsp to sericite; mica to chlorite (minor); biot to pyrite.
Modal comp.: 20-25% qz; 40-45% plag; 25-30% Kfsp; 1-3% mica.

**contd/**

**91.1018**

Hand specimen: Pyrite-rich granite, similar to but more mafic than 91.1017.
Mineralogy: Kfsp, plag, qz, biot, musc, sericite, pyrite, sphene (?).
Texture: Granitic.
Grain size: Plag 1-5mm; Kfsp 3-8mm; qz 1-4mm; mica 0.2-1mm.
Deformation: Severe fracturing; strain in qz led to recryst. and sub-grain growth; some granulation; micas flexed.
Alteration: Fsp to sericite; minor chlorite after biot; biot altered to pyrite; biot near colourless.
Modal comp.: 30% qz; 50-60% plag; 5-10% Kfsp; < 1% mica.

**91.1022**

Hand specimen: Fine, buff-coloured biotite granite.
Mineralogy: Qz, Kfsp (perthite, microcline), plag, green biot chlor, musc, colourless, high relief, low biref. mineral (?) in fsp.
Texture: Equigranular, granitic; less obvious clustering of fsp; relict euhedralism in plag; mostly anhedral.
Grain size: 0.5-1.5mm (qz, fsp).
Deformation: Strain extinct; not much crushing; little fract.
Alteration: Kaolinization of fsp; chlor after biot.
Modal comp: 25-30% qz; Kfsp $\geq$ plag.
Comment: Plag rather than Kfsp is strongly altered as is the case in all samples of granite here, indeed in Galway Granite in general. Implication is that K (from kaolin) was introduced, not remobilized from existing rock.

**91.1023**

Hand specimen: Med-grained granite; white fsp up to 10mm, generally 3-5mm.
Mineralogy: Qz, plag, Kfsp (perthite), biot, pyrite, sericite, chlorite, apatite.
Texture: Granitic; typical patchy Kfsp, euhedral-subhedral plag, patchy recrystallized qz; notably high content of apatite; biot wraps fsp.
Grain size: Plag 1-6mm, typically 2-4mm; Kfsp up to 8mm; biot in clusters of small (<0.1mm) grains.
Deformation: Strain extinction in qz; fracturing and granulation of qz; incipient foliation of biot; flattening of qz.
Alteration: Plag to sericite; minor chlorite after biot; pyrite after biot.
Modal comp.: 50-60% qz; 30-40% plag; 5-10% biot; Kfsp <5% in this section.
Comments: Texture and mineralogy suggest granite; modal comp. closer to that of gneiss.

**91.1025**

Hand specimen: Coarse-grained equigranular granite.
Mineralogy: Qz, plag, perth, microcline, chlor,biot,opaque.
Texture: Equigranular, anhedral qz, fsp; some fsp clustering.
Grain size: Fsp, 2-4mm mostly; qz patches, $\leq$ 7mm but these contain several grains.
Deformation: Fracturing; strain extinction.
Alteration: Kaolinization of Kfsp; biot -> chlor, opaque.
Modal comp: 35-45% qz; rest is mostly fsp.

contd/

Comment: Not very deformed compared to others.

**91.1026**

Hand specimen: Grey granite with white-buff large (up to 10mm) fsp; leucocratic.
Mineralogy: Qz, Kfsp (perthite, microcline), plag, biot, chlor, sericite.
Texture: Granitic; euhedral-subhedral plag intergrown with qz and irregularly shaped patches of Kfsp; qz shows flattening and fsp shows some tendency to be aligned with qz.
Grain size: Plag generally 1-3mm, up to 5mm; Kfsp typically c. 5mm; qz 0.5-3mm.
Deformation: Strain and flattening of qz; granulation of qz; flexing, fracturing and some rotation of plag.
Alteration: Plag, Kfsp to sericite; biot to pyrite.
Modal comp.: 30-35% qz; 20-25% plag; 35-40% Kfsp; <2% biot.
Comment: Notably high in Kfsp, abundant microcline.

**91.1042**

Hand specimen: Grey, appearance of wackestone - qz, fsp as rounded grains, 2-3mm in size: crushed granite?
Mineralogy: Qz, plag, Kfsp, chlorite, biot, musc, opaque.
Texture: Qz and fsp as interlocking grains - granitic; more often as fractured grains with sharp edges, corners; matrix of fragmented qz, fsp and calcite replaces these; chlorite and biot relatively abundant, possibly post-deformation.
Grain size: Larger qz, fsp grains up to 5mm; mostly 0.5-1.5 mm.
Deformation: fracturing, fragmentation of grains; severe strain extinction of qz; some flexing of sheet silicates.
Alteration: Intense - fsp to calcite, biotite to chlorite and opaque.
Modal comp.: Pre-alteration: ? In localized large patches which have not been granulated: 65% fsp, 30% qz.
Comments: Crushed granite? Thrust fault in vicinity?

**91.1052**

Hand specimen: Felsite, flow-banded vertically.
Mineralogy: Qz, fsp, white mica, unident. brown material.
Texture: V. fine matrix of qz, fsp, aligned white mica needles with porphyritic qz, fsp grains; zones of oolith-like spheroids with concentric outer zones of dark brown, limonitic(?) alteration.
Grain size: Matrix: < 0.1mm; phenocrysts: 0.2-0.5mm.
Deformation: Not apparent.
Alteration: Limonite? Brown material is opaque in Xnicols.
Comments: Felsite!

**contd/**

**91.1054**

Hand specimen: V. weathered, limonite-stained fractured granite.
Mineralogy: Qz, plag, Kfsp, biot, chlorite, pyrite, sericite.
Texture: Granitic; fsp near euhedral in places.
Grain size: Fsp up to 7mm, typically 2-4mm; qz sub-grains 2-5mm; biot, chlorite < 1mm.
Deformation: Strain extinction, granulation at edges of grains.
Alteration: Pervasive; fsp to sericite, biot to chlorite, opaque; pyrite in fractures.
Modal comp.: 10-20% qz, 60-80% fsp, < 2% mafics.

**91.1055**

Hand specimen: Coarse-grained greyish granite; prominent mafics; greenish fsp.
Mineralogy: Plag, Kfsp, qz, biot, chlorite, sericite, opaque, garnet, high-relief/biref. mineral = ? monazite.
Texture: Granitic; large Kfsp grains enclosing smaller plags and irregularly-shaped qz; plag euhedral-subhedral; biot as ragged flakes.
Grain size: Kfsp up to 15mm; plag typically 4-6mm; qz 2-7mm; biot 0.5-1.5mm.
Deformation: Fracturing common but granulation minor; strain extinction in qz; largely intact granite texture.
Alteration: Fsp to sericite, calcite; biot to chlorite, opaque.
Modal comp.: 25-40% qz, rest is mostly feldspar.
Comments: Relatively rare example of marginal granite which is essentially undeformed and little altered.

**91.1056F**

Hand specimen: Euhedral, cube-like crystals of qz (?) in v. fine grey-brown matrix; flow banding absent but reported from outcrop.
Mineralogy, texture, etc.: Resembles 91.1007; cracked, spherical grains, apparently of fsp with brown-yellow corona of indeterminate composition but with colour probably due to limonite; fine matrix of fsp, qz with strong greyish alteration which obscures much - calcite? structure of spherical grains appears to be radiate. Grains found in strings or chains. Occasional euhedral plag or rounded qz grains in place of spheroids.

**91.1056P**

Hand specimen: Supposedly a porphyry but resembles felsite.
Mineralogy, texture, etc.: V. like 91.1056F, perhaps less alteration.

**91.1057**

Hand specimen: Fine grey granite; much pyrite; suspected of being gneiss in field.
Mineralogy: Qz, Kfsp, plag, opaque, limonite, biot, calcite(?)
Texture: Abundant micrographic qz-fsp intergrowths; rest has granitic or microgranitic texture.
Grain size: Fsp grains rarely > 0.5mm; typical grain size is 0.1-0.3mm but micrographic patches can exceed 1mm.
Deformation: Fracturing, strain extinction.

**contd/**

Alteration: Limonite, ?calcite.
Modal comp.: Difficult to estimate (fine grain size).
Comments: Dyke rock?

**91.1059**
Hand specimen: Buff-coloured fsp; fragmented granite.
Mineralogy: Mineralogy identical to 91.1054 but grain size larger (4-10mm).
texture, etc. Deformation more intense, with granulation common at margins of grains leading to creation of finer, clastic "matrix". Pyrite and limonite along fractures.

**91.1060**
Hand specimen: Granite, greenish alteration of fsp; grey.
Mineralogy: Plag, Kfsp (perthite, microcline), qz, biot, opaque, sericite, calcite, limonite.
Texture: Granitic; large patches of kfsp with inclusions of smaller, often euhedral plag; limited biot between intergrown qz, Kfsp and plag.
Grain size: Large fsps > 10mm; qz 1-3mm; 2-4mm typical of fsp.
Deformation: Severe strain in qz, flattening also; fsp twin lamellae flexed; limited granulation.
Alteration: Fsp to sericite and calcite; limonite after pyrite.
Modal comp.: 50-75% fsp, rest mainly qz.

**91.1060A**
Hand specimen: Deformed granite, possibly foliated.
Thin section: Similar to 91.1060, strong limonite staining reflects filling of fractures by pyrite. More deformation than in 91.1060.

**MOY 107**
Hand specimen: Fractured, possibly brecciated pink aplite.
Mineralogy: Qz, plag, Kfsp (perthite, microcline), biot, pyrite, sericite, apatite.
Texture: Aplitic.
Grain size: Up to 1.5mm, typically 0.5-1mm.
Deformation: Fracturing; plag flexed.
Alteration: Fsp to sericite; pyrite to limonite.
Modal comp.: Grain size too fine for visual estimation.
Comments: Notable paucity of alteration compared to granites

**MOY 115**
Hand specimen: V. fine greenish-grey feldspathic rock with clear euhedral 1mm sized crystals of qz; porphyry.
Mineralogy,: V. fine, apparently sericitized qz-fsp matrix (<0.1mm); euhedral qz
texture, etc. porphyritic crystals and some fsp; plag and qz in lithic clasts; qz is rounded (resorbed? - fine rim of matrix material on it); qz phenocrysts are 0.5-1mm in size; lithic clasts up to 4mm.
Comments: Typical qz porphyry.

**B. Gneiss: field samples**

**91.1019**

Hand specimen: Grey qz-fsp-mica foliated rock; anhedral fsp up to 3mm in size not aligned in foliation; gneiss.
Mineralogy: Qz, plag (albite-andesine), biotite, opaque (pyrite), sericite.
Texture: Granitic in places; in general, qz and fsp do not interlock in granitic fashion; fsp anhedral, rounded; foliated biot intergrown with and wrapping fsp; qz strained, recryst., flattened; sutured qz-fsp boundaries.
Grain size: Fsp typically 1-2mm; qz similar but due to recryst. and sub-grain growth ranges from <0.1 to 3-4mm.
Deformation: Qz flattened, mica foliated, fsp slightly flattened.
Alteration: Fsp to sericite and pyrite; biot to pyrite.
Modal comp.: 60-65% qz; 25-30% fsp (mainly plag); < 10% biot.
Comments: Possible paragneiss; lack of Kfsp and biot abundance support this.

**91.1020**

Hand specimen: Schistose, grey qz-fsp-biot gneiss; white fsp coarser than in 91.1019, up to 5mm.
Mineralogy: Qz, plag, biot, pyrite, sericite.
Texture: More clearly schistose and gneissose than 91.1019: flattened qz patches wrapped by biot; fsp as elongate zones of small sub-grains; effectively banded with qz and fsp forming proto-bands.
Grain size: Qz, fsp patches 2-10mm long; individual fsp grains v. small; biot (<0.1mm) occurs as sheafs of small grains.
Deformation: High strain, flattening of qz, fsp; bending of biot; fracturing and granulation of qz, fsp.
Alteration: Fsp heavily altered to sericite; biot to pyrite.
Modal comp.: 40-50% qz; 40-50% plag; 5-10% biot.

**91.1021**

Hand specimen: Finer grained gneiss than 91.1019/20; grey, qz-fsp, pyrite-rich, schistose rock; high content of biot.
Mineralogy: Qz, plag, biot, pyrite, sericite.
Texture: Up to 5mm thick bands of recrystallized, flattened qz, not continuous over more than 30-40mm, inter-banded with fsp-rich qz-fsp bands and biotitic lamellae; fsp preserved as single crystals, wrapped by and intergrown with biotite.
Grain size: Fsp 1-2mm; qz more variable, much recryst.
Deformation: Flattening, fracturing of qz and fsp; biot bent; fractures filled by qz, pyrite.
Alteration: Heavy alteration of plag to sericite; biot to pyrite.
Modal comp.: 55-65% qz; 35-40% plag, 2-5% biot.

**contd/**

**91.1024**

Hand specimen: Cracked granite; coarse white-green fsp (>10mm); foliation?
Mineralogy: Qz, plag, biot, pyrite, sericite.
Texture: Proto-gneiss: flattened, elongated patches of qz but euhedral plag which is oriented parallel to qz; incipient development of banding; biot wraps fsp and is generally parallel to foliation.
Grain size: Plag 1-7mm, typically 3-5mm.
Deformation: Intensely fractured; qz flattened recrystallized.
Alteration: Plag to sericite; biot to pyrite.
Modal comp.: 40-50% qz; 45-55% plag; 5% biot.

**C. Breccia: field sample**

**91.1006**

Hand specimen: Breccia; rounded and more angular clasts of felsite.
Mineralogy: Qz-altered fsp matrix; clasts of v. kaolinized feldspathic material or fsp; chlor<-biot; ore; euhedral high birefringence = ?zircon.
Texture: Clast-supported breccia in most of section, with min. rotation; brecciated felsite (porph. fsp in fine qz-fsp matrix; chlor, ore along fractures.
Grain size: Matrix: 0.1mm; fsp clasts (porph. xtals): .5-2.5mm; mainly 0.5-1.5mm; hand spec: 20mm clasts.
Deformation: Chlor very flexed in places; otherwise, inherent.
Alteration: Intense kaolinization; limonite/pyrite on cracks.
Modal comp: Matrix > 60% qz. Matrix = 50% of rock in section.
Comment: Felsite breccia.

**D. Granites, porphyries and shale: borehole samples**

**DH 1**

**91.1063**

Hand specimen: Crushed rock immediately below thrust fault. Mylonitic appearance.
Mineralogy: Qz, plag, Kfsp (incl. perthite), musc, biot, sericite, calcite, kaolin, opaque, lithic frags, apatite, myremekite.
Texture: Almost aplitic; bimodal grain size; fine-grained material between grains of qz and fsp; grains rounded, equidimensional, often sharp-edged, jagged, fractured appearance; some euhedral fsp; grains touch but not intergrown.
Grain size: Qz, fsp 1-1.5 mm and 0.3-0.6 mm.
Deformation: Material between grains looks like crush product; fragmented appearance of grains and "sedimentary" appearance suggest mylonitization, dissaggregation.
Alteration: Fsp kaolinized & altered to calcite, sericite along fractures.
Modal comp.: > 95% qz and fsp, v. little biotite, main Fe phase is opaque (pyrite or Fe oxide).

**contd/**

Comments: Mineralogy and modal comp. suggest that this is crushed marginal granite.

**91.1067**

Hand specimen: Rel. competent white marginal gran, c. 4 m below contact zone.

Mineralogy: Qz, plag, Kfsp, biot, kaolin, chlor, calcite, apatite, opaque, unidentified red-brown mineral assoc with chlor (= biot or rutile?).

Texture: Granitic, basically intergrown qz and fsp; fragmentation at edges of typical granitic patches led to development of large areas of qz-fsp "matrix".

Grain size: Fsp up to 10mm, typically qz and fsp are 3-6 mm; deformation has created smaller grains; biot 0.5-1 mm.

Deformation: Crushing and fract. of fsp, fract. and granulation of qz at edges; qz highly strained; biot flexed.

Alteration: Fsp kaolinized, fractures filled by calcite; qz v. cloudy due to high density of fluid inclusions arrayed along fractures (evidence of circulation of water after granite emplacement); biot partly altered to chlor and opaque.

Modal comp.: c. 80% fsp, 15% qz, max. 5% biot & accessories.

Comments: Typical white marginal granite with above average fsp content in this section. Strong alteration and reaction with hydrothermal fluid indicated.

**91.1068**

Hand specimen: Fract., altered granite (green fsp); rel. high mafic content.

Mineralogy: Kfsp, plag, qz, biot., kaolin, pyrite, brown (cubic?) phase associated with biotite.

Texture: Strongly fract. granitic texture mainly; granulation at edges of larger grains and among smaller grains (qz).

Grain size: Variable: 5-8 mm on average before deformation.

Deformation: Fracturing; biot. bent; granulation of qz, fsp.

Alteration: Fsp to kaolin, sericite and calcite; calcite and pyrite along cracks; biot to pyrite; qz very turbid due to v. high fluid inclusion density.

Modal comp.: c. 60-70 % fsp, 20-30 % qz.

Comments: Sheared granite. Calcite limestone-related?

**91.1071**

Hand specimen: Grey-green porphyry, greenish alteration.

Mineralogy: Qz, plag, calcite, chlorite, sericite, opaque (= pyrite?).

Texture: Fine-grained matrix of qz and fsp; euhedral fsp and near euhedral, rounded qz; matrix-supported but extensive grain-grain contact among qz & fsp phenocrysts suggest felsite rather than porphyry; recrystallization of larger grains common.

Grain size: Fsp: 0.5 to 4 mm, mean .7-1.0 mm, some > 1.5 mm; qz usually 0.25 to 0.5 mm, up to 1.5 mm.

Deformation: Fractures and strain extinction in qz; little else.

Alteration: Most fsp to calcite or sericite; chlorite may be primary rather than alteration of biotite.

Modal comp.: c. 40 % fsp phenocrysts, 10 % qz; 40-50 % matrix; matrix 50-50 qz, fsp; overall, 30-35 % qz, 60-65 fsp, 2-3 % minors (excluding alteration of

**contd/**

fsp).

Comments: Extensive, Ca-rich alteration, lack of strong deformation.

**91.1072**

Hand specimen: Grey porphyry, apparently less altered than 91.1071.

Mineralogy: Fsp, qz, chlorite, calcite, sericite, opaque.

Texture: As 91.1071, a little more matrix-supported - more clearly porphyritic; more qz, in clusters of 3-6 grains.

Grain size: Qz, 0.2-1.5 mm, typically 0.3-0.5 mm; fsp, rarely > 1.5 mm, typically 0.3-0.7 mm; chlorite, 0.1-0.2 mm.

Deformation: Slight flexing of chlorite; some strain extinction of qz; in general, slight.

Alteration: Fsp heavily altered to calcite; rim of sericite on qz due to reaction?; few fluid inclusions in qz compared to granite.

Modal comp.: 15 % qz, 30 % fsp, rest is matrix, i.e. 40 % qz, 55-60 % fsp assuming matrix is 50 % qz and fsp.

**91.1075**

Hand specimen: Pink fsp granite near end of core.

Mineralogy: Fsp (mostly andesine plagioclase), qz, chlorite, sericite, calcite, apatite, opaque.

Texture: Granitic. Coarse, subhedral-anhedral fsp intergrown with qz; strong sutured contact between qz grains.

Grain size: Fsp up to 10 mm, typically 3-6 mm; qz, 2-4 mm; chlorite, 0.5-1.5 mm.

Deformation: Strong strain extinction and fract. in qz; some fract. of fsp; chlorite flexed.

Alteration: Fsp 80% altered to calcite/sericite; calcite in cracks in qz; opaque (pyrite?) replaces chlorite.

Modal comp.: Difficult to estimate: c. 45% qz, 50% fsp, 5-10% chlorite.

Comments: Typical of white granite in grain size; fsp mostly plag. so pink colour is presumbly due to alteration.

**91.1076**

Hand specimen: Shale with pyrite and zone rich in clastics - fossil debris and lithic clasts?

Mineralogy: Mixture of silicate and calcareous clasts; laminated clasts may be shelly

texture fragments; rounded ball-like calcareous material with concentric structure could be ooliths or crinoids; qz and fsp (andesine) clasts, qz very rich in fluid inclusions, fsp little altered compared to material in granite; fractures in qz and fsp filled by calcite; pyrite as irregularly-shaped replacive grains.

Comments: Qz looks like granitic qz but fsp less altered than in granite: ? derived from granite before last hydrothermal alteration?

**91.1080**

Hand specimen: Very friable, altered granite; sheared.

Mineralogy: Qz, fsp, opaques, calcite, minor musc and sericite.

Texture: Rock is broken up, texture not clear- granitic?

Deformation: Intense fracturing of fsp and qz; severe strain extinction in qz; calcite-filled

**contd/**

veins cut silicates; silicates fragmented.

Comments: This is very altered granite; soft matrix is mostly carbonate; greenish muscovite suspected during core logging is probably calcite and chlorite.

**91.1084**

Hand specimen: Competent granite; scattered pyrite; mafic-rich.

Mineralogy: Kfsp, plag, qz, chlorite, calcite, sericite, pyrite.

Texture: Fragmentation of grains disturbs normal granite texture; euhedral-subhedral fsp (esp. plag) broken up and replaced; granulation forms a secondary matrix.

Grain size: Kfsp up to 10mm, but fsp is typically 1-2mm; qz up to 8mm but is mostly fragmented and recrystalized, occurring as 1-2 mm grains; chlorite 0.5-0.8mm, mostly smaller.

Deformation: Intense - crushing, fragmentation, fracturing.

Alteration: Plag to calcite; Kfsp to calcite and sericite along fractures; chlorite to pyrite; pyrite on fractures also.

Modal comp.: qz 30-50%; fsp 60-70% (pre alteration); plag and Kfsp 1:1 prior to alteration.

Comments: Apparent lack of alteration in hand specimen belied by intense deformation and alteration seen in thin section.

**91.1087**

Hand specimen: Cataclasis has led to small rounded grains of qz in matrix composed of altered silicates; fsp survives as large distinct grains.

Mineralogy: Kfsp, plag, qz, biot, opaque, calcite, rutile(?)

Texture: Original texture largely lost - recrystallized, granulated, altered.

Grain size: Largest qz or fsp is c. 10mm; all other sizes below this are represented.

Deformation: Intense.

Alteration: Intense.

Modal comp.: Pointless to estimate.

Comments: Severe deformation and associated alteration render this granite friable; surprisingly, biotite is little altered to chlorite.

**91.1092**

Hand specimen: Fractured but competent granite; altered but biotite present.

Mineralogy: Kfsp, plag, qz, biot, pyrite, calcite, sericite.

Texture: Granitic.

Deformation: Qz strongly strained; fracturing.

Alteration: Fsp generally altered to calcite and sericite, plagioclase most strongly; biot to chlorite on cleavage.

Modal comp.: 25-30% qz, 20-40% Kfsp, 30% plag, 5% biot.

Comments: Alteration and deformation relatively mild; rock is from outside main zone of deformation.

# ANNEX 2

**Contribution of the Radiological Protection Institute of Ireland (formerly the Nuclear Energy Board)**

**J.S. Madden, J. T. Duffy and G. Mackin**

## 2.1 Introduction

The Moycullen area lies about 10 km northwest of Galway city, and straddles the NW-SE trending and NE dipping geological contact between the Main Galway Granite and the Carboniferous karstic limestone sequences.

The choice of the Moycullen area for this project originates in the discovery by University College Dublin in 1985-1989 of elevated indoor radon concentrations in houses on the limestone sequences. Regional follow-up studies by the Radiological Protection Institute (RPII) and UCD in 1989-1991 confirmed these earlier findings, and predicted that 14% $\pm$ 5% of houses in Co. Galway would exceed the adopted national Reference Level of 200 Bq $m^{-3}$. In addition the regional survey identified an anomalous area in Co. Galway, which incorporates Moycullen, in which 24% $\pm$ 9% of the houses were predicted to exceed the Reference Level. Radon concentrations monitored in houses in the Moycullen area during the regional survey ranged from 42 Bq $m^{-3}$ up to 1751 Bq $m^{-3}$.

## 2.2 Objectives

The objectives of the RPII in this project were:

(i) To approach and obtain on behalf of the Research Group the participation of householders, and to determine the geographical distribution of indoor radon concentrations in selected townlands within the Moycullen postal district.

(ii) To approach and obtain on behalf of the Research Group the further participation of specific householders whose houses were selected for detailed follow-up site investigations, and

(iii) To participate in site specific investigations

## 2.3 Geographical Distribution of Indoor Radon Concentrations

Sample Selection

A total of 494 householders in selected townlands within the Moycullen postal district were contacted by the RPII regarding participation in this project, and radon measurements were completed in 235 houses. The geographical distribution of participating houses is presented in Figure 2.1. One hundred and nineteen houses are located on the country rock to the NE of the granite/country rock geological contact with 116 houses located on the granite to the SW of the contact. All houses were plotted on 1: 10560 O.S. maps and subsequently digitised by the Geological Survey of Ireland (GSI).

Indoor Radon Gas Measurement Technique

Time integrated radon gas concentrations were measured using the standard RPII domestic radon dosemeter. This dosemeter is a passive, closed, alpha track radon detector which is left undisturbed in a ground floor bedroom or living area for a minimum exposure period of 90 days. It consists of a closed cylindrical plastic bottle with a screw-on lid. The alpha particle detecting medium i.e. polyallyl-diglycol carbonate or as it is commonly called

CR-39, is positioned inside the lid, and is held in place when the lid is closed by a small plastic insert placed inside the bottle. The lid on the bottle is sufficiently close fitting to exclude the ingress of radon decay products and airborne particulates into the sensitive volume, but quite easily permits the diffusion of radon gas.

On return the radon detectors were chemically etched, and counted by manual microscopy. The etching conditions used in this work were 10 N Sodium Hydroxide (Na OH) at 70°C for 8 hours. The radon dosemeters were calibrated by participation in the recent series of intercomparisons carried out by the CEC.

## 2.4 Site Specific Investigations

Site Selection

After consultation with our contract partners 20 houses, equally divided between the granite and limestone regions were selected for detailed site investigations. RPII personnel canvassed the support of these householders, and all subsequently agreed to participate further in the project. Site investigations were completed at 18 houses, and all site locations were plotted on 1: 2500 O.S. maps. The selected sites contained houses with both high and low indoor radon concentrations on both sides of the granite/country rock geological contact. All site investigations were jointly carried out by RPII, UCD and TCD personnel.

Site Investigations

At each site the following measurements were conducted.

(i) Soil gas radon concentrations were measured using passive, integrating CR-39 alpha track radon detectors. The detectors were buried in the soil at depths ranging from 30 cm up to 123 cm as close as possible to the house.

(ii) Instantaneous soil gas radon concentrations were measured using a grab sampling technique with Lucus cells and a Pylon AB-5 Radiation Monitoring System. Soil gas samples were taken from depths ranging from 30 cm to 70 cm as close as possible to the house.

(iii) Terrestrial gamma radiation measurements 1m above ground level were made at each site using a Mini Instruments Environmental Meter (Type 6-80).

In addition to the above measurements the RPII supplied passive radon detectors to University College Galway (UCG), a sub-contractor to the GSI. These detectors were displayed by UCG in several deep boreholes drilled by GSI in the Moycullen area.

## 2.5 Measurement Techniques

Passive Integrated Soil Gas Radon Measurements

Integrated soil gas radon concentrations were measured using the standard RPII domestic radon dosemeter. Site conditions permitting a portable Cobra drill with a 4.5 cm diameter soil sampling head was used to penetrate the overburden to a depth of at least 1 m. The borehole was then cased with tight fitting plastic tubing to preserve the hole, and sealed

at the surface end with an air-tight rubber cap. Passive detectors were displayed inside the casing by suspending them from the rubber cap (see Figure 2.2a). All detectors were suspended in the boreholes so as to hopefully remain above the water table.

Difficult and unfavourable ground conditions at most sites dictated that practically all passive radon detectors were deployed and retrieved by manual excavation of the soil. Holes were dug by pick and shovel to practical attainable depths, and the radon detectors positioned on top of a stable base, usually a small stone, and covered with a plastic cup for protection (see Figure 2.2b). The holes were then back filled and marked. After an exposure period of 190 hours the detectors were retrieved for processing. Where possible the measurements were taken in original soil as opposed to imported top soil.

Instantaneous Soil Gas Radon Measurements

Soil gas was extracted from the ground by sucking through a 4 mm internal diameter hydraulic pipe into Lucas cells (see Figure 2.2c). To ensure a representative sample of soil gas was obtained a flow-through method was adopted whereby at least 1 l of soil gas was flushed through the Lucas cells. The RPII Lucas cells have volumes of 161 ml and 271 ml respectively.

After a minimum delay period of at least 3 hours the Lucas cells were counted on a Pylon AB-5 Radiation Monitoring System. Radon concentrations were determined using appropriate calibration factors and sample decay corrections. Following completion of counting the cells were flushed through with outdoor air in preparation for use the following day. Likewise where possible all measurements were taken in original soil.

Terrestrial Gamma Radiation Measurements

Terrestrial gamma radiation measurements were taken at 2 locations at each site, at least 10 m away from the nearest building or outcrop. The energy compensated GM tube was placed in a vertical position with its centre approximately 1 m above ground level. The counting period was 1000 seconds and the results displayed in $\mu$Gy $h^{-1}$. An average cosmic ray contribution of 0.04 $\mu$Gy $h^{-1}$ was subtracted from each reading to give the terrestrial gamma radiation component.

Intercomparison of Instantaneous Soil Gas Radon Measurement Techniques

An intercomparison of the radon grab sampling techniques employed in the field by RPII and BGR was undertaken at the RPII Radon Calibration Facility in Dublin. The intercomparison was performed under laboratory controlled conditions in the walk-in Radon Chamber, and also under typical field conditions in the grounds of UCD.

## 2.6 Results

Geographical Distribution of Indoor Radon Concentrations

In the survey area indoor radon concentrations range from 8 Bq $m^{-3}$ up to 725 Bq $m^{-3}$ with an arithmetic mean concentration of 82 Bq $m^{-3}$ and a median concentration of 53 Bq $m^{-3}$. Ten percent of the houses have concentrations in excess of 200 Bq $m^{-3}$. there is no obvious systematic spatial pattern in the data, and high and low concentrations occur, often contiguously, over the granite and limestone.

From a purely lithological basis the indoor radon concentrations in general tend to be higher in houses underlain by country rock. Thirteen percent of such houses have radon

concentrations in excess of 200 Bq $m^{-3}$ as against 6% of houses on the granite. Indoor radon concentrations range from 10 Bq $m^{-3}$ up to 725 Bq $m^{-3}$ in houses underlain by country rock with an average concentration of 97 Bq $m^{-3}$ and a median concentration of 59 Bq $m^{-3}$. In contrast indoor radon concentrations range from 8 Bq $m^{-3}$ up to 440 Bq $m^{-3}$ in houses underlain by granite with an average concentration of 68 Bq $m^{-3}$ and a median concentration of 33 Bq $m^{-3}$.

Site Investigations

The results of all passive integrated soil gas radon measurements, instantaneous soil gas radon measurements and terrestrial gamma radiation measurements are presented in Tables 2.1 and 2.2.

Time integrated soil gas radon concentrations range from less than 100 Bq $m^{-3}$ up to 81,000 Bq $m^{-3}$ on the granite side of the geological contact in contrast to concentrations ranging from 1,400 Bq $m^{-3}$ up to 38,000 Bq $m^{-3}$ on the limestone side.

Instantaneous soil gas radon concentrations range from 330 Bq $m^{-3}$ up to 108,000 Bq $m^{-3}$ on the granite side of the contact and from 4,500 Bq $m^{-3}$ up to 165,000 Bq $m^{-3}$ on the limestone side. On both sides of the geological contact some of the highest recorded instantaneous soil gas radon concentrations are normally associated with the lowest indoor radon concentrations.

Terrestrial gamma radiation measurements indicate absorbed doses ranging from 38 nGy $h^{-1}$ up to 60 nGy $h^{-1}$ with an average value of 48 nGy $h^{-1}$ on the limestone side of the contact in contrast to doses ranging from 44 nGy $h^{-1}$ up to 70 nGy $h^{-1}$ with an average value of 58 nGy $h^{-1}$ on the granite side.

The higher values over granite are to be expected because of the uraniferous nature of the Galway Granite Batholith.

Intercomparison Exercise

The results of the intercomparison of RPII and BGR grab sampling techniques are presented in Table 2.3. Good agreement between both techniques under laboratory and field conditions is evident.

Passive Radon Detectors Deployed in Deep Boreholes

The results form passive radon detectors deployed in GSI boreholes are presented in Table 2.4. Soil gas radon concentrations range from 657 Bq $m^{-3}$ up to 12,874 Bq $m^{-3}$ with no apparent anomalous concentrations present. However, the degree of atmosphere dilution of radon in the boreholes is unknown, as is the degree of air mixing from the various open cavities encountered in the boreholes. As the first attempt at determining radon concentrations from boreholes which intersect sub-surface cavities the soil gas radon concentrations are not significantly elevated.

## 2.7 Conclusion

No apparent correlation between indoor radon concentrations and site specific soil gas radon concentrations is evident. The occurrence of high and low indoor radon concentrations, often contiguously over both granite and country rock, suggests that other parameters such as house characteristics and site specific geological geophysical and hydrogeological features must contribute in no small way to radon ingress into domestic

dwellings in the area.

**Table 2.1**

**Summary of time-integrated soil gas radon and terrestrial gamma radiation data for site specific investigations**

| House Number | Rock Type | Hole Number | Depth cm | Integrated Soil Gas Radon Conc. Bq m-3 | Indoor Radon Conc. Bq $m^{-3}$ | Absorbed Dose in Air 1m above ground level nGy $h^{-1}$ |
|---|---|---|---|---|---|---|
| 211 | LST | DH1 | 43 | 4395 | 430 | 45 |
| | | DH2 | 40 | 2843 | | |
| | | CH1 | 38 | 2282 | | |
| 210 | LST | DH3 | 50 | 5445 | 376 | 50 |
| | | DH4 | 65 | 7770 | | |
| 206 | LST | CH2 | 123 | 6670 | 44 | 46 |
| 6 | LST | CH4 | 100 | 8666 | 120 | 55 |
| | | CH5 | 100 | 11013 | | |
| 13 | LST | DH5 | 40 | 3943 | 12 | 40 |
| | | DH6 | 45 | 1818 | | |
| 8 | LST | DH7 | 46 | 9798 | 17 | 45 |
| | | DH8 | 45 | 17247 | | |
| 10 | LST | DH9 | 46 | 7457 | 725 | 55 |
| | | DH10 | 52 | 7699 | | |
| 269 | LST | CH12 | 100 | 38340 | 326 | 60 |
| | | CH13 | 60 | 6016 | | |
| | | CH14 | 110 | 24440 | | |
| 45 | LST | DH16 | 32 | 1485 | 231 | 38 |
| 453 | GNT | DH11 | 47 | 8460 | 28 | 60 |
| | | DH12 | 50 | 17470 | | |
| 464 | GNT | DH13 | 50 | 6626 | 440 | 70 |
| 454 | GNT | CH6 | 85 | 1784 | 29 | 70 |
| | | CH7 | 118 | 27298 | | |

/...

| House Number | Rock Type | Hole Number | Depth cm | Integrated Soil Gas Radon Conc. Bq m-3 | Indoor Radon Conc. Bq $m^{-3}$ | Absorbed Dose in Air 1m above ground level nGy $h^{-1}$ |
|---|---|---|---|---|---|---|
| 459 | GNT | CH8 | 100 | 26546 | 265 | 70 |
| | | CH9 | 110 | 28098 | | |
| 155 | GNT | DH14 | 40 | 3588 | 343 | 50 |
| | | DH15 | 45 | 81463 | | |
| 154 | GNT | CH10 | 110 | 37920 | 67 | 55 |
| | | CH11 | 100 | 588 | | |
| 301 | GNT | CH15 | 70 | 178 | 25 | 44 |
| | | CH16 | 100 | 8684 | | |
| 298 | GNT | CH17 | 76 | 60 | 10 | 57 |
| | | CH18 | 100 | 90 | | |
| 79 | GNT | DH17 | 33 | 2931 | 10 | 58 |

* LST = Limestone, GNT = Granite, DH = Dug Hole, CH = Cobra Hole

**Table 2.2**
**Summary of Instantaneous Soil Gas Radon Data for Site Specific Investigations**

| House Number | Rock Type | Hole Number | Depth cm | Instantaneous Soil Gas Radon Conc. Bq $m^{-3}$ | | Indoor Radon Concentration |
|---|---|---|---|---|---|---|
| 211 | LST | SG1 | 30 | 8290 | To the rear | 430 |
| | | SG2 | 60 | 19840 | of house | |
| | | SG3 | 40 | 41752 | To the front | |
| | | SG4 | 45 | 27386 | of house | |
| 210 | LST | SG5 | 35 | 16825 | To the rear | 376 |
| | | SG6 | 50 | 32210 | of house | |
| | | SG7 | 53 | 11398 | To the front of house | |
| 206 | LST | SG8 | 45 | 43557 | To the front | 44 |
| | | SG9 | 50 | 98585 | of house | |
| | | SG10 | 53 | 165,154 | To the rear of house | |
| 6 | LST | SG11 | 58 | 74987 | To the side | 120 |
| | | SG12 | 58 | 23650 | of house | |
| 13 | LST | SG13 | 40 | 36532 | To the rear | 12 |
| | | SG14 | 40 | 14507 | of house | |
| 8 | LST | SG15 | 40 | 13646 | To the rear | 17 |
| | | SG16 | 40 | 26013 | of house | |
| 10 | LST | SG17 | 50 | 4563 | To the rear | 725 |
| | | SG53 | 53 | 66860 | of house | |
| 269 | LST | SG41 | 55 | 33421 | To the front | 326 |
| | | SG42 | 58 | 60354 | To the rear | |
| | | SG43 | 55 | 51211 | To the side | |
| 45 | LST | SG35 | 45 | 18510 | To the side | 231 |
| | | SG36 | 65 | 45520 | of house | |
| | | SG37 | 40 | 17000 | To the front of house | |
| 453 | GNT | SG58 | 50 | 29281 | To the rear | 28 |
| | | SG59 | 50 | 1839 | of house | |
| 464 | GNT | SG19 | 60 | 15952 | To the rear | 440 |
| | | SG20 | 70 | 1608 | of house | |

/...

| House Number | Rock Type | Hole Number | Depth cm | Instantaneous Soil Gas Radon Conc. Bq $m^{-3}$ | | Indoor Radon Concentration |
|---|---|---|---|---|---|---|
| 454 | GNT | SG21 | 65 | 42026 | To the front | 29 |
| | | SG22 | 50 | 13569 | To the rear | |
| | | SG23 | 50 | 79971 | To the side | |
| 459 | GNT | SG24 | 65 | 75418 | To the front | 265 |
| | | SG25 | 65 | 29935 | To the rear | |
| 155 | GNT | SG26 | 60 | 10031 | To the front | 343 |
| | | SG27 | 40 | 28603 | of house | |
| 154 | GNT | SG28 | 50 | 108372 | To the front | 67 |
| | | SG29 | 40 | 43998 | To the rear | |
| 301 | GNT | SG30 | 50 | 2477 | To the front | 25 |
| | | SG31 | 50 | 18551 | To the rear | |
| 298 | GNT | SG32 | 65 | 750 | To the front | 10 |
| | | SG33 | 65 | 330 | of house | |
| | | SG34 | 65 | 33690 | To the rear | |
| 79 | GNT | SG38 | 40 | 24930 | To the side | 10 |

* SG = Soil Gas

**Table 2.3**

**Results of intercomparison of Radon equipment**

| | | Volume | Counts/10 min | Radon Concentration Bq $m^{-3}$ |
|---|---|---|---|---|
| Field Test | RPII | 161 ml | 4771 | 23320 |
| | BGR | 10 ml | 300 | 24630 |
| Lab. Test | RPII | 161 ml | 11359 | 54260 |
| | BGR | 10 ml | 660 | 55500 |

**Table 2.4 Borehole Passive Radon Detectors**

| Detector No. | Borehole Location | Radon Conc. Bq $m^{-3}$ |
|---|---|---|
| 6501 | Ballydotia, opposite House No. 10, vertical borehole, 1.2 m below ground level | 657 |
| 6502 | Ballydotia, opposite House No. 10, vertical borehole, 3.4 m below ground level | 3645 |
| 6510 | Ballydotia, under House No. 10, inclined borehole, 0.8 m along axis of hole | 9127 |
| 6512 | Ballydotia, under house No. 10, inclined borehole, 4.7 m along axis | 1480 |
| 6514 | Ballydotia, under House No. 10, inclined borehole, 9.6 m along axis | 12874 |
| 6505 | Clydagh Bridge, DH 2, inclined borehole, 1.5 m along axis of hole | 1741 |
| 6506 | Clydagh Bridge, DH 2, inclined borehole, 0.2 m along axis of hole | 1588 |

## Appendix
## Indoor $^{222}$Rn activities in houses in Moycullen area, Co. Galway

| | Original Bnumber | | Original Bnumber |
|---|---|---|---|
| 48.000 | 168 | 63.000 | 32 |
| 42.000 | 170 | 21.000 | 33 |
| 132.000 | 174 | 123.000 | 35 |
| 53.000 | 176 | 64.000 | 39 |
| 163.000 | 177 | 29.000 | 40 |
| 70.000 | 182 | 33.000 | 41 |
| 24.000 | 183 | 57.000 | 42 |
| 10.000 | 190 | 54.000 | 43 |
| 52.000 | 192 | 231.000 | 45 |
| 150.000 | 194 | 32.000 | 47 |
| 129.000 | 196 | 184.000 | 50 |
| 200.000 | 197 | 93.000 | 51 |
| 10.000 | 198 | 92.000 | 52 |
| 67.000 | 201 | 70.000 | 54 |
| 78.000 | 202 | 174.000 | 55 |
| 10.000 | 205 | 343.000 | 60 |
| 44.000 | 206 | 152.000 | 63 |
| 19.000 | 209 | 61.000 | 66 |
| 376.000 | 210 | 294.000 | 71 |
| 430.000 | 211 | 10.000 | 72 |
| 38.000 | 216 | 105.000 | 73 |
| 24.000 | 217 | 209.000 | 74 |
| 10.000 | 218 | 76.000 | 76 |
| 73.000 | 220 | 100.000 | 78 |
| 109.000 | 222 | 10.000 | 79 |
| 70.000 | 228 | 10.000 | 81 |
| 115.000 | 236 | 20.000 | 82 |
| 14.000 | 237 | 46.000 | 83 |
| 32.000 | 239 | 25.000 | 84 |
| 13.000 | 241 | 32.000 | 86 |
| 10.000 | 242 | 16.000 | 89 |
| 10.000 | 244 | 35.000 | 91 |
| 42.000 | 245 | 48.000 | 93 |
| 67.000 | 246 | 79.000 | 100 |
| 107.000 | 247 | 96.000 | 103 |
| 23.000 | 255 | 72.000 | 105 |
| 88.000 | 258 | 55.000 | 106 |
| 22.000 | 259 | 34.000 | 107 |
| 10.000 | 262 | 10.000 | 108 |
| 120.000 | 263 | 24.000 | 109 |
| 26.000 | 266 | 17.000 | 110 |
| 340.000 | 268 | 64.000 | 113 |
| 326.000 | 269 | 44.000 | 121 |
| 43.000 | 270 | 81.000 | 122 |
| 47.000 | 277 | 10.000 | 125 |
| 57.000 | 278 | 54.000 | 126 |
| 24.000 | 280 | 132.000 | 129 |
| 72.000 | 281 | 43.000 | 133 |
| 21.000 | 283 | 10.000 | 134 |
| 10.000 | 285 | 32.000 | 138 |
| 40.000 | 286 | 62.000 | 139 |
| 116.000 | 288 | 33.000 | 141 |
| 21.000 | 291 | 29.000 | 143 |
| 10.000 | 293 | 10.000 | 146 |
| 16.000 | 294 | 60.000 | 147 |
| 31.000 | 295 | 29.000 | 149 |
| 10.000 | 298 | 16.000 | 150 |
| 75.000 | 299 | 52.000 | 153 |
| 80.000 | 300 | 67.000 | 154 |
| 25.000 | 301 | 343.000 | 155 |
| 26.000 | 302 | 245.000 | 157 |
| 11.000 | 303 | 17.000 | 159 |
| 13.000 | 304 | 21.000 | 160 |
| 213.000 | 307 | 71.000 | 161 |
| 105.000 | 308 | 10.000 | 162 |
| 164.000 | 313 | 59.000 | 165 |

| | Original Bnumber | | Original Bnumber |
|---|---|---|---|
| 48.000 | 168 | 180.000 | 314 |
| 42.000 | 170 | 184.000 | 318 |
| 132.000 | 174 | 25.000 | 320 |
| 53.000 | 176 | 10.000 | 321 |
| 163.000 | 177 | 85.000 | 324 |
| 70.000 | 182 | 154.000 | 326 |
| 24.000 | 183 | 52.000 | 333 |
| 10.000 | 190 | 10.000 | 335 |
| 52.000 | 192 | 81.000 | 337 |
| 150.000 | 194 | 12.000 | 338 |
| 129.000 | 196 | 205.000 | 340 |
| 200.000 | 197 | 18.000 | 341 |
| 10.000 | 198 | 21.000 | 348 |
| 67.000 | 201 | 10.000 | 349 |
| 78.000 | 202 | 24.000 | 352 |
| 10.000 | 205 | 396.000 | 356 |
| 44.000 | 206 | 29.000 | 357 |
| 19.000 | 209 | 78.000 | 358 |
| 376.000 | 210 | 58.000 | 364 |
| 430.000 | 211 | 16.000 | 365 |
| 38.000 | 216 | 58.000 | 366 |
| 24.000 | 217 | 95.000 | 367 |
| 10.000 | 218 | 82.000 | 368 |
| 73.000 | 220 | 222.000 | 373 |
| 109.000 | 222 | 50.000 | 374 |
| 70.000 | 228 | 31.000 | 378 |
| 115.000 | 236 | 29.000 | 381 |
| 14.000 | 237 | 105.000 | 384 |
| 32.000 | 239 | 208.000 | 387 |
| 13.000 | 241 | 25.000 | 390 |
| 10.000 | 242 | 51.000 | 392 |
| 10.000 | 244 | 24.000 | 393 |
| 42.000 | 245 | 103.000 | 396 |
| 67.000 | 246 | 154.000 | 400 |
| 107.000 | 247 | 154.000 | 402 |
| 23.000 | 255 | 53.000 | 403 |
| 88.000 | 258 | 33.000 | 404 |
| 22.000 | 259 | 55.000 | 406 |
| 10.000 | 262 | 131.000 | 411 |
| 120.000 | 263 | 24.000 | 413 |
| 26.000 | 266 | 10.000 | 414 |
| 340.000 | 268 | 434.000 | 416 |
| 326.000 | 269 | 43.000 | 418 |
| 43.000 | 270 | 99.000 | 422 |
| 47.000 | 277 | 112.000 | 425 |
| 57.000 | 278 | 26.000 | 426 |
| 24.000 | 280 | 51.000 | 428 |
| 72.000 | 281 | 289.000 | 433 |
| 21.000 | 283 | 21.000 | 434 |
| 10.000 | 285 | 12.000 | 439 |
| 40.000 | 286 | 17.000 | 440 |
| 116.000 | 288 | 67.000 | 441 |
| 21.000 | 291 | 74.000 | 443 |
| 10.000 | 293 | 11.000 | 444 |
| 16.000 | 294 | 19.000 | 445 |
| 31.000 | 295 | 10.000 | 448 |
| 10.000 | 298 | 171.000 | 449 |
| 75.000 | 299 | 10.000 | 451 |
| 80.000 | 300 | 161.000 | 452 |
| 25.000 | 301 | 28.000 | 453 |
| 26.000 | 302 | 29.000 | 454 |
| 11.000 | 303 | 10.000 | 456 |
| 13.000 | 304 | 19.000 | 458 |
| 213.000 | 307 | 265.000 | 459 |
| 105.000 | 308 | 10.000 | 460 |
| 164.000 | 313 | 23.000 | 461 |

| | Original enumber |
|---|---|
| 26.000 | 462 |
| 440.000 | 464 |
| 90.000 | 465 |
| 37.000 | 467 |
| 77.000 | 469 |
| 112.000 | 470 |
| 70.000 | 472 |
| 42.000 | 473 |
| 99.000 | 476 |
| 280.000 | 477 |
| 60.000 | 478 |
| 99.000 | 479 |
| 97.000 | 480 |
| 213.000 | 484 |
| 63.000 | 485 |
| 237.000 | 488 |
| 36.000 | 491 |
| 39.000 | 492 |
| 57.000 | 493 |
| 53.000 | 494 |
| 109.000 | 496 |
| 97.000 | 497 |
| 194.000 | 498 |
| 87.000 | 499 |
| 115.000 | 500 |

# ANNEX 3

**Contribution of University College, Dublin**

**J.P. McLaughlin and S. Grimley**

# RADON MEASUREMENTS AND DETECTOR DEVELOPMENTS
# UNIVERSITY COLLEGE DUBLIN (CONTRACTOR No.3)

## 3.1 OBJECTIVES

The principal objective of University College Dublin ( U.C.D.), as part of the field work of this project was to examine soil gas radon concentrations near house sites in Moycullen, Co. Galway. To achieve this objective, it was proposed to make the following measurements at each site.

1) Time integrated soil gas measurements using CR-39 alpha track detectors buried in the ground at a depth of 1 m, as close to each house as possible.

2) Grab sample measurements using Lucas cells and a Pylon AB-5 taken at a depth of 0.7 m, as close to each house as possible.

3) Soil permeability measurements using a newly developed permeability probe.

In support of the above objective, it was also necessary for U.C.D. to develop in the laboratory, a new type of passive alpha track based radon detector and also a soil gas permeability probe (both of which are described below).

## 3.2 DESCRIPTION OF TECHNIQUES

### 3.2.1 Development of a new type of CR-39 detector for soil gas radon measurements.

CR-39 is an alpha sensitive plastic resin; Polyallyldiglycol carbonate or P.A.D.C.. When an alpha particle strikes the surface of the CR-39, it produces a damage trail which becomes clearly visible under a microscope after etching. The CR-39 used for this project was supplied by TASL (Bristol University) and it has displayed excellent track formation and optical properties. The CR-39 was etched in 6.25 molar Sodium Hydroxide at 98$^{\circ}$ for 1 hour. Typical CR-39 alpha track detectors consist of a single

chamber defining a particular sensitive volume. If the radon levels are very high, the CR-39 may rapidly become saturated with alpha tracks. This makes counting the tracks very difficult as they will overlap each other. Similarly, when the radon concentration is low, the chamber may not be sensitive enough and too few tracks will appear on the CR-39. To overcome this problem, a multichambered detector was developed. Each of the chambers has a different volume and therefore a different sensitivity. The detector was cut from solid perspex by a Kitamura C.N.C. high precision computerised Machine Tool Centre. Perspex was chosen as it has a low natural background radiation and it can be cut easily and accurately without spreading.

Figure 3.1 shows a schematic diagram of the new detector.

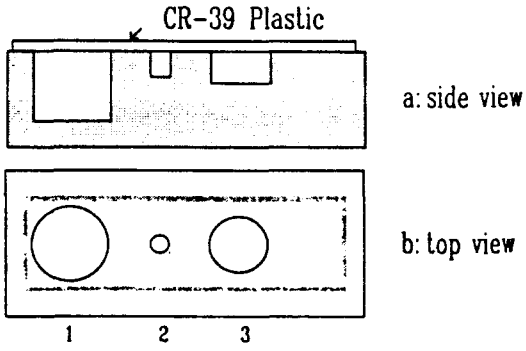


Figure 3.1 : New Multichamber Passive Detector
Chamber 1-$R_c$ = 0.0060m/D = 0.11m
Chamber 2-$R_c$ = 0.0015m/D = 0.04m
Chamber 3-$R_c$ = 0.0045m/D = 0.05m

The sensitivities were theoretically determined by developing equations to describe the alpha particle geometrical detection factors for a cylindrical detector. Four different factors were derived,

1) $G^a$ Geometry factor for airborne activities
2) $G^d$ Geometry factor for radon daughters deposited on the CR-39
3) $G^w$ Geometry factor for radon daughters deposited on the walls
4) $G^b$ Geometry factor for radon daughters deposited on the base.

These geometry factore are presented in Table 3.1.

The theoretical expression for the expected radon sensitivity of a cylindrical detector as shown in Figure 3.1 is

$$S = \mathcal{D}_\alpha \left( G^a + 2 ( G^d + G^w + G^b ) \frac{\text{volume}}{\text{surface}} \right) \text{tracks.m}^{-2}.\text{Bq}^{-1}.\text{m}^3.\text{s}^1$$

where $\mathcal{D}_\alpha$ is the track registration efficiency.

| Condition | $(D^2 + R_c^2)^{1/2} \leq R_\alpha$ |
|---|---|
| $G^a$ (airborne) | $\frac{1}{2}\left(R_c + D - (R_c^2 + D^2)^{1/2}\right)$ |
| $G^d$ (detector) | $\frac{1}{2}$ |
| $G^w$ (wall) | $\frac{1}{2}\left(1 - \frac{R_c}{(R_c^2 + D^2)^{1/2}}\right)$ |
| $G^b$ (base) | $\frac{1}{2}\left(1 - \frac{L}{(D^2 + R_c^2)^{1/2}}\right)$ |

**TABLE 3.1 - Geometry factors for cylindrical detector**

**D = depth of the chamber**

**$R_c$ = radius of the chamber**

Using this equation, a value for the expected radon activity is obtained. This allows the user to determine a mean radon concentration in absolute units such as $Bqm^{-3}$ instead of the less useful instrumental equivalent such as tracks $mm^{-2}$. The detectors were also intercalibrated against regular radon detectors calibrated at the N.R.P.B. (U.K.) as part of the ongoing C.E.C. radon detection intercalibration programme.

This detector is suitable for successfully measuring a much greater range of radon concentrations than conventional detectors. For accurate counting of the tracks either by eye or on a Image Analysis System, the track density should range from about 1500 tracks/$cm^2$ up to about 12500 tracks/$cm^2$. Figure 2 displays the expected number of tracks/$cm^2$/day (24 hours) for each of the chambers in the new detector. It also shows the expected number of tracks/$cm^2$/day for a typical CR-39 detector.

### 3.2.2 Passive Integrated Soil Gas Radon Measurements.

Time integrated soil gas radon concentrations were measured using the new type of passive CR-39 alpha track detector. A Cobra coring drill with a 4.5 cm drill bit was used to drill to a depth of about 1 m. The drilled hole was lined with tight fitting plastic piping and sealed from the open air with a rubber cap. As shown in Figure 3.3 ( A ), the detector was suspended from inside the cap, to remain about 3 cm above the bottom of the hole thereby avoiding the effects of any water in the ground. Ideally all the holes were to be drilled, lined and sealed in this way but due to difficult ground conditions, it was more than often necessary to abandon the drill for shovels and a pick. On such occasions, holes were dug by hand and the detectors were placed on a small stone and covered with a large plastic cup for protection (Figure 3.3 (B)). The holes were filled back and marked. The detectors remained undisturbed in the ground for a minimum of 190 hours. After recovery, they were chemically etched and counted using a Quantimet Q520 Digital Image Analysis System.

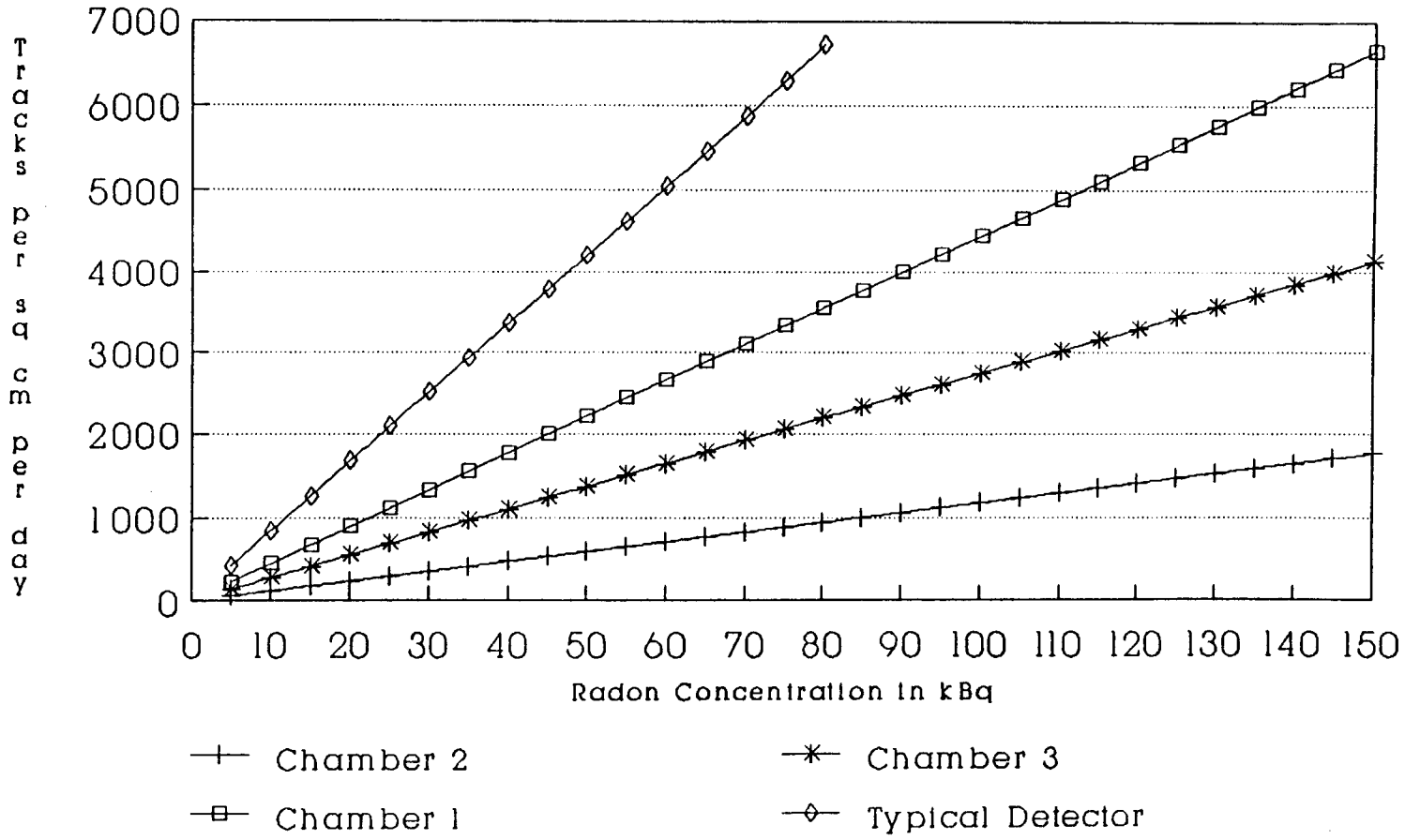


Fig 3.2:Track production vs Radon Conc.

### 3.2.3 Soil Gas Grab Sampling.

Instantaneous measurements of radon levels in soil gas were made using a grab sampling technique. Soil gas was pumped from the ground through a hydraulic pipe with a 4 mm internal diameter into a 100 ml Lucas cell (Figure 3.3 (C)). A flow-through method was used whereby at least 1 litre of soil gas was pumped through the Lucas cell , thereby ensuring a representative sample of soil gas. After at least a three hour period: the time required to allow the radon daughters to come into equilibrium with the radon gas, the cells were counted on a Pylon AB-5 scintillation counter for a series of five minute intervals. Using appropriate calibration factors and sample decay corrections, the radon concentration in each sample was calculated. After use each cell was flushed through with outdoor air using an electric pump for 15 minutes so that it could be used again the next day.

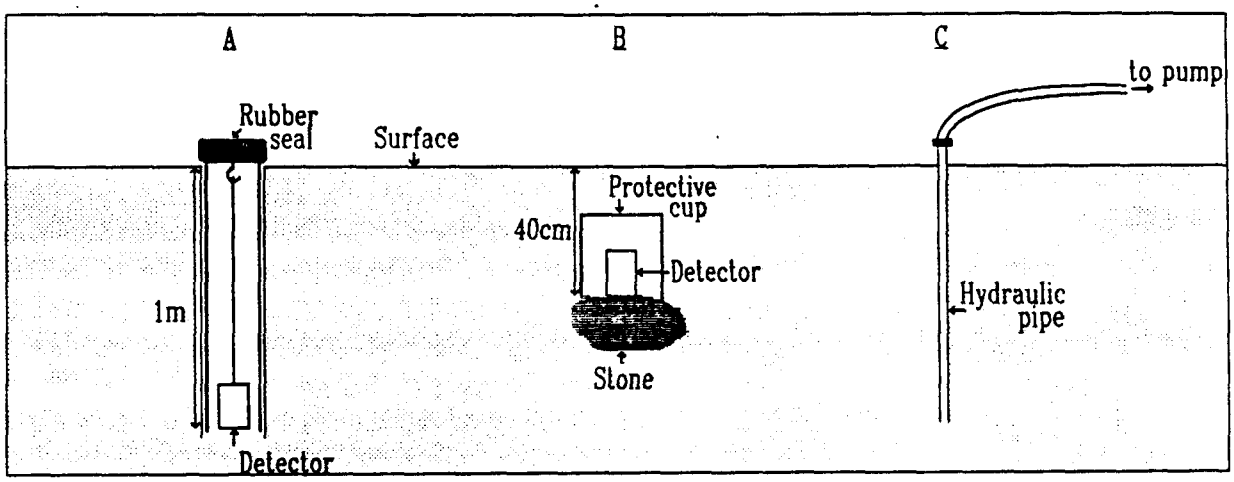


FIGURE 3.3

### 3.2.4 Development of soil gas permeability probe.

A soil gas permeability probe was designed and constructed based on a design by Anders Damkjaer at the Technical University of Denmark ( contract BI6 - 347f - 114), to make relative measurements of the soil permeability at all the sites. The probe developed consists of a steel rod 1 m in length. A detachable head, 0.25 m long was cut with six longitudinal slits (0.1 m ) and a pointed tip. The other end of the probe was fitted with an air tap and a pressure gauge. A hole in the ground was drilled to a depth

of 1 meter with the Cobra drill and lined it with tight fitting plastic piping. The probe is then be inserted into the hole pushing the pointed tip a further 0.25 m into the ground below the hole. The pipe is then be sealed and a known volume of air, under pressure, released through the probe and into the ground. By monitoring the pressure changes, the time taken for the air to diffuse through the soil can be measured and a relative determination of the soil permeability can be obtained.

To seal the probe tip from outside air, the probe was fitted with two metal rings 25 cm apart. Stretched between these was a section of rubber tubing which can be inflated, thus sealing off the pipe, by means of a copper tube running along the steel rod to the top of the probe. This tube was also fitted with an air tap and a pressure gauge. The rubber tube is inflated using a hand pump and the air tap is then closed. The pressure gauge is monitored to ensure that the pipe is sealed at all times, otherwise the air released to test the soil gas permeability will leak to the atmosphere and give a false reading on the pressure gauge .

Figure 3.4 shows a schematic diagram of the probe in situ.

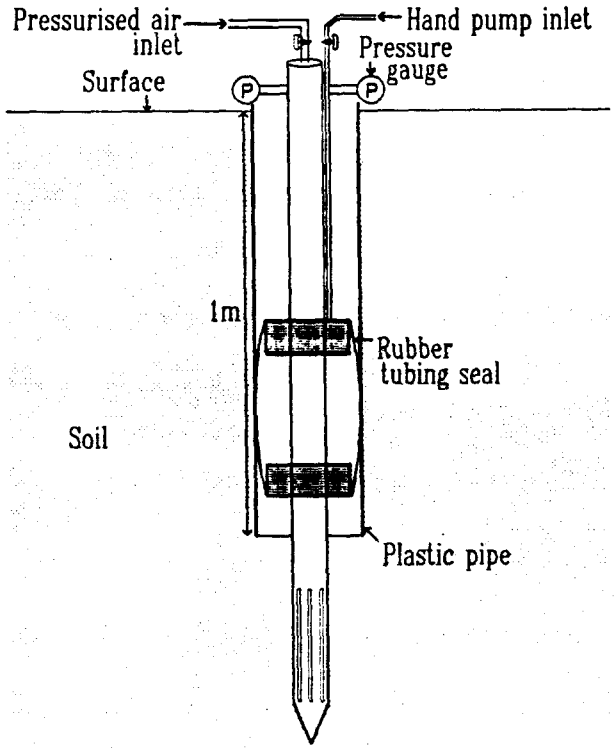


FIGURE 3.4

### 3.2.5 Soil Permeability Measurements

It was intended to make several measurements of soil gas permeability at each site as permeability plays an important part in the migration of radon from the ground into dwellings above. Unfortunately, the soil and ground conditions encountered at almost all the sites proved unsuitable for the permeability probe so it was not used. The probe was however tested in suitable soil sites in the Dublin area and proved to be successful in these more favourable conditions. The soil cover in the Moycullen area was very thin, as little as 3 cm in parts and even in areas where the soil cover was deeper, the soil was riddled with rocks and stones. However it proved possible to divide the soils in the area into two general types,

1) dry sandy porous soil,
2) wet clay rich soil.

Two factors were taken into account in this determination, the first being the general appearance and texture of the soil and the second being the ease of pumping soil gas through the Lucas cells.

## 3.3 RESULTS

Field work in Moycullen took place mainly in July 1991. Due to the close proximity of the bedrock to the surface and the stony ground, it was very difficult to take either type of measurement below half a meter. In places the soil cover was as shallow as 2 or 3 cm. Therefore the depths of the integrated measurements ranged from about 0.3 m to 1.25 m and the depths of the soil gas measurements from 0.3 m to 0.7 m. Where possible, the measurements were taken close to the house and in original soil as opposed to imported top soil which the owner had brought into the garden to overcome the general soil deficiency.

The results obtained are presented in the following tables. The time integrated soil gas radon measurements gave concentrations ranging from a few hundred $Bq/m^3$ up to 58000 $Bq/m^3$. Most of the higher concentrations occurred on the granitic side of the Moycullen area. The grab samples gave radon concentrations ranging from 330 $Bq/m^3$ up to 165000 $Bq/m^3$. Table 3.2

shows all the results from the passive time intgrated detectors while Table 3.3 shows some of the grab sample measurements. In Table 3.3, some of the results displayed are taken from Lucas cells belonging to the Radiological Protection Institute of Ireland (formerly the Nuclear Energy Board) as all the available cells were combined to allow more measurements to be made daily.

| HOUSE NUMBER | ROCK TYPE | HOLE NUMBER | DEPTH cm | RADON CONC. in Bq/m$^3$ Alpha track meas. | *INDOOR RADON (Bq/m$^3$) |
|---|---|---|---|---|---|
| 211 | Lst | DH1 | 43 | 5740 | 430 |
| | | DH2 | 40 | 5060 | |
| | | CH1 | 38 | 3360 | |
| 210 | Lst | DH3 | 50 | 21340 | 376 |
| | | DH4 | 65 | 21170 | |
| 206 | Lst | CH2 | 123 | 11810 | 44 |
| 6 | Lst | CH4 | 100 | 15130 | 120 |
| | | CH5 | 100 | 18150 | |
| 13 | Lst | DH5 | 40 | 6200 | 12 |
| | | DH6 | 45 | 5220 | |
| 8 | Lst | DH7 | 46 | 14250 | 17 |
| | | DH8 | 45 | 20020 | |
| 10 | Lst | DH9 | 46 | 7200 | 725 |
| | | DH10 | 52 | 11170 | |
| 453 | Gnt | DH11 | 47 | 24340 | 28 |
| | | DH12 | 50 | 31680 | |
| 464 | Gnt | DH13 | 50 | 9160 | 440 |
| 454 | Gnt | CH6 | 85 | 1770 | 29 |
| | | CH7 | 118 | 50930 | |
| 459 | Gnt | CH8 | 100 | 48410 | 265 |
| | | CH9 | 110 | 36020 | |
| 155 | Gnt | DH14 | 40 | 6180 | 343 |
| | | DH15 | 45 | 58760 | |
| 154 | Gnt | CH10 | 110 | 53590 | 67 |
| | | CH11 | 100 | 780 | |
| 269 | Lst | CH12 | 100 | 53010 | 326 |
| | | CH13 | 60 | 9050 | |
| | | CH14 | 110 | 47640 | |
| 301 | Gnt | CH15 | 70 | 600 | 25 |
| | | CH16 | 100 | 22860 | |
| 298 | Gnt | CH17 | 76 | 340 | 10 |
| | | CH18 | 100 | 340 | |
| 45 | Lst | DH16 | 32 | 2600 | 231 |
| 79 | Gnt | DH17 | 33 | 4930 | 10 |

Table 3.2

* R.P.I.I. Measurements

Lst - Limestone

Gnt - Granite

CH1 - Cobra Drilled Hole No.1

DH1 - Dug Hole No.1

| HOUSE NUMBER | ROCK TYPE | HOLE NUMBER | DEPTH cm | RADON CONC. in Bq/m$^3$ Lucas cell meas. | *INDOOR RADON in Bq/m$^3$ |
|---|---|---|---|---|---|
| 211 | Lst | SG1 | 30 | 8290 | 430 |
| | | SG2 | 60 | 19840 | |
| 210 | Lst | SG5 | 35 | 16820 | 376 |
| | | SG6 | 50 | 32210 | |
| 206 | Lst | SG8 | 50 | 98580 | 44 |
| | | SG7 | 53 | 165150 | |
| 6 | Lst | SG11 | 58 | 74980 | 120 |
| | | SG45 | 55 | 54370 | |
| 13 | Lst | SG13 | 40 | 36530 | 12 |
| | | SG14 | 40 | 14500 | |
| 8 | Lst | SG15 | 40 | 13640 | 17 |
| | | SG16 | 40 | 26010 | |
| 10 | Lst | SG17 | 50 | 4560 | 725 |
| | | SG53 | 53 | 66860 | |
| 453 | Gnt | SG58 | 50 | 29280 | 28 |
| | | SG59 | 50 | 1830 | |
| 464 | Gnt | SG19 | 60 | 15950 | 440 |
| 454 | Gnt | SG21 | 65 | 42020 | 29 |
| | | SG22 | 50 | 13560 | |
| 459 | Gnt | SG24 | 65 | 75410 | 265 |
| | | SG25 | 65 | 29930 | |
| 155 | Gnt | SG27 | 40 | 28600 | 343 |
| | | SG60 | 60 | 22550 | |
| 154 | Gnt | SG28 | 50 | 108370 | 67 |
| | | SG61 | 50 | 55830 | |
| 269 | Lst | SG41 | 55 | 33420 | 326 |
| | | SG42 | 58 | 60350 | |
| 301 | Gnt | SG30 | 50 | 2470 | 25 |
| | | SG31 | 50 | 18550 | |
| 298 | Gnt | SG32 | 65 | 750 | 10 |
| | | SG33 | 65 | 330 | |
| 45 | Lst | SG36 | 65 | 18510 | 231 |
| 79 | Gnt | SG39 | 40 | 24930 | 10 |

**Table 3.3**

* R.P.I.I. Measurements

Lst - Limestone

Gnt - Granite

SG1 - Soil Gas No.1

## 3.4 CONCLUSION

The general elevation of indoor radon levels in the Moycullen area appears to be due to the underlying uraniferous granite (see other sections of this report for a fuller discussion ). No direct correlation was found between the indoor radon concentrations and those in the ground; houses built side by side may have indoor concentrations differing by several hundred Bequerels. This would suggest that there are other important parameters governing the indoor radon concentrations besides the existance of the granite. Parameters such as

1) House structure, particularly foundations,
2) House heating and ventilation,
3) soil permeability,
4) localised faults and fractures in the underlying bedrock,

play very important parts in providing dwellings with radon gas.

From a measurement perspective, it was found that the newly designed multi-cell radon detector which was designed specifically for this work ), proved to be very suitable for field work in the unfavourable conditions found in the Moycullen area.

# ANNEX 4

**Contribution of Trinity College, Dublin**

**I.R.McAulay and D.Marsh**

## 4.1 Introduction

Initially a survey of indoor radon levels was carried out in the area in which over 400 households participated. From the results of this initial survey, 17 houses were selected for further study, including houses with low and elevated radon levels on each of granite and limestone bedrock. The objective of the soil measurements described in this section was to investigate the concentrations of $^{226}Ra$ (the precursor of $^{222}Rn$) in the soil surrounding these selected houses.

## 4.2 Sampling

At the location of each house, a soil sample was collected, usually by digging a hole 30-40 cm deep; the sample being removed at this depth using a normal garden spade. However, sometimes it was more convenient to use an existing excavation or natural soil face, again sampling at a depth of 30-40 cm. Care was taken to ensure that the collected sample was of natural soil, and not imported topsoil (which is common in this area due to poor quality natural soil). For this reason it was not always possible to sample directly adjacent to the house, however in all cases soil was sampled within 50 m of the house. In some cases a second soil sample was collected.

## 4.3 Gamma spectroscopy

When samples were returned to the laboratory they were then prepared for gamma activity measurement. Large stones and other debris were first removed from the samples which were then placed in foil trays and dried in a furnace at 110°C for about 24 hours. When dry, the soils were crushed to particles of less than 2mm diameter using a mechanical mortar and pestle. This powder was then placed in standard Marinelli beakers which have a sample volume of 450 ml. Typical sample masses were in the range 300-600 grams. Samples were measured for gamma activity using a high resolution HpGe solid state detector. The naturally occurring radionuclides of interest are $^{234}Th$ (93 KeV) and $^{226}Ra$ (186 KeV) from the uranium-238 series, $^{228}Ac$ (911 KeV) from the thorium-232 series and $^{40}K$ (1461 KeV). The figures in parenthesis indicate the energies in the spectrum at which the nuclide activity is measured. Sample measurement time varied but most were counted for approximately 24 hours which yields a lower detection limit of about 11 Bq $kg^{-1}$ for $^{226}Ra$. Rock samples taken from deep cores were supplied by the Geological Survey of Ireland in the form of a powder. These samples did not contain sufficient material to fill the Marinelli containers, so 200 ml plastic tubs (8 cm diameter) were used in these cases. Typical sample masses were in the range 200-300 grams. A Ge(Li) detector was used to measure some of these rock samples.

## 4.4 Results

### 4.4.1 Soils

The results of the gamma ray spectrometry on the soils collected at each of the houses sampled are shown in table 1, together with the radon levels measured in each of the houses.

No significant degree of correlation was found for radon levels when tested against any of the other quantities measured. However, the $^{226}Ra$ values found in the Moycullen soils were considerably less than those found in other parts of Ireland. Values up to 430 Bq $kg^{-1}$ had previously been found within 60 km of Moycullen and over 500 Bq $kg^{-1}$ in the Kerry area further to the south. The highest values for $^{234}Th$ in this survey were 149 Bq $kg^{-1}$ as compared with a maximum value of 543 Bq $kg^{-1}$ found in an earlier national survey consisting of 651 samples taken on the basis of the 10km grid. The disequilibrium found in the Moycullen soils was also much lower than found elsewhere in the country with the highest measured value for the $^{226}Ra/^{234}Th$ ratio in this series of measurements being 1.91 compared with up to 10 in some samples from Co. Clare. The average values of radium in soil found in the national survey was 46 Bq $kg^{-1}$ which compares with the Moycullen soils mean of 48 Bq $kg^{-1}$; the corresponding values for $^{234}Th$ were 39 Bq $kg^{-1}$ nationally and 49 Bq $kg^{-1}$ in the Moycullen samples.

4.4.2 Drillcore rock samples

The results of the activity concentrations determined for the rock core samples are shown in table 2. Again, for these figures no significant correlations were found for relationships between the different activity concentrations. The radium concentrations appear in general to be rather lower in the core samples than in the soils and there is even less evidence for disequilibrium in the $^{226}Ra/^{234}Th$ ratio.

4.4.3 Field rock samples

A series of surface or near-surface rock samples had also been obtained for Galway granites and for the rocks in the Moycullen area investigated in this project. The results of the gamma analysis of these is given in tables 3 and 4. In the case of the Galway granites, some degree of correlation was found (R2 = 0.[illegible]) between $^{234}Th$ and $^{226}Ra$ values and also between $^{226}Ra/^{234}Th$ ratio and $^{226}Ra$ (R2 = 0.811). This indicates a slight increase in degree of disequilibrium with activity concentrations of $^{226}Ra$, though it must be stressed that the degree of [illegible]n was never large and in most cases was not detectably different to unity. In [illegible]f the Moycullen rock samples, the radium values were lower than for the gran[illegible] reasonable degree of correlation (R2 = 0.759) was found between $^{226}Ra$ and $^{23}$[illegible] concentrations. For most of these samples the degree of disequilibrium appe[illegible]ss than one, but it should again be noted that for individual samples it would be di[illegible] to interpret this as having any relevance to the geological factors influencing the n[illegible]e of the rocks.

## 4.5 Above-ground gamma radiation dose

A number of measurements were made of gamma radiation dose rates above the ground in the Moycullen area. The dose rate obtained over exposed limestone slabs was 13 nGy $hr^{-1}$, which is extremely low but consistent with values measured elsewhere in the country over similar limestone terrain. Dose rates measured over soil in and around Moycullen and over granitic terrain averaged 70 nGy $hr^{-1}$, which is in the range recognised as the highest found in a series of measurements made over the whole country.

## 4.6 $^{40}K$ measurements

Potassium-40 was measured in all samples and the activity concentrations were high for all rock samples whether core or surface, with similar values being obtained for the means within each classification. In the case of the soil samples, generally lower values of $^{40}K$ were found, with the mean for this grouping being about 2/3 that of the means for the rock samples.

## 4.7 Conclusions

It may therefore be concluded that the $^{226}Ra$ activities present in the soils do not in this survey provide a reliable indicator to the radon levels found in houses built on such soils. The degree of disequilibrium between $^{226}Ra$ and $^{234}Th$ found in the measurements was not large and it would therefore not be justified to draw any general conclusions between this ratio and the potential for high radon levels in houses. The mean values for $^{226}Ra$ in the soil and in the rock core measurements were close to and below the national average respectively, which again does not provide any justification for drawing general conclusions.

# TABLE 1 MOYCULLEN SOIL SAMPLES AT HOUSES

| House | $^{234}$Th | | $^{226}$Ra | | $^{40}$K | | $^{228}$Ac | | Disequilibrium | | Indoor radon |
|---|---|---|---|---|---|---|---|---|---|---|---|
| | Bq/kg | ±% | Bq/kg | ±% | Bq/kg | ±% | Bq/kg | ±% | Ratio | ±% | Bq/m$^3$ |
| 6 | 44 | 15 | 65 | 14 | 785 | 6 | 43 | 10 | 1.47 | 18 | 120 |
| 8 | 43 | 11 | 83 | 14 | 666 | 6 | 41 | 8 | 1.91 | 18 | 17 |
| 10 | 34 | 11 | 52 | 11 | 821 | 6 | 34 | 8 | 1.54 | 17 | 725 |
| 13 | 47 | 14 | 89 | 14 | 696 | 7 | 41 | 11 | 1.87 | 20 | 12 |
| 79 | 149 | 7 | 86 | 9 | 922 | 6 | 69 | 7 | .58 | 13 | 10 |
| 154 | 67 | 13 | 47 | 19 | 1098 | 6 | 46 | 9 | .71 | 23 | 67 |
| 155 | 42 | 15 | 29 | 35 | 752 | 7 | 32 | 14 | .69 | 38 | 343 |
| 206 | 54 | 13 | 80 | 14 | 615 | 7 | 46 | 10 | 1.48 | 20 | 44 |
| 210 | 44 | 14 | 56 | 15 | 350 | 7 | 32 | 9 | 1.27 | 19 | 376 |
| 211 | 31 | 15 | 38 | 19 | 412 | 7 | 24 | 11 | 1.24 | 22 | 430 |
| 269 | 54 | 12 | 38 | 20 | 771 | 7 | 47 | 9 | .7 | 23 | 326 |
| 298 | 6 | 28 | 6 | 48 | 85 | 10 | 6 | 18 | 1.05 | 63 | 10 |
| 298B | <6 | | 7 | 88 | 62 | 16 | 3 | 55 | > 1.17 | | 10 |
| 301 | 57 | 9 | 25 | 23 | 16 | 26 | 24 | 9 | .43 | 24 | 25 |
| 453A | 54 | 9 | 47 | 13 | 992 | 6 | 41 | 7 | .87 | 13 | 28 |
| 453B | 44 | 12 | 52 | 14 | 904 | 6 | 43 | 9 | 1.17 | 18 | 28 |
| 454 | 37 | 15 | 26 | 26 | 1067 | 7 | 38 | 10 | .71 | 23 | 29 |
| 459 | 33 | 13 | 28 | 22 | 1020 | 6 | 45 | 8 | .83 | 27 | 265 |
| 464 | 54 | 6 | 31 | 12 | 915 | 6 | 55 | 7 | .58 | 13 | 440 |

# TABLE 2 MOYCULLEN ROCK CORE SAMPLES

| Sample | $^{234}$Th | | $^{226}$Ra | | $^{40}$K | | $^{228}$Ac | | Disequilibrium | |
|---|---|---|---|---|---|---|---|---|---|---|
| | Bq/kg | ±% | Bq/kg | ±% | Bq/kg | ±% | Bq/kg | ±% | Ratio | ±% |
| 91.1063 | 29 | 28 | 17 | 56 | 445 | 10 | 11 | 26 | .59 | 63 |
| 91.1064 | 71 | 17 | <11 | | 1547 | 7 | 137 | 7 | <.15 | |
| 91.1065 | 62 | 15 | <11 | | 1577 | 7 | 106 | 8 | <.18 | |
| 91.1066 | 62 | 26 | <11 | | 1368 | 7 | 88 | 9 | <.18 | |
| 91.1067 | 53 | 21 | <11 | | 1301 | 7 | 91 | 10 | <.21 | |
| 91.1068 | 47 | 22 | 21 | 82 | 1610 | 7 | 70 | 13 | .45 | 85 |
| 91.1069 | 23 | 41 | 42 | 31 | 1003 | 7 | 44 | 11 | 1.83 | 51 |
| 91.1070 | 32 | 30 | 44 | 34 | 943 | 7 | 43 | 11 | 1.38 | 45 |
| 91.1071 | 44 | 23 | 16 | 87 | 1084 | 7 | 35 | 18 | .36 | 90 |
| 91.1072 | 40 | 21 | 12 | 92 | 969 | 7 | 36 | 14 | .3 | 94 |
| 91.1073 | 50 | 22 | 15 | 92 | 1299 | 7 | 92 | 11 | .3 | 95 |
| 91.1074 | 77 | 17 | <11 | | 1950 | 7 | 109 | 10 | <.14 | |
| 91.1075 | 75 | 17 | <11 | | 1546 | 7 | 110 | 9 | <.15 | |
| 91.1076 | 25 | 40 | 15 | 79 | 478 | 8 | 22 | 14 | .6 | 89 |
| 91.1077 | 94 | 17 | 142 | 17 | 698 | 8 | 34 | 13 | 1.51 | 24 |
| 91.1078 | 17 | 26 | <11 | | 607 | 8 | 10 | 24 | <.65 | |
| 91.1079 | 10 | 65 | 13 | 66 | 17 | 52 | <3 | | 1.3 | 93 |
| 91.1080 | 51 | 19 | <11 | | 1426 | 7 | 85 | 10 | <.22 | |
| 91.1081 | 43 | 29 | 30 | 51 | 872 | 7 | 39 | 12 | .7 | 59 |
| 91.1082 | 35 | 18 | 32 | 26 | 1063 | 7 | 35 | 11 | .91 | 32 |
| 91.1083 | 45 | 20 | 21 | 67 | 981 | 8 | 39 | 15 | .47 | 70 |
| 91.1084 | 78 | 16 | <11 | | 1175 | 7 | 96 | 8 | <.14 | |
| 91.1085 | 122 | 14 | <11 | | 1222 | 7 | 82 | 8 | <.09 | |
| 91.1086 | 61 | 19 | 24 | 53 | 1401 | 7 | 64 | 12 | .39 | 56 |
| 91.1087 | 75 | 11 | 11 | 49 | 1989 | 6 | 93 | 7 | .15 | 50 |
| 91.1088 | 70 | 19 | 31 | 35 | 1357 | 6 | 80 | 8 | .44 | 40 |
| 91.1089 | 78 | 14 | 28 | 34 | 1498 | 6 | 88 | 8 | .36 | 37 |
| 91.1090 | 87 | 17 | 46 | 35 | 1503 | 7 | 73 | 11 | .53 | 39 |
| 91.1091 | 106 | 19 | 116 | 20 | 1291 | 7 | 86 | 9 | 1.09 | 28 |
| 91.1092 | 54 | 23 | 36 | 44 | 1536 | 7 | 58 | 9 | .67 | 50 |

# TABLE 3 GALWAY GRANITE SAMPLES

| Sample | $^{234}$Th | | $^{226}$Ra | | $^{40}$K | | $^{228}$Ac | | Disequilibrium | |
|---|---|---|---|---|---|---|---|---|---|---|
| | Bq/kg | ±% | Bq/kg | ±% | Bq/kg | ±% | Bq/kg | ±% | Ratio | ±% |
| 88.2001 | 239 | 7 | 236 | 9 | 1219 | 7 | 182 | 8 | .99 | 11 |
| 88.2020 | 48 | 8 | 14 | 27 | 940 | 5 | 60 | 7 | .29 | 28 |
| 88.2021 | 142 | 7 | 227 | 7 | 1241 | 5 | 110 | 8 | 1.6 | 10 |
| 88.2040 | 50 | 11 | 38 | 20 | 1195 | 5 | 62 | 9 | .76 | 22 |
| 88.2046 | 116 | 8 | 82 | 13 | 1292 | 5 | 108 | 8 | .7 | 15 |
| 88.2057 | 49 | 9 | 30 | 19 | 1050 | 5 | 66 | 8 | .6 | 21 |
| 88.2058 | 183 | 7 | 101 | 12 | 1266 | 5 | 156 | 7 | .56 | 14 |
| 88.2082 | 41 | 12 | 28 | 27 | 1058 | 5 | 41 | 11 | .68 | 30 |
| 88.2083 | 50 | 10 | 42 | 19 | 806 | 5 | 46 | 9 | .83 | 22 |
| 88.2138 | 188 | 5 | 267 | 6 | 1352 | 5 | 92 | 7 | 1.42 | 8 |
| 88.2143 | 79 | 8 | 49 | 15 | 1201 | 5 | 80 | 8 | .63 | 18 |
| 88.2146 | 81 | 11 | 87 | 11 | 1097 | 5 | 84 | 8 | 1.08 | 16 |
| 88.2148 | 166 | 6 | 367 | 6 | 1212 | 5 | 50 | 9 | 2.21 | 8 |

## TABLE 4 MOYCULLEN ROCK SAMPLES

| Sample | $^{234}Th$ | | $^{226}Ra$ | | $^{40}K$ | | $^{228}Ac$ | | Disequilibrium | |
|---|---|---|---|---|---|---|---|---|---|---|
| | Bq/kg | ±% | Bq/kg | ±% | Bq/kg | ±% | Bq/kg | ±% | Ratio | ±% |
| 91.1004 | 69 | 10 | 60 | 14 | 1274 | 5 | 97 | 8 | .87 | 18 |
| 91.1017 | 240 | 6 | 148 | 9 | 1128 | 5 | 206 | 7 | .59 | 11 |
| 91.1052 | 240 | 6 | 172 | 8 | 1934 | 5 | 191 | 7 | .72 | 10 |
| 91.1054 | 93 | 7 | 97 | 11 | 1191 | 5 | 78 | 8 | 1.05 | 13 |
| 91.1055 | 206 | 7 | 76 | 18 | 1184 | 5 | 114 | 7 | .37 | 20 |
| 91.1060 | 49 | 13 | 84 | 13 | 1205 | 5 | 37 | 13 | 1.69 | 19 |
| 91.1062(1) | 44 | 22 | < 15 | | 1053 | 5 | 26 | 12 | < .34 | |
| 91.1062(2) | 24 | 40 | 14 | 75 | 1075 | 5 | 25 | 12 | .6 | 85 |
| 91.1062(3) | 22 | 24 | 12 | 49 | 1069 | 5 | 24 | 9 | .54 | 54 |
| 91.1062(4) | 20 | 15 | 13 | 34 | 1078 | 5 | 23 | 11 | .68 | 37 |
| **Later Clay Samples:** | | | | | | | | | | |
| 91.1093 | 49 | 18 | 27 | 10 | 597 | 5 | 41 | 4 | .55 | 13 |
| 91.1094 | 83 | 10 | <15 | | 308 | 5 | 20 | 13 | < .18 | |

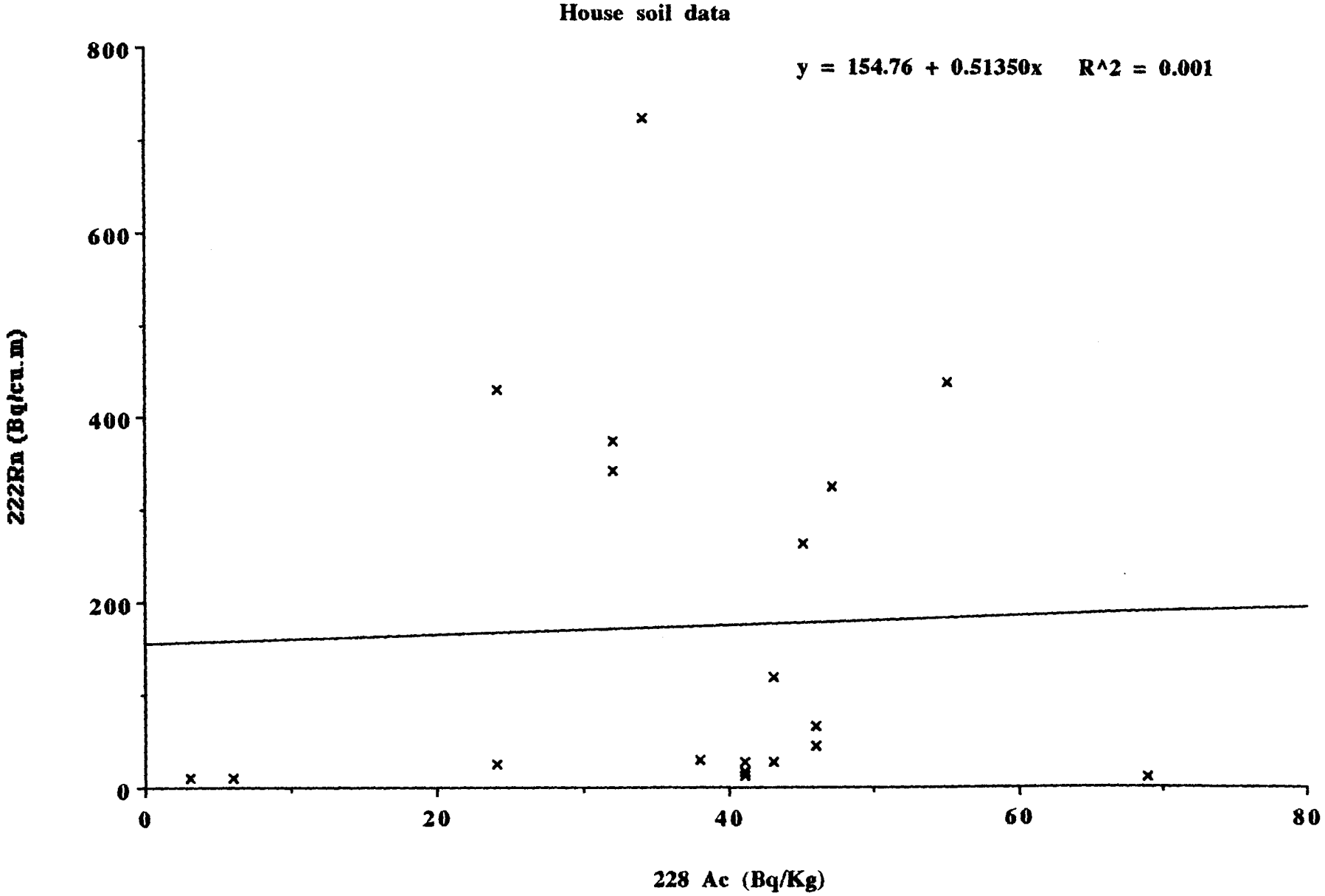
House soil data
y = 154.76 + 0.51350x R^2 = 0.001
800
600
400
200
0
222Rn (Bq/cu.m)
0
20
40
60
80
228 Ac (Bq/Kg)

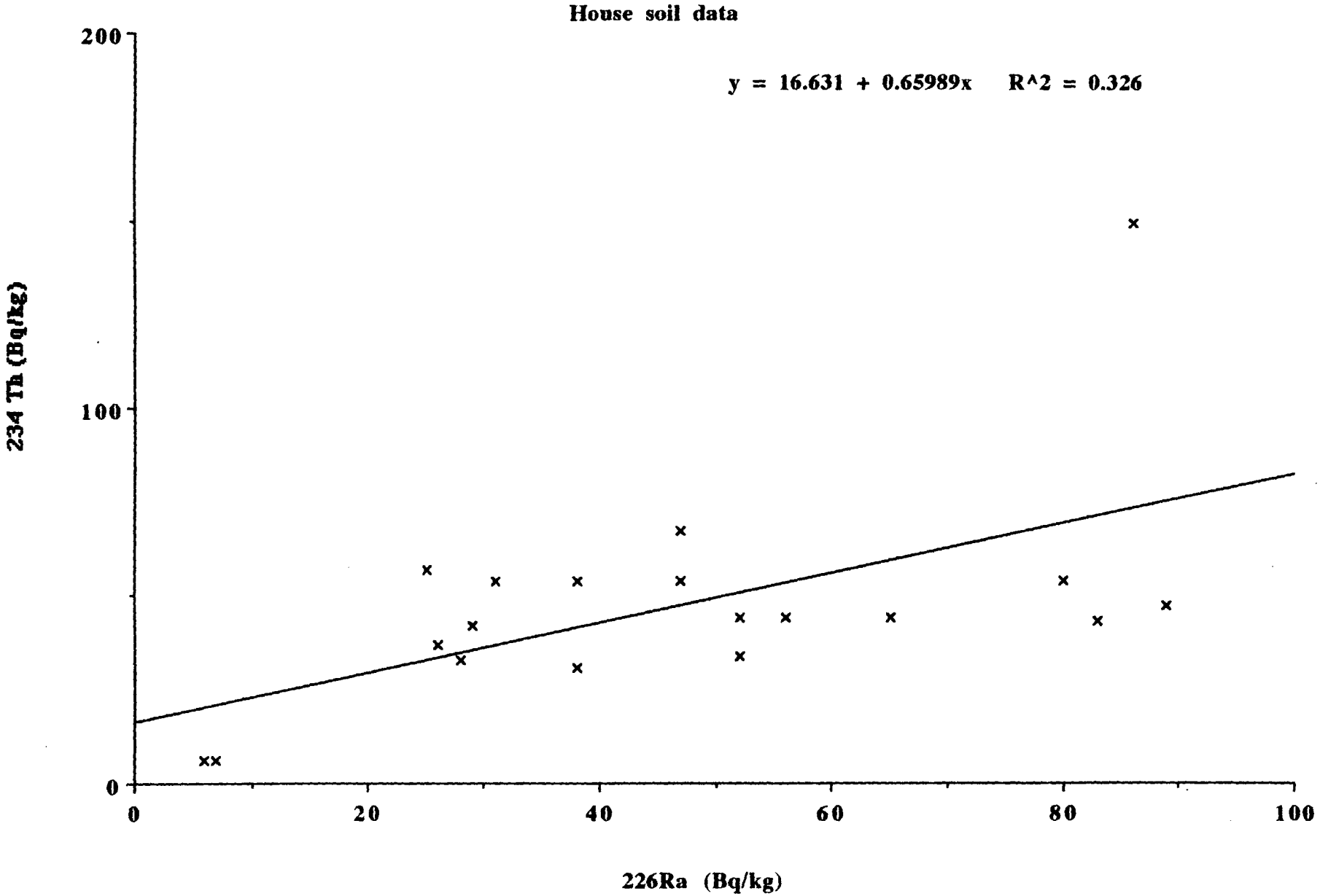
House soil data
y = 16.631 + 0.65989x R^2 = 0.326
234 Th (Bq/kg)
200
100
0
0
20
40
60
80
100
226Ra (Bq/kg)

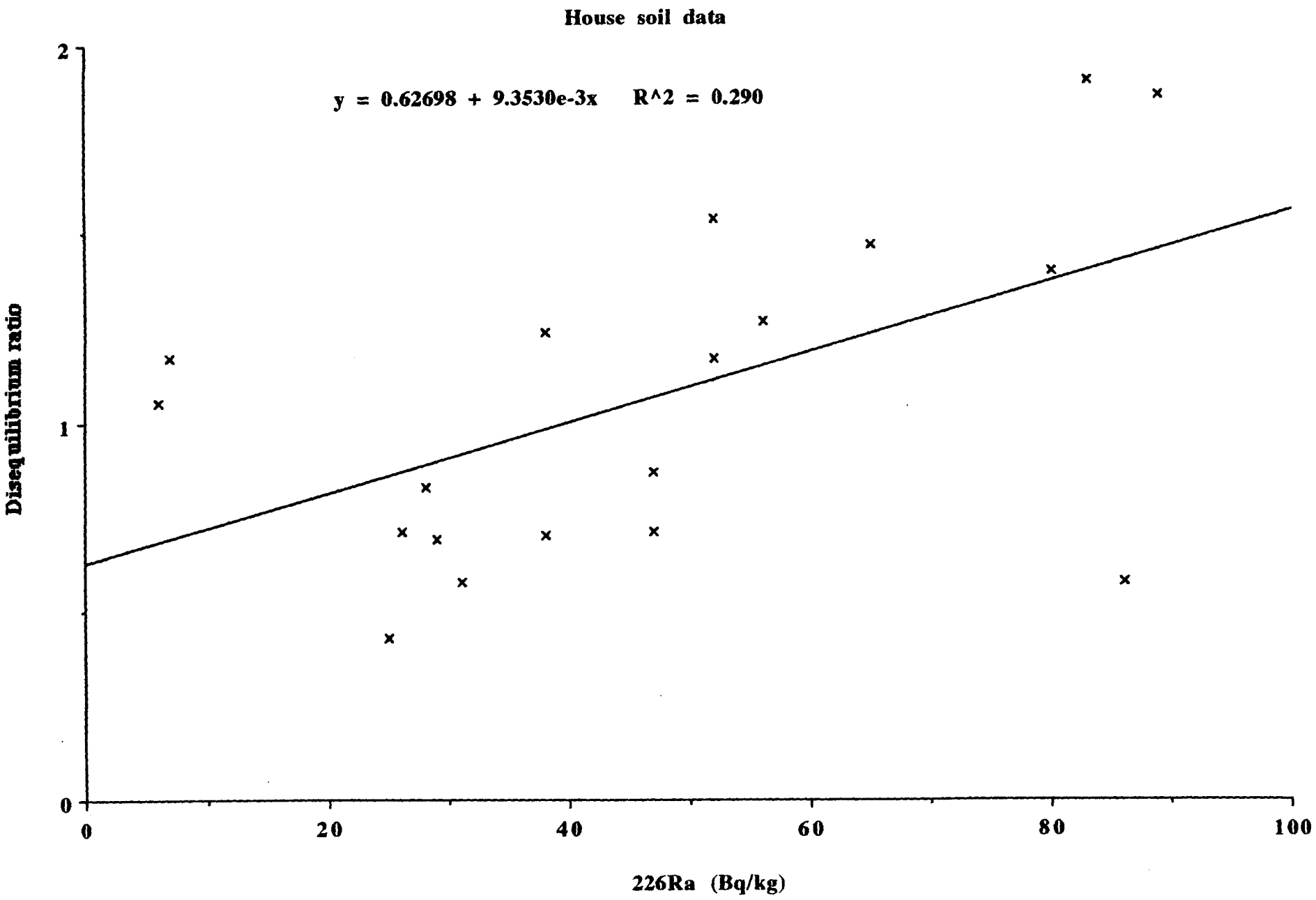
House soil data
y = 0.62698 + 9.3530e-3x R^2 = 0.290
Disequilibrium ratio
2
1
0
0
20
40
60
80
100
226Ra (Bq/kg)

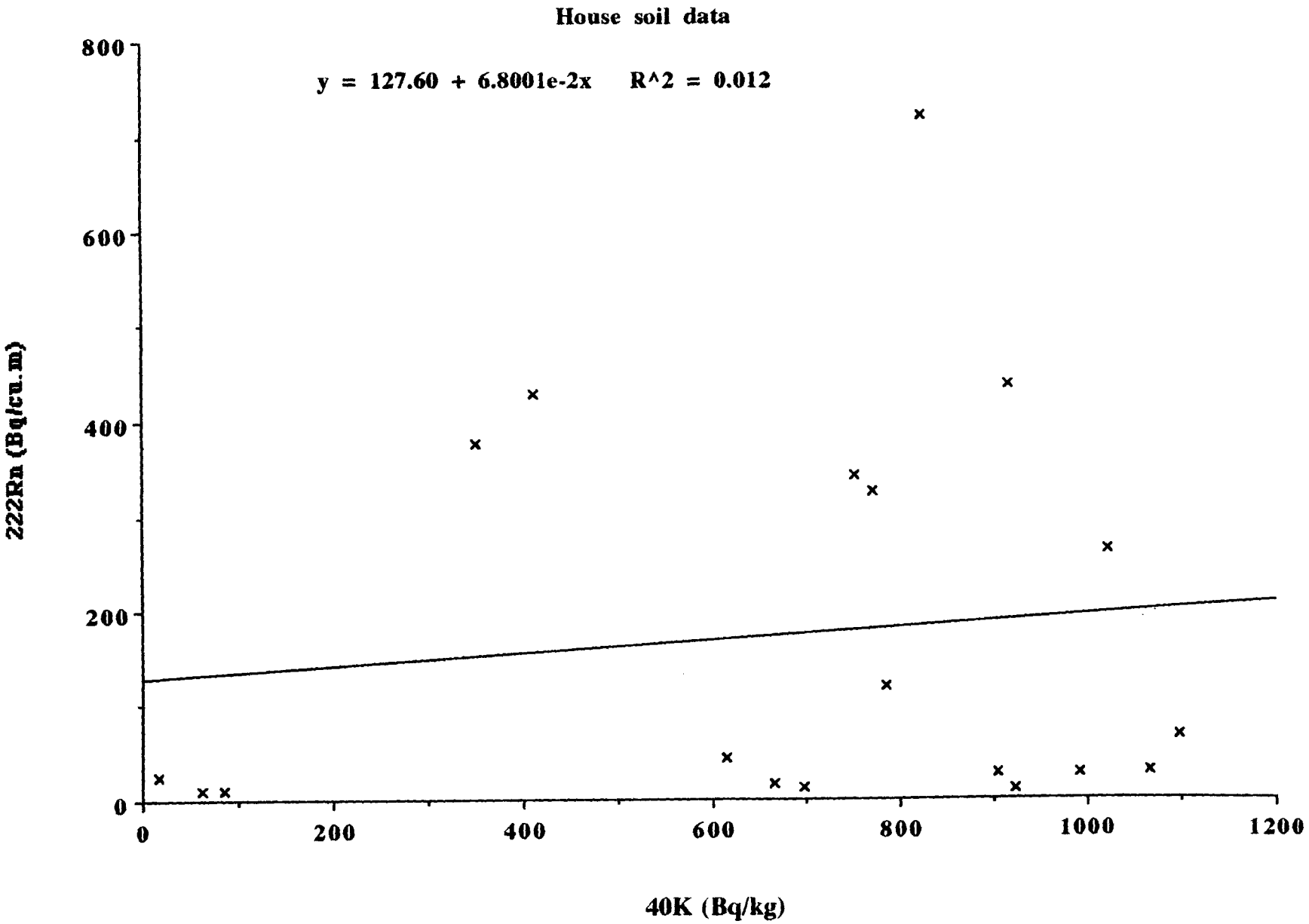
House soil data
y = 127.60 + 6.8001e-2x R^2 = 0.012
800
600
400
200
0
222Rn (Bq/cu.m)
0
200
400
600
800
1000
1200
40K (Bq/kg)

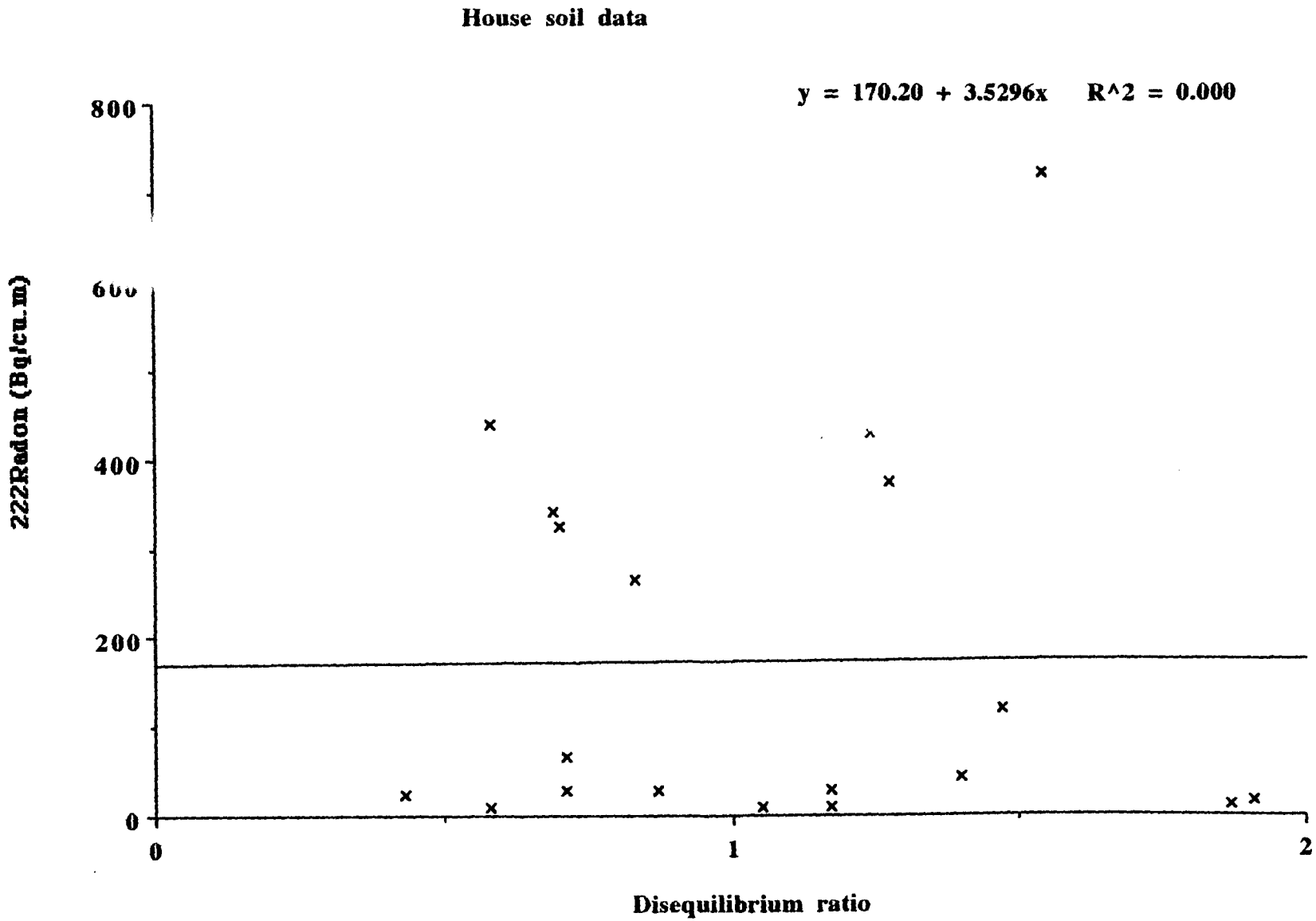
House soil data
y = 170.20 + 3.5296x R^2 = 0.000
800
600
400
200
0
222Radon (Bq/cu.m)
0
1
2
Disequilibrium ratio

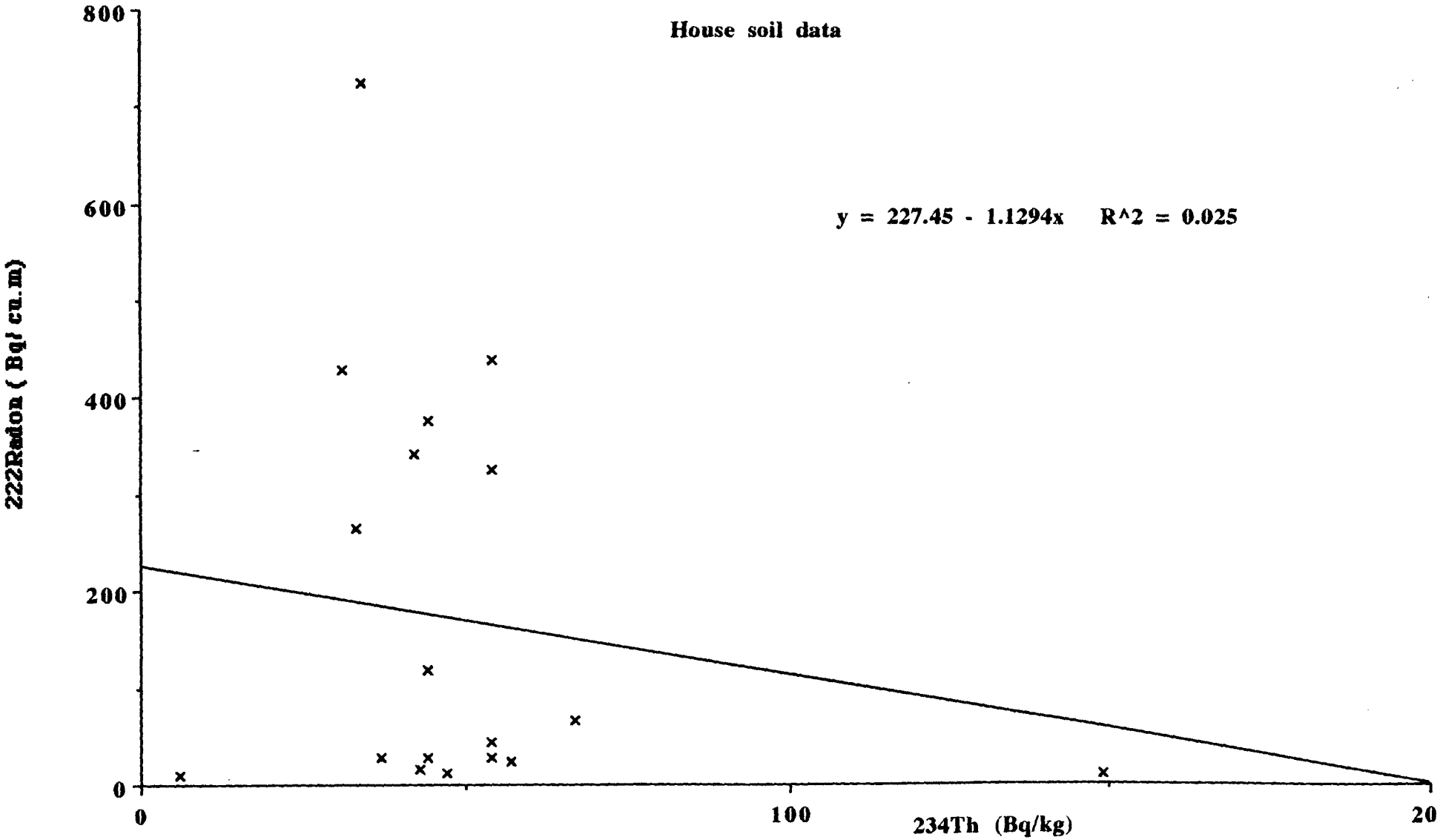
House soil data
y = 227.45 - 1.1294x R^2 = 0.025
222Radon ( Bq/ cu.m)
800
600
400
200
0
0
100
20
234Th (Bq/kg)

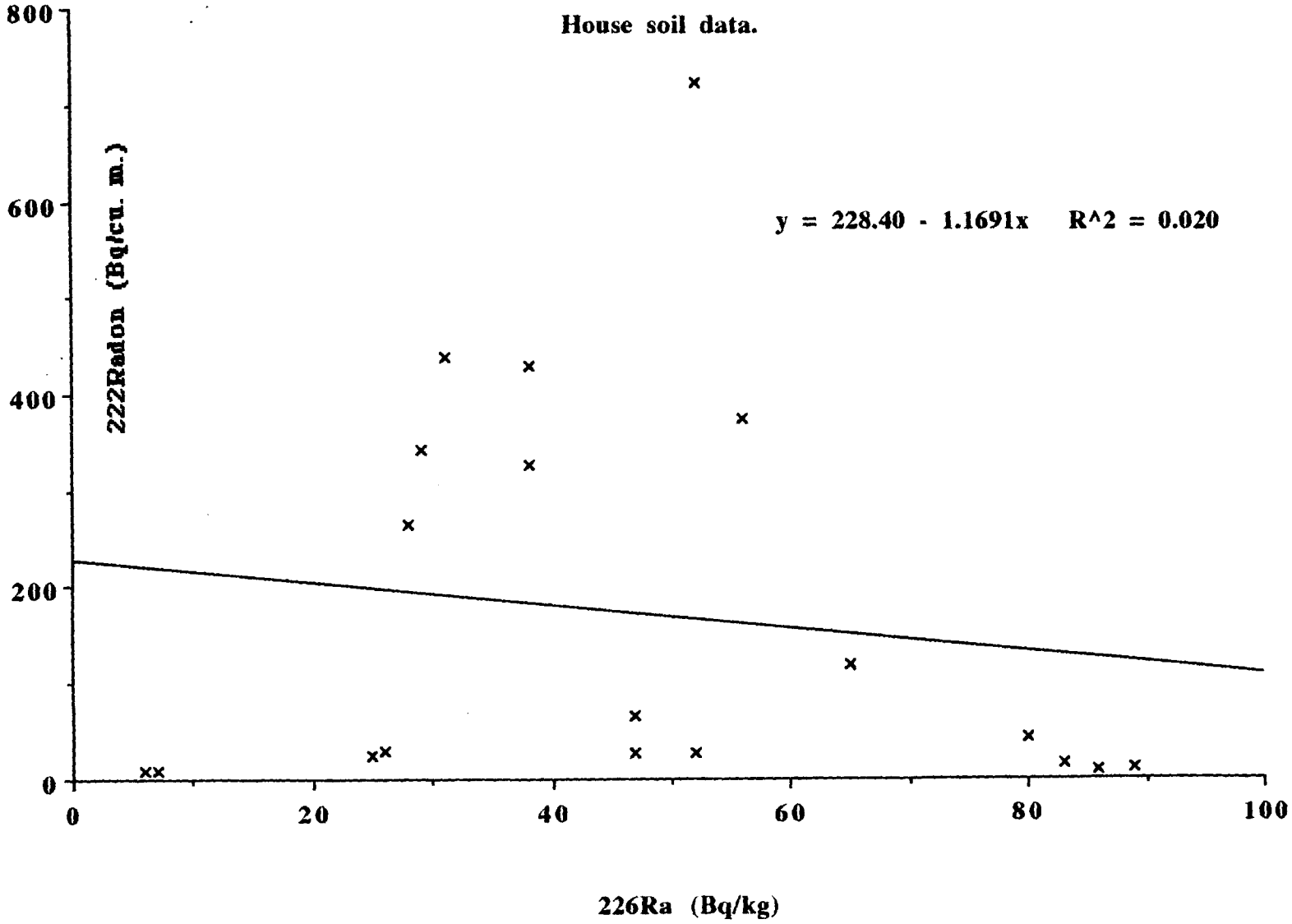
House soil data.
y = 228.40 - 1.1691x R^2 = 0.020
222Radon (Bq/cu. m.)
800
600
400
200
0
0
20
40
60
80
100
226Ra (Bq/kg)

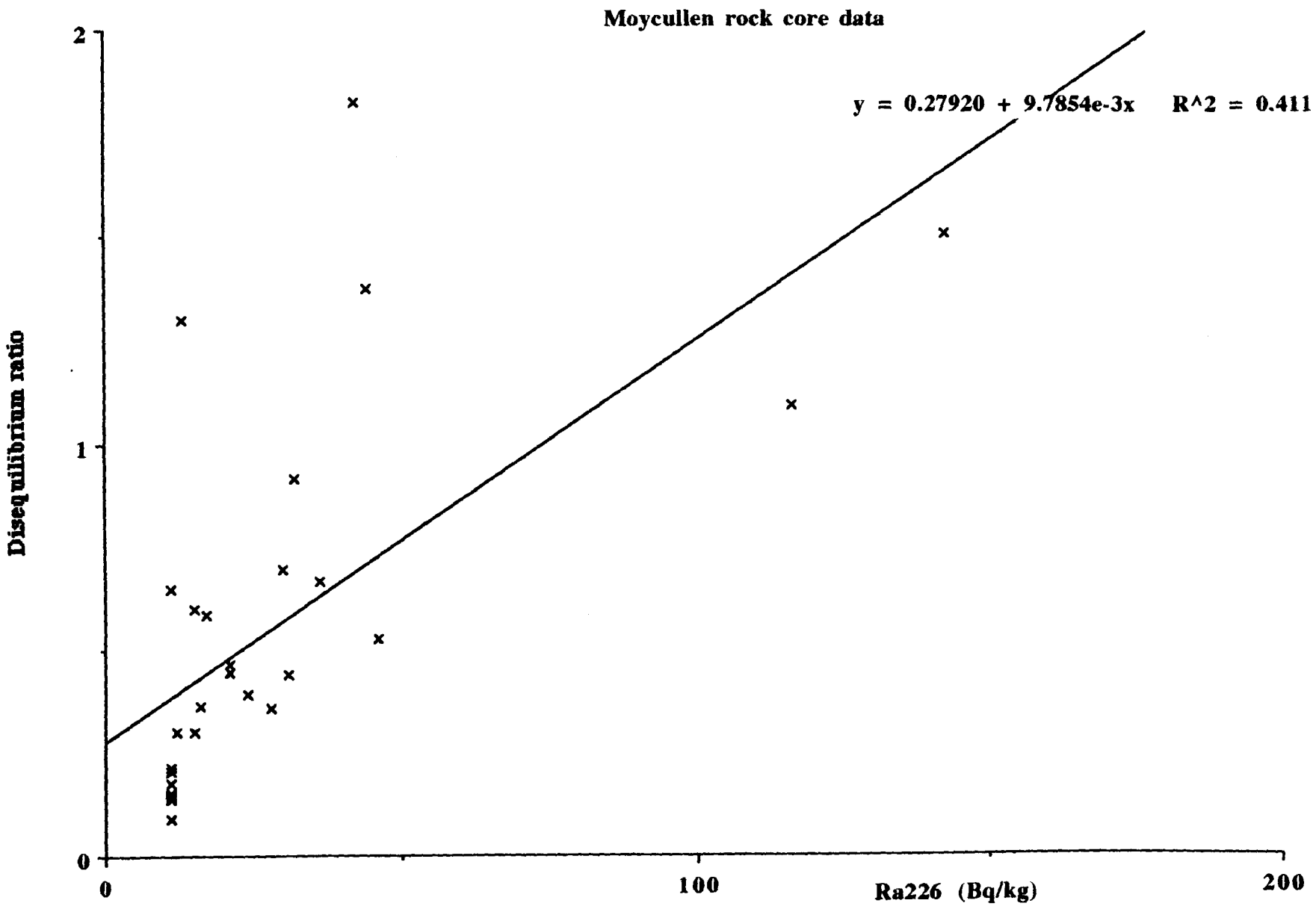
Moycullen rock core data
y = 0.27920 + 9.7854e-3x R^2 = 0.411
Disequilibrium ratio
2
1
0
0
100
200
Ra226 (Bq/kg)

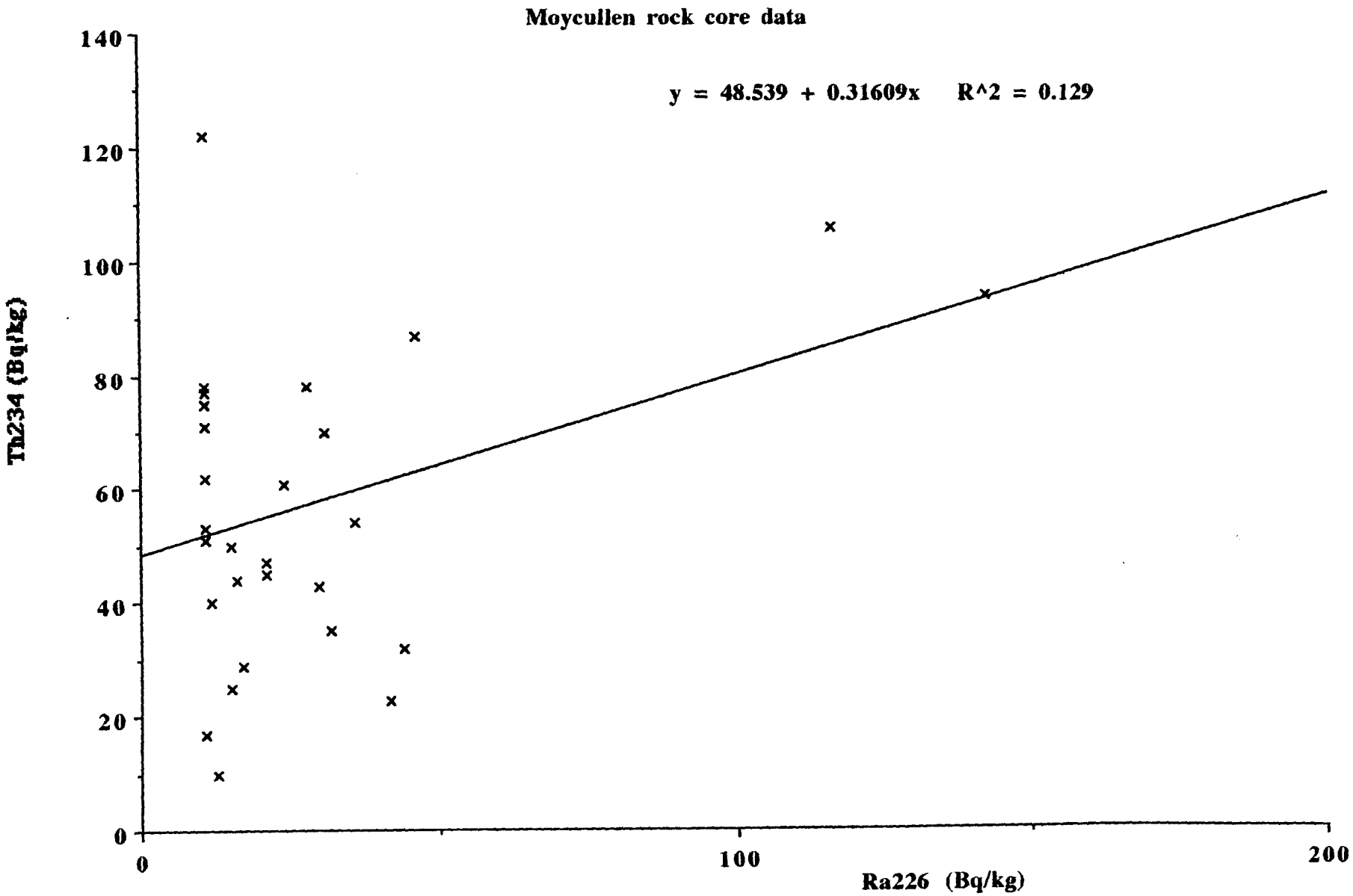
Moycullen rock core data
y = 48.539 + 0.31609x R^2 = 0.129
Th234 (Bq/kg)
140
120
100
80
60
40
20
0
0
100
200
Ra226 (Bq/kg)

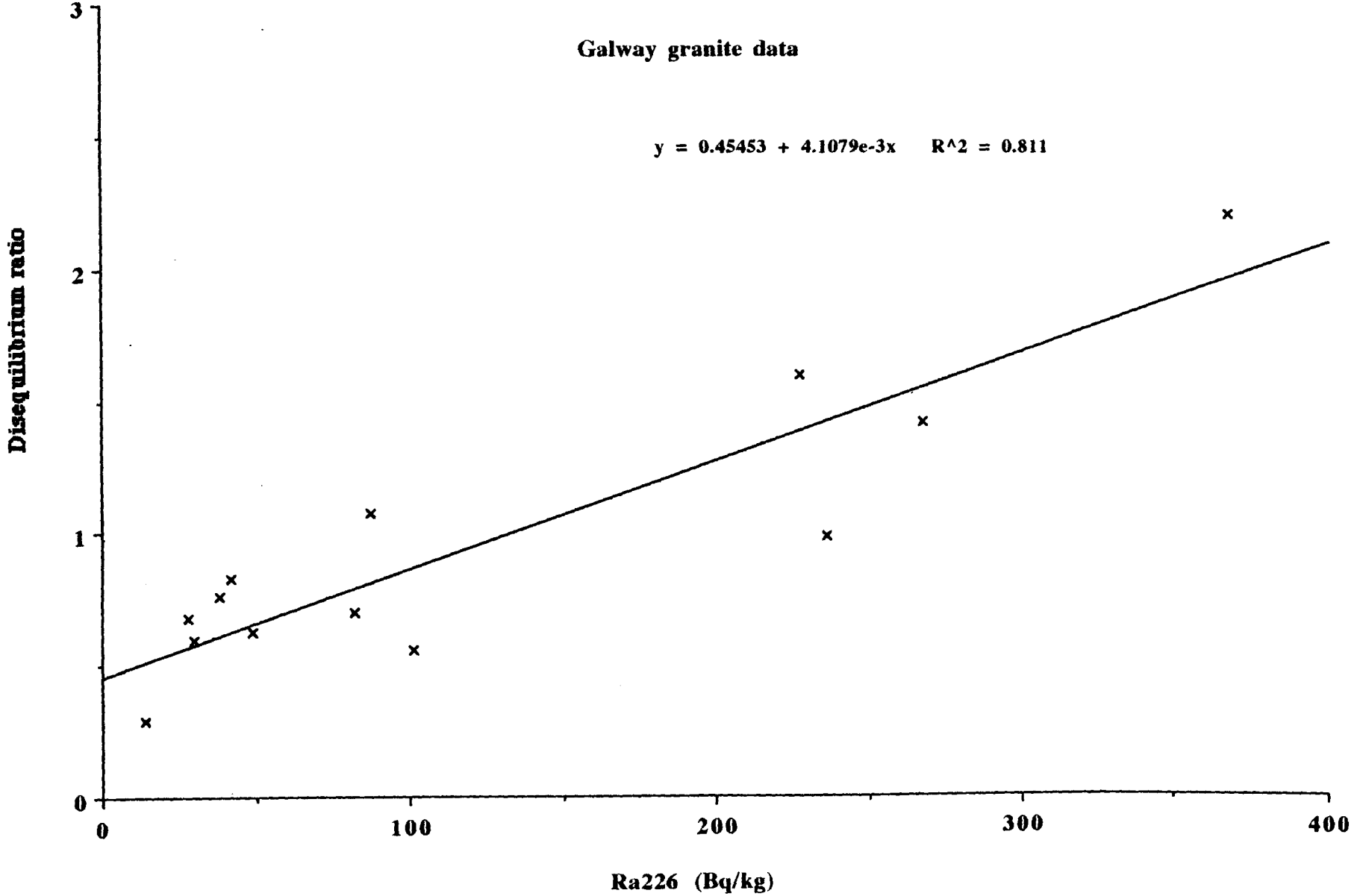
Galway granite data
y = 0.45453 + 4.1079e-3x R^2 = 0.811
Disequilibrium ratio
Ra226 (Bq/kg)
0
1
2
3
0
100
200
300
400

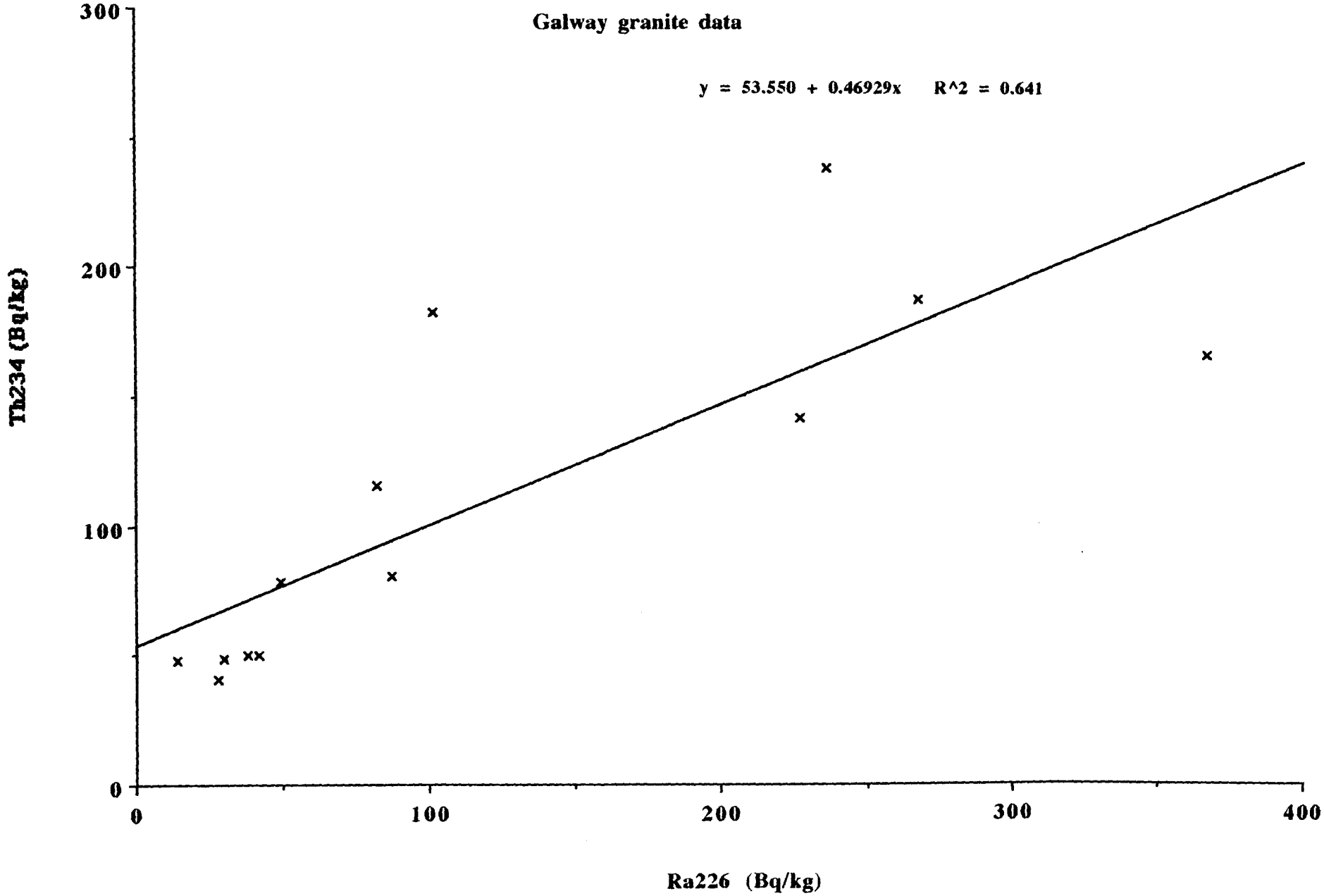
Galway granite data
y = 53.550 + 0.46929x R^2 = 0.641
Th234 (Bq/kg)
Ra226 (Bq/kg)
0
100
200
300
400

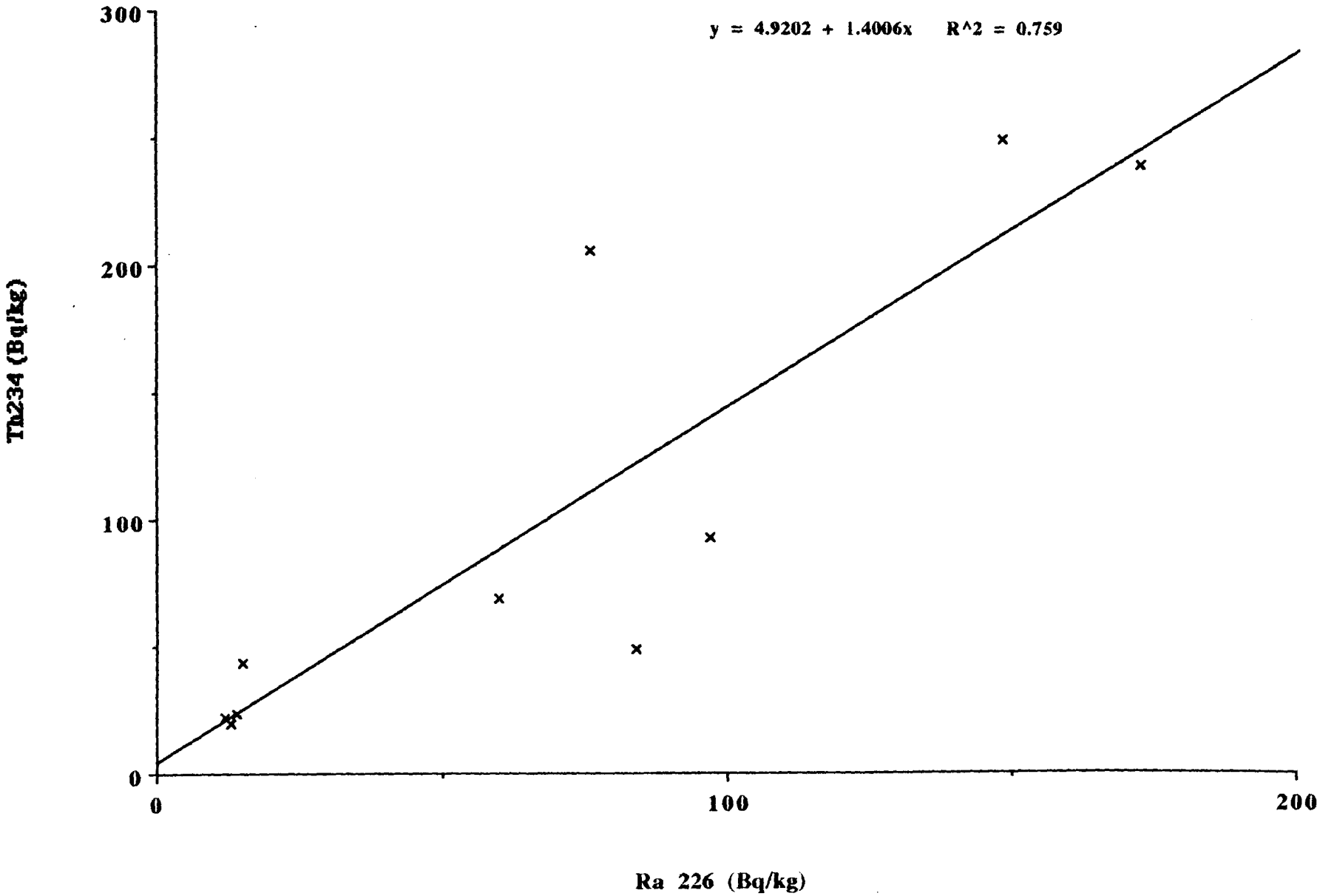
Moycullen rock data
y = 4.9202 + 1.4006x R^2 = 0.759
300
200
100
0
0
100
200
Th234 (Bq/kg)
Ra 226 (Bq/kg)

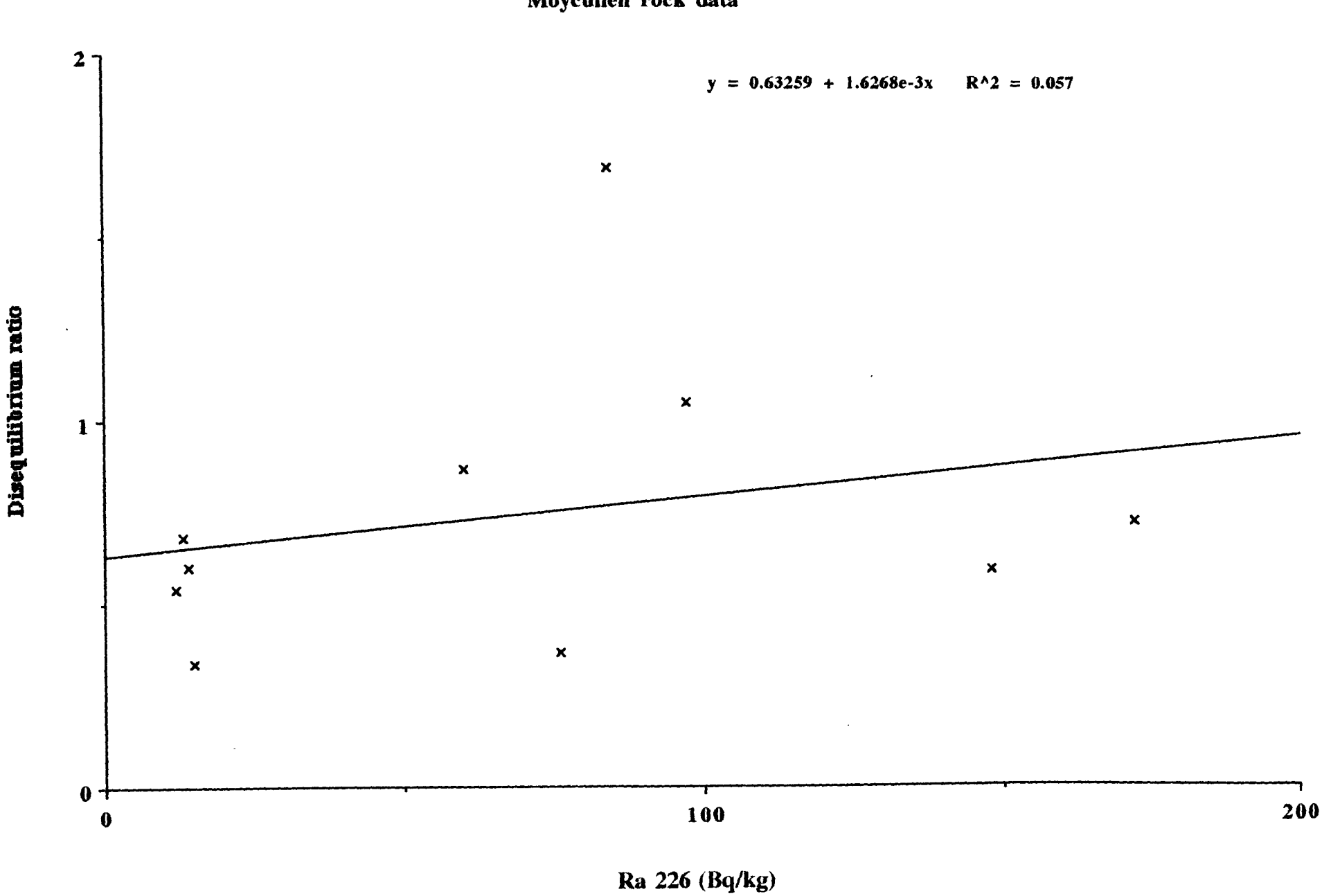
Moycullen rock data
y = 0.63259 + 1.6268e-3x R^2 = 0.057
Disequilibrium ratio
2
1
0
0
100
200
Ra 226 (Bq/kg)

# ANNEX 5

Contribution of
Bundesanstalt für Geowissenschaften und Rohstoffe

G. van den Boom and R. Müller

# Contents

## 5.1. Introduction

The application of gas-geochemical methods within the framework of geological and environmental investigations is largtely based on past experiences gained during mineral exploration. In recent years new techniques and new methodologies have been developed, tested and applied with new objectives mainly in the field of environmental protection investigations, especially in outdoor surveys. The method used for the studies in Ireland is a combined helium - radon technology which still is in a developing phase but has already shown some success in the following fields of application:

-Identification of concealed ground structures (e.g. fractures, faults, joints etc.) for geological, hydrological and environmental protection investigations

-Helium and radon as indicators for studies of the position of the natural floor of waste disposal sites (both toxic waste and household waste), especially for detection of subsurface zones with higher permeability

-Measurement of radon potentials of different lithological units and tracing of migration channels for terrestrial gases

-Accompanying geochemical measurements for detection and qualification of important fracture zones

-Application of the combined helium - radon method for identification of regional distribution patterns of tectonic structures in areas of geothermal anomalies

-Environmental protection investigations in areas with known radon contamination in populated districts where outdoor surveys using both helium and radon can provide additional additional and important information concerning the distribution of radon in soil air and the delineation of radon migration paths.

The last mentioned field of application is the objective of the current R & D Project carried out in a karstic terrain in western Ireland.

There is no documented previous experience in applying the helium-radon method in a region underlain by karstic limestone with a relatively thin cover of soil. Sampling methods and data evaluation had to be modified to meet the new conditions and to optimize the methodology for further tests and application in areas with similar geology, structural settings and pedology. The application of the helium-radon method in the area was therefore an exellent opportunity to test, modify and optimize the methodology. It will be necessary to test the method in another area of similar geology before the methodology is fully capable and ready for routine application. The second necessary step, however, will be undertaken in a second phase of the programme.

## 5.2. Methodology

The requirements for the application of gas-geochemical methodologies for the

determination of lithological radon potentials and their use in the detection of concealed tectonic structures are based on the fact that structural discontimuties of any kind might serve as migration channels for gases emanating from deeper portions of the crust or even the mantle. The design of the sampling pattern in any region has to be varied to obtain optimal results for the detection of subsurface zones with higher permeability. Even if these zones are covered by soil or unconsolidated sediments of many meters of thickness the detection of helium and radon anomalies is possible because there is a difference in permeability between fractures and the rocks in which they occur.

The possibility of application of gasgeochemical methods depends on gas conditions of the solid earth in general and other factors which control the distribution of terrestrial gases (Figure 5.1 and 5.2).

HELIUM occurs as two isotopes, $^{3}He$ and $^{4}He$, where the latter is 1.2 to 1.4 million times more abundoned than $^{3}He$. This is the reason for applying the general term "helium" to the $^{4}He$ - isotope.

$^{4}He$ derives by radioactive decay from :

$^{238}Uranium$ ---------> $^{206}Pb + 8\ ^{4}He$
$^{235}Uranium$ ---------> $^{207}Pb + 7\ ^{4}He$
$^{232}Thorium$ ---------> $^{208}Pb + 6\ ^{4}He$

According to Eremeev (1973) 96 % of lithospheric helium is formed below the granitic / sedimentary stratum in the lower crust. This helium has to migrate through the earth crust to reach the surface. The transport mechanism is very complex and transport in solution is thought to play the main role.

Helium is an ideal geological "tracer" because it is

-chemically inert
-physically stable and therefore capable of travel over long distances
-soluble in hydrocarbons
-highly volatile with high migration potential
-distributed worldwide at a constant concentration of 5240 ppb (by volume) in the atmosphere.

The helium distribution at the earth's surface depends on :

-the permeability of the crustal rocks through which it might migrate and the depth of occurrence within the crust (or mantle)
-presence of deep going fractures, which might serve as migration channels
-presence of radioactive mineral occurrences which form regionally limited helium sources
-presence of hydrocarbon deposits and geothermal resources, which trap helium and release it gradually.
-nature of fluids which transport helium in solution in the crust.

The second gas used as a partner in the methodology described is RADON - 222 ($^{222}Rn$). It is produced from the radioactive decay of radium-226 ($^{226}Ra$), which is in turn a product of the decay of uranium-238 ($^{238}U$). Other isotopes of radon occur naturally, but

are of less importance in terms of indoor radiological risk because of their short half-lives and less common occurrence. The exception to this is thoron (radon-220), which occurs in high enough concentrations to be of concern in a few local areas. In general the concentration and mobility of radon in a soil are dependent on several factors, the most important of which are the soil's radium content and distribution, porosity, permeability to gas movement, and moisture content. These characteristics are, in turn, determined by the character of the bedrock, glacial deposits or transported sediments from which the soil was derived, as well as the local climate and the soil's age or maturity.
Radon transport in soils occurs by two processes, convective or advective flow and diffusion. Diffusion is the dominant radon transport process in soils of low permeability (generally less than $10^{-7}$ $cm^2$), whereas convective transport processes tend to dominate in highly permeable soils (generally greater than $10^{-7}$ $cm^2$). Radon transport distance is limited in low-permeability soils because of the short distance radon may travel during its half-life (3.82 days).

When radium decays in the soil, not all radon produced will be mobile. The portion of radium that can potentially release radon into pore space and fractures of rocks and soils is called the emanating fraction. When a radium atom decays to radon, the energy generated is strong enough to propel the radon atom a distance of about 40 nanometers - this is known as alpha recoil. Depending on where radium is distributed in the soil, much of the radon produced could end up imbedded in adjacent soil grains rather than becoming mobile in the pore space between grains. Moisture greatly affects the recoil distance. Because water is more dense than air, a radon atom will travel a shorter distance in a water-filled pore than in an air-filled pore; therefore moisture lessens the chance of a recoiling radon atom becoming imbedded in an adjacent grain. However, too much moisture can block soil pores and impede radon movement out of the soil.

Soil-gas radon concentrations can vary in response to climatic and weather variations on hourly, diurnal, or seasonal time scales.

### 5.3. Description of the sampling technique for soil gas.

Many factors affect the concentration of radon in the soil : The Ra concentration, the emanation characteristics of the soil organic and mineral matter, the soil porosity, permeability, moisture content and meteorological conditions. Similarly, there are many factors that come into play when collecting a sample of soil gas for analysis. All sampling methods disturb the soil environment to some degree and they sample different regimes of the soil air, such as differing proportions of micro- or macropores. Therefore the selection of a specific soil-gas sampling method is based upon some compromises such as requirements for a special sample size, the need for unique pumping or pressure differential requirements, or for sampling at a particular soil horizon or depth.

The sampling method described here is one that has many advantages for measuring the relative distribution of radon and helium concentrations in the surficial environment. This method has been applied for many years by the U.S. Geological Survey ( Reimer, 1989) and has been further developed by BGR. The sampling method has advantages and limitations but both are definable.

The technique involves pounding a small diameter hollow steel probe into the ground and using a hypodermic syringe for collecting the sample (Figures 5.3 - 5.4 ).

The approach is very useful for samples that are analysed immediately in the field

area. The primary disadvantage of the method is that it is a "grab sample" defining the concentration only for the environmental and meteorologic conditions that exist at the time of collection.

Soil gas samples can be stored in the syringe if the needle is capped to prevent gas loss or exchange with the atmosphere. In our study, however, the radon sample was immediately transferred into a prepared Lucas cell after collection. Soil air samples for helium analysis were injected into special laser-welded bi-metal containers which were tested for helium leakage and proved to be tight for many days.

Radon analyses were carried out at least three hours after sampling. Helium samples were taken to the field laboratory in Galway University for mass-spectroscopic analysis.

## 5.4. Techniques used for helium and radon analyses.

### 5.4.1. Helium analysis.

For measurement of the helium concentration in soil air samples a Balzers helium mass spectrometer (Fig. 5.6.) was used. This instrument is equipped with a quadrupole magnetic system and focussed on the determination of the mass 4. Since the helium background concentration in ambient air is very low (5240 ppb(v)) and the contrast between background and anomaly often is less than 100 ppb the analytical equipment has to be very reliable, precise and capable of measuring up to 100 samples per day with the same precision.

The precision of the mass spectrometer is approximately +/- 20 - 25 ppb (v). This value has to be considered in connection with the helium background in ambient air and shows in this regard the instrument capability to measure $1/200^{th}$ of the natural background.

For the analysis of the helium concentration in a soil air sample approximately 5 - 10 ml of gas is used. Since the helium concentration in ambient air has a constant value worldwide, ambient air samples are used as a calibration gas and are measured alternatively with the soil gas samples.

The analytical procedures can be followed on a monitor and the data are stored and evaluated by a PC. All data for the project area are given in the Appendix.

### 5.4.2. The counting technique for radon analysis.

Field analytical instruments are commonly alpha scintillometers which contain a phosphor coated cell (Lucas cell). Evacuating the cells to a predefined vacuum before sample injection permits a small sample to be quantitatively introduced and, in turn, minimizes contamination of the cell with the radon progeny especially when high concentrations of radon are encountered. The procedure allows the repeated use of a single cell for an extended period before the cell background becomes significant.

With our technique, a gas sample of 10 ml volume is withdrawn from the probe with a plastic hypodermic syringe and then introduced into an evacuated Lucas cell of approximately 100 ml nominal volume. Counting begins at least 3 hours after sampling. At that time radon gas and its daughter products are in equilibrium in the cell. Counting time is usually ten minutes. Immediately after the analysis the cell has to be evacuated by a strong vacuum pump to keep the cell contamination as low as possible (Fig. 5.7.). Data are given in the Appendix.

## 5.5. Quality control.

### 5.5.1. Helium analysis.

For intercomparison and intercalibration purposes, approximately twice a year calibration gases and special samples are exchanged between BGR and Dr.G.M.REIMER of the U.S. Geological Survey in Denver.

### 5.5.2. Radon analysis.

Quality control of radon equipment and counting technique includes a technical check-up of the radon monitors and the Lucas cell. This inspection takes place once a year for determination of the cell efficiency and with our own radon source a monthly control of the AB 5 Monitors.

Furthermore an intercomparison test was carried out during the project with the radon equipment of RPII in Dublin. Table 1 shows the result of this calibration test. The test was performed under the technical conditions which normally apply during fieldwork. The two sampling methods used differ in the amount of soil air used for measuring the radon concentrations. When adjustment is made for this both instruments and methods show very similar results so that both applied methodologies are comparable.

| | | Volume Soil-Gas | Counts/10 Min. | Result |
|---|---|---|---|---|
| TEST 1 | BGR | 10 ml | 300 | 24 630 Bq/m$^3$ |
| | NEB | 161 ml | 4 771 | 23 320 " |
| TEST 2 | BGR | 10 ml | 660 | 54 260 Bq/m$^3$ |
| | NEB | 161 ml | 11 359 | 55 500 " |

Table 1 : Results of two Intercomparison Tests of Radon Equipment

## 5.6. Statistical evaluation of sample data

Statistical parameters of the helium and radon populations of the entire project area, the limestone area, and the granite area are shown in the following tables 2 and 3. Data are given in the Appendix.

| | WHOLE PROJECT AREA | LIMESTONE AREA | GRANITE AREA |
|---|---|---|---|
| Sample Size | 447 | 294 | 153 |
| Average | 5305 | 5296 | 5322 |
| Median | 5275 | 5267 | 5283 |
| Mode | 5255 | 5247 | 5255 |
| Geometric Mean | 5304 | 5295 | 5321 |
| Standard Deviation | 98.004 | 91.4 | 107.78 |
| Minimum | 5013 | 5092 | 5013 |
| Maximum | 5759 | 5759 | 5685 |
| Range | 746 | 667 | 672 |
| Lower Quartile | 5246 | 5244 | 5252 |
| Upper Quartile | 5344 | 5324 | 5384 |

Table 2 : Statistical Parameters of the Helium Concentration in the collected Soil-Gas Samples in Western Ireland

| | WHOLE PROJECT AREA | LIMESTONE AREA | GRANITE AREA |
|---|---|---|---|
| Sample Size | 367 | 255 | 112 |
| Average | 54300 | 47500 | 69900 |
| Median | 43800 | 36900 | 68050 |
| Mode | 21900 | 21900 | 76100 |
| Geometric Mean | 39500 | 34200 | 54800 |
| Standard Deviation | 39225 | 35837 | 42218 |
| Minimum | 400 | 400 | 2600 |
| Maximum | 186300 | 184400 | 186300 |
| Range | 185900 | 184000 | 183700 |
| Lower Quartile | 23400 | 20200 | 36450 |
| Upper Quartile | 76100 | 66900 | 89850 |

Table 3 : Statistical Parameters of the Radon Concentration in the collected Soil-Gas Samples in Western Ireland

Helium concentrations in the soil-gas samples show a wide range from 667 to 746 ppb. The highest value was observed in the limestone area (5 759 ppb He). In the granite area, the maximum value is approximately 100 ppb lower. However,if one considers the average values of the helium population, the granite area shows a population with higher helium values.

helium values.

The distribution of the soil-gas radon concentration shows in both sampled areas a range of > 180 000 Bq/m$^3$, while both the average and maximum values are highest in the granite area.

The frequency distribution for helium shows a lognormal distribution (Fig. 5.8., 5.10., and 5.12.) with a second population indicated at concentrations > 5 300 - 5350 ppb. Two populations occur in the radon distribution, also, but much more distinct at a threshold value of approximately 50 000 Bq/m$^3$ (see figures 5.9., 5.11., and 5.13.).

One would expect that the two radon populations are caused by the two different lithologic units that were sampled. However, comparing the frequency histograms of radon and helium in the segregated limestone and granite data sets it is obvious that this is not the case and that the two radon population still prevail in the limestone and in the granite area and that in both areas the thresholds are approximately at the same level of 50 000 Bq/m$^3$. However, the threshold values showing the beginning of the second helium population in the two different lithological units differ. Limestone samples show a threshold value between 5 300 and 5 350 ppb, while samples taken from the granite area show the threshold of a second helium population at approximately 5 400 ppb.

These statistical parameters were taken into account for defining normal and anomalous populations for both variables. Therefore, helium concentrations > 5 330 ppb (in limestone) and 5400 ppb (in granite), respectively, and radon values higher than 50 000 Bq/m$^3$ in both areas are considered as anomalous.

Interpretation of these results allow us to conclude that, in the case of the area sampled in Western Ireland, the radon hazard has almost the same impact on populated areas in both the limestone and granite area.

## 5.7. Regional distribution of radon and helium

### 5.7.1. Distribution of Radon Concentrations in Soil-Air Samples

5.7.1.1. Area I (Ballydotia - Moycullen) (Maps 1 and 2)

As shown in section 5.6 anomalous radon concentrations are values > 50 000 Bq/m$^3$. This threshold value is valid for samples collected in both the limestone and granite areas. Maps 1 and 2 show the spatial distribution of these high radon samples in the limestone and granite lithologies.

In the more northerly region (Ballydotia) two small areas with anomalous radon concentrations occur (Map 1). Between the two areas there is a small gap where several houses are located. House No. 10 shows an elevated indoor radon concentration of 725 Bq/m$^3$ (Annex 1, Map 3). The radon values measured in the close vicinity of this house are: 21 300, 37 300, 39 300, 11 700, 39 900, and 35 500 Bq/m$^3$. All outdoor soil-gas radon levels are below the defined threshold for anomalous radon concentrations in soil air. Besides there is one anomalous helium value of 5 350 ppb, that might point out to a small fractured area where radon could easily move upwards. The neighbouring houses show indoor radon values of less than 20 Bq/m$^3$ and only background helium concentrations in the soil-air samples. Although the statistical analysis shows a distinct break in the frequency histogram for radon at approximately 50 000 Bq/m$^3$ this value seems to be too high in relation to elevated indoor radon concentrations in the limestone area.

The statistical analysis made by the Geological Survey of Ireland (Annex 1) showed that radon values decrease with distance from the granite. This can also be observed from

the regional distribution map of radon (Maps 1 and 2). The high radon anomalies do not occur in the northern part of the limestone area. Therefore a threshold level of 30 000 Bq/m$^3$ seems to be more suitable for this part of the area investigated, especially if soil-gas samples in the vicinity of houses show elevated helium values demonstrating the possible presence of fractures. Areas showing radon samples higher than this limit of 30 000 Bq/m$^3$ are also included in the radon distribution map (Maps 1 and 2).

The largest area with anomalous radon concentrations lies in the central part of the region investigated (Moycullen). This area strikes SE-NW and might continue to both sides. No sampling has been performed in the assumed continuation. East of the main road in the southern portion of the sampled area a third zone with high and anomalous radon concentrations in soil air samples has been observed.

It should be mentioned here that in many parts of the project area sampling was very difficult because of very poor development of soil. This is the reason for gaps in the sampling pattern. In a number of sampling stations only one sample (helium) could be collected so that radon values are not available from all sample points. This is the case especially in the granite area close to the granite/limestone contact where soil development is poor over large areas. The radon values obtained do not allow a reliable interpretation of the sparse data.

5.7.1.2. Area II (UGGOOL) (Map 3)

The entire Uggool area is located in the granite region with very poor soil development.

The radon potential of this rock unit is in general higher than that of the limestone region. A total of 79 soil-gas samples were collected, 69 of which were analyzed for radon. Forty-nine soil-air samples sh[illegible]ncentrations higher than 50 000 Bq/m$^3$. 12 of these were in the range between 80 0[illegible]000 Bq/m$^3$ and 11 were > 100 000 Bq/m$^3$. The regional distribution is shown in Map [illegible].

The centre of the area investigated shows relatively low radon concentrations in soil-air. This centre is surrounded by a zone of high radon values >50 000 Bq/m$^3$ in which 5 cluster of even higher radon concentrations are located.

### 5.7.2. Distribution of Helium Concentrations in Soil-Air

5.7.2.1. Area I (Ballydotia - Moycullen) (Maps 1 and 2)

Abnormally high helium concentrations in soil-gas have been observed where soils overlie fault and fracture systems (Pierce et al.1964, Eremeev et al. 1973, Ovchinnikov 1973, and Jones and Drozd 1983).

Most soil-gases at depth less than 1 meter are in constant communication with the atmosphere and, as a result, measured soil-gas helium concentration is fairly close to that observed in the air itself. How[illegible]f a significant subsurface conduit for helium, such as a fault or fracture system, this m[illegible]ute abnormally large amounts of helium locally to the continuous flux and soil-gas he[illegible]oncentrations are observed on the order of tens or even hundreds of parts per billion [illegible]olume (vpb) above the normal atmospheric background.

In the area investigated certain faults and fractures are known and more are assumed to occur beneath th overburden. The vicinity of the granite underlying the limestone rock unit favour the conditions for helium sources. The tectonic pattern of faults, fractures and most probably karstic development in the limestone follows north-south directions.

Based on the results of the helium survey carried out in the limestone area and in the

contact zone limestone/granite, several approximately north-south striking lineaments were mapped. It is not possible to classify these concealed structures, but they probably represent the subsurface locations of joints and fractures. It must also be assumed that these lineaments serve as migration paths for terretrial gases, such as radon and helium.

A second preferred lineament is demonstrated by northwest-southeast striking elements which run parallel to the mapped granite/limestone contact. The contact itself was not detected by the helium survey. The question of whether this contact is tectonic or a normal geological contact could not be answered by the soil-gas sampling carried out in a small portion of the contact region. There is, however, some evidence from the helium survey for assumed faults in the granite close to the limestone contact. The existence of these structures are suggested by some low density He sampling in the granite.

Maps 3 and 4 in Annex 1 show the distribution of helium concentrations in soil-air samples and an interpretation of the results is given in Maps 1 and 2 of this Annex. Only a denser sampling pattern could clarify the situation in some parts of the area.

5.7.2.2. Area II (Uggool) (Map 3)

Most of the zones with very high radon concentrations in soil air also show anomalous helium values. The tectonic distribution pattern in the granite area is not as well known as in the limestone region. However, detection of tectonic lineaments based on the helium survey is relatively easy particularly as helium anomalies are well supported by radon anomalies. Two fracture systems were detected, a NE-SW direction which occurs several times in the relatively small surveyed area and an approximately N-S striking direction. All these lineaments are accompanied by radon haloes with > 50 000 Bq/m$^3$ activity concentration and in several cases by even much higher radon values.

## 5.8. Discussion of results and conclusions

The investigation in Western Ireland has shown that the application of a combined helium-radon method leads to important results regarding the radiation protection of the population. Knowledge of the occurrence of radon alone is not sufficient for further steps protecting the inhabitants of contaminated houses. It is very important to lead the investigations to the source of radon and the migration paths used by radon to reach the earth surface and to contaminate the soil cover or even the basement of buildings. Especially the detection of migration channels, normally tectonic lineaments such as faults, fractures or joints but also karst developments in the limestone may be possible by application of helium, which shows anomalous concentrations in soil air in the vicinity of the mentioned tectonic features. In many cases it is obvious that high helium concentrations in the soil air samples are not correlated with high radon values in soil air.

If one considers the genesis of both gases it is also obvious that one should not expect a good correlation between the two noble gases. Firstly the helium can migrate over much longer distances from its source than radon, because of the decay of the latter. It is therefore possible that the helium source is different from the radon source. Secondly radon has the ability to move laterally in the soil especially if a certain moisture is present. High radon values must not be necessarly in place. The bad correlation between the two gases is caused by the high radon values which are not connected with structures detected by helium. It can, however, be seen from the maps (Maps 1 - 3) that radon builds up haloes around lineament determined by the helium survey.

For the determination of the migration ways for terrestrial gases helium is the best "pathfinder.

Concerning the source of radon it was shown in the histograms from the radon soil-gas data taking into account the distance of the collected samples from the granite that samples taken from the granite area itself, from the marginal "white" granite and within a distance of 400 m from the granite in the limestone contain high radon concentrations between 100 000 and 180 000 Bq/m$^3$. Farer away from the granite (400 - 800 m) the highest radon value in the soil-gas samples is around 140 000 Bq/m$^3$. These maximum radon concentrations drop to 100 000 and 90 000 Bq/m$^3$ in 800 - 1200 and 1200 - 1600 m distance from the granite, respectively. This might allow a first conclusion that the source of the radon encountered in the limestone area might be located in the granite. Transportation and migration of the gas into the soil overlying the limestone rock unit is possible via deep reaching fractures, joints and faults.

## 5.9. Recommendations

The gas-geochemical soil gas helium-radon method has been tested and applied in a geologically and pedologically very difficult area. The results obtained from the survey are very promising. But there are still some problems to solve and open questions to answer. Based on our experience gained in the first application of the method in a karstic terrain further development of the techniques and evaluation procedures is strongly recommanded. It should be carried out in a second phase in an area of similar geological and tectonical conditions. There are still more tests necessary to design and test the optimal sampling density in a karstic limestone area. The sampling depth is very important and so many localities show only a very thin soil cover so that samples have to be taken from a depth much less than 1 meter. Is there a possibility to measure the radon flux in the soil cover and to correct all data received from shallow depth ?

More helium studies have to be carried out in the vicinity of buildings and houses to determine the importance of high helium concentration in connection with high indoor radon results. Last not least the application of the helium method can submit important results for determining radon availablity and soil permeability, two parameters for a better interpretation of high indoor radon concentrations.

## 5.10. Literature


**Boom, G.van den (1981)** Geochemische Prospektionsmethoden, Angew. Geowissensch., Bd.1,S.3327-3357, Enke Verlag, Stuttgart.

**Boom, G. van den (1986)** Weiterentwicklung und Anwendung gasgeochemischer Methoden, Vertrag MSM-001-D(B), Komm.d.Europ.Gemeinschaften

**Boom, G. van den (1986)** Korrekturen zur Bestimmung des heliumgehaltes in Bodenproben, *Geol.Jb.*,Reihe D,80,47-71

**Boom, G. van den Boom (1987)** Helium Distribution Pattern of measured and corrected Data around the Eldingen Oil-field, NW Germany, *J.of Geophysical Research*, Vol.92,No. 812, P.12547-12555.

**Boom, G. van den, et al.(1991)** Mapping of $^{222}$Rn and $^{4}$He in Soil Gas over a karstic Limestone-Granite boundary. Correlation of high Indoor $^{222}$Rn with Zones of

enhanced Permeability. Fifth International Symposium on the Natural Radiation Environment

**Boom, G. van den Boom & R. Müller (1991)** Bericht über die Durchführung von Helium -Radon Messungen in fünf Testgebieten in der CSFR. Umweltradioaktivität, Interdisziplinäre Umweltforschung, Marianska (CSFR), Vortrag und Bericht BGR Archiv Nr. 108990

**Eremeev,A.N. et al. (1973)** Application of Helium Surveying to Structural Mapping and Ore deposit Forecasting, Moscow State University and the Scientific Council for Geochemical Prospecting, Moscow, UdSSR

**Golubev,V.S.,et al (1970)** Some Characteristics of Migration of Helium in the Permeable Systems of the Upper Part of the Earth's Crust. *Geokhimiya*, No.11,pp.1341-1348.

**Ovchinnikov, L.N. et al. (1972)** Gaseous geochemical methods in structural mapping and prospecting for ore deposits. Inst. of Mineralogy, Geochemistry, and Cristallochemistry of Rare Elements, Moscow, USSR.

**Oxburgh, E.R. & K. O'Nions (Manuscript, no date)** Helium Loss, Tectonics, and Terrestrial Heat Budget. Deprtm. of Earth Sc., Univ. of Cambridge, England

**Reimer.G.M. (1985)** Fault Demarcation from Helium Soil-Gas Profiles near Oroville, California. U.S. Geological Survey, Denver

**Reimer, G.M. & L.C.S. Gundersen (1989)** A direct correlation among indoor radon, soil gas radon and geology in the Reading prong near Boyertown, Penn.. *Health Physics*, V. 57,No.1, p. 155-160.

**Reimer, G.M. (1990)** The Occurrence and Transport of Radon in the Natural Environment. American Geophysical Union

**Roberts,A. & J.B. Roen (1985)** Near-surface Helium Anomalies Associated with Faults and Gas Accumulations in western Pennsylvania, U.S. Dep. of the Interior, Geological Survey

## 5.11. List of figures

# Appendix

**$^{222}$Rn, $^{4}$He, ΔHe and grid co-ordinates (1:2500 maps) for soil gas samples collected in the Moycullen area**

| X | Y | Number | $^{4}$He, ppb | ΔHe | $^{222}$Rn,Bqm-3 |
|---|---|---|---|---|---|
| 121714 | 234224 | 1.001 | 5127 | -113 | 13900 |
| 121676 | 234221 | 1.002 | 5228 | -12 | 51000 |
| 121650 | 234227 | 1.003 | 5201 | -39 | 17700 |
| 121607 | 234241 | 1.004 | 5242 | 2 | 83300 |
| 121582 | 234230 | 1.005 | 5244 | 4 | 19600 |
| 121553 | 234210 | 1.006 | 5255 | 15 | 10400 |
| 121521 | 234206 | 1.007 | 5244 | 4 | 21800 |
| 121523 | 234156 | 1.008 | 5230 | -10 | 37300 |
| 121547 | 234165 | 1.009 | 5281 | 41 | 61800 |
| 121581 | 234170 | 1.010 | 5266 | 26 | 21300 |
| 121609 | 234182 | 1.011 | 5247 | 7 | 37300 |
| 121638 | 234174 | 1.012 | 5227 | -13 | 14700 |
| 121678 | 234150 | 1.013 | 5290 | 50 | 31100 |
| 121596 | 234186 | 1.014 | 5247 | 7 | 39300 |
| 121628 | 234154 | 1.015 | 5245 | 5 | 10300 |
| 121632 | 234129 | 1.016 | 5226 | -14 | 12700 |
| 121631 | 234082 | 1.017 | 5257 | 17 | 24600 |
| 121639 | 234055 | 1.018 | 5292 | 52 | 11900 |
| 121593 | 234166 | 1.019 | 5335 | 95 | 11700 |
| 121587 | 234129 | 1.020 | 5281 | 41 | 10000 |
| 121583 | 234088 | 1.021 | 5269 | 29 | 20500 |
| 121578 | 234057 | 1.022 | 5286 | 46 | 12400 |
| 121708 | 234212 | 1.023 | 5287 | 47 | 44600 |
| 121607 | 234241 | 1.024 | 5277 | 37 | 23800 |
| 121594 | 234319 | 1.025 | 5276 | 36 | 8100 |
| 121599 | 234286 | 1.026 | 5250 | 10 | 4500 |
| 121564 | 234222 | 1.027 | 5263 | 23 | 13000 |
| 121594 | 234154 | 1.028 | 5253 | 13 | 39900 |
| 121601 | 234193 | 1.029 | 5226 | -14 | 35500 |
| 121587 | 234129 | 1.030 | 5239 | -1 | 6400 |
| 121636 | 234068 | 1.031 | 5252 | 12 | 27500 |
| 121580 | 234067 | 1.032 | 5258 | 18 | 18300 |
| 121547 | 234165 | 1.033 | 5351 | 111 | 71400 |
| 121695 | 234125 | 1.034 | 5253 | 13 | 39000 |
| 121711 | 234076 | 1.035 | 5262 | 22 | 27600 |
| 121728 | 234049 | 1.036 | 5346 | 106 | 2700 |
| 121682 | 233990 | 1.037 | 5281 | 41 | 56900 |
| 121729 | 233881 | 1.038 | 5318 | 78 | 13300 |
| 121782 | 234031 | 1.039 | 5420 | 180 | 17900 |
| 121815 | 234022 | 1.040 | 5275 | 35 | 17600 |

| | | | | | |
|---|---|---|---|---|---|
| 121833 | 233995 | 1.041 | 5281 | 41 | 29700 |
| 121881 | 233966 | 1.042 | 5211 | -29 | 23500 |
| 121894 | 233969 | 1.043 | 5305 | 65 | 45600 |
| 121891 | 233984 | 1.044 | 5324 | 84 | 60500 |
| 121895 | 233989 | 1.045 | 5305 | 65 | 19200 |
| 121907 | 233990 | 1.046 | 5399 | 159 | 55800 |
| 121918 | 234004 | 1.047 | 5252 | 12 | 33900 |
| 121908 | 233953 | 1.048 | 5239 | -1 | 14800 |
| 121850 | 233953 | 1.049 | 5471 | 231 | 39400 |
| 121842 | 233983 | 1.050 | 5276 | 36 | 28400 |
| 121850 | 233930 | 1.051 | 5335 | 95 | 20900 |
| 121802 | 233934 | 1.052 | 5296 | 56 | 25100 |
| 121805 | 233961 | 1.053 | 5247 | 7 | 25000 |
| 121800 | 233915 | 1.054 | 5327 | 87 | 14400 |
| 121737 | 234075 | 1.055 | 5377 | 137 | 42200 |
| 121745 | 234056 | 1.056 | 5434 | 194 | 65600 |
| 121755 | 234017 | 1.057 | 5251 | 11 | 30800 |
| 121775 | 234004 | 1.058 | 5261 | 21 | 28300 |
| 121748 | 234041 | 1.059 | 5300 | 60 | 38500 |
| 121649 | 234205 | 1.060 | 5249 | 9 | 20500 |
| 121609 | 234218 | 1.061 | 5230 | -10 | 35700 |
| 121732 | 234277 | 1.062 | 5278 | 38 | 65900 |
| 121715 | 234431 | 1.063 | 5283 | 43 | 45500 |
| 121697 | 234356 | 1.064 | 5387 | 147 | * |
| 121689 | 234294 | 1.065 | 5334 | 94 | * |
| 121639 | 234291 | 1.066 | 5336 | 96 | 68200 |
| 121628 | 234357 | 1.067 | 5368 | 128 | * |
| 121614 | 234418 | 1.068 | 5436 | 196 | 64800 |
| 121643 | 234472 | 1.069 | 5484 | 244 | * |
| 121559 | 234431 | 1.070 | 5240 | 0 | * |
| 121584 | 234520 | 1.071 | 5372 | 132 | 34200 |
| 121525 | 234514 | 1.072 | 5249 | 9 | * |
| 121470 | 234488 | 1.073 | 5218 | -22 | 54300 |
| 121500 | 234403 | 1.074 | 5247 | 7 | 53600 |
| 121453 | 234416 | 1.075 | 5407 | 167 | * |
| 121375 | 234469 | 1.076 | 5238 | -2 | 58100 |
| 121396 | 234511 | 1.077 | 5256 | 16 | * |
| 121350 | 234443 | 1.078 | 5400 | 160 | * |
| 121407 | 234374 | 1.079 | 5369 | 129 | 87100 |
| 121454 | 234337 | 1.080 | 5380 | 140 | * |
| 121510 | 234294 | 1.081 | 5249 | 9 | 32300 |
| 121545 | 234256 | 1.082 | 5272 | 32 | * |
| 121898 | 233764 | 1.083 | 5246 | 6 | 16800 |
| 121918 | 233832 | 1.084 | 5272 | 32 | 18800 |
| 121922 | 233902 | 1.085 | 5461 | 221 | 67500 |
| 121844 | 233861 | 1.086 | 5304 | 64 | 25200 |
| 121819 | 233806 | 1.087 | 5328 | 88 | 14700 |
| 121800 | 233861 | 1.088 | 5236 | -4 | 28200 |

| | | | | | |
|---|---|---|---|---|---|
| 121797 | 233769 | 1.089 | 5344 | 104 | 29500 |
| 121837 | 233747 | 1.090 | 5331 | 91 | 34700 |
| 121881 | 233670 | 1.091 | 5369 | 129 | 13700 |
| 121829 | 233682 | 1.092 | 5280 | 40 | 43400 |
| 121770 | 233696 | 1.093 | 5328 | 88 | 98400 |
| 121722 | 233725 | 1.094 | 5338 | 98 | 36600 |
| 121764 | 233760 | 1.095 | 5284 | 44 | 9700 |
| 121739 | 233641 | 1.096 | 5427 | 187 | 132800 |
| 121808 | 233630 | 1.097 | 5255 | 15 | * |
| 121974 | 233655 | 1.098 | 5244 | 4 | 11200 |
| 121717 | 234157 | 1.099 | 5247 | 7 | 22200 |
| 121730 | 234101 | 1.100 | 5262 | 22 | 16600 |
| 121794 | 234114 | 1.101 | 5233 | -7 | 7000 |
| 121789 | 234170 | 1.102 | 5292 | 52 | 15300 |
| 121838 | 234175 | 1.103 | 5245 | 5 | 25000 |
| 121848 | 234107 | 1.104 | 5357 | 117 | * |
| 121894 | 234170 | 1.105 | 5243 | 3 | 17600 |
| 121925 | 234208 | 1.106 | 5241 | 1 | * |
| 121973 | 234233 | 1.107 | 5256 | 16 | 1300 |
| 121981 | 234314 | 1.108 | 5276 | 36 | 20100 |
| 121989 | 234381 | 1.109 | 5232 | -8 | 4100 |
| 121915 | 234365 | 1.110 | 5251 | 11 | 9000 |
| 121910 | 234291 | 1.111 | 5243 | 3 | 5500 |
| 121855 | 234262 | 1.112 | 5244 | 4 | 5800 |
| 121790 | 234241 | 1.113 | 5267 | 27 | 3800 |
| 121834 | 234349 | 1.114 | 5295 | 55 | 19000 |
| 121844 | 234410 | 1.115 | 5426 | 186 | 26300 |
| 121915 | 234449 | 1.116 | 5400 | 160 | 38300 |
| 121990 | 234429 | 1.117 | 5263 | 23 | 23200 |
| 121770 | 234368 | 1.118 | 5550 | 310 | 84100 |
| 121976 | 233583 | 1.119 | 5387 | 147 | 56300 |
| 121895 | 233590 | 1.120 | 5216 | -24 | 90200 |
| 121811 | 233577 | 1.121 | 5364 | 124 | 74900 |
| 121735 | 233579 | 1.122 | 5534 | 294 | 182300 |
| 121648 | 233621 | 1.123 | 5252 | 12 | 76800 |
| 121565 | 233673 | 1.124 | 5290 | 50 | 22400 |
| 121602 | 233726 | 1.125 | 5479 | 239 | 61900 |
| 121538 | 233767 | 1.126 | 5675 | 435 | 2500 |
| 121361 | 233914 | 1.127 | 5294 | 54 | 8000 |
| 121374 | 233979 | 1.128 | 5288 | 48 | 13400 |
| 121457 | 234160 | 1.129 | 5151 | -89 | 19800 |
| 121456 | 234205 | 1.130 | 5228 | -12 | 73300 |
| 121317 | 233150 | 2.001 | 5233 | -7 | 38000 |
| 121266 | 233132 | 2.002 | 5249 | 9 | 78700 |
| 121231 | 233105 | 2.003 | 5255 | 15 | 59800 |
| 121194 | 233073 | 2.004 | 5255 | 15 | 55400 |
| 121121 | 232989 | 2.005 | 5260 | 20 | 24200 |
| 121153 | 233012 | 2.006 | 5259 | 19 | 18300 |

| | | | | | |
|---|---|---|---|---|---|
| 121187 | 233038 | 2.007 | 5264 | 24 | 37800 |
| 121216 | 233098 | 2.008 | 5253 | 13 | 43800 |
| 121245 | 233068 | 2.009 | 5250 | 10 | 70500 |
| 121093 | 232967 | 2.010 | 5233 | -7 | * |
| 121067 | 232949 | 2.011 | 5255 | 15 | 19900 |
| 121031 | 232919 | 2.012 | 5269 | 29 | 11400 |
| 121003 | 232894 | 2.013 | 5271 | 31 | 180300 |
| 120965 | 232875 | 2.014 | 5199 | -41 | 37200 |
| 121050 | 232930 | 2.015 | 5570 | 330 | 54300 |
| 120945 | 233091 | 2.016 | 5447 | 207 | 90700 |
| 120841 | 233089 | 2.017 | 5325 | 85 | 85900 |
| 120819 | 233037 | 2.018 | 5369 | 129 | 155500 |
| 120754 | 233034 | 2.019 | 5275 | 35 | 164200 |
| 120614 | 233046 | 2.020 | 5451 | 211 | 99600 |
| 120559 | 232916 | 2.021 | 5558 | 318 | 65500 |
| 120535 | 232876 | 2.022 | 5466 | 226 | 152000 |
| 120632 | 232793 | 2.023 | 5283 | 43 | 66800 |
| 120786 | 232735 | 2.024 | 5446 | 206 | 24500 |
| 120953 | 233128 | 2.025 | 5366 | 126 | 79300 |
| 120974 | 233164 | 2.026 | 5254 | 14 | 28700 |
| 120940 | 233194 | 2.027 | 5271 | 31 | 109500 |
| 120877 | 233271 | 2.028 | 5479 | 239 | 74500 |
| 120902 | 233292 | 2.029 | 5369 | 129 | 80400 |
| 120920 | 233308 | 2.030 | 5443 | 203 | 118000 |
| 120935 | 233322 | 2.031 | 5314 | 74 | 116000 |
| 120969 | 233350 | 2.032 | 5255 | 15 | 30000 |
| 120990 | 233367 | 2.033 | 5258 | 18 | 12000 |
| 121018 | 233372 | 2.034 | 5286 | 46 | 64200 |
| 121049 | 233410 | 2.035 | 5308 | 68 | 88000 |
| 121067 | 233441 | 2.036 | 5399 | 159 | 72000 |
| 121088 | 233470 | 2.037 | 5331 | 91 | 18700 |
| 121094 | 233483 | 2.038 | 5248 | 8 | 7900 |
| 120852 | 233262 | 2.039 | 5252 | 12 | 26500 |
| 120831 | 233257 | 2.040 | 5257 | 17 | * |
| 120814 | 233242 | 2.041 | 5281 | 41 | 80400 |
| 121469 | 232587 | 2.042 | 5305 | 65 | 28500 |
| 121487 | 232598 | 2.043 | 5247 | 7 | 30900 |
| 121532 | 232629 | 2.044 | 5271 | 31 | 66100 |
| 121551 | 232652 | 2.045 | 5230 | -10 | 34600 |
| 121569 | 232673 | 2.046 | 5385 | 145 | 83300 |
| 121590 | 232697 | 2.047 | 5261 | 21 | 21000 |
| 121614 | 232711 | 2.048 | 5250 | 10 | 48500 |
| 121640 | 232740 | 2.049 | 5256 | 16 | 89500 |
| 121651 | 232759 | 2.050 | 5275 | 35 | 57700 |
| 121669 | 232783 | 2.051 | 5302 | 62 | 26200 |
| 121670 | 232816 | 2.052 | 5217 | -23 | 29300 |
| 121689 | 232826 | 2.053 | 5235 | -5 | 15400 |
| 121711 | 232826 | 2.054 | 5292 | 52 | 31900 |

| | | | | | |
|---|---|---|---|---|---|
| 121718 | 232859 | 2.055 | 5276 | 36 | 36600 |
| 121738 | 232881 | 2.056 | 5339 | 99 | 32900 |
| 121749 | 232908 | 2.057 | 5202 | -38 | 19800 |
| 121747 | 232931 | 2.058 | 5263 | 23 | 58700 |
| 121766 | 232989 | 2.059 | 5245 | 5 | 75600 |
| 121787 | 233040 | 2.060 | 5322 | 82 | 110000 |
| 121764 | 233084 | 2.061 | 5321 | 81 | 35400 |
| 121749 | 233158 | 2.062 | 5231 | -9 | 34500 |
| 121748 | 233213 | 2.063 | 5257 | 17 | 22500 |
| 121749 | 233251 | 2.064 | 5275 | 35 | 400 |
| 121770 | 233282 | 2.065 | 5312 | 72 | 17800 |
| 121398 | 232515 | 2.066 | 5348 | 108 | 30000 |
| 121384 | 232498 | 2.067 | 5283 | 43 | * |
| 121368 | 232482 | 2.068 | 5211 | -29 | * |
| 121354 | 232459 | 2.069 | 5198 | -42 | * |
| 121380 | 232403 | 2.070 | 5236 | -4 | * |
| 121362 | 232365 | 2.071 | 5258 | 18 | * |
| 121271 | 232377 | 2.072 | 5360 | 120 | 45200 |
| 121245 | 232353 | 2.073 | 5221 | -19 | * |
| 121239 | 232288 | 2.074 | 5013 | -227 | 60400 |
| 121199 | 232266 | 2.075 | 5192 | -48 | * |
| 120908 | 232114 | 2.076 | 5173 | -67 | * |
| 120713 | 232063 | 2.077 | 5505 | 265 | 54800 |
| 120654 | 232083 | 2.078 | 5256 | 16 | * |
| 121053 | 232333 | 2.079 | 5441 | 201 | * |
| 121065 | 232381 | 2.080 | 5216 | -24 | * |
| 121001 | 232418 | 2.081 | 5360 | 120 | * |
| 120947 | 232487 | 2.082 | 5130 | -110 | * |
| 120919 | 232522 | 2.083 | 5154 | -86 | * |
| 120929 | 232556 | 2.084 | 5337 | 97 | * |
| 120930 | 232589 | 2.085 | 5156 | -84 | * |
| 120817 | 232444 | 2.086 | 5321 | 81 | 186300 |
| 120798 | 232444 | 2.087 | 5252 | 12 | * |
| 120800 | 232477 | 2.088 | 5361 | 121 | 41200 |
| 120742 | 232499 | 2.089 | 5501 | 261 | * |
| 120711 | 232490 | 2.090 | 5521 | 281 | * |
| 120698 | 232480 | 2.091 | 5214 | -26 | 2600 |
| 120680 | 232467 | 2.092 | 5464 | 224 | 97800 |
| 120663 | 232455 | 2.093 | 5269 | 29 | * |
| 120640 | 232441 | 2.094 | 5237 | -3 | 4300 |
| 120614 | 232408 | 2.095 | 5546 | 306 | * |
| 121123 | 232211 | 2.096 | 5347 | 107 | 118000 |
| 121162 | 232189 | 2.097 | 5470 | 230 | 83500 |
| 121589 | 232805 | 2.098 | 5262 | 22 | 62600 |
| 121542 | 232809 | 2.099 | 5497 | 257 | 56400 |
| 121562 | 232823 | 2.100 | 5469 | 229 | 149500 |
| 121595 | 232908 | 2.101 | 5298 | 58 | 32500 |
| 121502 | 232831 | 2.102 | 5294 | 54 | 40800 |

| | | | | | |
|---|---|---|---|---|---|
| 121544 | 232898 | 2.103 | 5326 | 86 | 59600 |
| 121550 | 232948 | 2.104 | 5342 | 102 | 65900 |
| 121467 | 232921 | 2.105 | 5317 | 77 | 98100 |
| 121432 | 232915 | 2.106 | 5213 | -27 | 45100 |
| 121404 | 232895 | 2.107 | 5205 | -35 | 21900 |
| 121377 | 232879 | 2.108 | 5247 | 7 | 70500 |
| 121333 | 232849 | 2.109 | 5256 | 16 | * |
| 121312 | 232835 | 2.110 | 5233 | -7 | 19900 |
| 121853 | 233032 | 2.111 | 5182 | -58 | 4400 |
| 121849 | 233074 | 2.112 | 5221 | -19 | 26200 |
| 121848 | 232999 | 2.113 | 5199 | -41 | 2600 |
| 121718 | 233059 | 2.114 | 5209 | -31 | 8700 |
| 121587 | 233294 | 2.115 | 5252 | 12 | 54100 |
| 121577 | 233264 | 2.116 | 5249 | 9 | 21900 |
| 121550 | 233208 | 2.117 | 5416 | 176 | 79700 |
| 121545 | 233189 | 2.118 | 5232 | -8 | 95900 |
| 121532 | 233158 | 2.119 | 5226 | -14 | * |
| 121507 | 233101 | 2.120 | 5251 | 11 | 63000 |
| 121485 | 233085 | 2.121 | 5221 | -19 | * |
| 121470 | 233065 | 2.122 | | 37 | 28900 |
| 121415 | 233041 | 2.123 | | -24 | 30400 |
| 121367 | 232997 | 2.124 | 5273 | 33 | 41700 |
| 121311 | 232947 | 2.125 | 5092 | -148 | 40500 |
| 121343 | 232671 | 2.126 | 5287 | 47 | 41200 |
| 121324 | 232654 | 2.127 | 5511 | 271 | * |
| 121315 | 232644 | 2.128 | 5350 | 110 | 40800 |
| 121286 | 232622 | 2.129 | 5142 | -98 | * |
| 121232 | 232680 | 2.130 | 5277 | 37 | 19300 |
| 121268 | 232703 | 2.131 | 5309 | 69 | * |
| 121199 | 232716 | 2.132 | 5532 | 292 | * |
| 121170 | 232708 | 2.133 | 5430 | 190 | 30000 |
| 121125 | 232735 | 2.134 | 5326 | 86 | * |
| 121091 | 232697 | 2.135 | 5273 | 33 | * |
| 121081 | 232726 | 2.136 | 5238 | -2 | 127800 |
| 121060 | 232769 | 2.137 | 5372 | 132 | 81800 |
| 121483 | 232753 | 2.138 | 5641 | 401 | 131200 |
| 121497 | 232740 | 2.139 | 5684 | 444 | 182900 |
| 121529 | 232977 | | 5251 | 11 | 18800 |
| 121529 | 232978 | 2. | 5249 | 9 | 21900 |
| 121490 | 232956 | 2.142 | | 12 | 26900 |
| 121468 | 232943 | 2.143 | | -12 | 40400 |
| 121453 | 232929 | 2.144 | | 4 | 69600 |
| 121555 | 232994 | 2.145 | 5191 | -49 | 75500 |
| 121554 | 233013 | 2.146 | 5223 | -17 | 20200 |
| 121552 | 233049 | 2.147 | 5233 | -7 | 66600 |
| 121549 | 233072 | 2.148 | 5263 | 23 | 35800 |
| 121910 | 230994 | 2.149 | 5331 | 91 | 17800 |
| 121934 | 231008 | 2.150 | 5394 | 154 | * |

| | | | | | |
|---|---|---|---|---|---|
| 121954 | 231019 | 2.151 | 5196 | -44 | * |
| 121980 | 231031 | 2.152 | 5248 | 8 | * |
| 122019 | 231039 | 2.153 | 5233 | -7 | 29300 |
| 122042 | 231070 | 2.154 | 5275 | 35 | * |
| 122062 | 231090 | 2.155 | 5272 | 32 | 12700 |
| 122079 | 231107 | 2.156 | 5324 | 84 | * |
| 122097 | 231138 | 2.157 | 5254 | 14 | 122000 |
| 122120 | 231142 | 2.158 | 5370 | 130 | 122800 |
| 122137 | 231167 | 2.159 | 5384 | 144 | * |
| 122153 | 231185 | 2.160 | 5667 | 427 | 152800 |
| 122137 | 231228 | 2.161 | 5312 | 72 | 99600 |
| 122231 | 231251 | 2.162 | 5451 | 211 | 18400 |
| 122254 | 231269 | 2.163 | 5586 | 346 | * |
| 122273 | 231302 | 2.164 | 5401 | 161 | 51400 |
| 122299 | 231315 | 2.165 | 5523 | 283 | * |
| 122336 | 231332 | 2.166 | 5321 | 81 | 5000 |
| 122325 | 231388 | 2.167 | 5263 | 23 | * |
| 122387 | 231396 | 2.168 | 5269 | 29 | 57800 |
| 121865 | 231162 | 2.169 | 5250 | 10 | 46400 |
| 121856 | 231192 | 2.170 | 5248 | 8 | 84200 |
| 121850 | 231225 | 2.171 | 5278 | 38 | 78400 |
| 121800 | 231431 | 2.172 | 5276 | 36 | 69300 |
| 121805 | 231396 | 2.173 | 5410 | 170 | 35000 |
| 122076 | 231177 | 2.174 | 5261 | 21 | 76100 |
| 122058 | 231213 | 2.175 | 5268 | 28 | 70800 |
| 122056 | 231234 | 2.176 | 5245 | 5 | 60200 |
| 122087 | 231297 | 2.177 | 5305 | 65 | 34600 |
| 122078 | 231318 | 2.178 | 5227 | -13 | 72100 |
| 122114 | 231288 | 2.179 | 5277 | 37 | 76100 |
| 122150 | 231304 | 2.180 | 5479 | 239 | 72500 |
| 122318 | 231232 | 2.181 | 5290 | 50 | 90400 |
| 122289 | 231219 | 2.182 | 5280 | 40 | 23400 |
| 122256 | 231319 | 2.183 | 5318 | 78 | 37800 |
| 122229 | 231343 | 2.184 | 5255 | 15 | 26400 |
| 122194 | 231428 | 2.185 | 5259 | 19 | 56100 |
| 122205 | 231402 | 2.186 | 5255 | 15 | 85000 |
| 122158 | 231412 | 2.187 | 5218 | -22 | 40700 |
| 122173 | 231390 | 2.188 | 5307 | 67 | 65800 |
| 122131 | 231401 | 2.189 | 5256 | 16 | 90200 |
| 122141 | 231377 | 2.190 | 5413 | 173 | 133400 |
| 122094 | 231392 | 2.191 | 5232 | -8 | 137000 |
| 122187 | 231347 | 2.192 | 5266 | 26 | 135900 |
| 122364 | 231211 | 2.193 | 5258 | 18 | 83400 |
| 122387 | 231156 | 2.194 | 5306 | 66 | 86400 |
| 122376 | 231032 | 2.195 | 5411 | 171 | 76900 |
| 122350 | 231021 | 2.196 | 5236 | -4 | 77100 |
| 122342 | 230996 | 2.197 | 5449 | 209 | 69900 |
| 122239 | 230972 | 2.198 | 5445 | 205 | 79000 |

| | | | | | |
|---|---|---|---|---|---|
| 122195 | 230993 | 2.199 | 5202 | -38 | * |
| 122158 | 230999 | 2.200 | 5433 | 193 | 43700 |
| 122430 | 231068 | 2.201 | 5315 | 75 | 137200 |
| 122439 | 231052 | 2.202 | 5324 | 84 | 182800 |
| 122405 | 231098 | 2.203 | 5227 | -13 | 75200 |
| 122416 | 231176 | 2.204 | 5206 | -34 | 26600 |
| 122409 | 231237 | 2.205 | 5239 | -1 | 48500 |
| 122404 | 231203 | 2.206 | 5398 | 158 | 53300 |
| 122335 | 231038 | 2.207 | 5354 | 114 | 98800 |
| 122324 | 231084 | 2.208 | 5282 | 42 | 62100 |
| 122309 | 231110 | 2.209 | 5312 | 72 | 88200 |
| 122315 | 231135 | 2.210 | 5283 | 43 | 59300 |
| 122295 | 231078 | 2.211 | 5276 | 36 | 22300 |
| 122276 | 231096 | 2.212 | 5251 | 11 | 31400 |
| 122251 | 231075 | 2.213 | 5243 | 3 | 57500 |
| 122265 | 231060 | 2.214 | 5266 | 26 | 84500 |
| 122305 | 231036 | 2.215 | 5458 | 218 | 101400 |
| 121329 | 232537 | 2.216 | 5293 | 53 | 13500 |
| 121353 | 232516 | 2.217 | 5456 | 216 | 35700 |
| 121375 | 232488 | 2.218 | 5244 | 4 | 30500 |
| 121407 | 232455 | 2.219 | 5236 | -4 | 33900 |
| 122320 | 230998 | 2.220 | 5276 | 36 | 40000 |
| 122285 | 230959 | 2.221 | 5359 | 119 | 156700 |
| 122269 | 231040 | 2.222 | 5363 | 123 | 37500 |
| 122228 | 231064 | 2.223 | 5403 | 163 | 46500 |
| 122203 | 231083 | 2.224 | 5449 | 209 | 125100 |
| 122183 | 231112 | 2.225 | 5407 | 167 | 89500 |
| 122178 | 231139 | 2.226 | 5303 | 63 | 53800 |
| 122150 | 231100 | 2.227 | 5315 | 75 | 72000 |
| 122144 | 231051 | 2.228 | 5685 | 445 | 71400 |
| 121849 | 233355 | 2.229 | 5213 | -27 | 36900 |
| 121858 | 233408 | 2.230 | 5438 | 198 | 64400 |
| 121815 | 233381 | 2.231 | 5344 | 104 | 63500 |
| 121855 | 233444 | 2.232 | 5388 | 148 | 69000 |
| 121825 | 233495 | 2.233 | 5491 | 251 | * |
| 121768 | 233411 | 2.234 | 5759 | 519 | 134000 |
| 121767 | 233357 | 2.235 | 5396 | 156 | 89900 |
| 121796 | 233465 | 2.236 | 5273 | 33 | 65200 |
| 121696 | 233431 | 2.237 | 5255 | 15 | 99400 |
| 121748 | 233484 | 2.238 | 5240 | 0 | * |
| 121683 | 233392 | 2.239 | 5673 | 433 | 103200 |
| 121654 | 233479 | 2.240 | 5259 | 19 | 87300 |
| 121660 | 233261 | 2.241 | 5195 | -45 | 56400 |
| 121631 | 233[illegible]4 | 2.242 | 5233 | -7 | 80800 |
| 121600 | 233352 | 2.243 | 5205 | -35 | 41900 |
| 121522 | 233323 | 2.244 | 5235 | -5 | 34000 |
| 121453 | 233340 | 2.245 | 5266 | 26 | 77400 |
| 121411 | 233359 | 2.246 | 5271 | 31 | 61400 |

| | | | | | |
|---|---|---|---|---|---|
| 121376 | 233384 | 2.247 | 5275 | 35 | 35200 |
| 121346 | 233396 | 2.248 | 5282 | 42 | 36100 |
| 121322 | 233429 | 2.249 | 5260 | 20 | 78000 |
| 121294 | 233457 | 2.250 | 5259 | 19 | 88000 |
| 121264 | 233472 | 2.251 | 5209 | -31 | * |
| 121298 | 233350 | 2.252 | 5441 | 201 | 174600 |
| 121328 | 233296 | 2.253 | 5368 | 128 | 122700 |
| 121644 | 233172 | 2.254 | 5248 | 8 | 9900 |
| 121628 | 233108 | 2.255 | 5244 | 4 | * |
| 121661 | 232615 | 2.256 | 5349 | 109 | 150900 |
| 121657 | 232552 | 2.257 | 5323 | 83 | 87300 |
| 121735 | 232548 | 2.258 | 5278 | 38 | 61700 |
| 121722 | 232628 | 2.259 | 5321 | 81 | 184400 |
| 121752 | 232576 | 2.260 | 5241 | 1 | * |
| 121785 | 232608 | 2.261 | 5246 | 6 | * |
| 121754 | 232666 | 2.262 | 5320 | 80 | 70500 |
| 121825 | 232670 | 2.263 | 5436 | 196 | * |
| 121790 | 232691 | 2.264 | 5418 | 178 | 52200 |
| 121810 | 232716 | 2.265 | 5426 | 186 | * |
| 121858 | 232773 | 2.266 | 5317 | 77 | * |
| 121781 | 232911 | 2.268 | 5296 | 56 | 104600 |
| 121814 | 232917 | 2.269 | 5429 | 189 | 67200 |
| 121795 | 232861 | 2.270 | 5227 | -13 | 34300 |
| 121834 | 232857 | 2.271 | 5255 | 15 | 54600 |
| 121841 | 232888 | 2.272 | 5123 | -117 | * |
| 121858 | 232858 | 2.273 | 5234 | -6 | 59600 |
| 121887 | 232842 | 2.274 | 5454 | 214 | 72400 |
| 121914 | 232771 | 2.275 | 5239 | -1 | * |
| 121887 | 232806 | 2.276 | 5273 | 33 | 113700 |
| 121945 | 232800 | 2.277 | 5296 | 56 | 22600 |
| 121863 | 232799 | 2.278 | 5235 | -5 | 114900 |
| 121834 | 232826 | 2.279 | 5265 | 25 | 97900 |
| 121782 | 232736 | 2.280 | 5260 | 20 | * |
| 121714 | 232719 | 2.281 | 5294 | 54 | 94700 |
| 121694 | 232702 | 2.282 | 5231 | -9 | 23300 |
| 121667 | 232677 | 2.283 | 5236 | -4 | 98200 |
| 121696 | 232646 | 2.284 | 5340 | 100 | 137500 |
| 121637 | 232650 | 2.285 | 5276 | 36 | 66900 |
| 121661 | 232615 | 2.286 | 5267 | 27 | 42000 |
| 121643 | 232590 | 2.287 | 5264 | 24 | * |
| 121615 | 232558 | 2.288 | 5277 | 37 | 83900 |
| 121628 | 232527 | 2.289 | 5234 | -6 | * |
| 121619 | 232508 | 2.290 | 5437 | 197 | 99000 |
| 121601 | 232486 | 2.291 | 5384 | 144 | 58900 |
| 121567 | 232477 | 2.292 | 5245 | 5 | * |
| 121527 | 232471 | 2.293 | 5233 | -7 | * |
| 121772 | 233230 | 2.294 | 5676 | 436 | * |
| 121808 | 233227 | 2.295 | 5222 | -18 | * |

| | | | | | |
|---|---|---|---|---|---|
| 121832 | 233207 | 2.296 | 5489 | 249 | 11400 |
| 121835 | 233150 | 2.297 | 5223 | -17 | * |
| 121864 | 233180 | 2.298 | 5453 | 213 | 39900 |
| 121967 | 232879 | 2.299 | 5411 | 171 | 59000 |
| 121658 | 232895 | 2.300 | 5256 | 16 | * |
| 121639 | 232912 | 2.301 | 5352 | 112 | 57800 |
| 121617 | 232925 | 2.302 | 5168 | -72 | * |
| 121590 | 232943 | 2.303 | 5276 | 36 | 33400 |
| 121590 | 232956 | 2.304 | 5241 | 1 | * |
| 121619 | 232953 | 2.305 | 5311 | 71 | 42200 |
| 121645 | 232949 | 2.306 | 5247 | 7 | * |
| 121665 | 232941 | 2.307 | 5288 | 48 | 67800 |
| 121700 | 232946 | 2.308 | 5292 | 52 | 14300 |
| 121677 | 232980 | 2.309 | 5287 | 47 | 94600 |
| 121650 | 232981 | 2.310 | 5282 | 42 | 17800 |
| 121630 | 232983 | 2.311 | 5340 | 100 | 82800 |
| 121594 | 232987 | 2.312 | 5250 | 10 | 24900 |
| 121626 | 233048 | 2.313 | 5430 | 190 | 72600 |
| 121652 | 233044 | 2.314 | 5258 | 18 | 75000 |
| 121641 | 233069 | 2.315 | 5206 | -34 | 51700 |
| 121684 | 233064 | 2.316 | 5273 | 33 | 30000 |
| 121681 | 233097 | 2.317 | 5297 | 57 | 27500 |

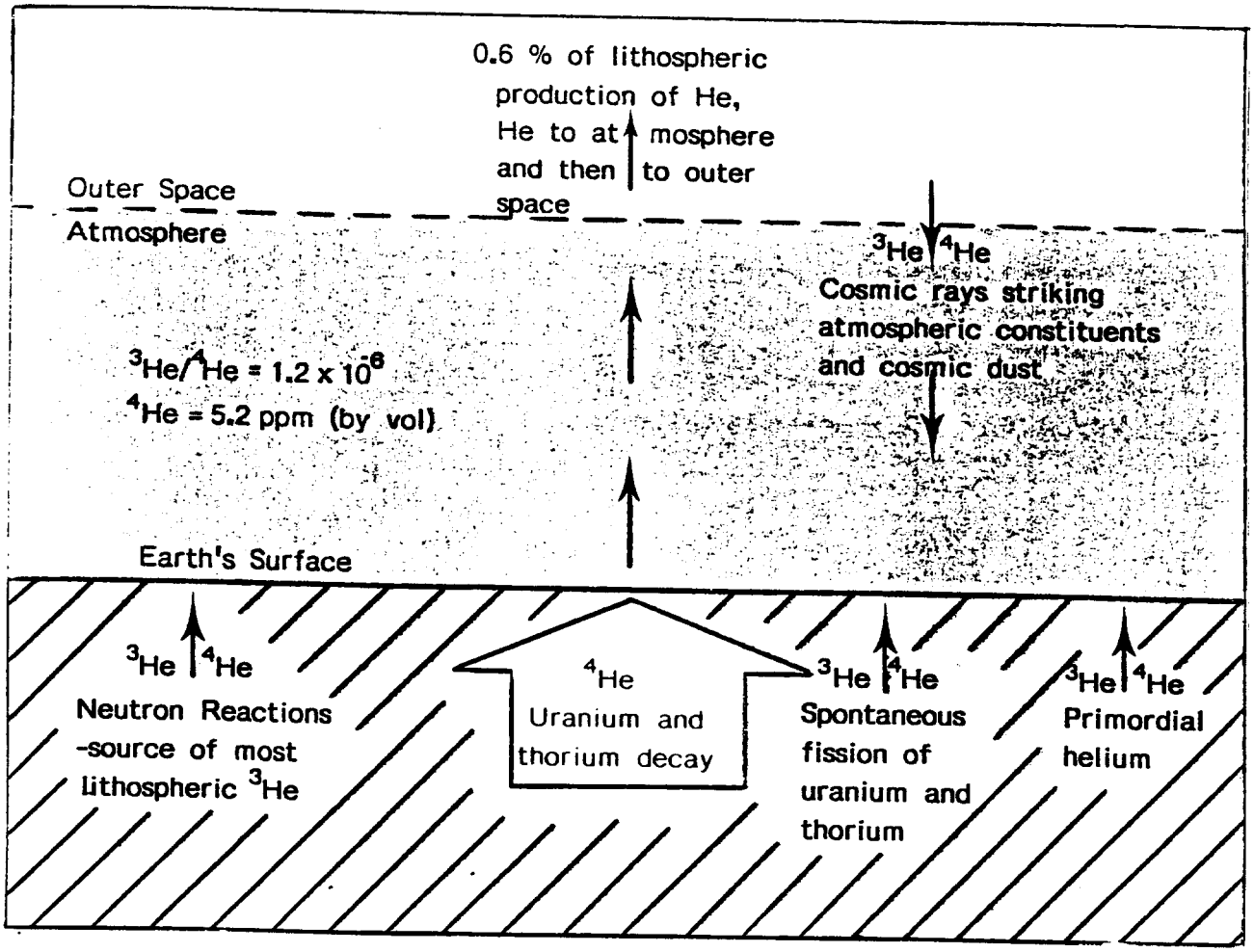


Fig 5.1 Origin of Helium ( after POGORSKY & QUIRT, 1981 )

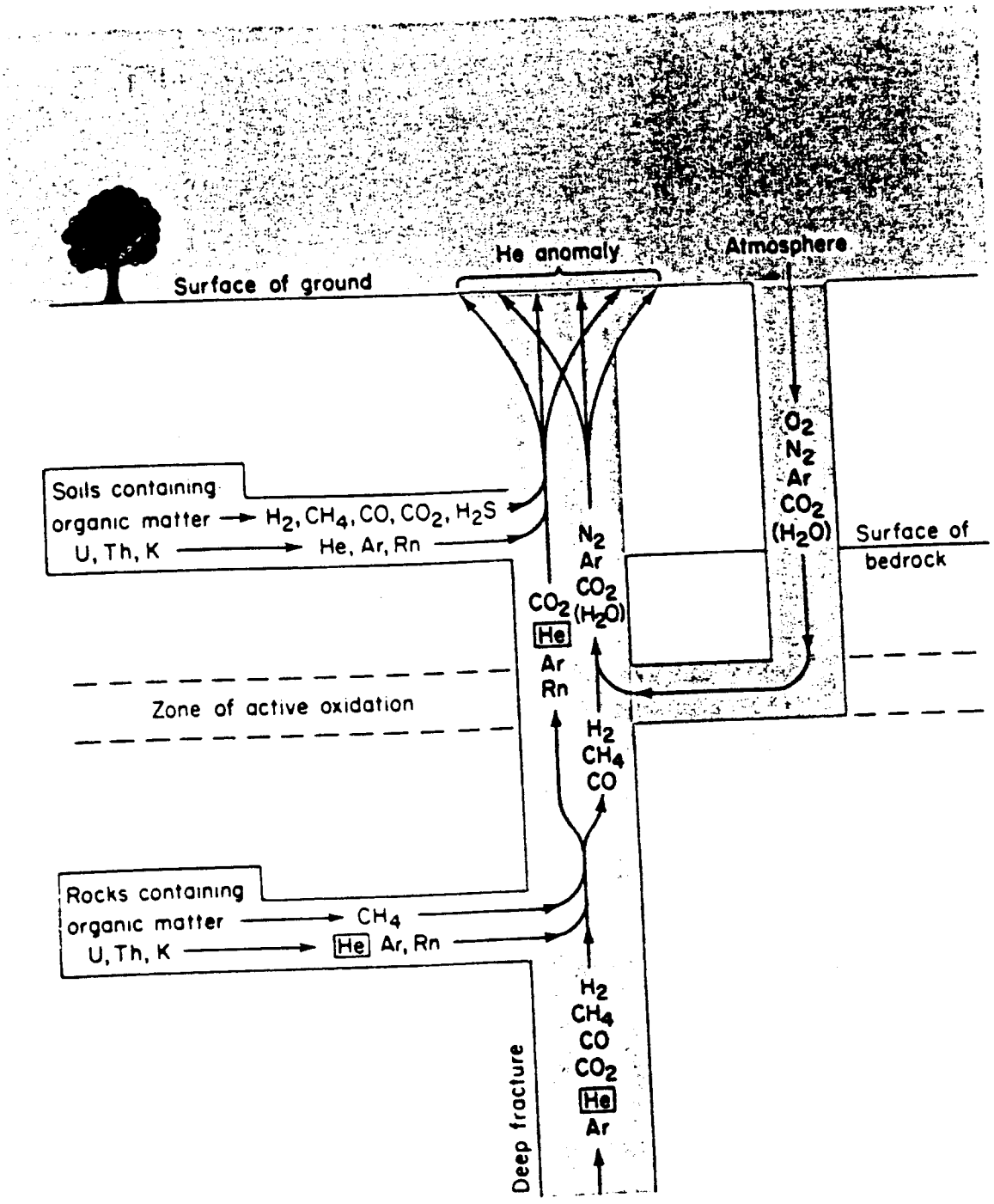


Fig. 5.2 Origin and migration of some terrestrial gases over deep reaching fault zones (after A.W. ROSE, H.E. HAWKES and J.S. WEBB, 1979)

Fig. 5.3 Soil gas sampling ( hammer )

Fig. 5.4 Soil gas sampling with hypodermic syringe

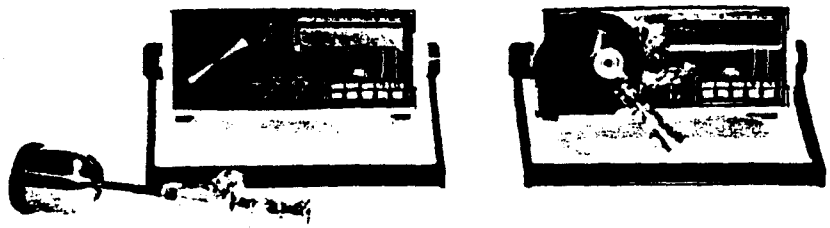

Fig. 5.7 Portable radiation monitor (AB-5) Pylon and Lucas cells used for $^{222}Rn$ measurements (outdoor)

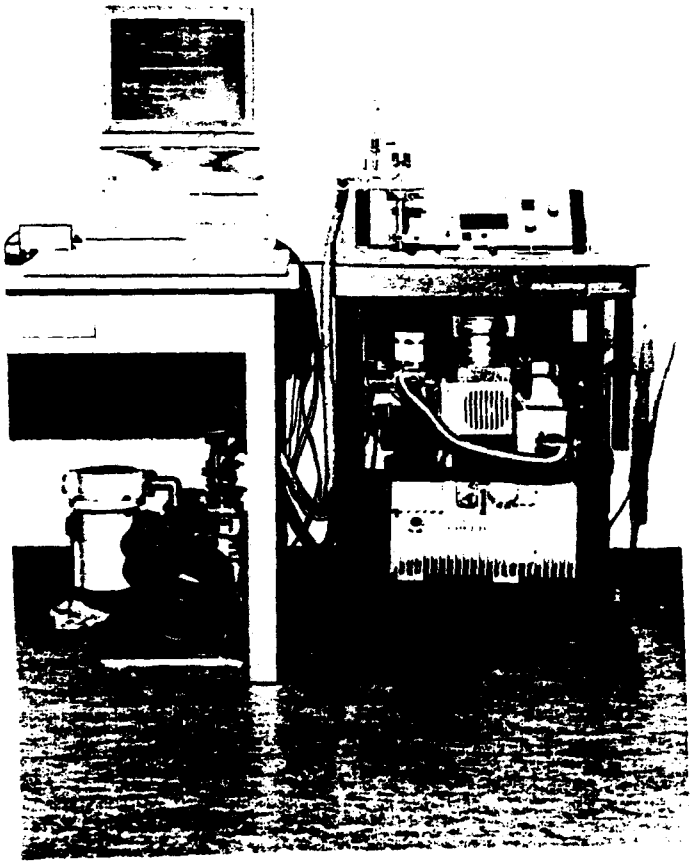

Fig. 5.6 Quadruple mass spectrometer, $^{4}Helium$ analysis of soil gas samples, Bratislava area

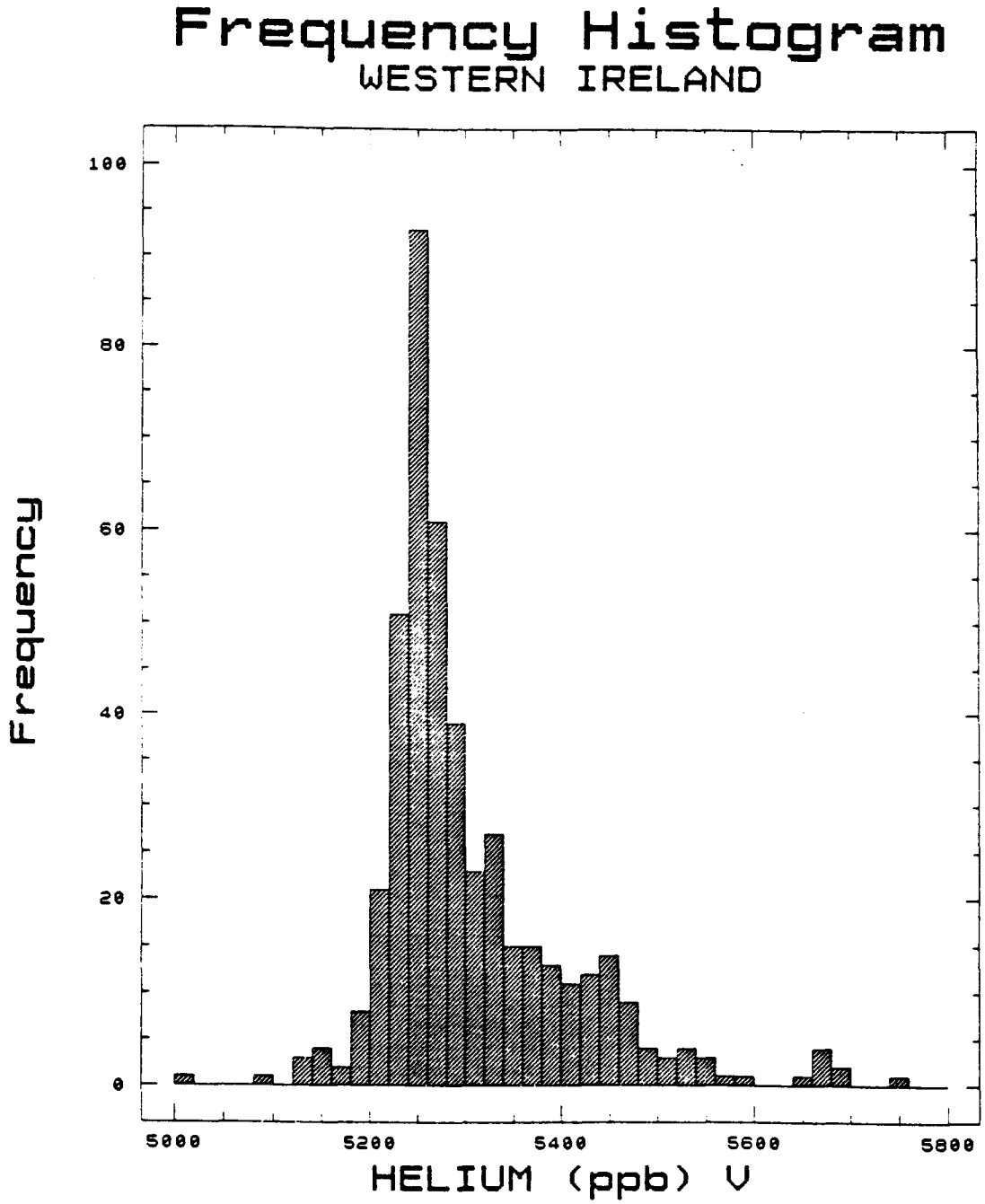


Fig. 5.8 Frequency histogramme of Helium (all data)

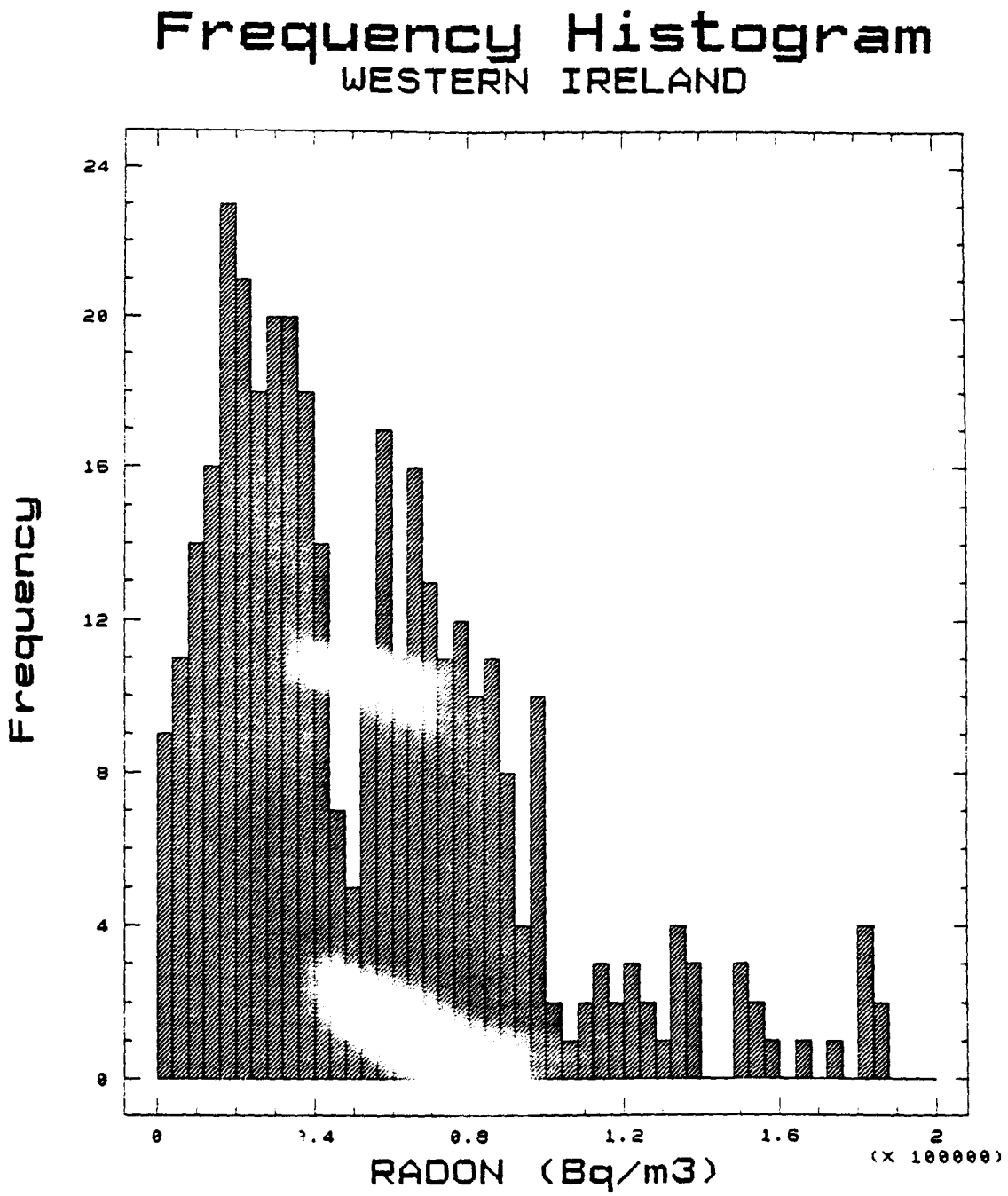


Fig. 5.9 Freque histogramme of radon (all data)

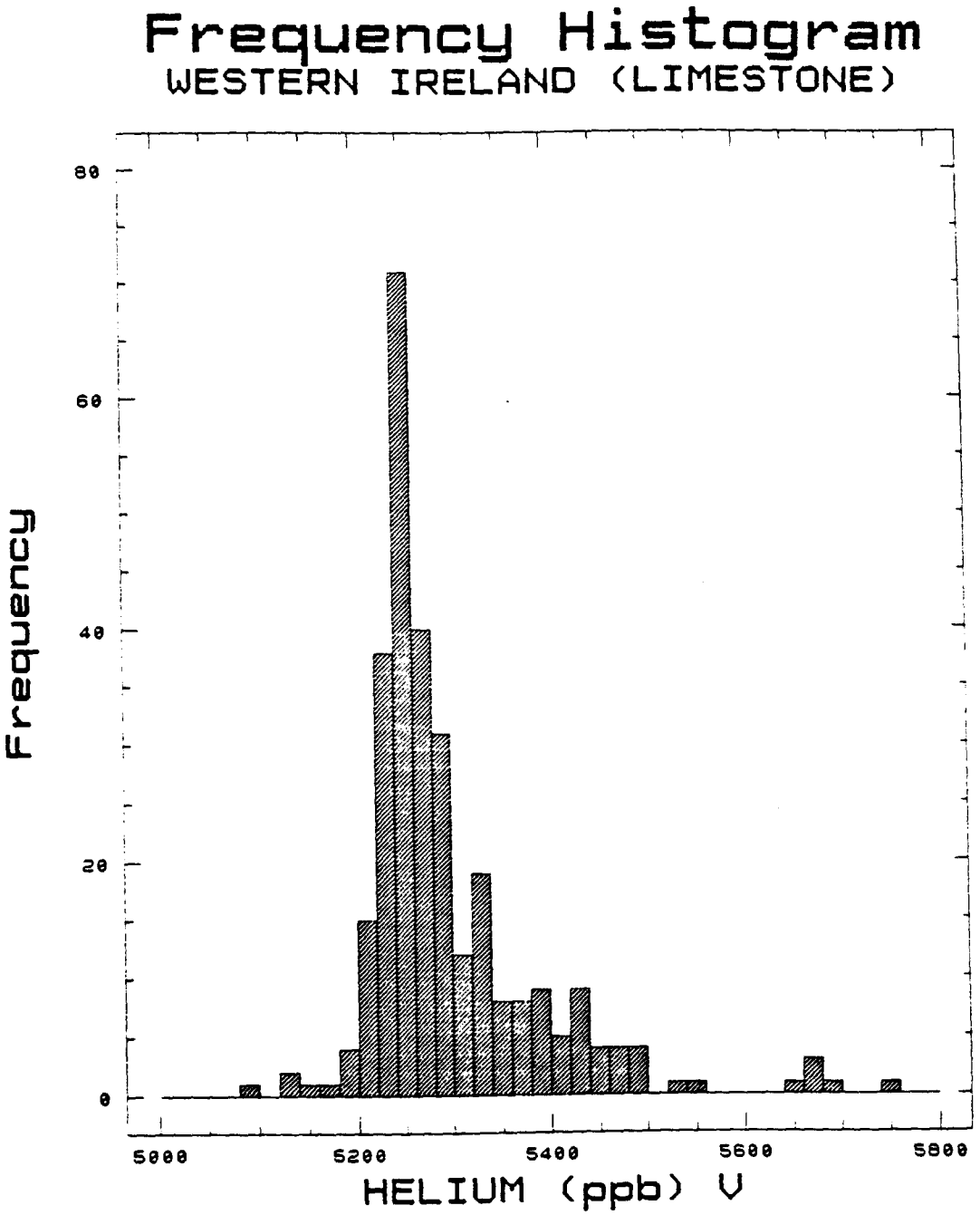


Fig. 5.10 Frequency distribution of helium in limestone samples

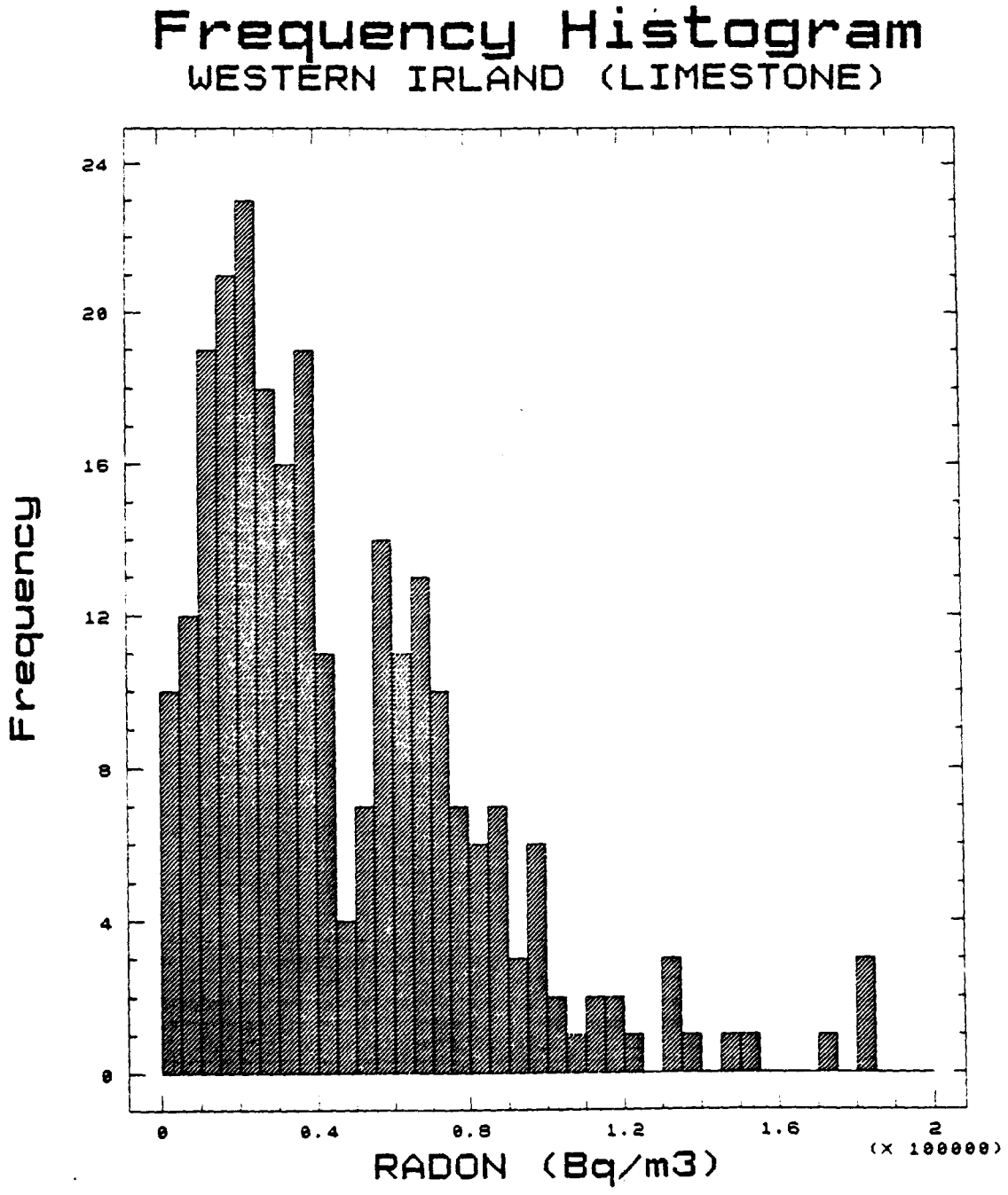


Fif. 5.11 Frequency distribution of radon in limestone samples

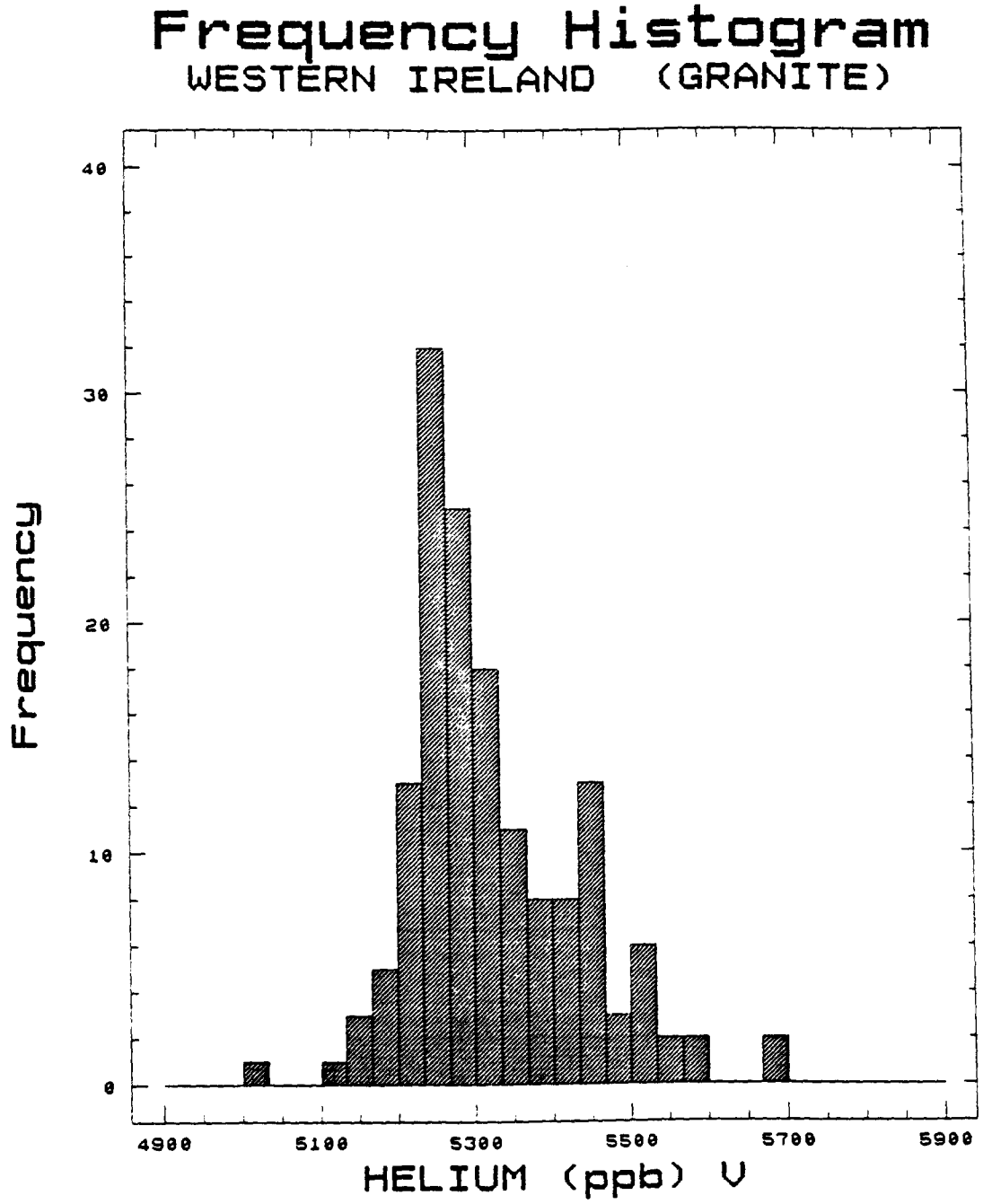


Fig. 5.12 Frequency distribution of helium in granite samples

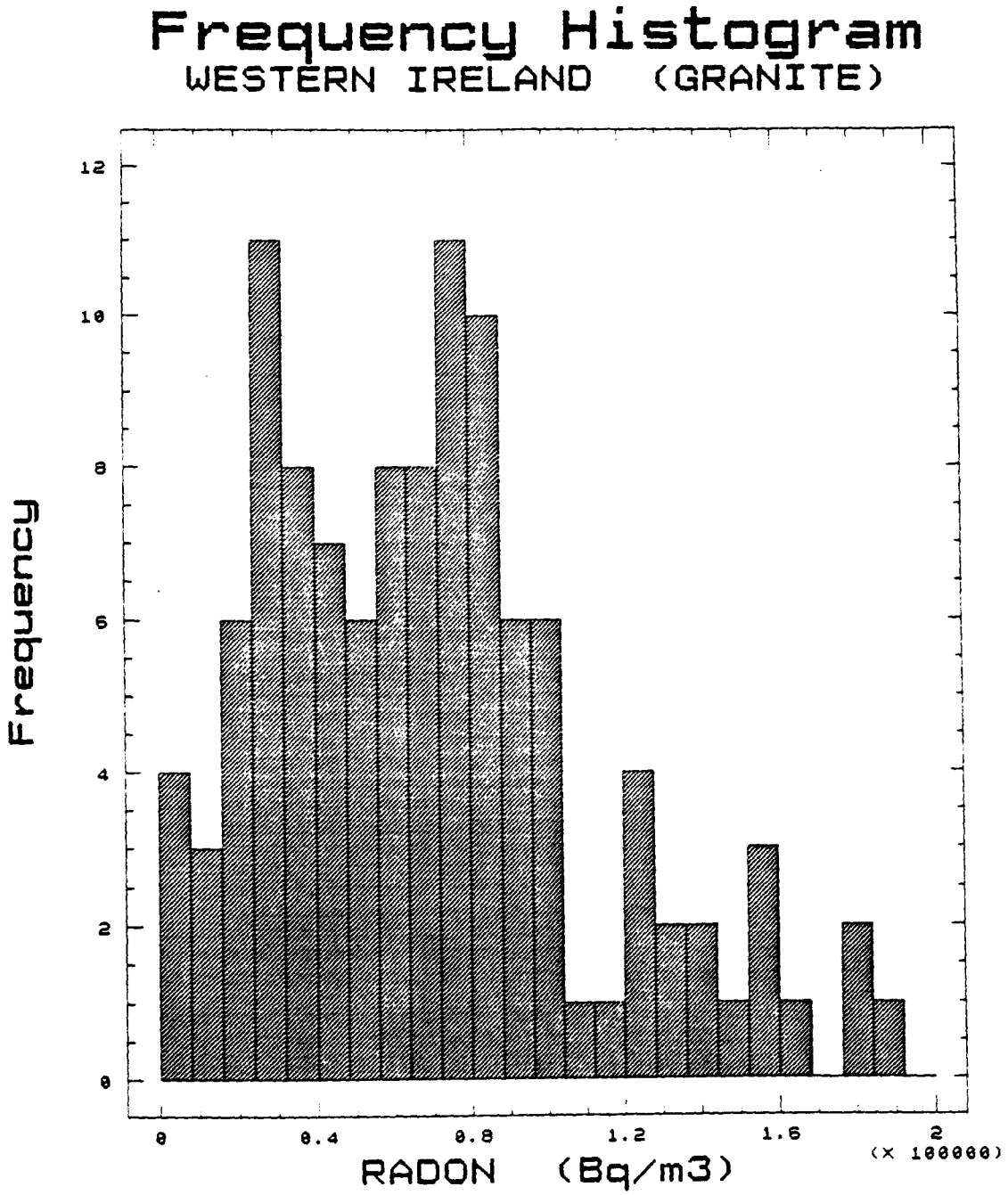


Fig. 5.13 Frequency distribution of radon in granite samples

# ANNEX 6

**Contribution of University College, Galway**

**K. J. Barton and C. Mac Niocaill**

# Contents

**6.6 Conclusions**

- 6.6.1 Ballydotia
  - 6.6.1.1 Ballydotia West
  - 6.6.1.2 Ballydotia East
- 6.6.2 Moycullen
- 6.6.3 Uggool

**6.7 Recommendations**

- 6.7.1 Ballydotia
  - 6.7.1.1 Ballydotia West
  - 6.7.1.2 Ballydotia East
- 6.7.2 Moycullen
- 6.7.3 Uggool

**6.8 Acknowledgements**

**6.9 References**

## 6.1 Introduction

### 6.1.1 Project scope and organization

This EC-funded Radiation Protection Project concerns the investigation of controls on radon migration in the Moycullen area of County Galway. The area lies some 10 km NW of Galway City and straddles the NW -- SE trending and NE dipping geological contact between the Galway granite and Carboniferous limestone.

The EC contract was let to a consortium of German and Irish institutions with the Geological Survey of Ireland (GSI) acting as project co-ordinator. The work reported here was commissioned by the GSI and forms a sub-contract with that institution. The main objective of the geophysical work was to help to define any regional or local geological structures which might influence radon migration in the region.

The zones with high in-house radon levels within the area were defined by means of a survey of indoor radon levels in domestic premises using passive radon detectors. Further work on measurement of radon and helium in soil gas helped to further define possible follow-up areas. Subsequently three follow-up areas were selected for more detailed investigation; they were designated Ballydotia, Moycullen and Uggool (Fig. 1).

Ballydotia is underlain by a thick limestone sequence, Moycullen lies on the contact between the granite and the limestone and Uggool lies on the granite. The Ballydotia area comprises flat, open farmland, the Moycullen area is largely occupied by the Village and a housing estate and Uggool has a very varied topography and is intersected by roads, powerlines and a river.

The geophysical work, with the guidance of the GSI, was subsequently focused on targets in these three areas which all had high in-house radon and/or soil gas anomalies in isolated houses.

### 6.1.2 Summary of geophysical work programme

Initial work concentrated on the compilation of available regional geophysical datasets which consisted of (i) the regional gravity data and (ii) ground, total count, gamma-ray survey data which was collected by the GSI. Work in the three designated areas mainly consisted of an Electromagnetic-Very Low Frequency (EM-VLF) survey which was used in the resistivity-mode. This technique, which was used to map sub-surface variations in apparent resistivity, provided a rapid reconnaissance of the designated areas and helped define more localised anomalous zones. These localised zones were then investigated further using conventional resistivity profiling and sounding techniques. A number of shallow, cored boreholes were drilled by the GSI is support of the geophysical surveys (Annex 1). All boreholes were collared in limestone on geophysical anomalies. In some cases it was possible to preserve the boreholes by inserting slotted, plastic casing once the drillers' rods and casing had been recovered. A string of passive radon detectors was generally deployed above the watertable in these preserved boreholes. Prior to the completion of the geophysical surveys a series of shallow, inclined boreholes were drilled to intersect the granite/limestone contact in the Uggool/Clydagh Bridge area. A continuous, total count, natural gamma-ray log was run in two of these boreholes (DH1 and DH2).

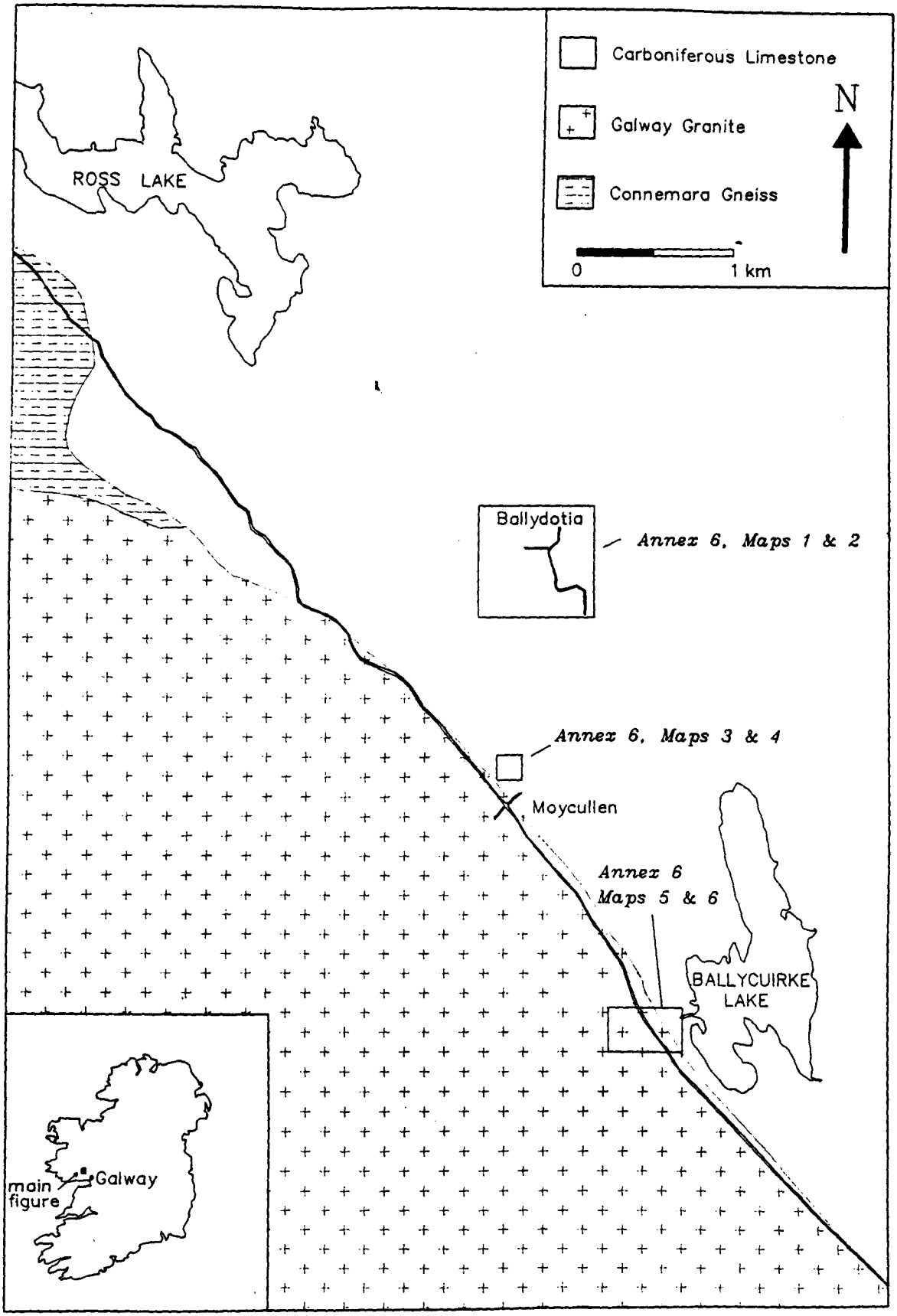


**Figure 1. Project area: location and geology map.**

## 6.2 Regional geophysical data

### 6.2.1 Simple Bouguer Anomaly gravity map

The regional gravity data for the Galway granite have been collected by the Dublin Institute of Advanced Studies (DIAS) and University College Galway (UCG). No terrain corrections have been applied to the data as the topographic relief is generally low in this region. The most recent regional gravity interpretation relevant to the study area is due to Madden (1987) who produced a 3-D model of the Galway granite using the combined DIAS and UCG datasets. The work, connected with a gamma-ray survey of the Galway Granite, was focussed on modelling the granite in relation to the surrounding country rocks. There is quite a good distribution of gravity stations on the granite, but the station coverage on the country rocks is considered poor. The data used in this study have been extracted from the Regional Gravity Dataset for Ireland, a digital copy of which has kindly been provided to UCG by DIAS.

The station density is, as noted, very poor in the study area and the stations are very randomly distributed. For these reasons it is not possible to arrive at a detailed interpretation. An attempt to contour these data using a grid cell size of 1000m yielded the machine contoured Smoothed Contour Map (Fig 2). The map shows a gentle gradient perpendicular to the NW -- SE trending granite/limestone contact. This gradient, of about 1 mgal per km, becomes progressively more negative in a SW direction. Moycullen Village lies within a few tens of metres to the SW of the inferred granite/limestone contact.

In Fig 2 it is seen that Moycullen Village lies between the -2 and the - 3 mgal contours and some 2 km SW of the 0 mgal contour. This would imply that the granite contact is further to the NE than inferred from geological mapping in the area. The reason for this apparent discrepancy is that the granite/limestone contact in this area is not vertical but dips very gently NE from its inferred surface trace in the Moycullen area. The negative gravity values NE of Moycullen reflect the presence of the granite at a deeper level and upon which rests the limestone sequence which thickens to the NE.

Previous gravity work by Reilly (1983) showed the granite-limestone contact in the vicinity of Galway City to dip about 35° to the NE. An attempt to quantify the dip-angle of the contact using a detailed gravity traverse in the Uggool area was not sucessful as the interpretation was disproved by subsequent drilling. The gravity data were collected by Cummins (1991) who subsequently tried to model the attitude of the contact using a two-and-a-half dimensional computer modelling program. The data could satisfy a number of model configurations and the one chosen indicated that the contact dipped at an angle of 75° to the NE. Later drilling by the GSI (Annex 1) showed the contact to dip at 25 - 30° NE which is very much in accord with the observed gentle gravity gradient in the area. A possible explanation for this discepancy is in the choice of density values used for the granite and limestone in the model by Cummins (1991). Granite and limestone densities in this area are likely to be similar, perhaps in the region of 2.68 - 2.70 gm $cm^{-3}$. With such a small density contrast it is difficult to model with any degree of confidence.

#### 6.2.1.1 Conclusions

The perusal of the limited regional gravity data for the Moycullen area therefore provide no evidence of any hidden, major, deep structural features but rather confirm the gentle NE dip of the granite/limestone contact.

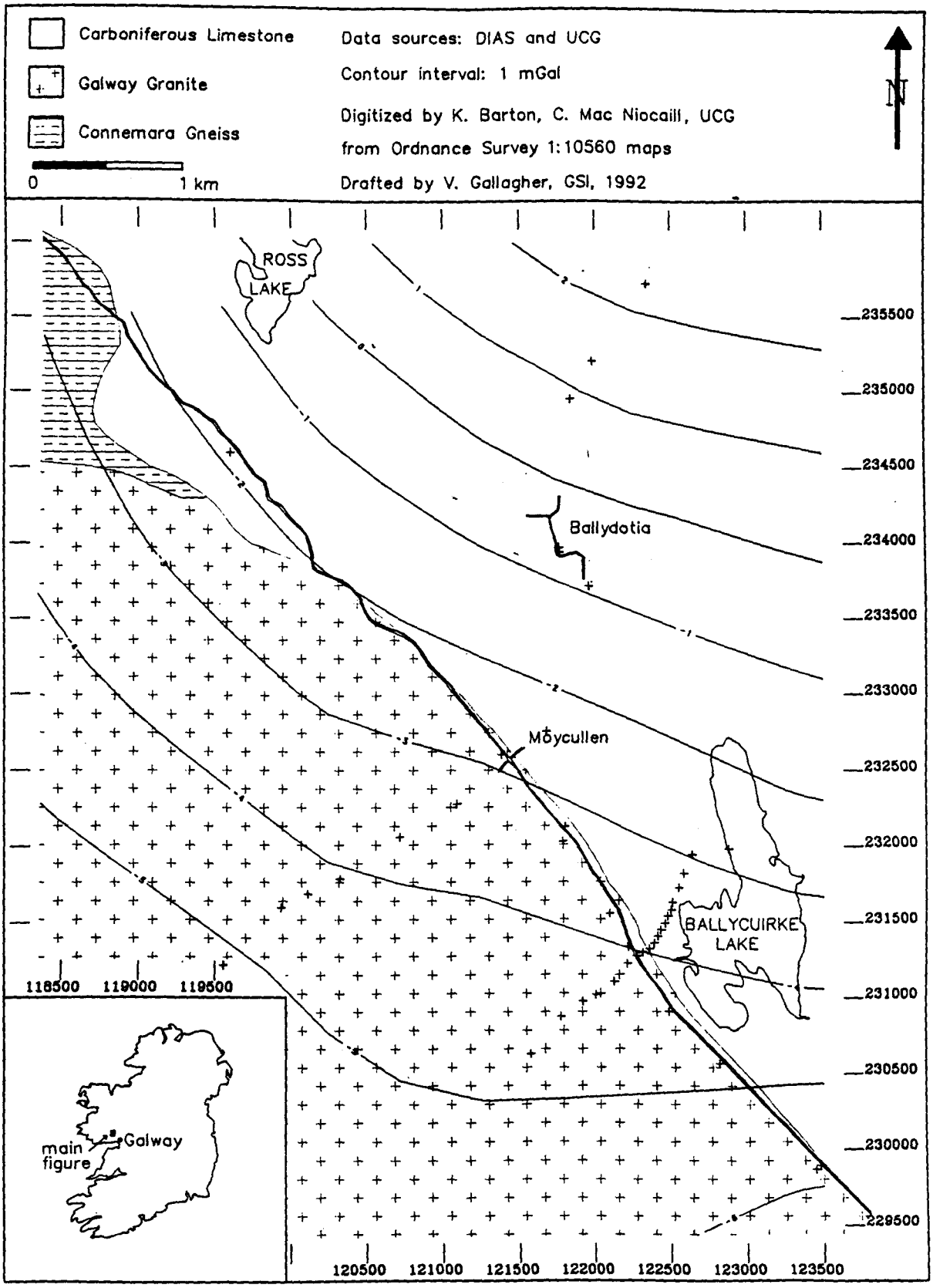


**Figure 2. Smoothed contour map of gravity data.**

### 6.2.2 Ground, Total-count Gamma-ray survey

This survey was carried out by the GSI in 1990 during a preliminary ground reconnaissance of the area. The data presented in Fig 3 were digitized as point data from a 1:10560 tracing supplied by the GSI. Utilising the GeoSoft 2-D Mapping Package, the data were then gridded with a grid-cell size of 500 m and contoured using a contour interval of 2 counts per second (cps).

The station density over most of the map region is quite good and the stations are quite well spatially distributed. The main feature is the NW - SE trend of increased gradient (50 to 70 cps) which coincides with the granite/limestone contact. Moycullen Village lies within this zone. Higher values generally occur to the SW of the contact over granite (above 60 cps) with lower values ( 40 - 60 cps) occuring over the glacial gravels and limestones to the NE. There are a number of broad 'highs' and 'lows' in the area but no really strong contrasts which might indicate any major structural features or localized radioelement concentrations. An interesting feature is the slightly elevated gamma levels immediately to the NE of Moycullen Village which may be due to granitic debris smeared over the area by glacial action.

#### 6.2.2.1 Conclusions

The total-count gamma ratemeter data define the granite/limestone contact zone better than the gravity data and show a number of broad highs and lows which may be related to glacial action. No other major structural features can be recognized.

## 6.3 Geophysical surveys in the Ballydotia area

### 6.3.1 Introduction

This rural area overlies limestone bedrock to the NE of Moycullen Village. The area is generally free from 'cultural noise' in the form of powerlines etc and access for geophysical surveys was relatively easy at the time of survey. There are a number of isolated houses with high indoor radon values and which also have helium and/or soil-gas anomalies in their vicinity. Topographically the area has gentle relief with a relatively thin, but variable, covering of glacial overburden resting on limestone bedrock. Limestone outcrops can be seen at a number of localities in the area and some of these are close to the houses with high radon concentrations. There are a number of sinkholes in the area which can be recognised by depressions in the ground surface.

Geophysical surveys were carried out in two adjacent areas designated Ballydotia West and Ballydotia East. Both areas had an isolated house with high indoor radon concentrations (Annex 1, Map 1) and a number of helium and/or radon in soil-gas anomalies which were found within 200 m of the houses. In the house in Ballydotia West repeat indoor radon measurements confirmed high levels found earlier while repeat measurements in the house at Ballydotia East showed the levels were quite variable with time. The reason for this is not known. There were other measured houses in both localities which did not have pronounced indoor radon anomalies. A working sand and gravel pit lay to the south of the anomalous house in Ballydotia West.

### 6.3.2 EM-VLF-R field survey

EM-VLF-R measurements, using a Geonics EM16R instrument, were made at an average station spacing of 50 m over the two areas. The 16 kHz transmitter at Rugby (GBR)

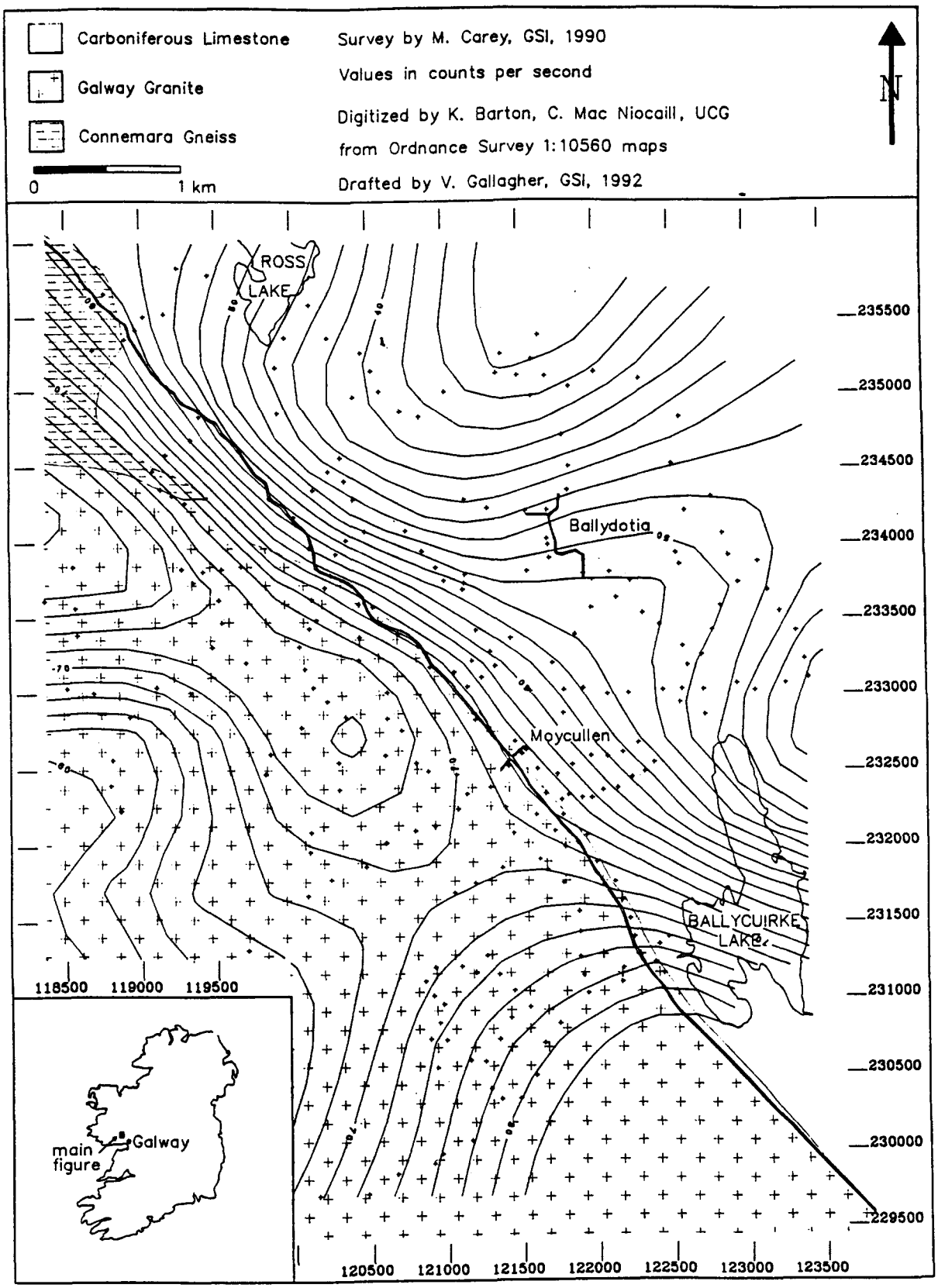


**Figure 3. Total count gamma-ray survey contour map.**

in England was used and measurement points were located relative to field boundaries so as to minimise surveying time. The stations were then plotted relative to the field boundaries shown on the 1:2500 scale field maps used for all surveys.

At each measurement point, or station, an apparent resistivity and phase value was recorded and the location plotted on the field map. A brief reconnaissance survey was carried out first in order to assess the likely range of values to be found and then in-fill stations were positioned so as to constrain any anomalies or trends recognised. As the survey progressed it became apparent that there was a major anomaly present in Ballydotia West which was located near house No 10. In Ballydotia East the EM-VLF-R response in the locality of house No 6 was different and trends were recognised which aligned with data collected in Ballydotia West. Accordingly it was decided to merge the data from the two survey areas and from then on the area was designated Ballydotia.

#### 6.3.2.1 Data reduction and processing

Since apparent resistivity and phase angle data were read directly from the field instrument, there was no data reduction required for this survey.

The data were processed using the computer-based, GeoSoft 2-D mapping system. The apparent resistivity and phase values were separately gridded with a grid-cell size of 50 m and machine contoured using contour intervals of 1000 Ohm-metres and 2° respectively. The results are presented on Maps 1 and 2.

#### 6.3.2.2 Interpretation

The main feature of the apparent resistivity map (Map 1) is the closed resistivity high in Ballydotia West which underlies house No 10. In Ballydotia East house No 6 straddles a high resistivity gradient. Resistivity values range from 3000 Ohm-metres to 30000 Ohm-metres, which is the upper measurement limit of the Geonics EM16 instrument used in the survey. The resistivity values measured are somewhat high for limestone terrain where experience has shown that values in the range 1000 - 10000 Ohm-metres would normally be expected. The Phase Map (Map 1) shows a closed low (less than 45°) in the west lying against a closed high (greater than 45°) to the east. These closed anomalies are not fully coincident with those anomalies found on the Resistivity Map. Phase values less than 45° indicate a two layer structure with a more resistive lower layer while values greater than 45° also indicate a two layer structure but this time the lower layer is more conductive.

The EM-VLF-R technique uses a distant electromagnetic source (i.e. Transmitter GBR) to energise the ground and the field instrument measures certain components of the resultant electromagnetic field which have been modified by the physical properties of the ground under investigation. This modification can largely be attributed to the electrical resistivity of the underlying geological strata and the relative thicknesses of these strata. The depth of investigation of the technique largely depends on the ground resistivity, higher resistivity generally gives deeper penetration. For the GBR transmitter used in this survey a theoretical depth of investigation of 40 m would be achieved with a homogenous ground of 100 Ohm-metre resistivity, about 100 m with a resistivity of 700 Ohm-metres and about 300 m with a resistivity of 10000 Ohm-metres. In glaciated limestone areas in Ireland, lower resistivity values (up to about 100 Ohm-metres) can be attributed to surface sediments with high clay content, medium resistivity values (200 - 300 Ohm-metres) can be attributed to sandy/gravelly tills and limestone bedrock usually has a resistivity of 500 Ohm-metres and upwards. Lower values (500 - 1500 Ohm-metres) may indicate saturated, weathered bedrock.

The measured resistivities are considered high for the karst limestone in this area and

therefore there must be another factor influencing the response of the instrument. It is possible that the measured, resultant electromagnetic field in the area has been at least partially modified by a phenomenon known as "current channeling". Where this effect is seen it can be attributed to possible high resistivity "channels" in the subsurface. These "channels" could be a single air-filled void or a zone of voids or a high resistivity contrast caused by lithological variation. The presence of voids can cause primary current flowlines to deviate and this results in higher-than-normal measured apparent resistivity and a relative phase low over the area of disturbance. Ogilvy et al. (1991) have exploited this phenomenon to map air-filled drainage galleries in Spain and Barton and Mac Niocaill (1991) have observed this effect during a survey to map a known, air-filled cave located at a depth of 30 m in karst limestone terrain in Co Clare.

#### 6.3.2.3 Conclusions

It is concluded that the high resistivity, closed anomaly may possibly be an artifact of a nearby zone, or zones, of cavities in the limestone and that the nearly coincident phase low indicates a more resistive lower layer at this location. The phase high to the east of the marked resistivity high indicates a more conductive layer at depth. This seems a reasonable hypothesis given the existence of a sinkhole some 20 m NW of house No 10 in Ballydotia West. Local householders also reported that, when a waterwell was being dug by hand, in the vicinity of the sinkhole a very large cavity was encountered at a depth of about 12 feet. Further evidence for cavities in the bedrock comes from the construction of a local sports facility some 500 m north of the survey area. Here cavities were encountered during the laying-down of a sportsfield.

### 6.3.3 Resistivity - Colinear dipole-dipole traverses

#### 6.3.3.1 Field survey

Subsequent to the EM-VLF-R survey and in order to obtain further information on the nature of the bedrock in the area of the interpreted zone of cavities, two resistivity traverses were completed using the colinear dipole-dipole array. The location of these traverses is plotted on Maps 1 and 2. One traverse (BYDDP1) was run across the closed resistivity high, near the sinkhole, in Ballydotia West and the other (BYDDP2) ran acros the high resistivity gradient, near the turlough, at the rear of house No 6 in Ballydotia East

The colinear, dipole-dipole array had a dipole length, or 'a' spacing, of 25 m. Th array was expanded in multiples (n) of 'a' from n=1 to n=5 for each position of the curre electrodes. This gave a theoretical depth of investigation in a homogenous ground approximately 35 m at the n=5 expansion (Roy and Apparao, 1971). The results of th surveys in the form of resistivity pseudosections are given in Fig 4 and 5.

The contoured resistivity pseudosections should not be regarded as true depth secti as the depth of investigation does not conform to a linear relationship. Also, the plo convention used precludes the resistivity distribution being viewed as a direct analogue o geological variation which may give rise to it. This means that shapes and attitudes obs on the contoured resistivity section do not strictly relate to shapes and dips which mig observed on the true geological section.

#### 6.3.3.2 Interpretation

In BYDDP1 (Fig 4) there is a general increase in resistivity as one move station 25 m in the West to station 125 m. Resistivity values range from 600 to 300

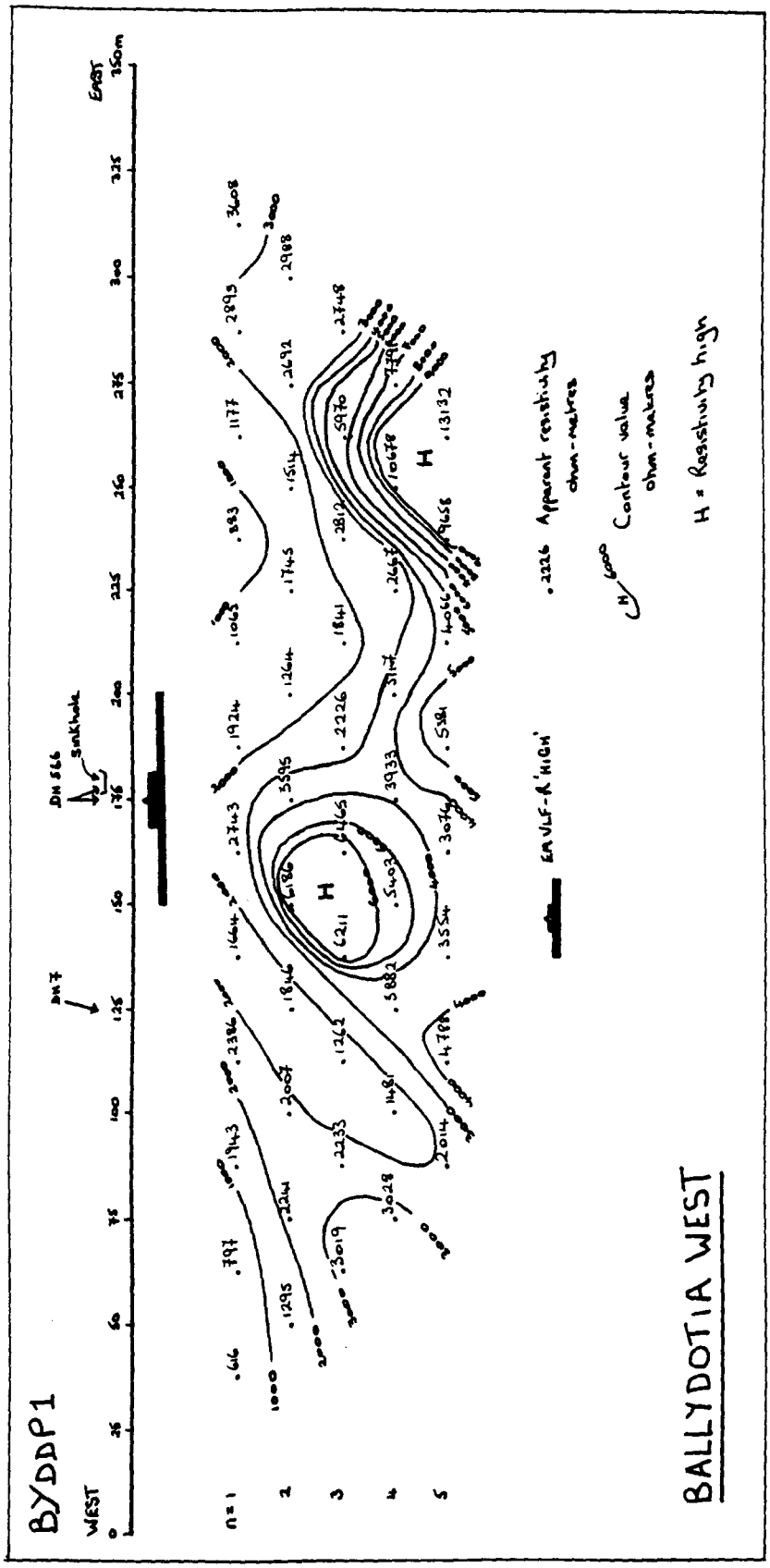


**Figure 4. Ballydotia West: Resistivity pseudosection BYDDP1**

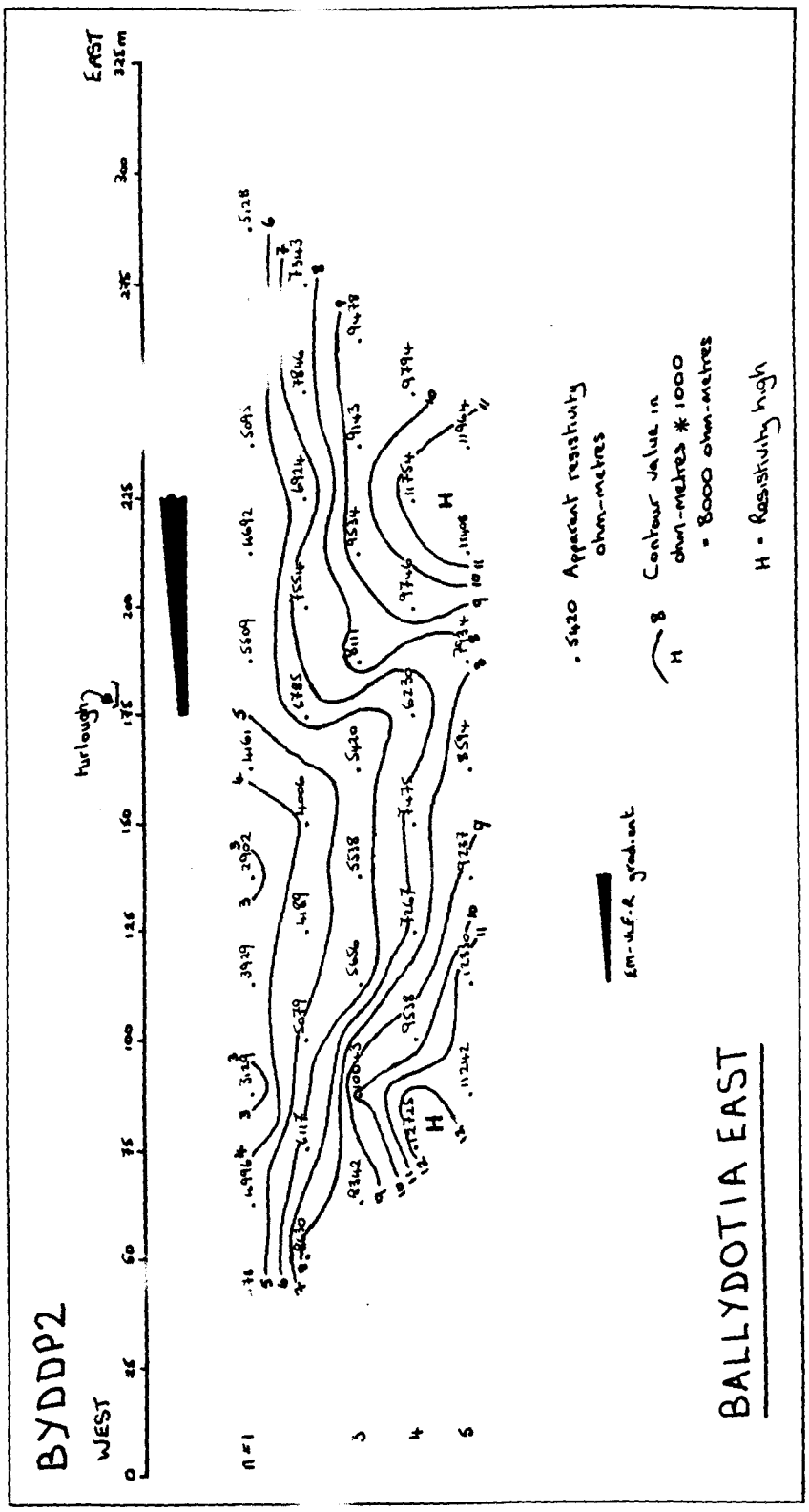


**Figure 5. Ballydotia East: Resistivity pseudosection BYDDP2**

metres across this portion of the section. This resistivity distribution can possibly be interpreted as being due to thin, sandy/gravelly till overlying karst limestone bedrock at depth. Between 125 m and 150 m there is a relative resistivity low, trending at 45° westwards, lying against a resistivity high. It can be shown (Hohmann, 1982) that resistivity zones on a pseudosection which contour at 45° can be related to the edges of vertical, or sub-vertical, geological features. This resitivity low therefore could represent the presence of a weathered zone resulting from a small, vertical or sub-vertical joint or fault in the limestone. This part of the resistivity pseudosection also corresponds with a small topographic rise in ground surface. From 150 m to 175 m, at the edge of the sinkhole, there is a closed resistivity high with values rising to over 6000 Ohm-metres underlain by lower resistivity values in the region of 3000 Ohm-metres. This feature may represent a relatively competent block of limestone underlain by less competent material. Continuing eastwards from 175m, a broad trough of lower resistivity material is encountered which is underlain by a high resistivity "basement". The sinkhole lies just to the east of 175 m and it is likely that the lower resistivity material is karstified limestone lying on more competent limestone at depth. It may also be inferred that the transition zone between karstified and competent limestone may occur in the zone between the 3000 - 4000 Ohm-metre contour lines. In this area an approximate depth to this zone would be 20 m at station 200 m. The pseudosection shows that a zone to the north of house No 10 is karstified, possibly to a depth of 20 m.

Fig 5 shows the contoured resistivity pseudosection for BYDDP2. It should be noted that the overall resistivity values are higher than those found on BYDDP1. This may result from less karstification in this area. Outcrop is seen in the immediate vicinity of the dipole-dipole traverse line. In the zone from station 25 m in the west to 175 m there is a broad, deepening 'trough' with relatively 'low' resistivity values ranging from about 3000 Ohm-metres at the surface to 7000 Ohm-metres at depth. This trough lies between two resistivity highs which are seen at about 75 m and 225 m. The highs have values greater than 8000 Ohm-metres. The highs may be due to massive, competent limestone while the 'low' zone could reflect an area of karstified material possibly related to a joint or fracture. The high surface resistivities indicate shallow, or absent, overburden along the line of the traverse. There is a water-filled turlough about 20 m north of the traverse line near station 175 m. The location of the turlough coincides with the eastern edge of the resistivity low. It is possible that the turlough is fed from water percolating up or along the eastern edge of the resistivity low which may be a zone of high permeability.

### 6.3.3.3 Conclusions

Both resistivity pseudosections image largely similar features and differ only in the magnitude and range of resistivities measured. In Ballydotia West a moderately thin overburden gives rise to lower surface resistivities. The overall bulk resistivity here is low indicating more extensive, and deeper, karstification of the limestone compared to that in Ballydotia East where resistivities are higher. The edge of a trough of low resistivities on BYDDP1 coincides with a dry sinkhole. In Ballydotia East surface resistivities are high due to little or no overburden. A trough of relatively low resistivity has been encountered which may be due to a zone of karstification.

The edge of this zone coincides with a water-filled turlough.

### 6.3.4 Resistivity - Vertical Electric Soundings

#### 6.3.4.1 Field survey

In order to gain further quantitative information on the sub-surface structure and resistivities in the Ballydotia West area, two Vertical Electric Soundings (VES) were carried out. The method used an Offset Wenner array, which was expanded about the centrepoint of the array, to collect resistivity data at increasing depths vertically beneath the centrepoint. The locations of BYVES1 and BYVES2 are shown on the EM-VLF-R map (Map 1). BYVES1 was sited to the north of the dipole-dipole traverse BYDDP1 for logistic reasons. It was targetted to intersect the edge of the EM-VLF-R resistivity high and also the resistivity high on the dipole-dipole traverse. It was assumed that the latter high extended north of the traverse line.

The linear distance the array could be expanded to was limited by obstructions such as houses and roads and the final 'a' spacing achieved was 64 m. This gave a total array length of 192 m which corresponds to an approximate depth of investigation of about 30 m.

#### 6.3.4.2 Data reduction and modelling of VES data

The data collected and calculated resistivities are given in Table 1.

The data reduction programme extrapolates readings for the 'a' spacings at 96 m and 128 m from the measured data and then calculates apparent resistivities for all data thus giving a final apparent 'a' spacing of 128 m and apparent array length of 384 m. This implies a depth of investigation of about 55 m but this estimate should be treated with caution in view of the extrapolation made by the software during computer processing. Using the Offset Wenner array, there is some in-built quality control on the data collected. This can be seen by inspecting the Offset Differences column in the tabulated results. BYVES1 has rather high offset differences values which can be attributed to lateral variations in resistivity due to non-homogenous ground. The RMS errors for BYVES1, which are high at 22%, are just within acceptable limits and result in a 'noisy' plotted field curve. The field curve (crosses) and model curve (squares) are given in Fig 6.

Sounding BYVES1 has been modelled as a 3-layer case using a forward modelling program. The model parameters used were a surface layer of resistivity 225 Ohm-metres down to 0.6 m, a second layer of 1150 Ohm-metres to 5.5 metres and a third layer of 12000 Ohm-metres. The RMS fitting error is poor at nearly 18%. This is largely attributable to noisy data. There are a number of possible model fits to the field data and the one presented in Fig 6 represents a number of compromises within the constraints of noisy data, and available geological/geophysical knowledge. The model can be interpreted as 0.6 m of sand/gravelly, possibly permeable, overburden overlying karstified limestone, or a sand/gravel horizon, to 5.5 m and finally underlain by competent limestone.

VES sounding BYVES2 is situated south of house No 10 within the EM-VLF-R resistivity high. The field data and calculated results are given in Table 2.

The data quality from this sounding is better than BYVES1 as can be seen from the RMS error of about 11%. In very crude terms this could indicate a change in ground conditions i.e. the ground is more homogenous to the south of the road. The plotted resistivity sounding curve (crosses) and modelled curve (squares) are shown in Fig 7.

These data have been modelled as a 2-layer case with a 0.6 m thick surface layer of 350 Ohm-metres underlain by bedrock with a resistivity of 9000 Ohm-metres. Again the surface layer resistivity is attributed to a sandy/gravelly till and the bedrock is competent and unweathered. The RMS fitting error is on the high side and can be attributed to 'noise' due

**Table 1. Ballydotia West: Field data and calculated resistivities - BYVES1**

Ballydotia-VES

OFFSET WENNER SOUNDING 1

OBSERVED RESISTANCES

| SPACING | RA | RB | RC | RD1 | RD2 |
|---|---|---|---|---|---|
| 0.5 | 110.1 | 6.4 | 103.7 | 82.3 | 64.9 |
| 1.0 | 90.140 | 7.089 | 83.070 | 64.790 | 56.920 |
| 2.0 | 77.340 | 4.329 | 73.020 | 53.250 | 50.020 |
| 4.0 | 63.420 | 3.265 | 60.170 | 47.290 | 35.170 |
| 8.0 | 44.600 | 2.875 | 41.650 | 33.450 | 27.700 |
| 16.0 | 38.700 | 1.897 | 36.730 | 28.630 | 21.270 |
| 32.0 | 26.550 | 2.722 | 23.850 | 22.730 | 16.420 |
| 64.0 | 31.400 | 0.471 | 30.910 | 18.790 | 18.330 |

CALCULATED SOUNDING CURVE AND ERROR INFORMATION

| SPACING m | APPARENT RESISTIVITY | OBSERVED ERROR | OFFSET DIFFERENCE |
|---|---|---|---|
| 0.5 | 231.221 | 0.00 | 23.64 |
| 1.0 | 382.363 | -0.02 | 12.93 |
| 1.5 | 536.583 | | |
| 2.0 | 648.865 | -0.01 | 6.26 |
| 3.0 | 823.217 | | |
| 4.0 | 1036.223 | -0.02 | 29.40 |
| 6.0 | 1313.375 | | |
| 8.0 | 1536.867 | 0.17 | 18.81 |
| 12.0 | 2064.050 | | |
| 16.0 | 2508.248 | 0.19 | 29.50 |
| 24.0 | 3209.532 | | |
| 32.0 | 3935.788 | -0.08 | 32.23 |
| 48.0 | 5998.557 | | |
| 64.0 | 7463.419 | 0.06 | 2.48 |
| 96.0 | 11695.545 | | |
| 128.0 | 19879.963 | | |

RMS OBSERVED ERROR = 0.10 percent
RMS OFFSET DIFFERENCE = 22.08 percent

**Table 2: Ballydotia West: Field data and calculated resistivities - BYVES2**

Ballydotia-VES

OFFSET WENNER SOUNDING 2

OBSERVED RESISTANCES

| SPACING | RA | RB | RC | RD1 | RD2 |
|---|---|---|---|---|---|
| 0.5 | 225.4 | 11.4 | 213.9 | 139.0 | 151.9 |
| 1.0 | 192.4 | 12.6 | 179.7 | 122.5 | 130.4 |
| 2.0 | 173.1 | 10.5 | 162.6 | 113.8 | 115.4 |
| 4.0 | 155.8 | 8.3 | 147.5 | 113.9 | 88.0 |
| 8.0 | 121.5 | 7.5 | 113.9 | 85.1 | 77.9 |
| 16.0 | 82.300 | 7.361 | 74.950 | 58.930 | 62.380 |
| 32.0 | 51.020 | 3.029 | 47.990 | 38.110 | 39.600 |
| 64.0 | 35.000 | 5.000 | 30.000 | 21.050 | 21.050 |

CALCULATED SOUNDING CURVE AND ERROR INFORMATION

| SPACING m | APPARENT RESISTIVITY | OBSERVED ERROR | OFFSET DIFFERENCE |
|---|---|---|---|
| 0.5 | 456.945 | 0.04 | -8.87 |
| 1.0 | 794.509 | 0.05 | -6.25 |
| 1.5 | 1147.238 | | |
| 2.0 | 1440.106 | 0.00 | -1.40 |
| 3.0 | 1991.865 | | |
| 4.0 | 2537.150 | 0.00 | 25.66 |
| 6.0 | 3356.164 | | |
| 8.0 | 4096.637 | 0.08 | 8.83 |
| 12.0 | 5299.032 | | |
| 16.0 | 6097.706 | -0.01 | -5.69 |
| 24.0 | 7481.377 | | |
| 32.0 | 7812.261 | 0.00 | -3.83 |
| 48.0 | 7727.118 | | |
| 64.0 | 8464.707 | 0.00 | 0.00 |
| 96.0 | 12935.905 | | |
| 128.0 | 14396.036 | | |

RMS OBSERVED ERROR = 0.04 percent
RMS OFFSET DIFFERENCE = 10.62 percent

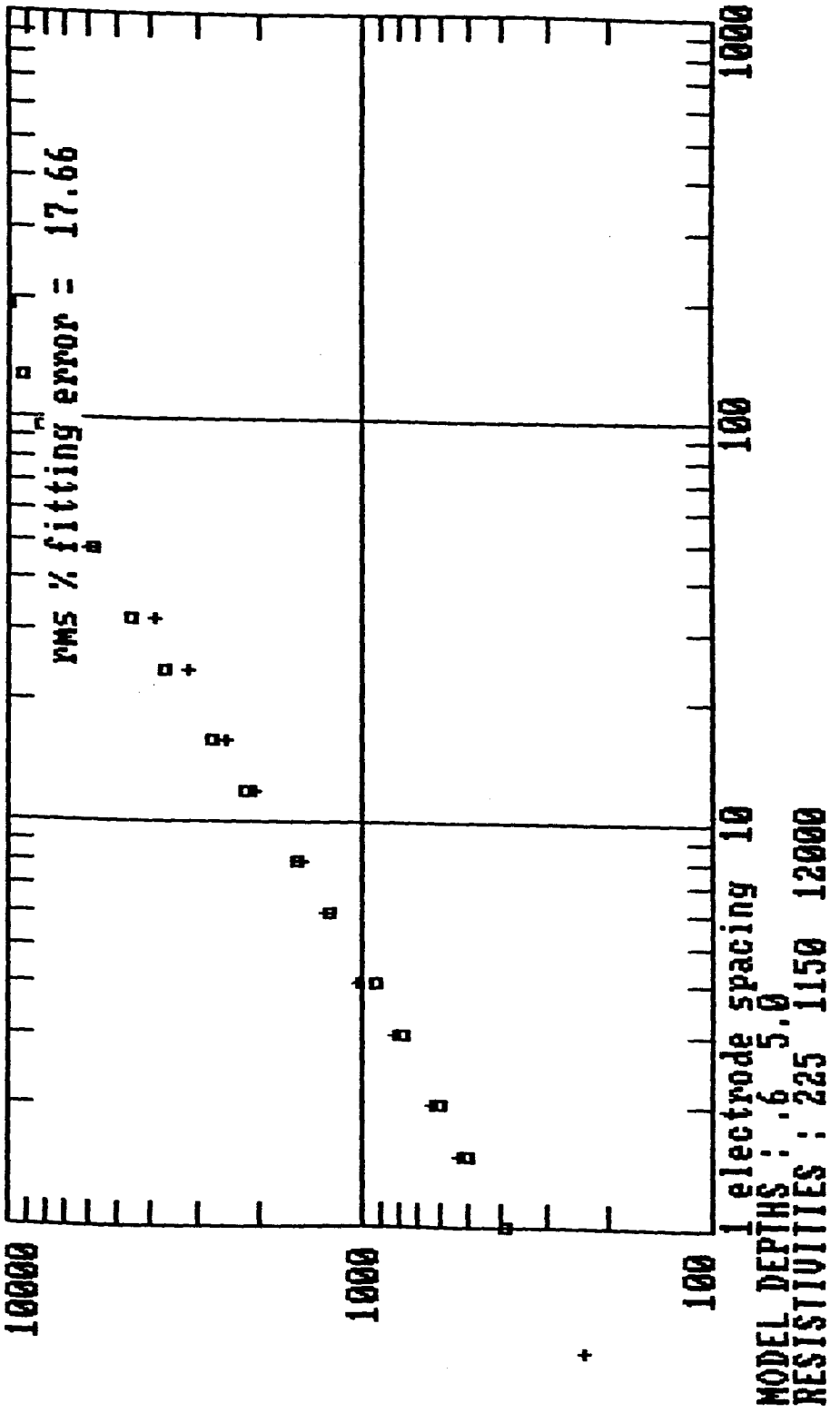


**Figure 6. Ballydotia West: Field resistivity and modelled curves - BYVES1**

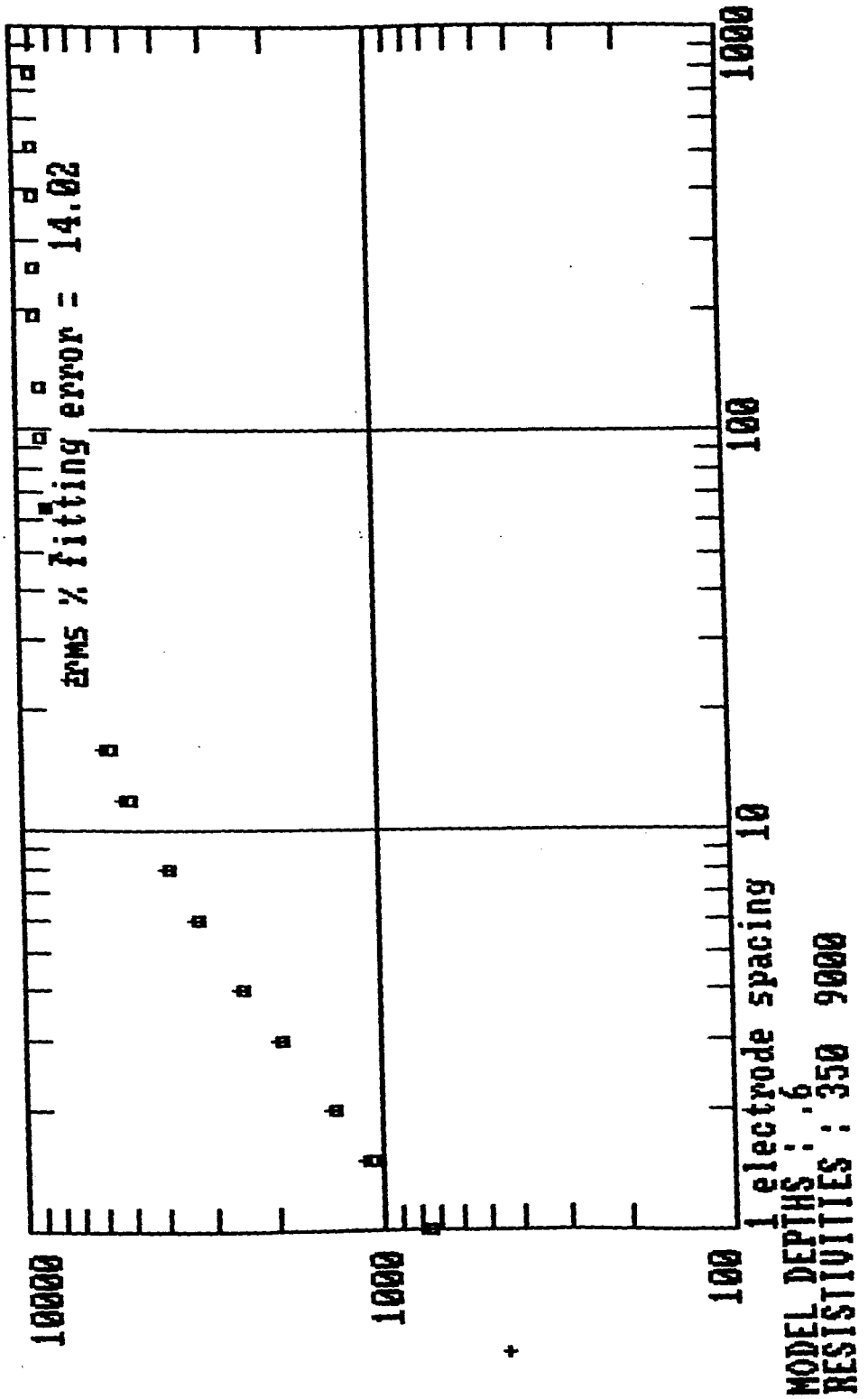


**Figure 7. Ballydotia West: Field resistivities and modelled curves - BYVES2**

to some lateral variation at the smaller 'a' spacings.

#### 6.3.4.3 Conclusions

The VES data indicate a change in ground conditions as one moves from north to south of house No 10. To the north there may be sand/gravel or, more likely, karstified limestone resting on competent limestone bedrock and to the south overburden is thin and rests on mainly competent bedrock. Lateral changes in resistivity, with increasing sounding depth, appear smaller to the south of the house. Limestone outcrop can be seen at the surface in the immediate vicinity of the house which tends to confirm the thin overburden indicated by BYVES2.

### 6.3.5 Discussion and integration with drilling results

Most of the geophysical work on this project was carried out in the Ballydotia area as the initial reconnaissance EM-VLF-R survey found distinct anomalies in the vicinity of the houses with high indoor radon values. The lack of major obstructions and 'cultural noise' also greatly aided the geophysical surveying.

All geophysical methods deployed responded to varying degrees of karstification detected to depths of about 20 m. There is a distinct and mappable resistivity contrast between the weathered or karstified limestone and the massive, unweathered limestone found in the area. At each high radon house there was surface evidence, in the form of sinkholes and turloughs, of karstification of the limestone bedrock and hence there was a likelihood of more widespread, buried air or water-filled cavities being present.

#### 6.3.5.1 Ballydotia West

In Ballydotia West the EM-VLF-R method mapped a broadscale resistivity high, the apparent resistivities measured may have been influenced by current channeling due to the presence of buried cavities in the limestone. A resistivity pseudosection (Fig 4) showed the central area of the EM-VLF-R resistivity high to be underlain by a possible competent zone of limestone. This competent zone is underlain, and abutted to the east, by a zone of low resistivity material interpreted as up to 20 m of karstified limestone. The EM-VLF-R phase data (Map 2) , also possibly influenced by current channneling, indicate a more resistive layer at depth here. It is in the zone between the high resistivity block and the resistivity low on the pseudosection BYDDP1 (Fig 4), and the resistivity high and phase low on the EM-VLF-R maps (Maps 1 and 2) that a dry sinkhole occurs. From the occurence of the sinkhole and the pervasive resistivity lows on the pseudosection BYDDP1, we must assume that this area is prone to deep karstification and to the possibility of cavities being associated with this pervasive weathering. The VES BYVES1 (Fig 6) shows that north of pseudosection BYDDP1 there is about 5 m of karstified limestone overlying massive limestone, while BYVES2 (Fig 7) to the south of house No 10 shows massive competent limestone at the surface. The suggestion of lateral surface layer and/or bedrock inhomogeniety, found as a by-product of carrying out the VES surveys, show that there is more lateral variation to the north of house No 10. BYVES2 (Fig 7) suggests that bedrock is almost at the surface in this area and this is confirmed by limestone outcrop immediately to the east of house No 10. However 100 m - 200 m further south, in the working sand/gravel pit, bedrock is not seen. The topographic level of the quarry floor is perhaps some 10 m lower than that of the outcrop near house No 10. Clearly, there must be a major E-W discontinuity (fault or fracture zone) to the south of house No 10 such that its foundations rest on a pronounced bedrock high.

Subsequent to the geophysical surveys, in Ballydotia West, a borehole (DH4) was

drilled some 25m to the south of house No 10 and 3 further boreholes (DH 5,6 and 7) were drilled on the line of pseudosection BYDDP1 to test whether resistivity lows represented a zone of buried cavities. Borehole locations are shown on Map 1 and also on pseudosection BYDDP1 (Fig 4). In Ballydotia East, 3 boreholes (DH 8,9 and 10) were drilled to test the resistivity gradient seen in the EM-VLF-R map and resistivity low on the pseudosection. The following account of borehole results is summarised from Annex 1. Depths quoted from inclined boreholes refer to the depth along the axis of the borehole and not the true vertical depth.

DH4 was a vertical hole, drilled 25 m south of house No 10, which encountered about 2 m of overburden before passing into massive limestone. At 19.1 m depth a small, 0.1 - 0.4 m cavity was intersected which contained pink granite pebbles. This borehole was sited near BYVES2 and confirmed the interpretation of thin overburden resting on massive, high resistivity limestone.

DH5, some 40 m NW of house No 10, was drilled at an angle of 55° into the sinkhole north of the house. About 3.5 m of overburden was encountered before the borehole entered a small fault or joint in the bedrock surface. Massive limestone was then recovered until a small zone of cavities was found between 15.5 m and 16.8 m depth, the largest cavity being 1.0 m across. Fragments of limestone and granite pebbles were recovered from the cavity. This borehole intersected the edge of the resistivity low seen on pseudosection BYDDP1 (Fig 4) and confirmed the presence of cavities in this zone.

DH6 was collared close to DH5 and was a vertical borehole. Very little overburden was encountered here and fractured limestone was found down to about 5 m depth. Massive limestone was encountered down to 40 m. This borehole most likely intersected the edge of the high resistivity 'block' on BYDDP1 (Fig 4) which was, thus, confirmed as due to massive limestone. The borehole did not intersect any cavities or the lower resistivity zone at the base of the block. This borehole was preserved using slotted, plastic agricultural drainage pipe. Two passive radon detectors were deployed above the watertable and recovered after 15 days. The radon concentrations found are given in Table 3 and are discussed in Annex 2.

DH7 was an inclined borehole which was targetted at the coincident topographic rise and resistivity low at the western end of BYDDP1 (Fig 4). About 5 m of overburden was encountered before passing into a thick zone of fractured and broken limestone which extended to about 18.5 m. Only 0.4 m of core was recovered in the depth interval 15.6 to 18.6 m indicating the presence of a possible 2.6 m cavity. Pebbles were found in the base of the cavity indicating water flow in this zone.

DH11 was subsequently drilled at 45° at the NE side of house No 10. The objective of this borehole was to drill under house in a SW direction to test if any cavities were disposed in a N-S zone under the house. The borehole was collared in massive, crinoidal limestone which extended to the end of the hole at 52 m. Two very small dissolution features were found at about 11 m and 14.5 m, they both had a maximum width of 1 - 2 cm. At a distance of 21 m to 22 m along the core axis two small cavities were encountered. At 21.3 m a narrow cavity, of possible width 0.45 m, containing buff-coloured clay, was encountered. A total of 0.15 m of clay was recovered from this zone with core loss making up the remaining 0.30 m. At 22.0 m a red-brown clay and granite fragments, preceded by fractured limestone, was encountered in a small cavity. The clay recovered was 0.1 m thick and some 0.7 m of core was missing, thus, giving a cavity possibly 0.8 m across. This borehole was also preserved using a slotted, plastic liner and 3 passive radon detectors deployed. The radon concentrations measured are given in Table 3.

The drilling results largely confirmed the interpretation of pseudosection BYDDP1 and VES surveys in that DH4 proved shallow, massive bedrock, DH5 proved weathered or karstified limestone and the presence of cavities, DH6 proved the high resistivity zone on the pseudosection and DH7 encountered a large cavity in low resistivity material at the western end of BYDDP1. DH11, under house No 10, also intersected clay-filled fractures or cavities. Here, the drilling results did not confirm if the cavities found were totally infilled with clay and granitic debris or if they had an air-water interface with clay and granitic debris lying on the floor of the cavity. None of the geophysical surveys imaged cavities directly, but delineated zones in which they were likely to occur.

The shallow drilling did not identify the cause of the EM-VLF-R resistivity anomaly which must be due to a deeper source which was not encountered in drilling. The size and number of the small cavities found do not fully explain the EM-VLF-R resistivity high nor the phase low. Either (i) current channeling effects are large and a zone of larger cavities exists at a deeper level which were not encountered in drilling , or (ii) the main zone of cavities was missed by drilling, or (iii) the EM-VLF-R survey is imaging a very resistive target at depth and the current channeling effects are small. Assuming a constant, contact dip of 30° between the granite and the limestone and a horizontal distance of 2 km between Ballydotia and the surface expression of the granite contact in Moycullen Village, the roof of the granite under Ballydotia would be about 1000 m below the surface. This estimated depth is supported by the 3-D modelling of Madden (1987) albeit with the limited gravity data available in the area. It is unlikely that the granite at 1000 m is the cause of the EM-VLF-R anomaly. It is possible that the roof of the granite is closer to the surface in this area, but unfortunately the sparse regional gravity data cannot be used to help resolve this problem. It is interesting to note however, that if we make the large assumption that the mid-point (0 mGal contour) of the SW--NE gravity gradient to the NE of the Moycullen area (Fig 2) defines the edge of the granite then, this edge may occur in the NE of the Ballydotia area (Fig 2). This 'edge' may exert some control on the fracture and/or jointing patterns in the area which in turn might be related to karstification in the limestone. In must be stressed, however, that this hypothesis may be seriously flawed due to (i) the sparse gravity data, (ii) lack of knowledge on granite-limestone density contrasts and (iii) lack of knowledge on the attitude and depth of the granite-limestone contact.

#### 6.3.5.2 Ballydotia East

In Ballydotia East the resistivity pseudosection BYDDP2 (Fig 5) indicates a weakly weathered zone which may be related to a master joint. A water-filled turlough lies adjacent to the edge of this weathered zone which probably strikes in the direction of house No 6 which has a high, but variable, indoor radon concentration. To the south of house No 6, and on line with the latter strike directon, lies a dry sinkhole (Map 1).

3 boreholes were drilled in the vicinity of BYDDP2 to test the relatively low resistivity zone and the resistivity high to the east (Map 1).

DH8, a vertical borehole, was targetted on the relatively low resistivity zone and encountered little overburden and then limestone with minor fracturing and alteration to a depth of about 6 m. The borehole then entered massive limestone to a depth of 24.5 m. At this depth a small channel containing exotic pebbles of sandstone and para-gneiss was found. The hole was completed in massive limestone at a depth of 34.8 m.

DH9 was an inclined borehole drilled westwards across the strike of the resistivity gradient towards the resistivity low. The borehole encountered 1 m of overburden and 2 m of fractured limestone followed by massive limestone to about 34 m. Here a small zone (0.3

m) of exotic pebbles of granite and gneiss was found which indicated a flowing channel. The borehole then continued in massive limestone to 39.5 m.

DH10, another inclined borehole, was drilled in the same direction as DH9 but was sited further to the west. The borehole encountered little overburden and was drilled largely in massive limestone.

In the Ballydotia East area the overburden is thin giving rise to the high surface resistivities.The nature of the limestone found in drillcore in this area was largely massive giving rise to the higher measured bulk resistivities compared with those in Ballydotia West. This indicates less pervasive weathering. The relative resistivity low, when drilled, did not reveal any cavities which may confirm that weathering is again not as pervasive as in Ballydotia West. The high resistivity gradient, when drilled, did not reveal any discernable joint system except for a small channel found at depth. This may be a feeder for the water-filled turlough. In this area the geophysical surveys did not image any structures likely to provide conduits for radon migration. On the whole, water movement in the area is likely to be via small channels deep in the massive limestones. In this area the EM-VLF-R high resistivity gradient is confirmed by a resistivity high on the pseudosection. It can again be concluded that either the EM-VLF-R is imaging the high resistivity, massive limestone or is imaging a higher resistivity source at depth.

## 6.4 Geophysical survey in the Moycullen area

### 6.4.1 Introduction

This area (Fig 1) largely lies on limestone bedrock in the NE of Moycullen Village. The surface trace of the NW--SE trending granite-limestone contact lies in the extreme SW of the area surveyed. In the Village 'cultural noise', in the form of powerlines, underground services etc., made surve very difficult. A modern housing estate, with a high density of houses, in the centre o rea and associated access roads reduced the number of possible survey sites in this loc

High soil-gas values wer in the vicinity of the housing estate and it was therefore decided to target the estat nvirons for the geophysical survey. At the time of survey no houses had been measur or radon concentrations.

### 6.4.2 EM-VLF-R field survey

The Geonics EM16R was used, with the Rugby (GBR) 16 kHz transmitter as a source. The number of survey stations was restricted due to cultural noise and access problems. Some 40 measurements were made and they display an uneven distribution (Map 3).

#### 6.4.2.1 Data reduction and processing

The data were gridded using the GeoSoft 2-D Mapping Package with a grid-cell size of 50 m. The gridded data were then machine contoured with a contour interval of 500 Ohm-metres and for the apparent resistivity and phase maps respectively.

#### 6.4.2.2 Interpretation

The main feature of the EM-VLF-R Map (Map 3) is a strong, uniform gradient (2000 Ohm-metres-11000 Ohm-metres) across the map from west to east. This gradient pattern is curved with its axis trending WSW-ENE. The curved nature, and increasing values, of the

resistivity contour pattern to the NE could be related to the thinning overburden in a NE direction. Outcrop is seen in the NE of this area.

The Phase Map (Map 4) also shows a uniform gradient which largely follows a similar trend, in the northern part of the area, to that seen on the Apparent Resistivity Map. However, in the southern part of the area, the contour pattern does not curve around to the SE but maintains a SW trend. Phase values greater than 45° lie to the NW of the area, with those less than 45° lying to the SE. This would indicate that a high resistivity second layer exists in the SE and a low resistivity second layer in the NW. The variations seen in the phase data could be explained by the underlying granite-limestone contact zone in the NW of the area being sufficiently weathered by localised fracturing and jointing so as to reduce the measured bulk resistivity in the NW. This would result in a less resistive second layer being observed in the NW of the map. The high resistivity second layer to the SE may be related to a thickening of the massive limestone in this area, this would result in low phase values being observed.

The trend of both the apparent resistivity and phase contour patterns do not correlate with the granite-limestone contact which is the general structural trend in the Moycullen area. It is possible that the mapped trends are related more to localized fracturing and jointing than to the general structural trend of the area..

#### 6.4.2.3 Conclusions

The general geophysical trend in this area does not follow the general geological trend and may be related to localised fracturing or jointing. The gradient in the Apparent Resistivity and Phase Map can be attributed to thinning overburden to the east in the case of the resistivity data and a weathered granite--limestone contact zone in the NW. In the Phase Map thickening, massive limestone to the east and the weathered granite-limestone contact would account for the observed values. Apparent resistivity values measured in this area are generally lower than those for the Ballydotia area. This could be related to the limestone in this area being more weathered as it thins towards the surface trace of the granite-limestone contact. Current channeling does not appear to be a major contributing factor in the resistivity values measured in this area.

### 6.5 Geophysical surveys in the Uggool area

#### 6.5.1 Introduction

This area lies entirely on granite with the surface trace of the granite-limestone contact lying some 100 m to the NE of the survey area (Map 5). Two granite types have been recognised; the NW-SE contact between the Coarse Foliated Granite and the Errisbeg Townland Granite lying in the centre of the area. Granite outcrop is seen in the SW of the area, the overburden covering most of the area comprises clayey soils of varying thickness.

The geophysical survey was targetted on house No 157 which had high indoor radon concentrations (Map 5). There were also a number of soil-gas anomalies in the vicinity of this house. The general area, especially in the vicinity of house No 157, was difficult to survey as the main Galway-Moycullen road runs through the area. There are also a large number of 110 kV powerlines and a river in the area. Access to suitable EM-VLF-R survey sites was also made difficult by the large number of private, walled gardens and dense vegetation.

### 6.5.2 EM-VLF-R field survey

The Geonics EM16R instrument was utilised in this survey with the Rugby 16 kHz transmitter being used as a source. Some 75 stations were occupied despite the restricted access and powerline interference problems. The station distribution is quite good in the west and southwest of the area, the station density falls going eastwards.

#### 6.5.2.1 Data reduction and processing

The field data were processed using the GeoSoft 2-D mapping package, both the resistivity and phase data were gridded with a grid-cell size of 50 m. The gridded data were then machine contoured using a contour interval of 100 Ohm-metres and 0.5° for the apparent resistivity and phase data respectively.

#### 6.5.2.2 Interpretation

The main feature seen in both the Apparent Resistivity and the Phase Maps (Maps 5 and 6) is the NNW--SSE trend. This trend broadly follows the contact between the two granite types recognised in the area. Resistivity values in this area are much lower than those found in the Ballydotia and Moycullen areas. They range from 1000 Ohm-metres to 2700 Ohm-metres with the higher values found in the west where the granite outcrops. The low resistivity values are likely to be caused by the clayey nature of the overlying soils which will reduce the bulk resistivity measured. The NNW--SSE zone (Map 5) with values of 1000 Ohm-metres, and less, coincides with the main Galway- Moycullen road and associated powerlines which may have influenced measurements in this area. To the east of this possible zone of interference, resistivity values lie in the range 1000 Ohm-metres to 1300 ohm-metres. The limited resistivity data here possibly reflects the occurence of thicker overburden compared with that found in the western portion of the survey area.

The phase values (Map 6) are less than 45° for the whole survey area indicating a more resistive second layer as would be expected with high resistivity granite underlying low resistivity, clayey overburden. There is some variation in the phase values with the lowest values being found in the west where overburden is thin and granite outcrops. In the SE corner of the area a limited number of stations show higher phase values which may indicate the zone of the weathered, and less resistive, granite-limestone contact which lies some 150 m to the NE.

#### 6.5.2.3 Conclusions

The NNW-SSE trend in the geophysical data coincides with the general trend of the contact between the two types of granite recognised in the area. Comparatively low resistivity values found on the granite may be related to the clayey nature of the soils which mask the true granite resistivity. Phase values indicate a more resistive second layer to the west which is likely to be the granite underlying the thinner soils in this area. House No 157 lies in an area of apparent change in resistivity and phase gradient, this could be speculatively related to features associated with the contact between the two granite types. However, station density is poor in the area around house No 157 and there is a possibility of powerline interference causing spurious results.

### 6.5.3 Down-hole natural gamma logging

#### 6.5.3.1 Field survey

The gamma logs were run from the bottom to the top of boreholes DH 1 and DH2

using a Mount Sopris 1000C handwinched logger. The thalium activated scintillation crystal used was 3.81 cm long and had a diameter of 1.27 cm. A continuous log of total counts per second versus depth in metres was recorded on an integral chart recorder which had a fixed depth scale of 1 : 100.The gamma probe was winched up the borehole at approximately 6 m per minute. The logging datum was ground level.

**6.5.3.2 Data processing**

The analogue chart records were digitised at an interval of 0.5 m and plotted using the Geosoft data processing package. The digitising process resulted in some smoothing of the log response. When the digitised log was compared to the original log (at the same scale i.e. 1 : 100) it was found that no major changes in log character were discernable provided that they extended over 0.5 m on the original log.

**6.5.3.3 Interpretation**

The log response in DH 1 (Fig 8), which was drilled at 45°, shows a low, but variable, gamma intensity averaging about 10 cps (counts per second) in the upper 10 m of the borehole. This possibly results from the fractured and broken nature of the core in this zone. From 10 m to 20 m the gamma response is uniformly low at just under 5 cps, this corresponds with the uniform limestone sequence seen in the core log. Just below 20 m there is a rise in the response reflecting the more muddy/shaley nature of the limestone as it passes into a shale sequence at about 24 m. The shale sequence continues to about 29 m and the response in this zone averages above 27 cps. The gamma log response in sedimentary sequences is largely derived from $^{40}K$ in clay minerals or shell debris and higher values would therefore be expected in muddy, or highly fossilised, limestones or shales. There is a sharp peak at just below 30 m which corresponds to the breccia zone which may have a higher concentration of clay minerals. The sharp trough from 31 m to about 32 m corresponds to highly fractured zone where many small rock fragments were recovered. The log here is likely to be responding to the fracture zone. Sheared granite found from about 32 m to 39 m shows an overall higher average response of just over 35 cps. This probably reflects the increase in radioelement (K,U Th) concentrations found in granites. The response is not particularly strong possibly indicating weak concentrations. The porphyry from about 39 m to just over 50 m shows a distinct response which averages just over 20 cps. This may indicate lower radioelement concentrations in this zone. From the base of the porphyry to the end of the hole the response rises again to average at 35 cps in the granite found at the bottom of the hole.

The response in DH 2, which was drilled at 66°, is broadly similar to that found in DH 1. The bioclastic limestone found down to about 20 m gives an average response of about 5 cps with a gradational increase to a response of 25 cps in the shale at about 26 m. The sheared granite sequence is thinner in this borehole than that found in DH 1 but is just recognisable as an increase in intensity from 27 m to 30 m. Again the porphyry is recognisable as a zone of uniform intensity averaging 20 cps between 30 m and 45 m. The sheared granite from 45 m to 60 m shows a higher, but variable response, compared to the porphyry and averages about 35 cps. There appears to be a graduation in the response with slightly higher values found with increasing depth to the base of this unit. The porphyry found at 60 m to 62 m is quite thin and cannot easily be distinguished from the granite. The sequence of sheared granite -- porphyry -- sheared granite from 62 m to the end of the hole at just over 80 m shows a variable character and has an average value of about 35 cps. The porphyry from 69 m to 75 m shows a slightly higher intensity than that found between

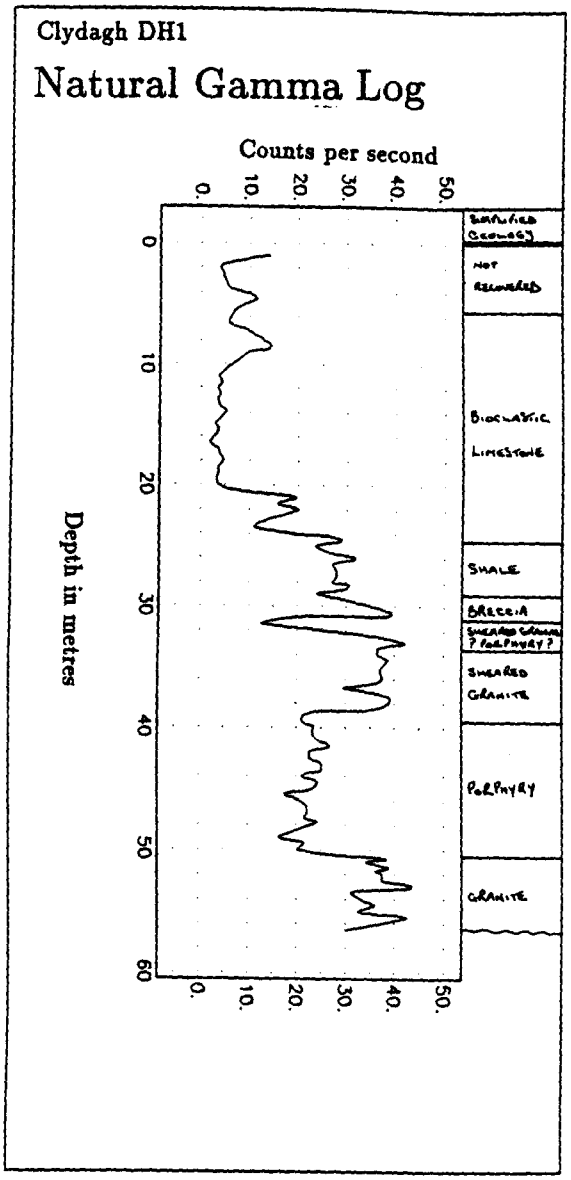


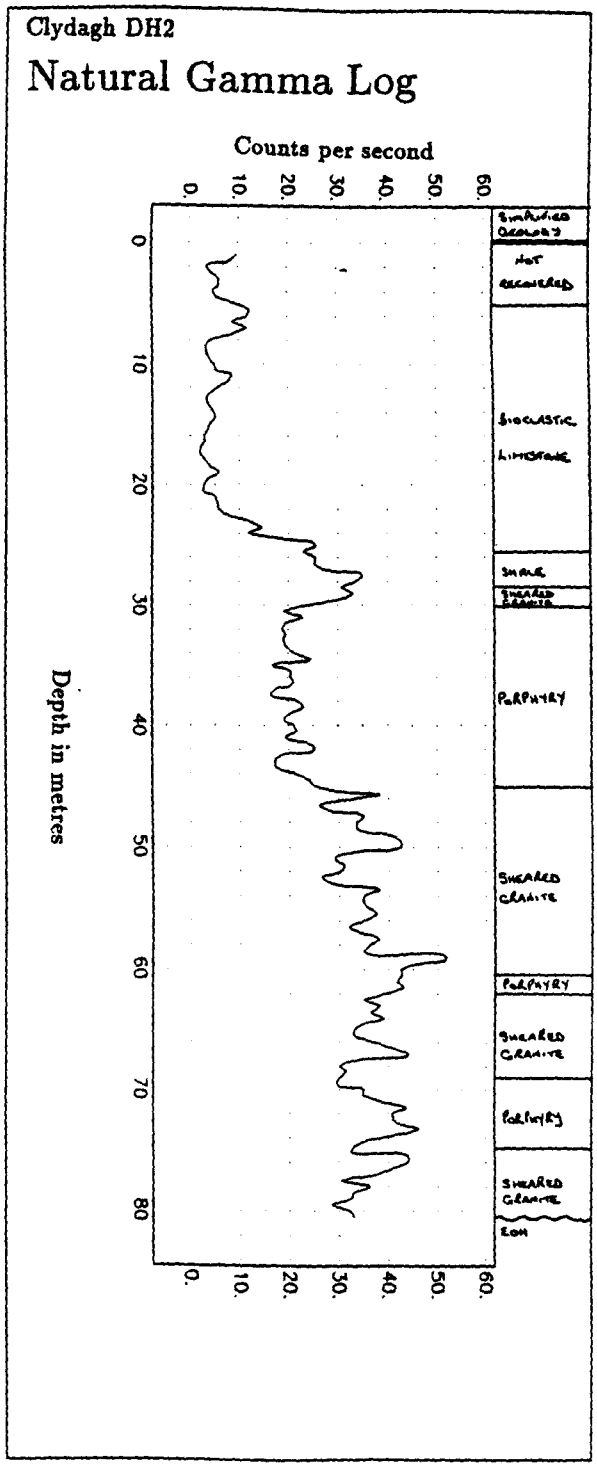


**Figure 8. Ballycuirke: Downhole gamma logs, DH1 and DH2**

30 m and 45 m. this may indicate slightly higher radioelement concentrations.

**Table 3: results from passive radon detectors deployed in boreholes**

| Det.No. UCG/ | Det.No RPII/ | Bh.No, Position along axis | Deployed D M Y | Recovered D M Y | Radon Conc. Bq $m^{-3}$ (RPII results) |
|---|---|---|---|---|---|
| 43 | 6501 | DH6,1.2m | 20-02-92 | 06-03-92 | 657 |
| 44 | 6502 | DH6,3.4m (below watertable) | 20-02-92 | 06-03-92 | 3645 |
| 45 | 6503 | B'ground | – | – | – |
| 46 | 6505 | DH2,1.5m | 02-10-91 | 17-10-91 | 1741 |
| 47 | 6506 | DH2,0.2m | 02-10-91 | 17-10-91 | 1588 |
| 48 | 6507 | B'ground | – | – | – |
| 49 | 6508 | B'ground | – | – | – |
| 50 | 6509 | B'ground | – | – | – |
| 51 | 6510 | DH11,0.8m | 27-02-92 | 06-03-92 | 9127 |
| 52 | 6511 | B'ground | – | – | – |
| 53 | 6512 | DH11,4.7m | 27-02-92 | 06-03-92 | 1480 |
| 54 | 6514 | DH11,9.6m | 27-02-92 | 06-03-92 | 12874 |

#### 6.5.3.4 Conclusions

Both gamma logs show characteristic responses in the limestone, sheared granite and porphyritic units found in both boreholes. The log response at the contact between the sedimentary sequence in DH 1 and the granite is not as distinct as that found in DH 2. The overall gamma response in both boreholes does not indicate any strong increase in radioelement concentrations.

## 6.6 Conclusions

### 6.6.1 Ballydotia

#### 6.6.1.1 Ballydotia West

1. A zone of cavernous, weathered limestone has been delineated north of house No 10. This zone contains a dry sinkhole at surface about 15 m north of the house.
2. The foundation of house No 10 rests on a bedrock high which comprises massive limestone. The limestone contains some thin, soft clays bands which may represent fracture or cavity infills, or coat the bottom of cavities.
3. Overburden immediately to the east and south of the house No 10 is thin or absent and massive limestone is close to the surface.
4. Some 100 m to the south of the house No 10, in the sandpit, the bedrock surface is at least 10 m topographically below the bedrock surface found at the house
5. The current geophysical survey and drilling have confirmed that there are small cavities under the foundation of house No 10.
6. The current geophysical survey has not proven any conduits linking the cavities, found to the north, to those found under the foundation of the house.
7. It is likely that the source of EM-VLF-R anomalies has not been intersected by drilling to depths of 40 m.

#### 6.6.1.2 Ballydotia East

1. The geophysical survey and drilling has confirmed the presence of massive limestone to the NW of house No 6.
2. Overburden in the vicinity of house No 6 is thin or absent. 3. There is a water-filled turlough to the NW of the house and a dry sinkhole to the SE.
4. House No 6 lies on a linear resistivity trend running between the water-filled turlough and the dry sinkhole.
5. When drilled, the linear resistivity trend revealed a 0.2 m thick channel or cavity at a depth of about 24 m.
6. The source of the EM-VLF-R anomaly has not been found by drilling to a depth of 35 m.
7. No information about the nature of the foundation of the house is available from the present geophysical survey.
8. No migration path to the house from the NW has been identified by the present geophysical survey.

### 6.6.2 Moycullen

1. Geophysical trends evident from the EM-VLF-R survey do not correlate with the general geological trend in this area.
2. Overburden thins to the east of the housing estate.
3. Apparent resistivity values in this area are generally lower than those found in Ballydotia possibly indicating more weathered limestone.
4. Limestone to the east of the area appears to be more massive.
5. The granite-limestone contact to the NW of the area is likely to be weathered.

### 6.6.3 Uggool

1. The geophysical trend found in this area generally coincides with the trend of the contact between the granite types recognised in the area.
2. Overburden in this area may have a high clay content giving rise to the low resistivities measured.
3. Overburden may be thicker in the east of the survey area.
4. 'Cultural noise' is likely to have obscured any EM-VLF-R anomalies in the vicinity of house No 157.

## 6.7 Recommendations

### 6.7.1 Ballydotia

This area offers the best possibility to build on the work carried out so far. Here we have identified two houses in different limestone terrains one of which has a reasonably constant high level of indoor radon values and the other may have levels which are time varying. There is a need to focus on these two houses and quantify the radon levels in relation to a wide variety of variables such as time, temperature, pressure etc and to also investigate the local geological controls (at or near foundation level which may have some influence on the radon values. The following recommendations would provide the geological/geophysical input to such a project. A detailed specification for the radon and other measurements is beyond the competence of the authors.

#### 6.7.1.1 Ballydotia West

1. 3 further Resistivity dipole-dipole pseudosections need to be carried out: the first parallel to BYDDP1 but south of house No. 10, the second and third at 90° to BYDDP1 and to the west and east of house No 10 respectively in order to further define the geological structure in the immediate vicinity of the house.

2. A number of resistivity VES to be sited on any anomalies found from the pseudosection data in order to aid interpretation.

3. A detailed gravity survey within a geographical area of 200 m of house No 10 to see if this technique can be used to quantify the distribution of cavities in the area.

4. A gravity survey, with a station interval of 200 m, along all roads and tracks in the Ballydotia area in order to assist interpretation of the depth to the granite in this area.

5. A Ground Probing Radar (GPR) survey on all the floors inside the house to see if there are any significant irregularities in the foundations of the house that can be recognised.

6. A test of the GPR outside, in the immediate vicinity, of house No 10 to see if this method can be used to map any anomalies associated with the foundations of the house and bedrock fracture zones.

7. Borehole topography between DH6 and DH11 to test for conduits linking the cavities.

8. Long term active in-house radon measurements to be carried out in house No 10.

9. Meteorological data to be regularly recorded for the Ballydotia area.

10. Water levels in DH6 and DH11 to monitored regularly.

11. Tracer test to see if any of the cavities intersected are connected internally or with the sinkhole.

12. DH7 to be reamed-out and cased with plastic, perforated casing and included in any longterm monitoring programme.

#### 6.7.1.2 Ballydotia East

1. 3 or 4 further resistivity dipole-dipole surveys to further refine the geological structure adjacent to house No 6.

2. A number of VES in support of the interpretation of the above.

3. Detailed gravity and GPR measurements as appropriate.

4. Meteorological and indoor radon data to be collected.

5. DH8 to be reamed-out and cased to allow for water level monitoring along with observations of water levels in the turlough.

6. A tracer test to see if the channel intersected is linked to the turlough or sinkhole.

### 6.7.2 Moycullen

The area in the vicinity of the housing estate, subsequent to the geophysical survey, has been found to contain a number of houses with high indoor radon concentrations. This area should be targetted for further follow-up. It will be difficult to carry out geophysical surveys in the vicinity of the estate due to 'cultural noise' and problems of access. The following could be attempted :

1. Ground probing radar to be used, if possible, in and around any houses with high indoor radon concentrations in order to map any anomalous zones associated with the foundations of the houses.

2. Fill-in EM-VLF-R stations, where possible, in the area in order to further define the resistivity and phase trend identified.

3. A resistivity dipole-dipole survey across the curved resistivity gradient to determine the geological structure in this area.

4. A number of VES surveys to test any anomalies resolved with the resistivity survey.

### 6.7.3 Uggool

House No 157 presents a difficult target for geophysical surveys due to 'cultural noise' and problems of access. If any further work is contemplated in this area, then the following could be attempted :

1. Two E-W resistivity dipole-dipole pseudosections to be carried out; one to the north and one to the south of house No 157 to try and delineate the possible geophysical gradient observed.

2. Ground probing radar survey in, and in the immediate vicinity of, house No 157 to further delineate any anomalies found during the resistivity dipole-dipole array survey.

## 6.8 Acknowledgements

We thank Dr Pat O'Connor and Dr Vincent Gallagher of the GSI for the opportunity to work on this project and for much helpful advice. Dr Jack Madden of the Radiological Protection Institute is acknowledged for much advice on radon, radon measurements and for arranging for provision and measurement of the downhole passive radon detectors. Kevin Crilly (GSI) is thanked for his patience and care in drilling and his expertise in inserting casing to preserve boreholes. Kevin O'Callaghan and Teresa Tully of UCG are thanked for assistance with fieldwork. Finally, the local population of the Moycullen area, especially Ballydotia, are thanked for allowing access to their property.

## 6.9 References

**Barton,K.J. and Mac Niocaill,C. (1991).** Trial EM-VLR-R and Detailed Gravity Survey at Pol-an-Ionain, Doolin, Co Clare. Unpublished Confidential Report, *AGU Report Series*, AGR 91/1, Applied Geophysics Unit, University College Galway.

**Cummins,P.A. (1991).** A PC-Based interactive program for 3-D gravity modelling. Unpublished MSc. minor Thesis, Applied Geophysics Unit, University College Galway.

**Hohmann,G.W. (1982).** Numerical Modeling for Electrical Geophysical Methods. *Proc. Int. Symp. Appl. Geophy. Trop. Reg.*, Univ. do Para, Belem, Brazil, pp308-384, 1982.

**Madden,J.S. (1987).** Gamma-ray Spectrometric Studies of the Main Galway Granite Connemara, West of Ireland. Unpublished PhD Thesis, National University of Ireland.

**Ogilvy,R.D., Cuadra,A., Jackson,P.D. and Monte,J.L. (1991).** Detection of an Air-filled Drainage Gallery by the VLF Resistivity Method. *Geophysical Prospecting*, 39, pp845-859, 1991.

**Reilly,S.G. (1983).** A Gravity Survey of Galway City. Unpublished M.Sc. minor Thesis, Applied Geophysics Unit, University College Galway.

**Roy,A. and Apparao, A. (1971).** Depth of Investigation in Direct Current Methods. *Geophysics*, 36, pp943-959, 1971.

# ANNEX 1 MAP 1: Moycullen area, Co. Galway: Geology and sample locations

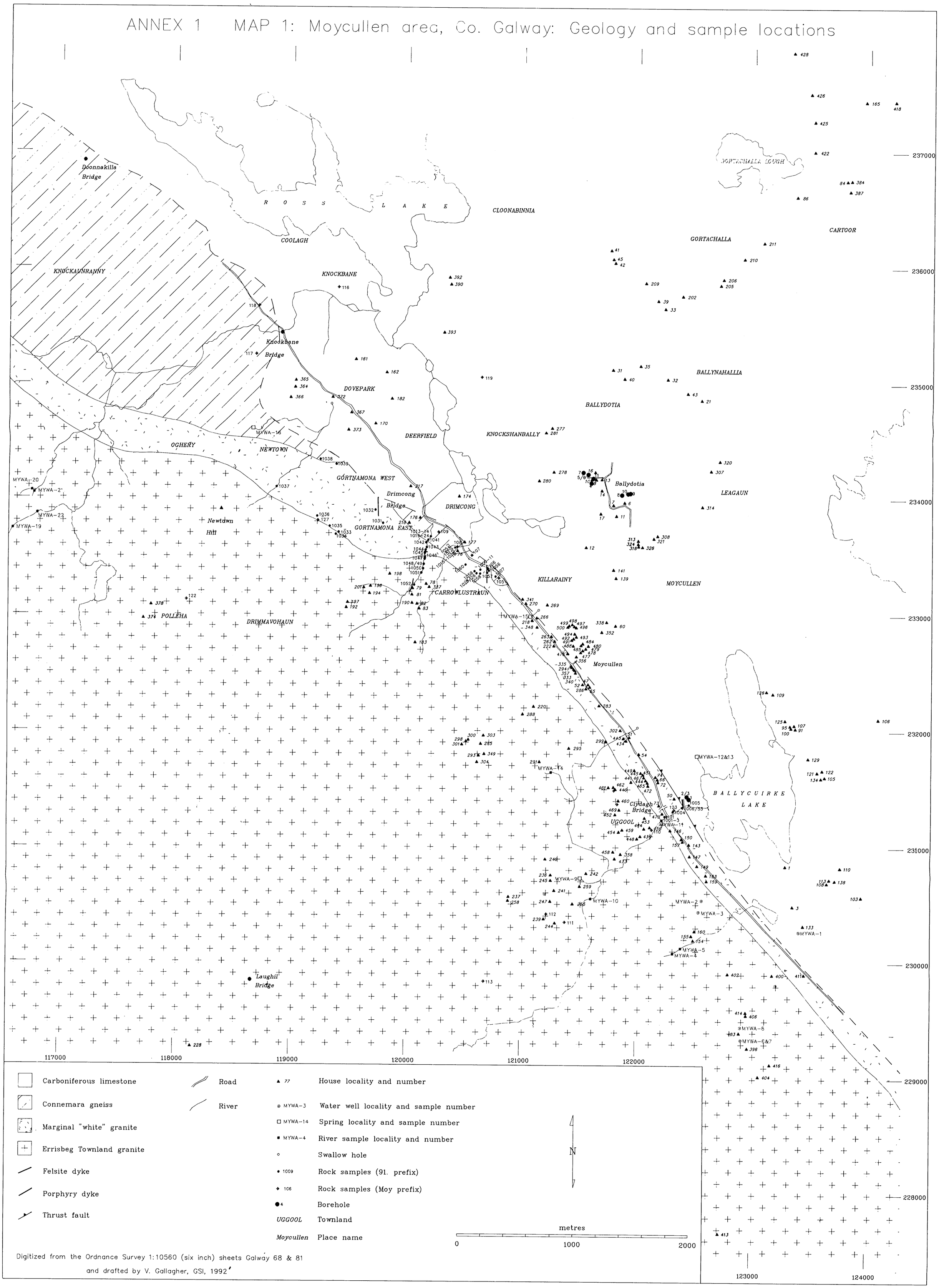


- Carboniferous limestone
- Connemara gneiss
- Marginal "white" granite
- Errisbeg Townland granite
- Felsite dyke
- Porphyry dyke
- Thrust fault
- Road
- River
- ▲ 77 — House locality and number
- ⊙ MYWA-3 — Water well locality and sample number
- □ MYWA-14 — Spring locality and sample number
- ■ MYWA-4 — River sample locality and number
- ○ — Swallow hole
- • 1009 — Rock samples (91. prefix)
- ✦ 106 — Rock samples (Moy prefix)
- ● 4 — Borehole
- *UGGOOL* — Townland
- *Moycullen* — Place name

N

metres: 0, 1000, 2000

Digitized from the Ordnance Survey 1:10560 (six inch) sheets Galway 68 & 81
and drafted by V. Gallagher, GSI, 1992

# ANNEX 1 MAP 2: Moycullen area, Co. Galway: Quaternary and bedrock geology

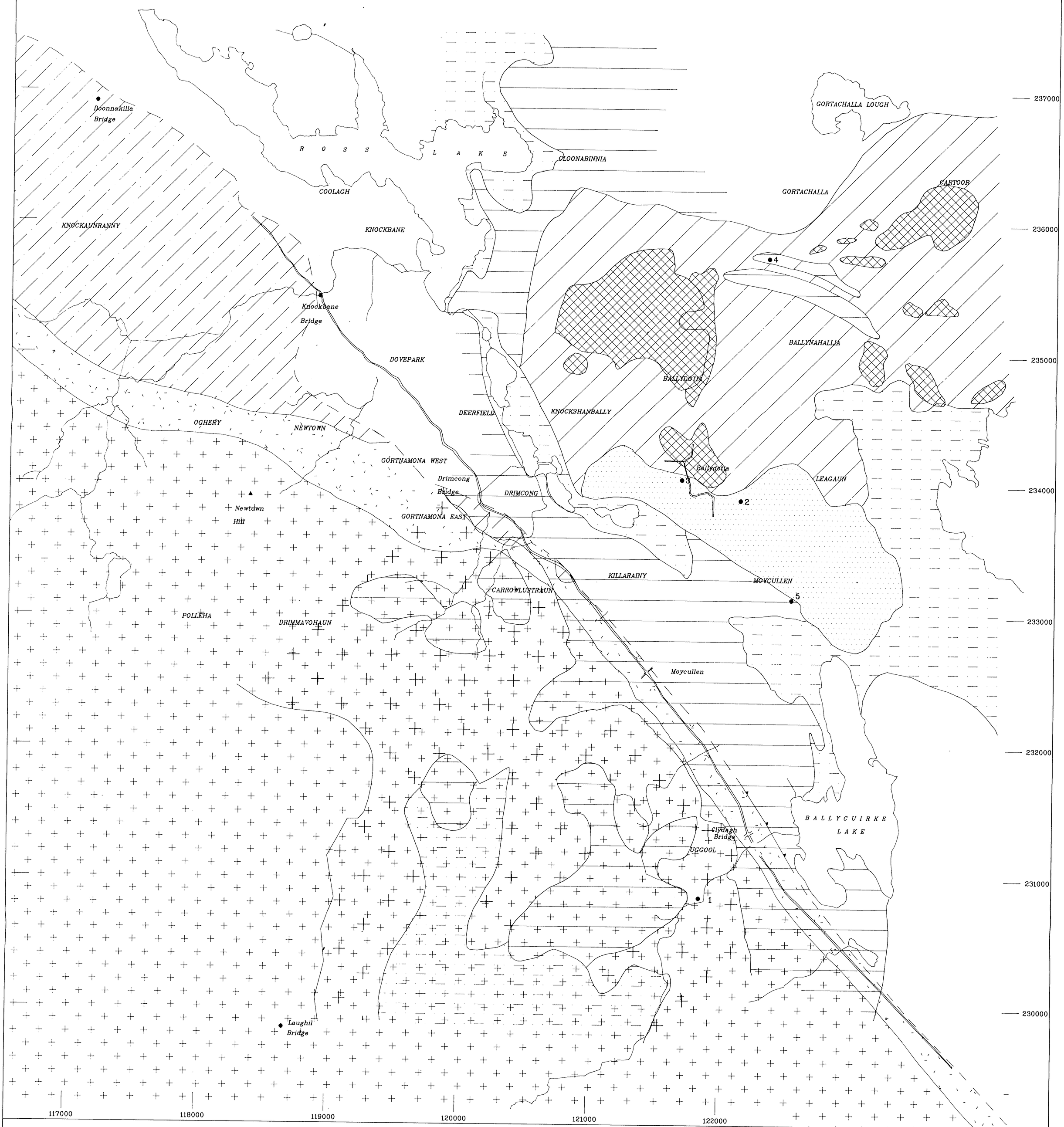


Original quaternary map compiled by C. Delaney, 1991

Transferred to 1:10560 map, digitized and drafted by V. Gallagher, GSI, 1992

# ANNEX 6

## MAP 1 BALLYDOTIA AREA

### EM–VLF–R SURVEY

### APPARENT RESISTIVITY MAP

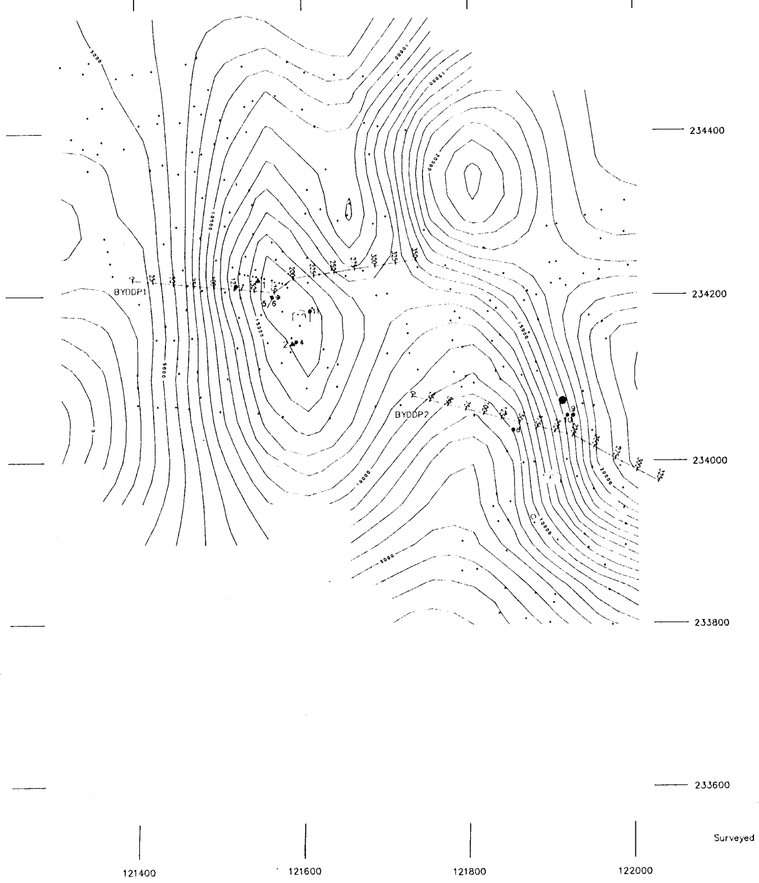


LEGEND

Contours for resistivity in Ohm–metres

· Station location

▲ VES locations

Resistivity – colinear dipole–dipole traverse (distance in metres)

[19] Location, number of house of interest

Drillhole, location and number

Well ○ Swallow hole ● Turlough

N

0 100 200 300 400

metres

Surveyed and digitized from the Ordnance Survey 1:2500 map by C. Mac Niocaill, UCG

Drafted by V. Gallagher, GSI, 1992

# ANNEX 6

## MAP 2: BALLYDOTIA AREA

### EM–VLF–R SURVEY

### PHASE MAP

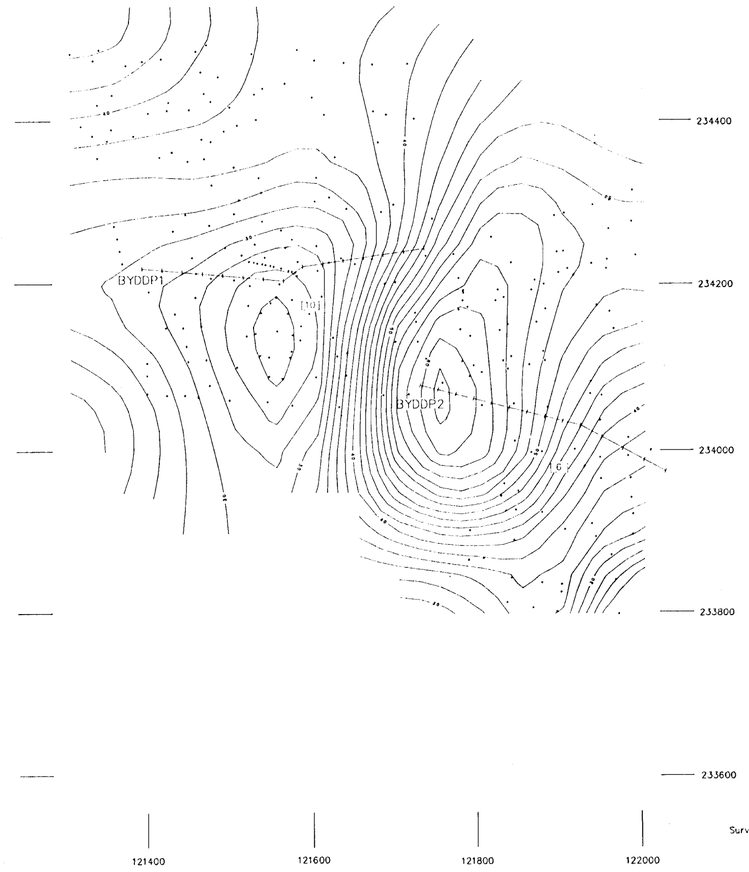


LEGEND

Phase contours at 2° intervals

· Station location

Resistivity – colinear dipole–dipole traverse

[19] Location, number of house of interest

N

0 100 200 300 400

metres

Surveyed and digitized from the Ordnance Survey 1:2500 map by C. Mac Niocaill, UCG

Drafted by V. Gallagher, GSI, 1992

# ANNEX 6

## MAP 3: MOYCULLEN AREA

### EM–VLF–R SURVEY

### APPARENT RESISTIVITY MAP

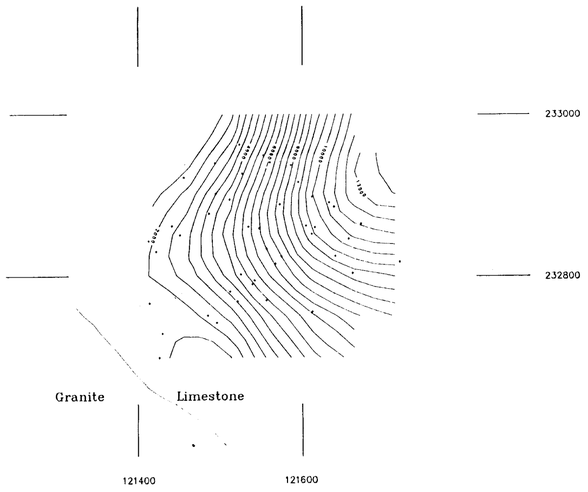


LEGEND

Contours for resistivity in Ohm–metres

· Station location

N

0 100 200 300 400

metres

Surveyed and digitized from the Ordnance Survey 1:2500 map by C. Mac Niocaill, UCG

Drafted by V. Gallagher, GSI, 1992

# ANNEX 6

## MAP 4: MOYCULLEN AREA

### EM–VLF–R SURVEY

### PHASE MAP

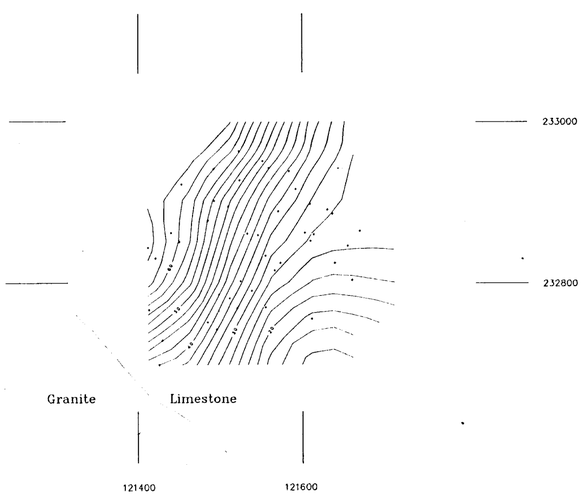


LEGEND

Phase contours at 2° intervals

· Station location

N

0 100 200 300 400

metres

Surveyed and digitized from the Ordnance Survey 1:2500 map by C. Mac Niocaill, UCG

Drafted by V. Gallagher, GSI, 1992

# ANNEX 6

## MAP 5: UGGOOL AREA

### EM–VLF–R SURVEY

### APPARENT RESISTIVITY MAP

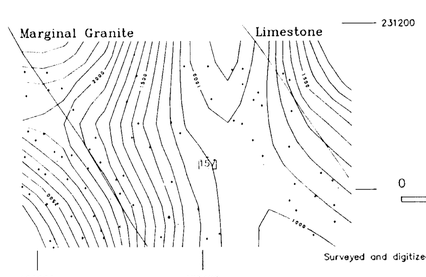


LEGEND

Contours for resistivity in Ohm–metres

· Station location

[15] Location, number of house of interest

N

0 100 200 300 400

metres

Surveyed and digitized from the Ordnance Survey 1:2500 map by C. Mac Niocaill, UCG

Drafted by V. Gallagher, GSI, 1992

# ANNEX 6

## MAP 6: UGGOOL AREA

### EM–VLF–R SURVEY

### PHASE MAP

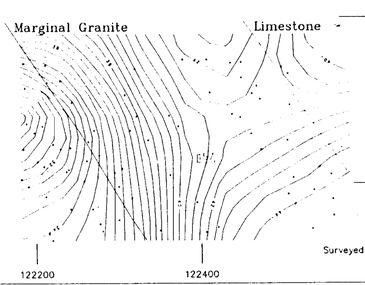


LEGEND

Phase contours at 0.5°

· Station location

[15] Location, number of house of interest

N

0 100 200 300 400

metres

Surveyed and digitized from the Ordnance Survey 1:2500 map by C. Mac Niocaill, UCG

Drafted by V. Gallagher, GSI, 1992

ANNEX 1

MAP 3: BALLYDOTIA AREA

$^{222}$Rn, $^{4}$He in soil gas (BGR)

$^{222}$Rn in dwellings (RPII)

$^{226}$Ra in soil (TCD)

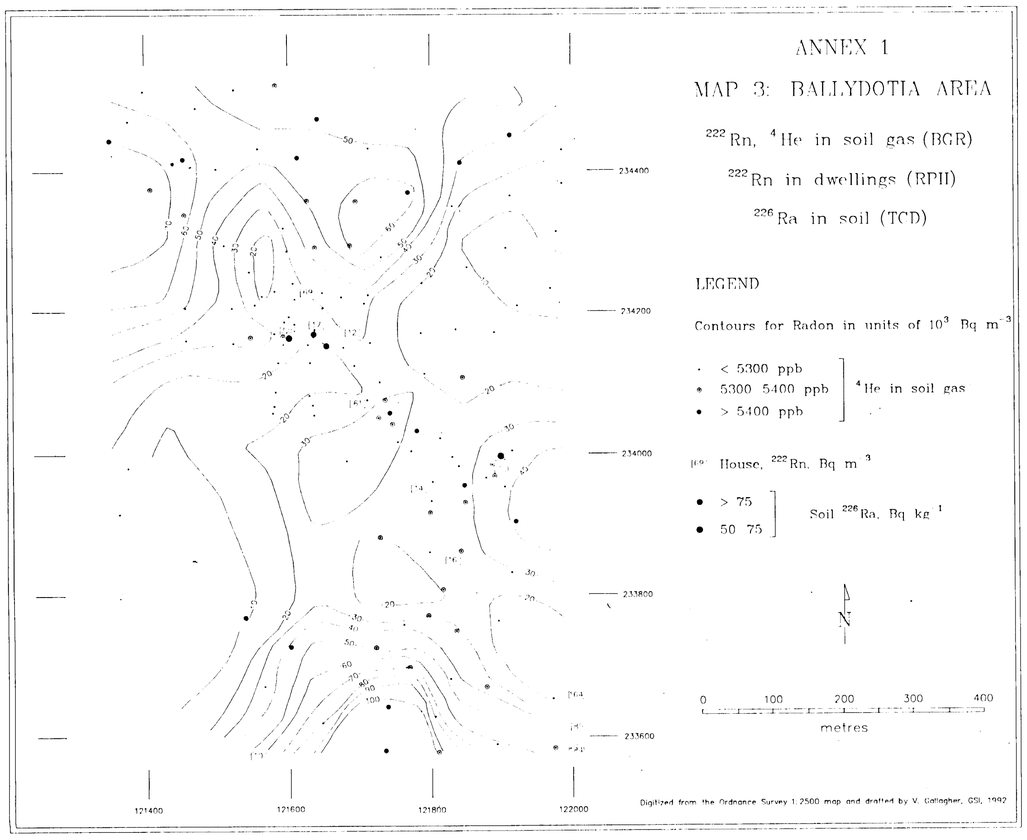


LEGEND

Contours for Radon in units of $10^3$ Bq m$^{-3}$

- < 5300 ppb
- 5300 5400 ppb
- > 5400 ppb

$^{4}$He in soil gas

[89] House, $^{222}$Rn, Bq m$^{-3}$

- > 75
- 50 75

Soil $^{226}$Ra, Bq kg$^{-1}$

N

0 100 200 300 400

metres

Digitized from the Ordnance Survey 1:2500 map and drafted by V. Gallagher, GSI, 1992

ANNEX 5

MAP 1: BALLYDOTIA AREA

Regional distribution of Radon in soil air and interpretation of Helium data

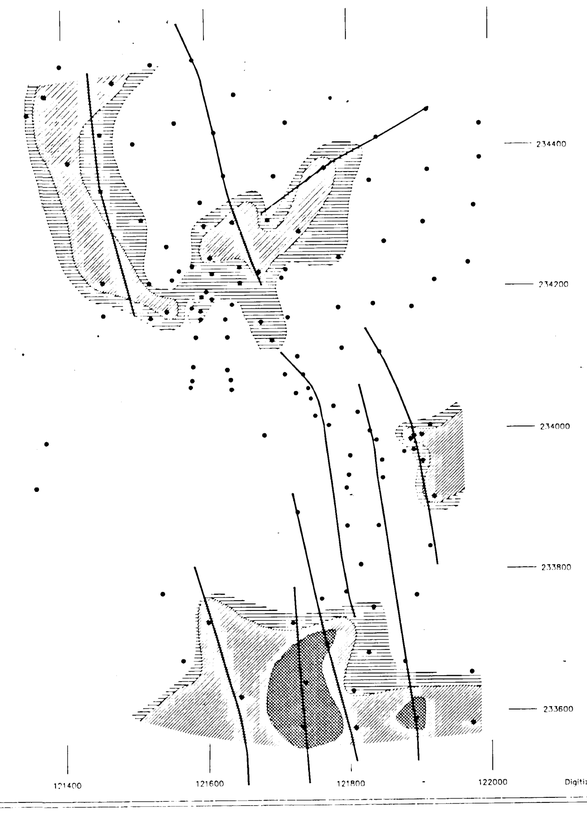


LEGEND

- $^{222}$Rn, 30000 49950 Bq m$^{-3}$
- $^{222}$Rn, 50000 90000 Bq m$^{-3}$
- $^{222}$Rn, > 90000 Bq m$^{-3}$
- Inferred fractures based on $^{4}$He survey
- Sample locations

N

0 100 200 300 400

metres

Survey and interpretation by G. van den Boom & R. Muller, BGR

Digitized from the Ordnance Survey 1:2500 map and drafted by V. Gallagher, GSI, 1992

ANNEX 1

MAP 4: MOYCULLEN AREA

$^{222}$Rn, $^{4}$He in soil gas (BGR)

$^{222}$Rn in houses (RPII)

$^{226}$Ra in soil (TCD)

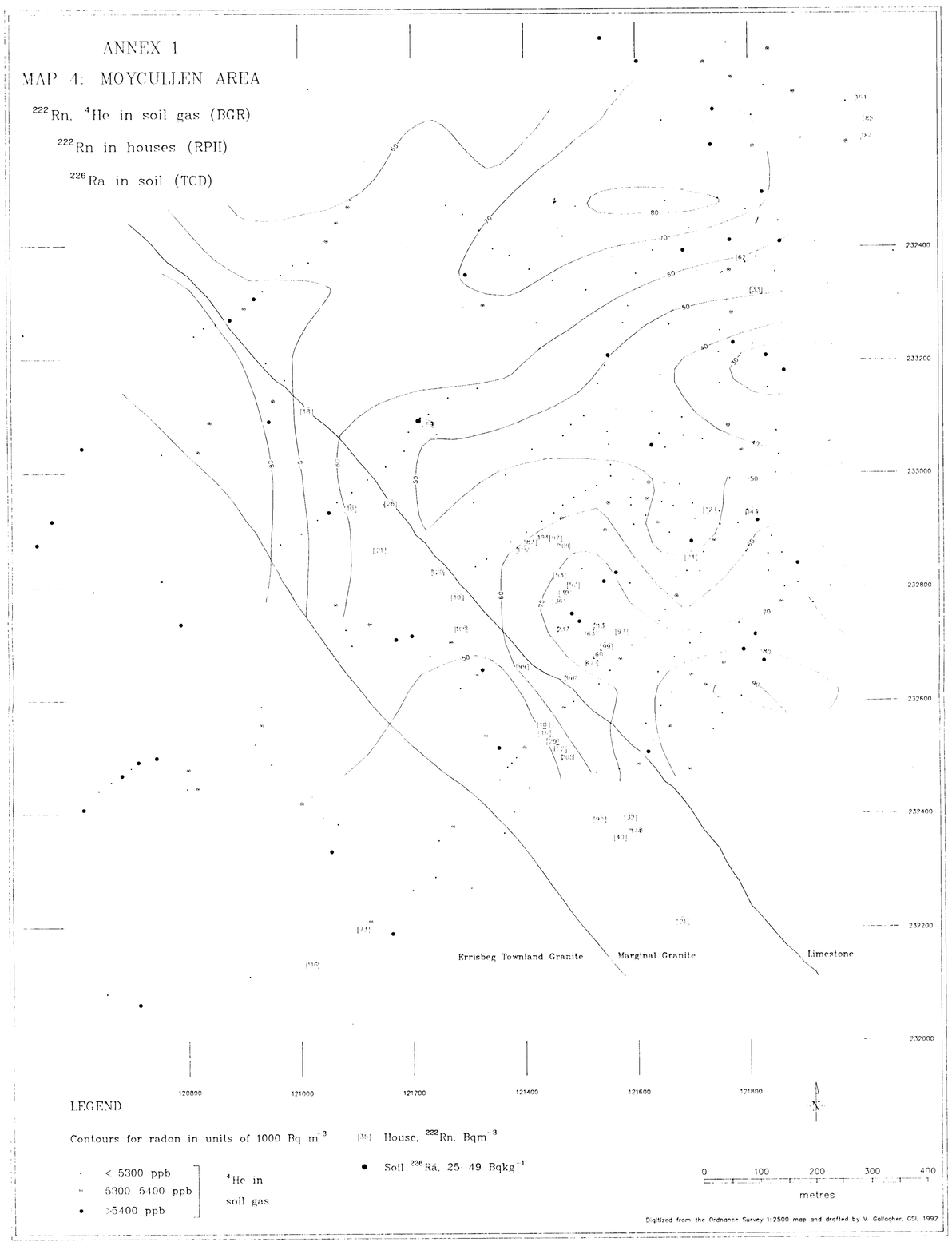


LEGEND

Contours for radon in units of 1000 Bq m$^{-3}$

- < 5300 ppb
- 5300 5400 ppb
- >5400 ppb

$^{4}$He in soil gas

[35] House, $^{222}$Rn, Bqm$^{-3}$

- Soil $^{226}$Ra, 25 49 Bqkg$^{-1}$

N

0 100 200 300 400

metres

Digitized from the Ordnance Survey 1:2500 map and drafted by V. Gallagher, GSI, 1992

ANNEX 5

MAP 2: MOYCULLEN AREA

Regional distribution of Radon in soil air and interpretation of Helium data

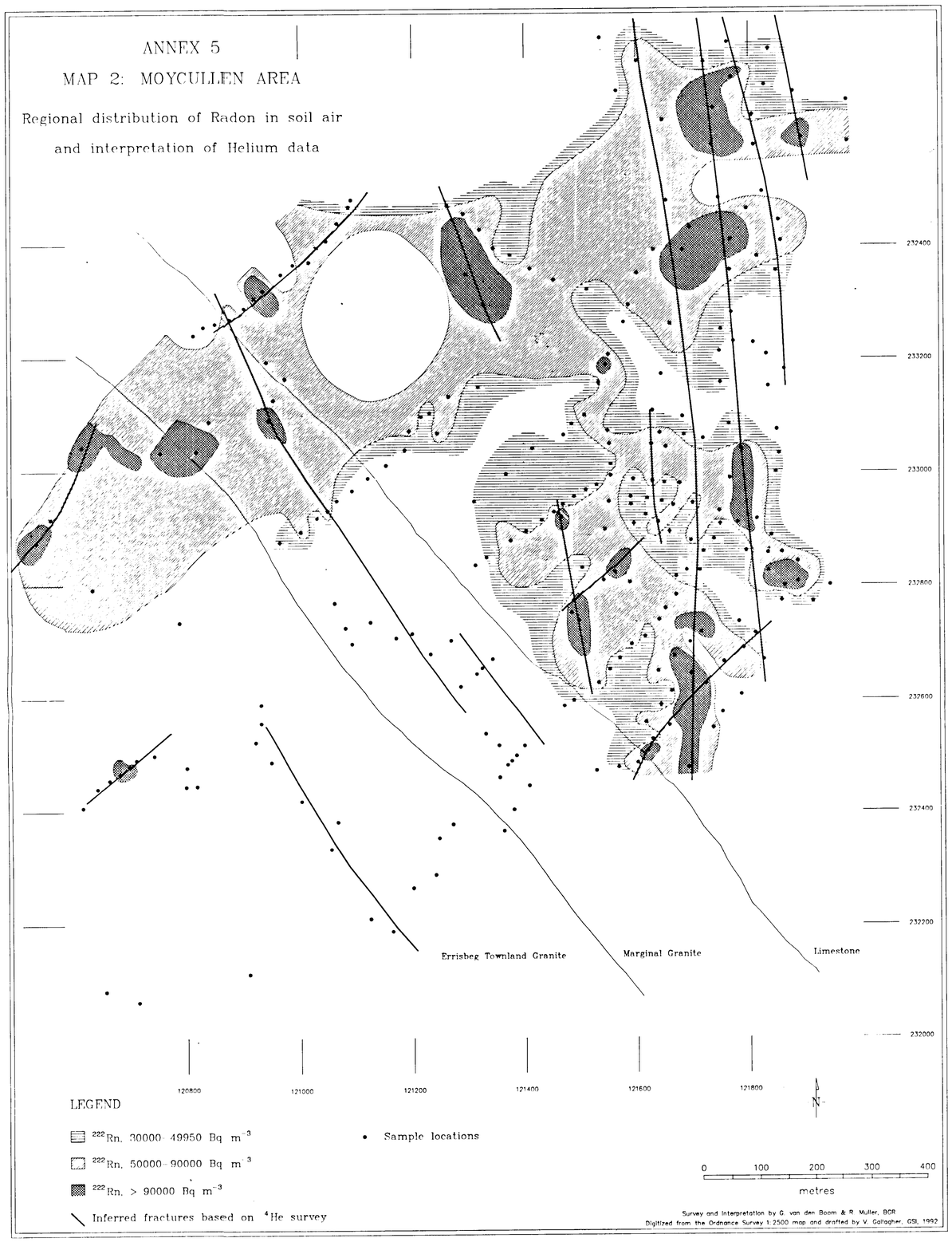


LEGEND

- $^{222}$Rn, 30000 49950 Bq m$^{-3}$
- $^{222}$Rn, 50000 90000 Bq m$^{-3}$
- $^{222}$Rn, > 90000 Bq m$^{-3}$
- Inferred fractures based on $^{4}$He survey
- Sample locations

N

0 100 200 300 400

metres

Survey and interpretation by G. van den Boom & R. Muller, BGR

Digitized from the Ordnance Survey 1:2500 map and drafted by V. Gallagher, GSI, 1992

ANNEX 1

MAP 5: UGGOOL AREA

$^{222}$Rn, $^{4}$He in soil gas

$^{222}$Rn in houses

$^{226}$Ra in soil

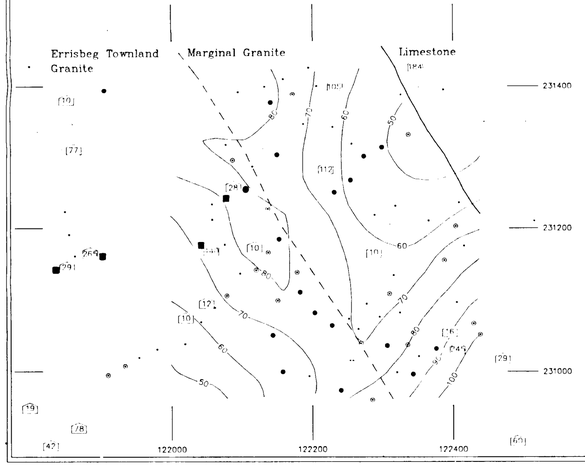


LEGEND

[50] Soil gas $^{222}$Rn, Bqm$^{-3}$ (x10$^{-3}$)

- < 5300 ppb
- 5300 5400 ppb
- >5400 ppb

$^{4}$He in soil gas

[10] House, $^{222}$Rn, Bqm$^{-3}$

- 50 75
- 25 49

Soil $^{226}$Ra, Bqkg$^{-1}$

N

0 100 200 300 400

metres

Digitized from the Ordnance Survey 1:2500 map and drafted by V. Gallagher, GSI, 1992

ANNEX 5

MAP 3: UGGOOL AREA

Regional distribution of Radon in soil air and interpretation of Helium data

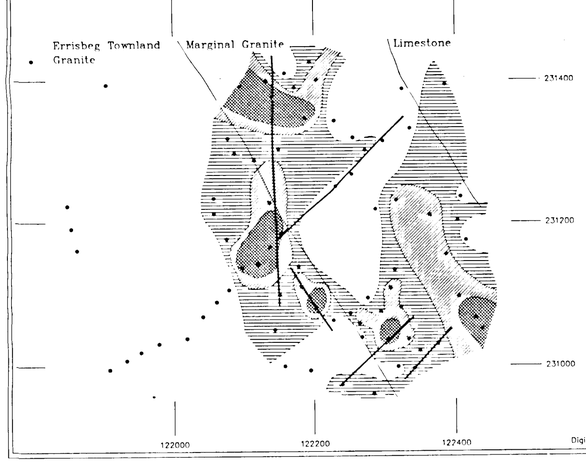


LEGEND

- $^{222}$Rn, 50000 80000 Bq m$^{-3}$
- $^{222}$Rn, 80000 100000 Bq m$^{-3}$
- $^{222}$Rn, > 100000 Bq m$^{-3}$
- Inferred fractures based on $^{4}$He survey
- Sample locations

N

0 100 200 300 400

metres

Survey and interpretation by G. van den Boom & R. Muller, BGR

Digitized from Ordnance Survey 1:2500 map and drafted by V. Gallagher, GSI, 1992